Hitoshi Michibata *Editor*

Vanadium

Biochemical and Molecular Biological Approaches

Springer

Vanadium

Hitoshi Michibata
Editor

Vanadium

Biochemical and Molecular Biological Approaches

Springer

Editor
Hitoshi Michibata
Department of Biological Science
Graduate School of Science
Hiroshima University
1-3-1 Kagamiyama
Higashihiroshima 739-8526
Japan
hmichi@hiroshima-u.ac.jp

ISBN 978-94-007-0912-6 e-ISBN 978-94-007-0913-3
DOI 10.1007/978-94-007-0913-3
Springer Dordrecht Heidelberg London New York

Library of Congress Control Number: 2011937453

Preface

Publishing the book "Vanadium: Biochemical and Molecular Biological Approaches" is particularly timed. It becomes exactly 100 years since Professor Martin Henze first reported high levels of vanadium in the blood cells of an ascidian (tunicate) collected in the Gulf of Naples in 1911. Subsequently, his discovery had a great influence not only on analytical, natural product, organic and inorganic chemistry but also on physiology, biochemistry and molecular biology. Vanadium, atomic number 23, is one of the most interesting transition elements. Average of its crustal abundance is estimated to be 100 μg/g, which is approximately twice that of copper, 10 times that of lead, and 100 times that of molybdenum (Nriagu 1998). In seawater, vanadium is dissolved in the average concentration of approximately 35 nM in the +5 oxidation state (Cole et al. 1983, 1984). Vanadium is also known to be present in crude oil, coal and tar sand. Western Venezuelan crude oil contains approximately 257 mg/g of vanadium. Vanadium can be recovered as V_2O_5 from smoke dust after the combustion of oil (Nriagu 1998). Approximately 50% of the vanadium in oil is in the form of a vanadyl ($V^{IV}O$) porphyrin complex, which resembles chlorophyll and hemoglobin (Barbooti 1989).

As far as the biochemical aspects, in the 1930s many analytical chemists analyzed the vanadium content of various organisms. In 1933, Hans Bortels suggested that vanadium compounds substituting for molybdenum compounds have a positive effect on nitrogen fixation by *Azotobacter*. In the 1970s, the biological significance of vanadium was the focus of several reports. Schwarz and Milne reported that vanadium is necessary for growing rats (1971). Bayer and Kneifel isolated a pale-blue vanadium compound from the toadstool *Amanita muscaria* and designated amavadin (1972). Cantley et al. determined that vanadate acts as a potent inhibitor of the Na^+-K^+-ATPase (1977). In the 1980s the inhibition of the Na^+-K^+-ATPase by quabain was also found to activate glucose transport and glucose oxidation in rat adipocytes. Shechter and Karlish (1980) found new inhibitors in the form of vanadium salts (vanadate and vanadyl) that stimulated glucose oxidation in rat adipocytes. In 1985, Heyliger et al. reported that vanadate appeared to have insulin-like effects. Meyerovitch et al. (1987) showed that the oral administration of vanadate normalized blood glucose

levels in streptozotocin-induced diabetic rats. The inorganic and organic vanadium-containing compounds have been of interest as insulin mimics and have been studied in clinical trials. Vanadium compounds have been further found to be effective as anti-cancer agents in several variants of leukemia. In 1984, Vilter first revealed the presence of vanadium bromoperoxidase in the marine macroalga *Ascophyllum nodosum*. This finding triggered the discovery of various vanadate-dependent haloperoxidases, including iodo-, bromo-, and chloro-peroxidases not only in marine algae but also in terrestrial fungi and lichens, which harbor enzymes that catalyze the halogenation of organic substrates by H_2O_2 and halides. In 1986, Robson et al. reported that the alternative nitrogenase of *Azotobacter chroococcum* was a vanadium enzyme. Subsequent genetic and physiological studies showed that V-nitrogenases are widely distributed but are only synthesized when molybdenum is a limiting nutrient.

At the time, the inorganic and coordination chemistry of vanadium has been investigated intenisively. The beautiful color changes depending on chemical species of vanadium in aquous solutions have fascinated inorganic and coordination chemists. Baes and Mesmer (1976) described diagram as a function of redox potential and pH. Thereafter, speciation of various vanadium species in solution and structures of many vanadium compounds have been reported by Chasteen (1983), Petterson (1985), Rehder (2008), Crans et al. (2000) and many other investigators. The reason why vanadium attracts scientists, covering such so extensive scientific fields, fundamentally attributes to its wide range of oxidation states (from -2 to $+5$), which can be converted by one-electron redox process. A variety of organic reactions, in which vanadium plays as a Lewis acid and produces many vanadium complexes, depend on the oxidation states of vanadium. Vanadium, in proteins such as vanabins isolated from ascidians, is revealed to participate in the redox chemistry. In addition, vanadium, included in enzymes such as haloperoxidases, is known to be involved in an oxygen-transfer reaction. Vanadium compounds have been revealed to induce or catalyze various potential organic reactions and polymerizations.

In the book, after you could learn the basics of vanadium by the first Part I "Featuring Chemistry of Vanadium", you would be filled with surprise on the unusual phenomena "Hyper-Accumulators of Vanadium". The skilful mechanism of enzymes described in the Part III would satisfy your scientific interest. The Part III "Enzymatic Roles of Vanadium" would show you the other side of vanadium function. The last Part IV "Medicinal Functions of Vanadium" would be expected for future practical use of vanadium.

Hiroshima University Hitoshi Michibata

Contents

Contributors

Farida Louise Assem ICF International, 9300 Lee highway, Fairfax, VA 22031, USA, lAssem@icfi.com

Daniel A. Barrio Cátedra de Bioquímica Patológica, Facultad de Ciencias Exactas, Universidad Nacional de La Plata, 47 y 115 (1900), La Plata, Argentina, barrio@biol.unlp.edu.ar

Md Shenuarin Bhuiyan Department of Pharmacology, Graduate School of Pharmaceutical Sciences, Tohoku University, 6-3 Aramaki-Aoba, Aoba-ku, Sendai 980-8578, Japan, shenuarin@hotmail.com

Malay Chatterjee Chemical Carcinogenesis and Chemoprevention Laboratory, Department of Pharmaceutical Technology, Jadavpur University, Kolkata 700 032, West Bengal, India, mcbiochem@yahoo.com

Mary Chatterjee Chemical Carcinogenesis and Chemoprevention Laboratory, Department of Pharmaceutical Technology, Jadavpur University, Kolkata 700 032, West Bengal, India, mary.chatterjee@gmail.com

José A.L. da Silva Centro de Química Estrutural, Complexo I, Instituto Superior Técnico, Technical University of Lisbon, Av. Rovisco Pais, Lisbon 1049-001, Portugal, pcd1950@ist.utl.pt

Subhadeep Das Chemical Carcinogenesis and Chemoprevention Laboratory, Department of Pharmaceutical Technology, Jadavpur University, Kolkata 700 032, West Bengal, India, subhadeepdasfaea@gmail.com

Ana L. Di Virgilio Cátedra de Bioquímica Patológica, Facultad de Ciencias Exactas, Universidad Nacional de La Plata, 47 y 115 (1900), La Plata, Argentina, aldivirgilio@biol.unlp.edu.ar

Susana B. Etcheverry Cátedra de Bioquímica Patológica, Facultad de Ciencias Exactas, Universidad Nacional de La Plata, 47 y 115 (1900), La Plata, Argentina

CEQUINOR (UNLP-CONICET), 47 y 115 (1900), La Plata, Argentina, etcheverry@biol.unlp.edu.ar

Daniele Fattorini Dipartimento di Scienze della Vita e dell'Ambiente, Università Politecnica delle Marche, Via Ranieri (Montedago) 65, Ancona 60131, Italy, d.fattorini@univpm.it

João J.R. Fraústo da Silva Centro de Química Estrutural, Complexo I, Instituto Superior Técnico, Technical University of Lisbon, Av. Rovisco Pais, Lisbon 1049-001, Portugal, pcd1950@ist.utl.pt

Kohji Fukunaga Department of Pharmacology, Graduate School of Pharmaceutical Sciences, Tohoku University, 6-3 Aramaki-Aoba, Aoba-ku, Sendai 980-8578, Japan, fukunaga@mail.pharm.tohoku.ac.jp

Toshikazu Hirao Department of Applied Chemistry, Graduate School of Engineering, Osaka University, Yamada-oka, Suita, Osaka 565-0871, Japan, hirao@chem.eng.osaka-u.ac.jp

Muthumani Janarthan Chemical Carcinogenesis and Chemoprevention Laboratory, Department of Pharmaceutical Technology, Jadavpur University, Kolkata 700 032, West Bengal, India, janarthan_mpharm@yahoo.co.in

Kan Kanamori Department of Chemistry, Graduate School of Science and Technology, University of Toyama, Gofuku 3190, Toyama 930-8555, Japan, kanamori@sci.u-toyama.ac.jp

Leonard Stephen Levy Institute of Environment and Health, Cranfield University, Cranfield, Bedfordshire MK43 0AL, UK, len.levy@cranfield.ac.uk

Hitoshi Michibata Department of Biological Science, Graduate School of Science, Hiroshima University, 1-3-1 Kagamiyama, Higashihiroshima 739-8526, Japan, hmichi@hiroshima-u.ac.jp

Toshiyuki Moriuchi Department of Applied Chemistry, Graduate School of Engineering, Osaka University, Yamada-oka, Suita, Osaka 565-0871, Japan, moriuchi@chem.eng.osaka-u.ac.jp

Armando J.L. Pombeiro Centro de Química Estrutural, Complexo I, Instituto Superior Técnico, Technical University of Lisbon, Av. Rovisco Pais, Lisbon 1049-001, Portugal, pombeiro@ist.utl.pt

Hari Ramachandran Department of Surgery, Columbia University, 17-401, 630W, 168th street, New York 10032, USA, 2harikar@gmail.com

Francesco Regoli Dipartimento di Scienze della Vita e dell'Ambiente, Università Politecnica delle Marche, Via Ranieri (Montedago) 65, Ancona 60131, Italy, f.regoli@univpm.it

Kiyoshi Tsuge Department of Chemistry, Graduate School of Science and Technology, University of Toyama, Gofuku 3190, Toyama 930-8555, Japan, tsuge@sci.u-toyama.ac.jp

Tatsuya Ueki Department of Biological Science, Graduate School of Science, Hiroshima University, 1-3-1 Kagamiyama, Higashihiroshima 739-8526, Japan, ueki@hiroshima-u.ac.jp

Ron Wever Van 't Hoff Institute for Molecular Sciences, University of Amsterdam, Science Park 904, Amsterdam 1098 XH, The Netherlands, r.wever@uva.nl

Abbreviations

2-AAF	2-acetylaminofluorene
2-ME	2-mercaptoethanol
6-PGDH	6-phosphogluconate dehydrogenase (EC1.1.1.44)
8-OHdG	8-hydroxydeoxyguanosine
acac	acetylacetonate
ACF	aberrant crypt foci
ACGIH	American Conference of Governmental Industrial Hygienists
AcOH	acetic acid
ACP	amorphous calcium phosphate
AGE	advanced glycation end
AHF	altered hepatocyte foci
ALP	alkaline phosphatase
AsGST-I	vanadium binding glutathione S-transferase-I
AsGST-II	vanadium binding glutathione S-transferase-II
BMPs	bone morphogenetic proteins
BrdU	bromodeoxyuridine
Caco-2	human colon adenocarcinoma
cAMP	cyclic adnosine 3′,5′-monophosphate
CAN	cerium(IV) ammonium nitrate
Cas	chromosomal aberrations
CD	Circular Dichroism
cDNA	complementary DNA
CSA	chondroitin sulfate A
CVD	cardiovascular disease
CYP	cytochrome P450
CYP2E1	cytochrome P45062E1
cyt	cytosolic fraction
DCT	divalent cation transporter
DEAE	diethylaminoethyl
DENA	diethylnitrosamine
DMA	dimethylarsinic acid

DMBA	dimethylbenzanthracene
DMH	dimethylhydrazine
DNA	deoxyribonucleic acid
DOPA	3,4-dihydroxylphenylalanine
DPCs	DNA-protein crosslinks
DTT	dithiothreitol
EAT	Ehrlich ascites tumor
ECM	extracellular matrix
EDTA	ethylenediaminetetraacetic acid
EGF	epidermal growth factor
enos	endothelial nitric oxide synthase
EPR	Electron Paramagnetic Resonance
ERK	extracellular regulated kinase
ESEEM	Electron Spin Echo Envelope Spectroscopy
ESRF	The European Synchrotron Radiation Facility
Et	ethyl
EXAFS	Extended X-ray Absorption Fine Structure
FGF	fibroblast growth factor
FOXO	forkhead transcription factor
G6PDH	glucose-6-phosphate dehydrogenase (EC1.1.1.49)
GGT	γ-glutamyltransferase
GP	glycogen phosphorylase (EC 2.4.1.1)
GR	glutathione reductase
GSH	glutathione
GSH-Px	glutahtione peroxide
GSH-R	glutathione reductuse
GSK-3	glycogen synthase kinase-3
GSSG	oxidized glutathione
GST	glutathione-S-transferase
H	heavy pellet
H_3HIDA	*N*-hydroxyiminodiacetic acid
H_3HIDPA	*N*-hydroxyimino-(2,2′)-dipropionic acid
IARC	International Agency for Research on Cancer
IMAC	immobilized metal ion affinity chromatography
iNOS	inducible nitric oxide
IP_3	Inositol trisphosphate
L	liter(s)
L-*dopa*	L-3,4-dihydroxyphenylalanine
LPL	lipoprotein lipase
m	microsomial fraction
MAPK	mitogen activated protein kinases
Me	methyl
MeCN	acetonitrile
MEK	acronyms of MAPK and ERK
ML	mitochondria and lysosomes enriched fraction

mol	mole(s)
MVs	matrix vesicles
NADPH	nicotinamide adenine dinucleotide phosphate
NADH	nicotinamide adenine dinucleotide
NMR	nuclear magnetic resonance
Nramp	natural resistance-associated macrophage protein
NTP	National Toxicology Program
PCNA	proliferating cell nuclear antigen
PCR	polymerase chain reaction
PDGF	platelet-derived growth factor
Ph	phenyl
PI3-K	phosphatidyl inosytol-3 kinase
PKB/Akt	protein kinase B
PKC	protein kinase C
PTPases	protein tyrosine phosphatases
$PTS \cdot H_2O$	*p*-toluenesulfonic acid monohydrate
R,S-H_3HIDBA	*meso*-*N*-hydroxyimino-2,2′-dibutyric acid
ROS	reactive oxygen species
SCE	sister chromatid exchanges
SDS-PAGE	sodium dodecyl sulfate-poly-acrylamide gel electrophoresis
SOD	superoxide dismutase
SQUID	superconducting quantum interference device
SSBs	DNA single-strand breaks
S,S-H_3HIDPA	(S,S)-*N*-hydroxyimino-(2,2′)-dipropionic acid
TBS	*tert*-butyldimethylsilyl
TFA	trifluoroacetic acid
TGF-β	transforming growth factor beta
TKL	transketolase (EC2.2.1.1)
TRAP	tartrate resistant acid phosphatase
Triflates	*trifl*uoromethane sulfon*ates*
UDPGT	UDP-glucoronyl transferase
V-ATPase	Vacuolar-type H^+-ATPase
VBP129	vanadium-binding protein 129
VBrPO	vanadium bromoperoxidase
VCPO	vanadium chloroperoxidase
vdacac	vanadocene acetylacetonate
VDC	vanadocene dichloride
VIPO	vanadium iodoperoxidase
VOHesp	VO(IV) hesperidin
VO(OPT)	bis(1-oxy-2-pyridinethiolato)
XAS	X-ray Absorption Spectrometry

Part I
Featuring Chemistry of Vanadium

Chapter 1
Inorganic Chemistry of Vanadium

Kan Kanamori and Kiyoshi Tsuge

Abstract Stereochemistry and redox property are essential factors in considering the roles of vanadium in biological systems. Coordination geometries adopted by vanadium ions with oxidation numbers +3, +4, and +5 are summarized in this chapter to provide a clue for determining the structure-function relationship of biological vanadium species. Vanadium can have a variety of geometries and its geometry is sometimes flexible. This property may be important for metals in biological systems. The electrochemical properties of complexes in each oxidation state are described by referring to typical mononuclear complexes. The redox potentials of the complexes depend largely on the ligand combination. A comparison of complexes with and without oxo ligands reveals that strong electron donation from oxo ligands stabilizes vanadium ions in higher oxidation states. Additionally, the proton-coupled equilibrium between oxo and aqua ligands imposes a significant effect on the redox behavior of vanadium complexes. Chemical redox reactions related to vanadium catalysts are also described.

Keywords Coordination stereochemistry • Coordination number • Redox chemistry • Redox potential

1.1 Introduction

Vanadium is a transition metal with a wide range of oxidation states (from −1 to +5) and it can adopt a variety of coordination numbers (CN) and coordination geometries. Among the oxidation states, the +3, +4, and +5 states have been found in biological systems. In this chapter, the coordination stereochemistry of

K. Kanamori (✉) • K. Tsuge
Department of Chemistry, Graduate School of Science and Technology, University of Toyama, Gofuku 3190, Toyama 930-8555, Japan
e-mail: kanamori@sci.u-toyama.ac.jp; tsuge@sci.u-toyama.ac.jp

H. Michibata (ed.), *Vanadium: Biochemical and Molecular Biological Approaches*,
DOI 10.1007/978-94-007-0913-3_1,

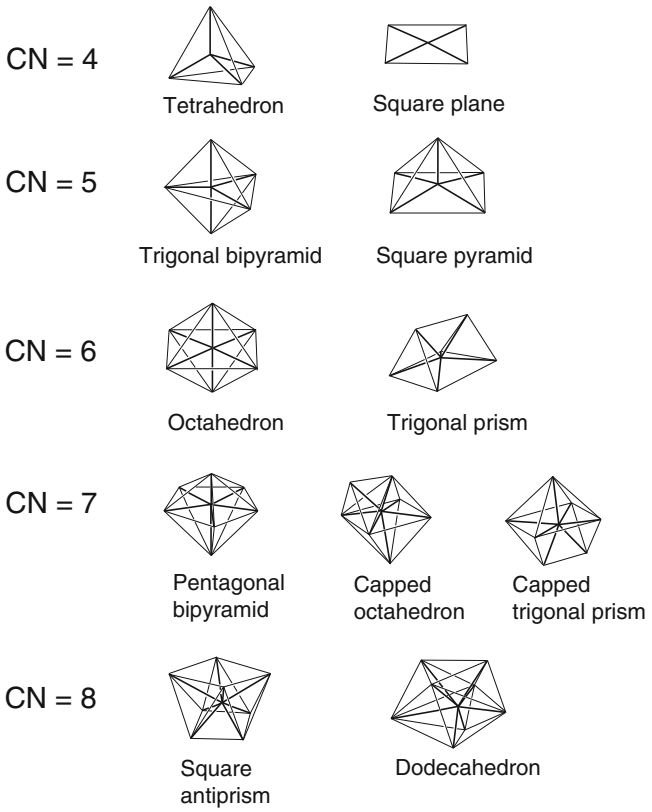

Fig. 1.1 Coordination geometries of CN 4 through 8

vanadium(III), –(IV), and –(V) complexes and their redox behaviors, including the lower oxidation states, will be presented as the basis of the biological chemistry of vanadium.

Ideal coordination polyhedra from CN 4 through 8 are presented in Fig. 1.1 [1]. Although the real coordination geometries adopted by most vanadium complexes are distorted from the ideal polyhedron to some extent, each of the polyhedra, except the square-plane and the square antiprism, has been found in vanadium complexes. This property of vanadium, adopting versatile coordination geometries, is distinct from other first-row transition metals: *e.g.*, chromium(III) and cobalt(III) give exclusively hexacoordinate octahedral complexes and the stereochemistry of copper(II) is dominated by square planar geometry.

Transition metals in biological systems are generally classified as having either a structural role in stabilizing protein structure or a functional role, involved in biological reactions [2]. However, these roles cannot be separated conclusively because it is believed that the biological function of a transition metal depends on its structure. Generally, coordinating groups of metals in biological systems are

supplied by proteins surrounding the metal ion, and the arrangement of coordinating groups in proteins does not always provide ideal coordination geometries for the metal ions. Proteins sometimes fold in a specific manner that forces the metal ion to adopt a largely distorted structure, far from the ideal geometry. This is termed an *entatic state*, which is believed to be closer to a structure in the transition state of the enzymatic reaction involving the transition metal, giving an energetically favorable pathway for the reaction [2]. Thus, flexibility in coordination geometry should be a key factor for metals in biological systems.

In the following sections, we will present the variety of coordination geometries adopted by vanadium. Typical organometallic compounds and metal clusters of vanadium will not be discussed here.

1.2 Structural Aspects of Vanadium

1.2.1 Coordination Number 4

Tetracoordination (CN = 4) generally adopts tetrahedral or square planar geometries. Square planar geometry is typically found for the d^8 metal complexes, such as Pt(II) and Pd(II), whereas, a square planar vanadium complex has not been found, so far. Tetrahedral complexes are favored for complexes with small central ions coordinated by large ligands, such as halogeno anions [1]; typical examples include $[FeCl_4]^{2-}$ and $[CoCl_4]^{2-}$. However, this is not the case for vanadium complexes because the vanadium atom has a large ionic radius among the first-row transition metals. Another example of a tetrahedral complex is the oxoanion of d^0 metals situated in the left side of the *d* block, such as $[VO_4]^{3-}$, $[CrO_4]^{2-}$, and $[MnO_4]^{-}$.

The electron-rich oxo (O^{2-}) anion can donate its electrons to a metal center through two π bonds between *p* orbitals of the oxo ion and *d* orbitals of the metal ion, in addition to a normal coordination bond of σ type, resulting in a bond order of up to three (Fig. 1.2). This multiple donation of electrons (multiple bonds) results in the stabilization of electron-poor d^0 metals.

The oxoanion of vanadium(V) (usually called "vanadate") exhibits a complex behavior in aqueous solution due to protonation equilibria, as well as oligomerization. The simple vanadate $[VO_4]^{3-}$ ion can only exist at very alkaline pH (>12). Below pH 12, various polyoxovanadium(V) species are formed, depending on the total concentration of vanadium and the ionic medium concentration. Speciation of the vanadium(V) oxoanion in aqueous solution has been studied thoroughly using a combination of potentiometric and ^{51}V NMR spectroscopic data [3]. ^{51}V NMR spectroscopy is a powerful tool and has been widely used in the study of vanadium(V) solution chemistry [4]. Formulations of the species in solution have been presented with their formation constants [3]. Well-characterized structures of the oligomeric species are shown in Fig. 1.3. The oligomerization of vanadate occurs by sharing a corner of the tetrahedron of a VO_4 unit. As shown in Fig. 1.3,

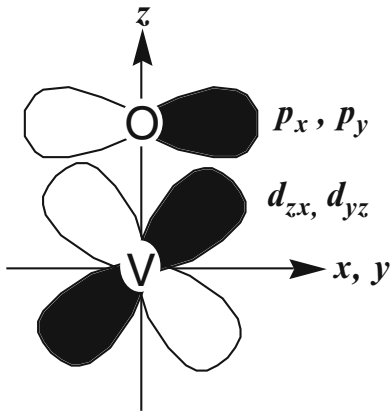

Fig. 1.2 π-Bonding between the *p* orbital of an oxo ligand and vanadium *d* orbital

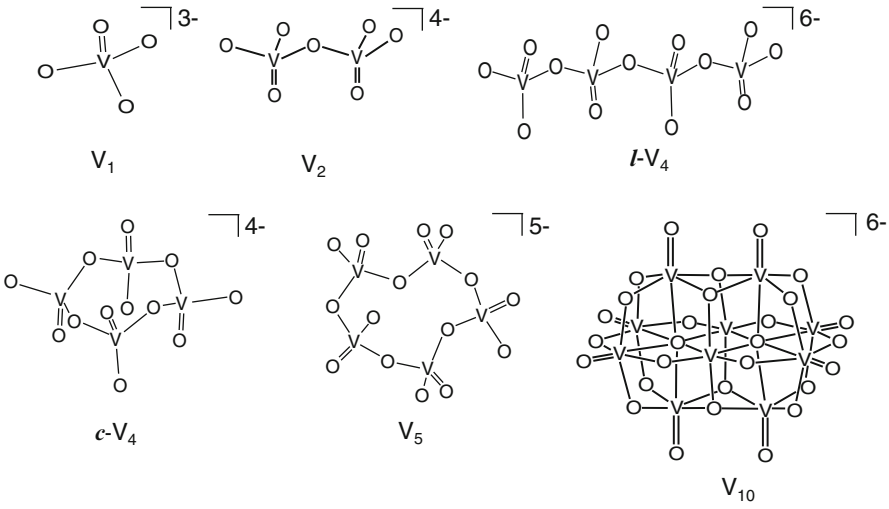

Fig. 1.3 Structures of vanadate species formed in solution

cyclic oligomers are formed in addition to linear ones. This behavior is distinct from that of chromium (neighboring atom of vanadium in the periodic table), in which only linear oligomers, such as $Cr_2O_7^{2-}$ and $Cr_3O_{10}^{2-}$, are recognized. Instead, vanadate oligomerization more closely resembles that of phosphate, for which the tetracyclo anion, $P_4O_{12}^{4-}$, has been found. This similarity in oligomerization behavior between vanadate and phosphate may relate to a biological role of vanadium because phosphate is an inorganic ion found commonly in living systems.

In contrast to polyoxovanadate species with nuclearity from 2 to 5, decavanadate (V_{10}) formed in slightly or moderately acidic solutions, as well as monomeric species formed in a very acidic solutions, consist of octahedral units.

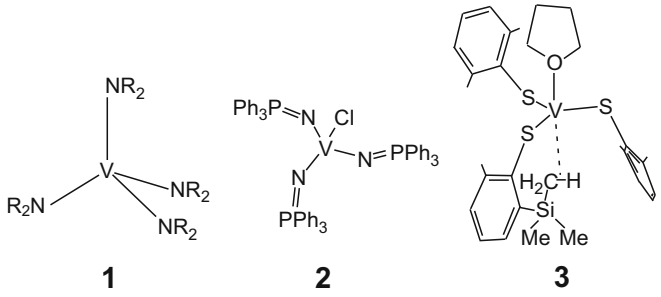

1 2 3

Fig. 1.4 Tetrahedral vanadium complexes

Tetrahedral vanadium complexes other than oxovanadium(V) species are very rare. R_2N^- ligands have been shown to give tetrahedral vanadium complexes (Fig. 1.4; **1** and **2**). Interestingly, the oxidation state of vanadium in **1** changes depending on the R group: $[V(V)(NEt_2)_4]^+$ [5], $[V(IV)(NMe_2)_4]$ [6], and $[V(III)(NPh_2)_4]^-$ [7], although the reason why is unclear. Although these species will not relate directly to the biological chemistry of vanadium because they are fairly unstable, it should be noted that the R_2N^- ligand has a strong donating ability, like the O^{2-} ligand.

A unusual trigonal monopyramidal structure for CN = 4 has been found (Fig. 1.4, **3**) [8]. In this complex, $[V(III)(SC_6H_3\text{-}2,6\text{-}(SiMe_3)_2)_3(THF)]$, the vacant site *trans* to the THF ligand is occupied by an agostic C–H bond from a SiMe group of the thiolate ligand. Thus, the coordination geometry of this complex would be better described as a trigonal bipyramid, by including the agostic interaction.

1.2.2 Coordination Number 5

Pentacoordinate vanadium is important with regard to the biological chemistry of vanadium because the vanadium ion in the active center of vanadium-dependent haloperoxidases (VHPOs) adopts pentacoordination. The ideal geometries of pentacoordinate metal complexes are trigonal bipyramid and square pyramid [1]. The natural form of VHPO adopts a trigonal bipyramidal structure, whereas the reaction intermediate coordinated by a peroxo ligand forms a square pyramidal structure (Fig. 1.5, **4** [9], **5** [10]). Real complexes frequently take an intermediate structure between the two ideal geometries. Distortion from the ideal geometries can be evaluated using the τ value, defined in Fig. 1.6 [11]. Because the energies of the trigonal bipyramid and square pyramid differ little from one another, pentacoordinate complexes are often fluxional, as illustrated by the observations that two types of complexes have been obtained with the same ligand or closely related ligands. Examples of such complexes are shown in Fig. 1.5.

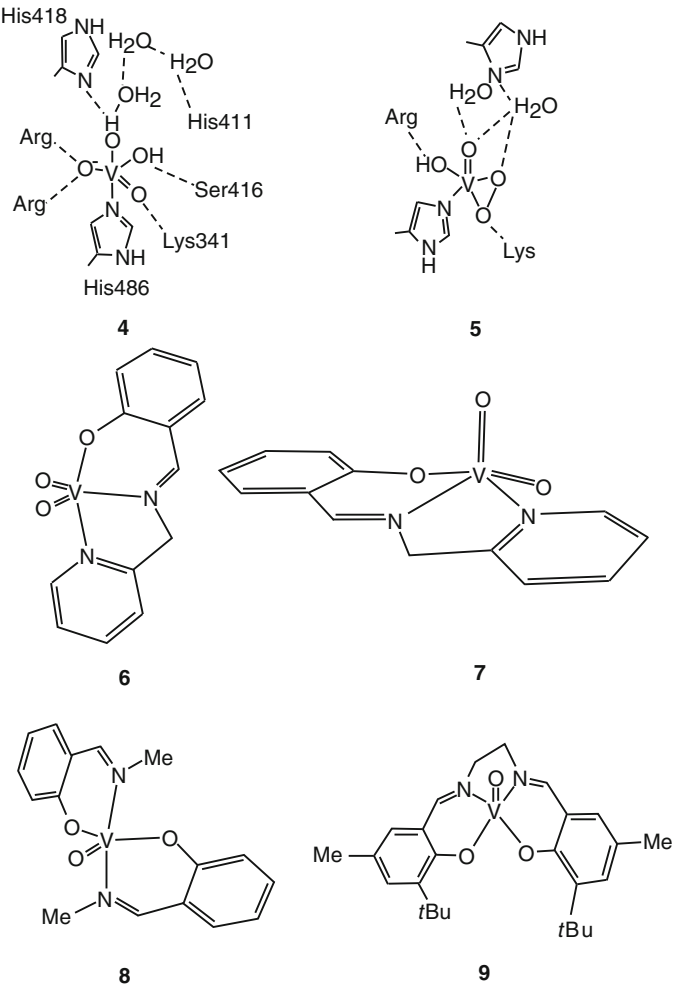

Fig. 1.5 Pentacoordinate vanadium complexes

Fig. 1.6 Definition of τ

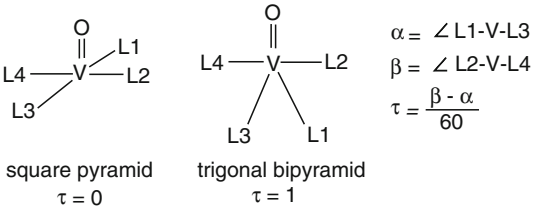

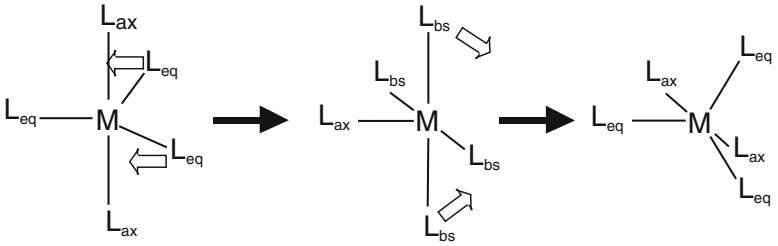

Fig. 1.7 Berry pseudorotation

Two types of crystals (greenish-yellow and green) have been obtained by the reaction of the tridentate salicylaldimine of 2-picolylamine with $[V(IV)O(acac)_2]$ (acac = acetylacetonate) in different solvents. The former crystal prepared in methanol contains the trigonal bipyramidal complex, $[V(V)(O)_2(L)]$ ($HL = C_6H_4(OH)CHNCH_2C_5H_4N$) (**6**: $\tau = 0.55$), whereas the latter (**7**: $\tau = 0.20$), prepared in acetonitrile, contains the square pyramidal complex [12], indicating solvent-specific dimorphs. Compounds **8**, [V(IV)O(*N*-methylsalicylaldiminato)$_2$] and **9**, [V(IV)O(*N,N′*-ethylenebis(*o-tert*-butyl-*p*-methylsalicylaldiminato))] are an example in which a bis(Schiff base) vanadium(IV) complex adopts a trigonal bipyramidal structure, while a square pyramidal vanadium(IV) complex can be obtained by linking the two azomethine groups with an ethylene group [13].

In solution, pentacoordinate complexes are often highly fluxional, resulting in an interconversion between the axial ligand and the equatorial ligand within a short period. This conversion may occur by Berry pseudorotation, via a square pyramidal geometry as an intermediate species (Fig.1.7). This dynamic behavior is exemplified by a model complex of VHPO, [V(V)O(OMe)(L)] ($H_2L = N(CHPhCH_2OH)_2(CH_2COO(t\text{-Bu}))$ [14] and $= N(CH_2CHMeOH)_2(CHPhMe))$ [15]. Two ^{51}V NMR signals of comparable intensity were observed for the complexes [V(V)O(OR)L]. This was explained by assuming that the two trigonal bipyramidal complexes with the oxo group mutually in the equatorial and axial positions are equilibrated in solution (Fig. 1.8, **10** and **10′**).

Although a trigonal bipyramidal structure minimizes ligand-ligand repulsions for pentacoordinate complexes, the stereochemistry of oxovanadium(IV) (usually called "vanadyl") complexes is dominated by square pyramidal geometry, as in $[V(IV)O(acac)_2]$. This preference is thought to be a result of the strong multiple bonding induced by an oxo ligand (discussed in Sect. 1.2.1). In octahedral complexes of oxovanadium(IV), the bond distances *trans* to the oxo group are considerably longer than those *cis* to the oxo group. This phenomenon is called "*trans* influence" (not to be confused with the kinetic "*trans* effect"), which is considered to be a result of the strong V(IV)-O^{2-} bond. Because two ligands situated

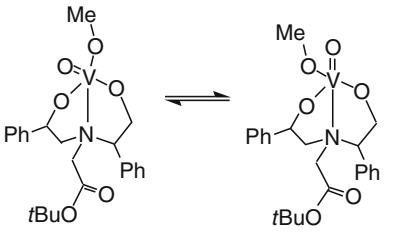

Fig. 1.8 Fluxional pentacoordinate vanadium complex

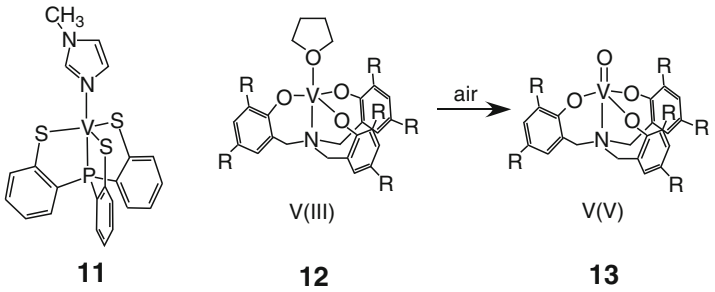

Fig. 1.9 Trigonal bipyramidal complexes

in *trans* positions with each other use common *d* orbitals for bonding with the central metal ion, strong electron donating from O^{2-} makes an attachment of the ligand *trans* to O^{2-} unfavorable. Thus, the square pyramidal geometry adopted by vanadyl complexes may be considered to be an extreme case of *trans* influence where a weakly bound ligand *trans* to the O^{2-} group leaves the coordination sphere (*e.g.*, in crystallization), making a vacant site. Thus, in a solution in which the solvent molecule has a coordinating ability, it is plausible that the solvent molecule weakly coordinates in the sixth position, *trans* to the O^{2-} group, even if the complex adopts a square planar geometry in the solid state.

Square pyramidal and trigonal bipyramidal structures can be formed selectively by designing the ligand structure. For example, tetradentate ligands with high planarity, such as porphyrin, yield exclusively square pyramidal complexes. On the other hand, tetradentate tripodal ligands tend to yield a trigonal bipyramidal geometry, as shown in Fig. 1.9, **11**, [V(III)($P(C_6H_4\text{-}2\text{-}S^-)_3$)(1-methylimidazole)] [16], **12**, [V(III)($N(CH_2C_6H_2R_2O^-)_3$)(THF)] and **13,** [V(V)O($N(CH_2C_6H_2R_2O^-)_3$)] [17]. Structural similarity among the complexes in different oxidation states (**12** and **13**) is an important factor for constructing a readily accessible pathway in redox reactions.

Other examples of pentacoordinate vanadium complexes are shown in Fig. 1.10. Compounds **14**, $[V(V)(O)_2(dipic)]^-$ [18] and **15,** $[V(V)(O)_2((S)\text{-}N\text{-}$salicylidene-3-aminopyrrolidine)] [19] are examples showing that dioxovnadium(V) complexes

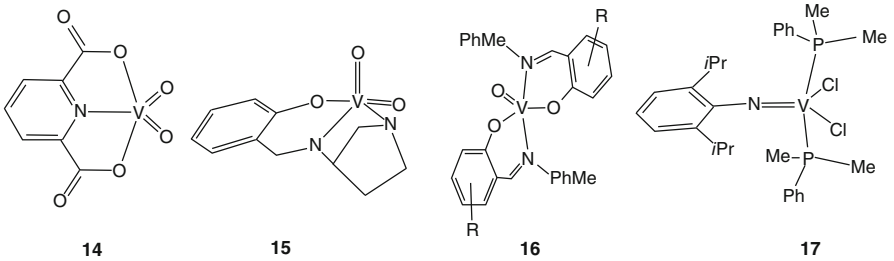

Fig. 1.10 Other pentacoordinate vanadium complexes

with a tridentate ligand can adopt both trigonal bipyramidal and square pyramidal structures. Compound **16**, [V(IV)O(OC_6H_3(R)CNCHPhMe)] [20] has a structure similar to **8**. Compound **17**, [V(IV)(N-2,6-*i*-$Pr_2C_6H_3$)(PMe_2Ph)] [21] is a rare example of an arylimido complex of vanadium(IV).

1.2.3 Coordination Number 6

A hexacoordinate octahedral arrangement is the most common structure for transition metal complexes. This structure is found for vanadium complexes in all biologically relevant oxidation states, +3, +4, and +5. In contrast, trigonal prismatic geometry is unusual. However, dithiolene ligands ($S_2C_2R_2^{2-}$) can specifically constrain the complex into a trigonal prism. Gray et al. attributed the stability of the trigonal prismatic structure to two types of π-bonding interactions between *p* ligand orbitals and the metal *d* orbitals [22]. Vanadium compounds having a trigonal prismatic structure are also seen in tris(dithiolene) complexes, as shown in Fig. 1.11. Distortion from the regular trigonal prism to an octahedron can be characterized by the twist angle, θ between two triangle faces opposite each other ($\theta = 0°$ for trigonal prism; $\theta = 60°$ for an octahedron). [$V(S_2C_2H_2)_3$] [23], [$V(S_2C_2Ph_2)_3$] [24], and [$V(DDDT)_3$]$^-$ ($DDDT^{2-}$ = 5,6-dihydro-1,4-dithin-2,3-dithiolate) [25] complexes adopt perfect or nearly perfect trigonal prismatic structures with $\theta = 0°$, 8.5°, and 3.7°, respectively, whereas [$V(S_2C_2(CN)_2)_3$]$^{2-}$ [26], [$V(bdt)_3$]$^{2-}$ (bdt^{2-} = 1,2-benzenedithiolate) and [$V(tdt)_3$]$^{2-}$ (tdt^{2-} = 3,4-toluenedithiolate) [23] have a structure distorted towards octahedral geometry.

For the dithiolene complexes, the oxidation state of the metal ion cannot be determined readily because the ligands themselves can be oxidized up to dithioketones, as shown in Fig. 1.11. In [$V(S_2C_2H_2)_3$], the oxidation state of vanadium has been determined to be +4 on the basis of an observed EPR spectrum characteristic of vanadium(IV) [23]. Thus, it has been concluded that the negative charge of −4 could be delocalized equally over the three $S_2C_2H_2$ ligands; nevertheless, it can be regarded formally that one ligand has a charge of −2 and two ligands have a charge of −1.

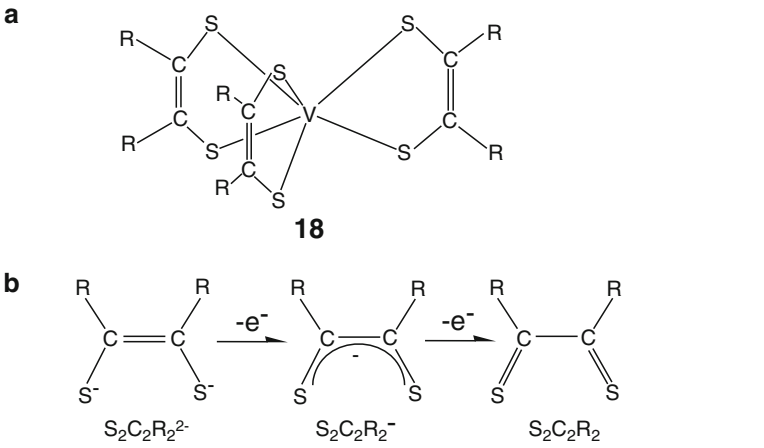

Fig. 1.11 Structure of tris(dithiolene) vanadium complex (**a**) and the oxidation of dithiolene (**b**)

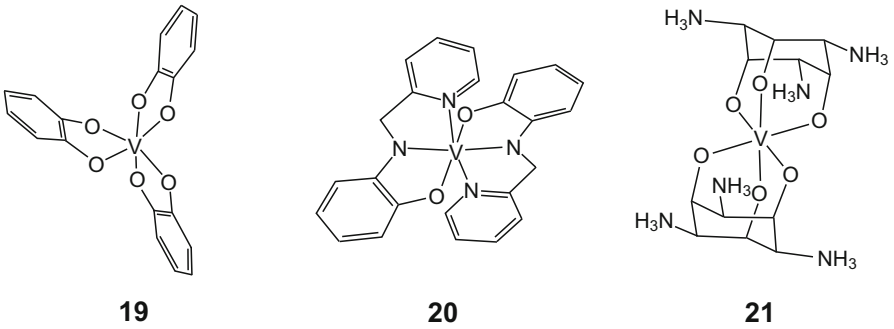

Fig. 1.12 Bare or non-oxo vanadium(IV) complexes

Although coordination compounds of vanadium(IV) are dominated by oxovanadium (vanadyl) species, several complexes without oxo ligands have been prepared and structurally characterized. This type of complex is called "bare" or "non-oxo" vanadium(IV). To obtain a bare vanadium(IV) complex, a ligand that can serve as a strong π donors must be introduced to the coordination sphere to compensate for the strong electron donation from the oxo group. Representative ligands with such ability are catecholates. In fact, a hexacoordinate bare vanadium(IV) complex, $[V(IV)(cat)_3]^{2-}$ (cat = catecholate) has been obtained (Fig. 1.12, **19** [27, 28]). Although, in general, vanadium(V) complexes also contain one or two oxo groups, 3,5-di-*tert*-butylcatecholate yields a bare vanadium(V) complex $Na[V(V)(DBcat)_3]$ [29]. Vanadium(V) complexes without strongly bound oxo ligands are quite rare. In addition to the above vanadium(IV) and –(V) complexes, a vanadium(III) complex, $K_3[V(III)(cat)_3]$ has been obtained and their redox behaviors were examined [27].

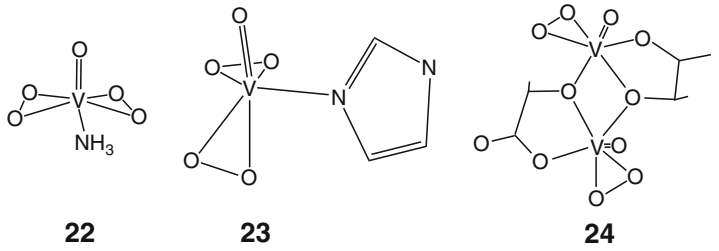

22 **23** **24**

Fig. 1.13 Hexacoordinate pentagonal pyramidal complexes

The reaction of oxovanadium(IV) ion with two equivalents of *N*-(2-hydroxyphenyl)-*N*-(2-pyridylmethyl)amine (H_2hppma) ligands yields another example of a bare vanadium(IV) complex (Fig. 1.12, **20** [30]). In this complex, the amino group of hppma is deprotonated and the ligand acts as a dianion. This N^- atom, in addition to the phenolate oxygen atom, can act as strong π donors, like catecholates, resulting in the formation of a bare vanadium(IV) complex. Compound **21** is an example of a bare vanadium(IV) complex with a biologically relevant ligand, 1,3,5-triamino-1,3,5-trideoxy-*cis*-inositol (taci) [31].

Some oxo(peroxo)vanadium(V) complexes adopt a geometry that can be best described as a pentagonal pyramid (Fig. 1.13, **22** [32], **23** [33], **24** [34]). This geometry is very unusual for hexacoordinate complexes. Thus, it may be better to consider this geometry as a special case of the pentagonal bipyramidal structure, which is found commonly in oxo(peroxo)vanadium(V) complexes. Specifically, the seventh ligand opposite to the oxo group in the pentagonal bipyramidal structure may leave the coordination sphere due to a strong *trans* influence of the oxo group in crystallization, resulting in a pentagonal pyramidal geometry.

1.2.4 Coordination Number 7

A coordination number greater than six is encountered rarely in first-row transition metal complexes because 3d metal ions do not have an ionic radius large enough to accommodate more than six ligands. Recently, however, heptacoordinate vanadium complexes have become less rare. This may be explained by considering that vanadium ions (especially vanadium(III)) have a slightly larger ionic radius than other first-row transition metal ions. The ideal geometries for heptacoordination include a pentagonal bipyramid, capped octahedron, and capped trigonal prism; these three geometries are, however, similar in energy to heptacoordination [1]. Thus, heptacoordinate vanadium complexes are often fluxional and most of them adopt intermediate structures.

Because cyanide is a small ligand, vanadium(III) can accommodate seven cyano ligands to yield the heptacoordinate vanadium(III) complex, $[V(III)(CN)_7]^{3-}$ with pentagonal bipyramidal geometry, as shown in Fig. 1.14, **25** [35]. The bent

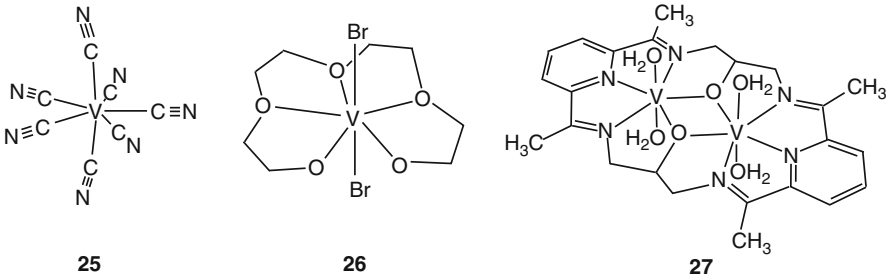

Fig. 1.14 Heptacoordinate pentagonal bipyramidal complexes

coordination of cyanide found in **25** has been attributed to the interaction of the ligand with the cations surrounding the complex. The pentagonal bipyramidal geometry of this complex has been explained in terms of crystal field stabilization, rather than the size of the vanadium(III) ion.

One strategy to obtain pentagonal bipyramidal complexes is to employ a ligand in which five donor atoms are arranged in a pentagonal plane. Examples of this type of complex are illustrated in Fig. 1.14, **26** and **27**. Compounds **26**, $[V(III)(teg)Br_2]^+$ (H_2teg = tetraethylene glycol) [36] and **27**, $[V(III)_2L(H_2O)_4]^{4+}$ (H_2L = 1,7,14,20-tetramethyl-2,6,15,19-tetra-aza[7, 7](2,6)-pyridinophane-4,7-diol) [37] have a highly planar structure with regard to the equatorial coordination. Preparation of **26** is worth noting because it accompanied a unique redox reaction. Specifically, compound **26** was prepared by the reaction of vanadium(V) species with tetraglyme, $CH_3O(CH_2CH_2O)_4CH_3$ in the absence of dioxygen. This indicates that the vanadium-catalyzed oxidation of hydrogen bromide to bromine,

$$2V\,(V)\,O + 4HBr \rightarrow 2V\,(III) + 2Br_2 + 2H_2O\,\left(V^{5+}/V^{3+}\text{ redox couple}\right)$$

occurred with scission of the terminal ether bond of the glyme by hydrogen bromide. As discussed later, generally, a strong reducing agent is necessary to reduce vanadium(IV) to vanadium(III). Thus, the above reaction is unique from the viewpoint that a weak reducing agent can reduce vanadium(V) to vanadium(III) by choosing a ligand to assist the reduction, and may relate to the reduction mechanism used to yield vanadium(III) species in biological systems.

Although heptacoordinate pentagonal bipyramidal vanadium compounds are still rare with conventional ligands, monoperoxo and diperoxo vanadium(V) complexes with chelate ligand(s) usually adopt this structure, as illustrated in Fig. 1.15, **28** $[V(V)O(O_2)(oxalate)_2]^{3-}$ [38], **29** $[V(V)O(O_2)$(picolinato)(picolinamide)] [39], and **30** (X = O) $[V(V)O(O_2)_2(bpy)]^-$ [40]. Persulfide, S_2^{2-} ligand also behaves in the same manner as O_2^{2-}, **30** (X = S) $[V(V)O(S_2)_2(bpy)]^-$ [41], and **31** $[V(V)O(S_2)_2$ (terpyridine)$]^-$ [42]. The small bite angles of the three-membered chelate ring formed by the side-on coordination of the peroxo or persulfido group (45° and 51°, respectively) would enable the arrangement of five donor atoms in the equatorial plane. Other examples in which ligands giving a small bite angle enable vanadium

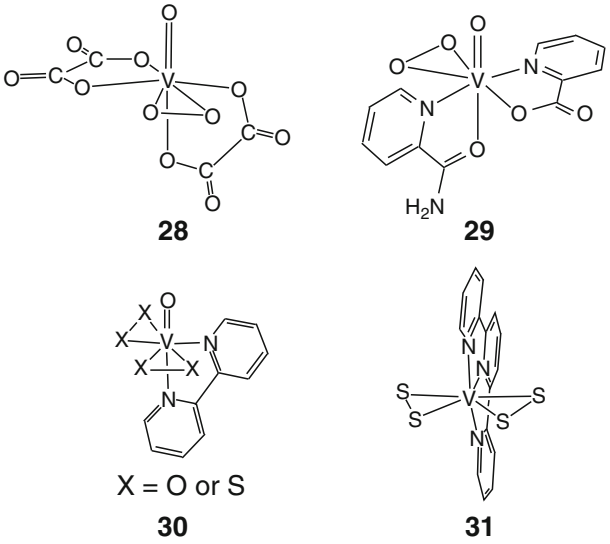

Fig. 1.15 Structures of peroxo and persulfido complexes

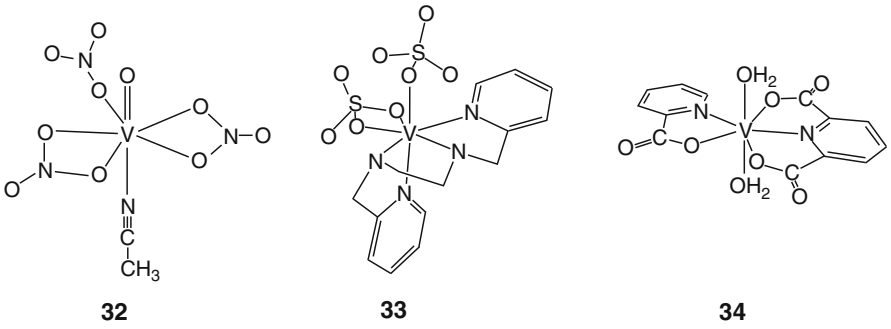

Fig. 1.16 Heptacoordinate complexes including ligands with small bite angles

to form a pentagonal equatorial plane are shown in Fig. 1.16. The bidentate coordination of nitrate in **32**, $[V(V)O(NO_3)_3(CH_3CN)]$ [43] and sulfate in **33**, $[V(III)_2(SO_4)_3(N,N'$-bis(2-pyridylmethyl)-1,2-ethanediamine$)_2]$ [44] forming four-membered chelate rings gives bite angles of ca. 61° and 66.6°, respectively. These bite angles can be regarded as small enough to allow five donor atoms to arrange in the equatorial plane. Compound **34**, $[V(III)$(dipicolinato)(picolinato)$(H_2O)_2]$ [45] is a unique example of a heptacoordinate complex that includes neither the three-membered chelate ring nor the four-membered chelate ring; instead, the tridentate meridional coordination of dipic is highly distorted from the ideal angle for meridional coordination (180°), giving an O-V-O angle of 142.1°, and thus leaves enough space to accommodate a normal bidentate ligand on the opposite side of the dipicolinate (dipic).

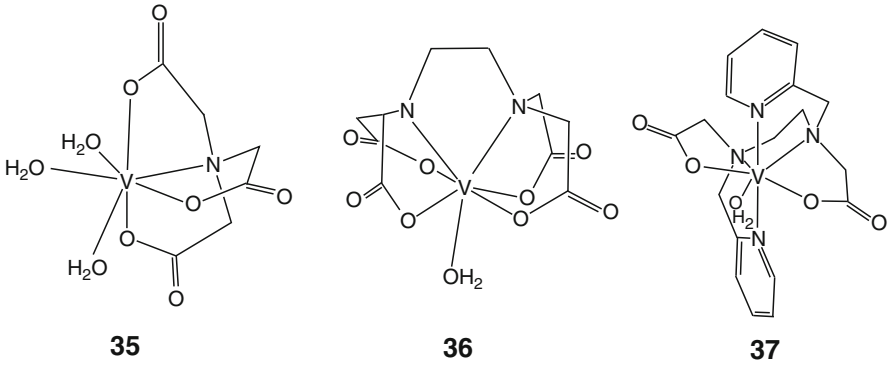

Fig. 1.17 Heptacoordinate complexes with tetradentate and hexadentate ligands

Among the three ideal geometries of seven-coordination, the capped octahedron and capped trigonal prism are rare. Nonetheless, these geometries as well as the pentagonal bipyramidal geometry, though distorted to some extent, have been realized for vanadium(III) complexes using aminopolycarboxylates and its analog with a pyridyl functionality (Fig. 1.17). The geometry of compound **35**, $[V(III)(OH_2)_3(nta)]$ (nta = nitrilotriacetate) [46] can best be described as a capped octahedron, with the amino nitrogen occupying the capping position, whereas compound **36**, $[V(III)(edta)(H_2O)]^-$ [47] has been shown to adopt a capped trigonal prism with the water molecule occupying the capping position. A 4:3 piano stool or tetragonal base-trigonal base geometry has been proposed as an alternative description for the geometry of **36**. $[V(III)(hedtra)(H_2O)]^-$ (hedtra = *N*-hydroxyethyl-*N,N′,N′*-triacetate) [48] and $[V(III)(Hedta)(H_2O)]$ [49] have been found to adopt a structure similar to that of **36**. An edta-like hexadentate ligand, H_2bpedda, in which the two acetate groups of edta were substituted by two pyridyl methyl groups, was prepared. This ligand also gives the heptacoordinate vanadium(III) complex **37**, $[V(III)(bpedda)(H_2O)]^+$ of which the structure is different from that of the edta complex and has been described as a distorted pentagonal bipyramid [50]. The reason why such tetra- and hexadentate ligands afford the heptacoordinate vanadium(III) complexes has been explained; these ligands would be too small to encircle the vanadium(III) ion, leaving an additional coordination site for the seventh ligand [51].

As shown above, the geometries of vanadium(III) complexes are flexible, depending on the ligand structure and functional groups. This flexibility may be an important property for metal ions in biological systems. An interesting example illustrating the flexibility in coordination mode of vanadium(III) is presented in Fig. 1.18. Compounds **38**, $[V(III)_2(dpot)(m\text{-hydroxybenzoato})(H_2O)]$ (H_5dpot = 2-hydroxy-1,3-diaminopropane-*N,N,N′,N′*-tetraacetic acid) [52] and **39**, $[V(III)_2(benzoate)(OH)(tphpn)(H_2O)_2]^{3-}$ (Htphpn = *N,N,N′,N′*-tetrakis(2-pyridylmethyl)-2-hydroxy-propane-1,3-diamine) [53] both contain a heptadentate binucleating ligand with a bridging alkoxo group (dpot or tphpn) and a bridging carboxylate

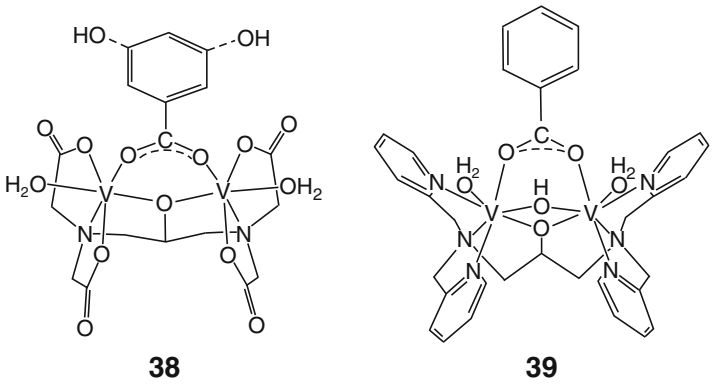

Fig. 1.18 Various structures of vanadium(III) complexes consist of closely related ligands

group (*m*-hydroxybenzoate or benzoate). The frameworks of dpot and tphpn are very similar, but the terminal coordinating groups of dpot are carboxylates, whereas those of tphpn are pyridyl groups. Interestingly, compound **38** adopts a normal hexacoordinate structure, whereas compound **39** forms a heptacoordinate structure with an additional hydroxo bridging group. This hydroxo group would be introduced to reduce the high positive charge not neutralized by the coordination of the neutral pyridyl groups. On the other hand, the negative charge of $dpot^{5-}$ in **38** would not require an additional negative charge to the complex.

Dinuclear units that contain the carboxylato and oxo (or hydroxo) bridges have been found in iron-containing biomolecules, such as hemerythrin, ribonucleotide reductase (RR), and methane monooxygenase (MMO) [2]. That vanadium(III) yields a similar dinuclear complex may indicate a potential role for vanadium(III) in biological systems.

1.2.5 Coordination Number 8

Ideal geometries for octacoordination are the dodecahedron and square antiprism. Although vanadium complexes with CN 8 are very rare, a natural vanadium(IV) compound isolated from *Amanita muscaria*, named amavadin, has been shown to adopt a unique octacoordinate structure. Figure 1.19, **40** illustrates the structure of amavadin [54]. In **40**, a fully deprotonated form of *N*-hydroxyimino-2,2′-diisopropionic acid (H_3hidpa) coordinates to a bare vanadium(IV) center as a tetradentate ligand through three O and one N atoms. Although the eight donor atoms coordinate to the vanadium(IV), the geometry of this compound would better be described as a special case of octahedron if the side-on coordination of the NO group is regarded to occupy one coordination site of the octahedron. The monoanionic vanadium(V) compound with hidpa, $[V(V)(hidpa)_2]^-$ [55] and the

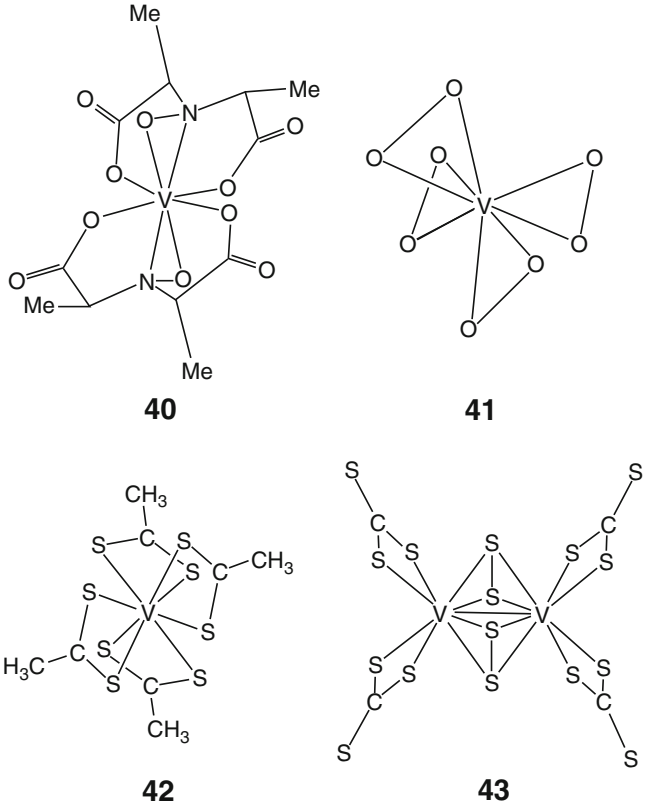

Fig. 1.19 Octacoordinate vanadium complexes

model compound with *N*-hydroxyiminodiacetatic acid (H_3hida), $[V(IV)(hida)_2]^{2-}$ [56] adopt almost the same structure as amavadin. The structures of these compounds are rare examples of bare vanadium(IV) and –(V) complexes and they contributed very much to determining the structure of amavadin.

The tetraperoxovanadium(V) complex, $[V(V)(O_2)_4]^{3-}$ (**41**) is the complex with the highest number of peroxides among structurally well-characterized peroxovanadium(V) complexes and it adopts a dodecahedral structure [57]. Dithiocarboxylate yields a dodecahedral vanadium complex, **42**, [V(IV)(dithioacetato)$_4$] [58, 59]. Dithiobenzoate and phenyldithioacetate [60] also give vanadium(IV) complexes with coordination geometry similar to that of **42**. Another type of octacoordinate vanadium complex surrounded by sulfur donors, **43**, $[V(IV)_2(\mu-\eta^2-S_2)_2(CS_3)_4]^{4-}$ [61] was prepared and characterized. Compound **43** and its analog, $[V(IV)_2(\mu-\eta^2-S_2)_2(S_2CCH_3)_4]$ [62] have a direct bond between the two vanadium centers. If this V-V bond is counted into the coordination number, the vanadium center can be regarded as a nonacoordinate complex and its geometry can be described as a tri capped trigonal prism.

1.3 Redox Behaviors of Vanadium

1.3.1 Oxidation States of Vanadium

Vanadium is known as a redox-active element that assumes oxidation states from −1 to +5 [63, 64]. Compounds with oxidation states of +2 or higher are more common. Although vanadium compounds with an oxidation number less than +2 may not be relevant to biological systems, as mentioned in the previous section, we will treat them in this chapter to present a complete view of the redox chemistry of vanadium.

As shown in the following sections, the redox potentials of vanadium complexes are largely affected by the ligands. Thus, V(III)-H_2O species, V(IV)-oxo species, and V(V)-dioxo species can exist in the same solution when the ligands are selected appropriately, indicating that the redox reaction can proceed on ligand substitution. The presence of the oxo ligand in the coordination sphere is especially important in the case of V(IV) and V(V) species. The dianionic oxo ligand stabilizes the vanadium ions in higher oxidation states by its strong electron-donating ability. Additionally, acid-base equilibrium between the oxo and the aqua ligand plays an important role in the redox behavior of the vanadium center. As shown by the Pourbaix diagram (Fig. 1.20), the redox behavior of vanadium ions in aqueous

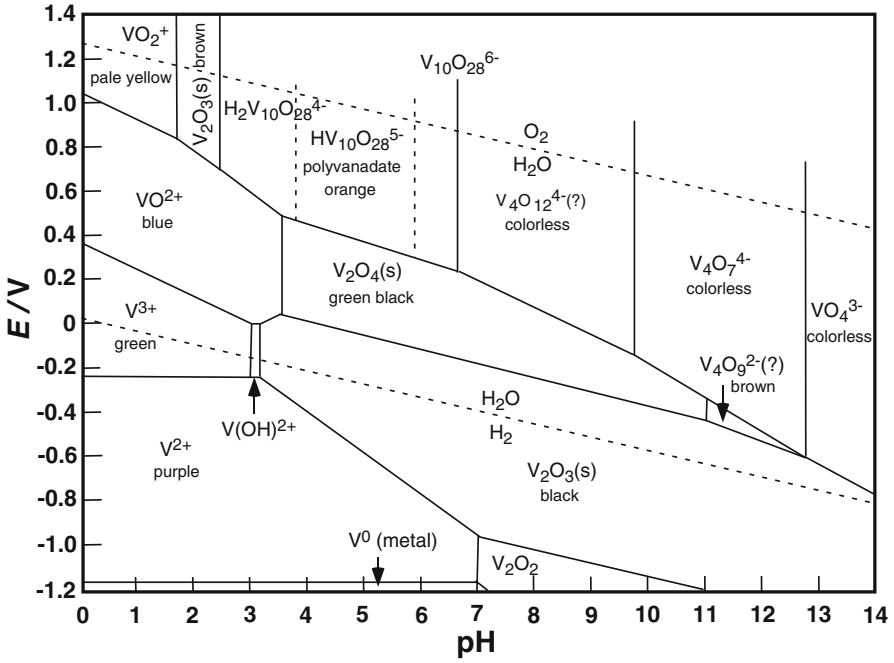

Fig. 1.20 Pourbaix diagram of vanadium species

solution is highly affected by pH. At around 0 V, the V(III) species exist under acidic conditions, whereas the V(IV) and V(V) species are dominant under neutral or basic conditions, reflecting the protonation/deprotonation of oxo and aqua ligands. In the following sections, the electrochemical and chemical redox behaviors of vanadium complexes will be described by focusing primarily on the mononuclear complexes studied by using electrochemical methods to show the characteristics of vanadium ions in each oxidation state.

1.3.2 Redox Properties of Each Oxidation State

1.3.2.1 Oxidation States Lower Than +I

Most vanadium complexes in lower oxidation states are organometallic ones where the large electron density on the metal center is stabilized by a π-acidic ligand, such as carbonyl or arenes. One of the interesting vanadium(−I) complexes is $[V(CO)_6]^-$, which is reversibly oxidized to the neutral complex at –0.54 V versus Fc/Fc^+ [65]. Several bis(arene) vanadium complexes are known to undergo reversible redox processes among −1, 0, and +1 charges. The redox potentials of bis(benzene)vanadium are −2.71 and −0.35 V versus SCE for −/0 and 0/+, respectively [66]. The redox potentials of this type of complex can be controlled by the arene and its substitution groups [64]. As indicated by their redox potentials, vanadium complexes in lower oxidation states are generally oxidized readily under ambient conditions.

1.3.2.2 Oxidation State of +II

For the +2 oxidation state, an aqua complex cation $[V(H_2O)_6]^{2+}$ is known, the oxidation potential of which is −0.26 V versus NHE under strongly acidic conditions, demonstrating its strong reducing ability [63]. $[V(H_2O)_6]^{2+}$ is also susceptible to oxygen even in the solid state, especially when it has moisture. An octahedral V(II) complex with two 2,2′:6″,2″-terpyridine (trpy) has also been reported [67]. It is reversibly oxidized to V(III) species at 0.46 V versus NHE, showing the considerable stability of $[V(II)(trpy)_2]^{2+}$ under ambient conditions. The difference in redox potentials between the hexa aqua complex and the terpyridine complex are ascribed to the better π-acidity of the trpy ligand than the aqua ligand. The related pyridine (py) complexes $[V(II)X_2(py)_4]$ (X = Cl, Br, I) are also oxidized at similar potentials [68]. Differences in donating ability among halogeno ligands are reflected in the redox potentials of −0.06, 0.15, and 0.27 V for chloro, bromo, and iodo complexes, respectively. Vanadocene, $[V(Cp)_2]$ is another typical V(II) complex, being reduced to V(I) species at −2.74 V versus SCE and oxidized to V(III) species at −0.55 V in THF [69]. The more negative oxidation potential for the +II/+III process indicates that the V(II) center in vanadocene is more electron-rich than that in $[V(II)(trpy)_2]^{2+}$.

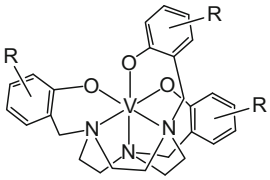

44

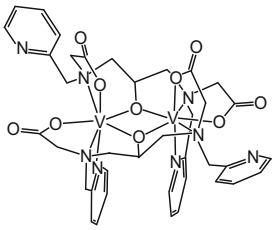

45

Fig. 1.21 Vanadium(III) complexes showing reversible oxidation

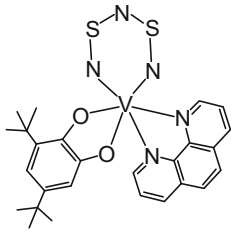

46

Fig. 1.22 Vanadium(V) complex with $N_3S_2^-$ ligand

1.3.2.3 Oxidation State of +III

As mentioned in the previous section, $[V(II)(H_2O)_6]^{2+}$ is oxidized to $[V(III)(H_2O)_6]^{3+}$ at −0.26 V versus NHE, whereas the edta complex $[V(III)(edta)(H_2O)]^-$ is reduced to $[V(II)(edta)(H_2O)]^{2-}$ at a more negative potential of −1.01 V versus NHE [70]. Related V(III) complexes with tetra(carboxylate)diamine ligands display similar reduction potentials, demonstrating the considerable electron donating nature of carboxylate groups. The oxidation process of V(III) to V(IV) is not simple when the complex has aqua ligands due to their deprotonation upon oxidation. The V(III) aqua ion $[V(III)(H_2O)_6]^{3+}$ is oxidized at 0.34 V into the oxovanadium(IV) species, $[V(IV)O(H_2O)_6]^{2+}$ at pH = 0, which manifests that V(IV), a hard Lewis acid, requires strong donation from an aqua ligand, resulting the release of protons. On the other hand, rigid chelating ligands can stabilize the V(IV) and even V(V) centers without oxo ligands. The hexadentate ligand derived from triazacyclononane (tacn) by adding three pendent hydroxybenzyl arms has been used to produce an octahedral V(III) complex (Fig. 1.21, **44**) [71]. In this case, the complex shows reversible oxidation to the +4 and +5 states at −0.55 and 0.33 V versus Fc/Fc^+, respectively. An alcoholato bridged dinuclear V(III) complex with hpnbpda (H_3hpnbpda = *N,N′*-bis(2-pyridylmethyl)-2-hydorxy-1,3-propanediamine-*N,N′*-diacetic acid), where each V(III) adopts a hepta coordination environment with two chelating ligands (Fig. 1.22, **45**), shows reversible oxidations at 0.65 and 1.02 V versus Ag/AgCl, which corresponds to the redox process of V(III)V(III)/V(III)V(IV) and V(III)V(IV)/V(IV)V(IV) [52].

1.3.2.4 Oxidation States of +IV and +V

Vanadium ions in the +4 and +5 oxidation states widely adopt the oxo ligand(s), the redox behavior of which will be discussed separately in Sects. 1.3.3.1 and 1.3.3.2. Other than an oxo-ligand, anionic and/or strongly electron-donating ligands are known to stabilize V(IV) complexes. The tris(catecholate) complex (**19**) has been reported to show oxidation and reduction processes at −0.42 and −1.24 V versus Fc/Fc^+ [72]. A similar complex with mercaptophenolato, $[V(mp)_3]^{2-}$ is reversibly oxidized at −0.27 V and irreversibly reduced at $E_{pa} = -1.08$ V versus Ag/AgCl [73]. A dithiol complex $[V(mnt)_3]^{2-}$ (**18**, R = CN, mnt = maleonitriledithiolato) is also known to show an oxidation and reduction at 0.17 and −0.87 V versus Fc/Fc^+ [74]. On the other hand, the tris(acetylacetonato)vanadium(IV) complex $[V(IV)(acac)_3]^+$ is reduced to $[V(III)(acac)_3]^0$ at a more positive potential of 0.76 V versus SCE [75]. Thus, the electron-donating properties of the ligands are reflected by the redox potentials of V(IV) species.

Electrochemical studies on vanadium(V) complexes without the oxo ligand have been more limited, except for those produced by electrochemical oxidation. Without the oxo ligand, highly charged anionic ligands are required to stabilize a vanadium(V) ion. It has been reported that a vanadium(V) complex with $N_3S_2^{3-}$ $[V(N_3S_2)(dtbc)(phen)]$ (Fig. 1.22, **46**) (dtbc = 3,5-di-*t*-butylcatecholato) is reversibly reduced to the V(IV) complex at 0.37 V versus NHE [76].

1.3.3 Redox Behaviors of Vanadium Complexes with Oxo Ligands

Highly charged vanadium ions, such as V(IV) and V(V), being small hard ions, prefer the oxo ligand, O^{2-}, which provides lone pairs not only by σ donation, but also by π donation, to provide a V = O double bond. Donation from the oxo ligand is so prominent that the reduction potentials are almost comparable among dioxo-vanadium(V), oxo-vanadium(IV), and vanadium(III) complexes with the same ligand, in several cases. The redox behaviors of oxo-vanadium complexes tend to be complex in the presence of H^+ because the conversion of an oxo ligand to an aqua ligand often triggers further change in the coordination sphere by ligand substitution [77].

1.3.3.1 Oxovanadium(IV) Complexes

Vanadium(IV) complexes with an oxo ligand tend to assume square pyramidal coordination geometry with the oxo ligand at the apical position because of its strong *trans* influence. The reduction process of these complexes is usually irreversible and is observed at relatively negative potentials because of the preference of the resulting

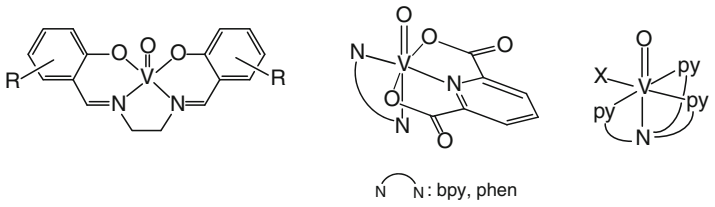

47 **48** **49**

Fig. 1.23 Oxovanadium(IV) complexes with salen (47), dicarboxypyridine (48) and tpa (49)

V(III) species for an octahedral coordination geometry, and because of the strong σ- and π-electron-donation from the oxo ligand. The acac complex $[V(IV)(O)(acac)_2]$ is irreversibly reduced to a V(III) species at $E_{pc} = -2.10$ V versus $Ag/AgClO_4$ in the presence of Hacac in an acetonitrile solution, whereas, under the same conditions, the V(III) acac complex, $[V(III)(acac)_3]$ is reversibly reduced at $E_{1/2} = -1.78$ V [78]. Similar behavior was observed in DMSO solution [75]. These results demonstrate that V(IV) = O species are more tolerant of reduction than V(III) species, reflecting the large stabilization of the V(IV) state by the presence of an oxo ligand.

The change in coordination geometry caused by protonation of the oxo ligand is also important in the redox chemistry of oxo vanadium(IV) complexes. The catechol complex $[V(IV)O(cat)_2]^-$ itself does not show a reversible reduction process, whereas, in the presence of excess catechol, it shows a reversible reduction at −0.72 V versus SCE [27]. Addition of catechol leads to the formation of H_2O and $[V(IV)(cat)_3]^{2-}$, which is reversibly reduced to $[V(III)(cat)_3]^{3-}$. In the case of the salen complex [VO(salen)] (Fig. 1.23, **47**), the proton-coupled redox behavior is more complicated. The reversible oxidation of [V(IV)O(salen)] to $[V(V)O(salen)]^+$ was observed at 0.55 V versus Ag/AgCl, and an irreversible reduction of [V(IV)O(salen)] was observed below −1.6 V in the absence of acid [79]. Under acidic conditions, the formation of $[V(III)(salen)]^+$ was observed by the reduction of [V(IV)O(salen)]. The reaction is formally represented as $[V(IV)O(salen)] + 2\ H^+ + e^- \rightarrow [V(III)(salen)]^+ + H_2O$. However, a detailed electrochemical study has indicated that this reaction actually proceeds via the reduction of dimeric species. The key reaction is the protonation of [V(IV)O(salen)], resulting in the formation of $[\{V(IV)(salen)\}_2(\mu\text{−}O)]^{2+}$, which leads to the more feasible reduction of vanadium centers [80].

On the other hand, several hexacoordinated oxovanadium(IV) complexes undergo reversible reductions to vanadium(III) complexes. The oxovanadium(IV) complex with dicarboxypyridine and bpy or phen (Fig. 1.23, **48**) is reversibly reduced at −1.08 V versus SCE in DMF [81]. Hexacoordinated oxovanadium complexes with glutathione derivatives also show reversible reduction at around −1.3 V versus NHE [82]. Thus, the reversibility of the reduction process of oxo V(IV) complexes is strongly affected by the coordination geometry.

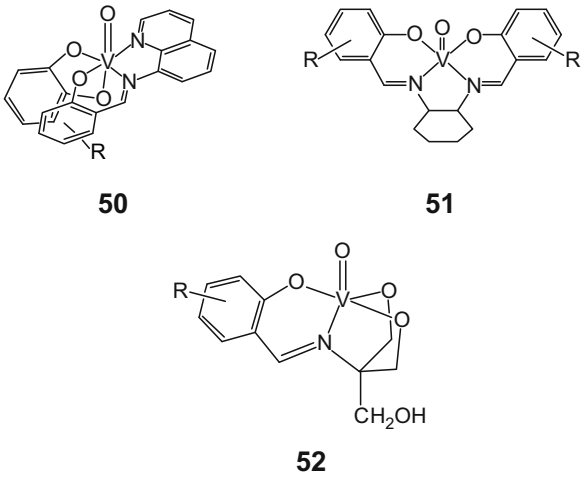

Fig. 1.24 Oxovanadium(V) complexes showing reversible reduction

The effect of protonation upon redox potential has been evaluated for the octahedral oxovanadium(IV) complex with the tpa ligand (Fig. 1.23, **49**) by varying the proton concentration. $[V(O)Cl(tpa)]^+$ was reversibly reduced at −1.59 V versus Fc/Fc^+, whereas the reduction potential of the corresponding $[V(H_2O)Cl(tpa)]^{3+}$ was estimated to be −0.59 V, indicating a 1 V positive shift of reduction potential by protonation [83].

1.3.3.2 Oxovanadium(V) Complexes

Most mono-oxovanadium(V) complexes undergo a reversible reduction process when the coordination geometry is intact during the redox processes. The hexacoordinated oxovanadium(V) complexes with catecholato and tridentate Schiff base ligands derived from aminoquinoline (Fig. 1.24, **50**) are reversibly reduced between −0.24 and −0.37 V [84]. Reversible reduction is also observed for the oxovanadium(V) complexes with tetradentate Schiff base ligands derived from cyclohexanediamine and salicyladehyde derivatives (Fig. 1.24, **51**). Although the oxo ligand and tetradentate Schiff base afford square pyramidal coordination geometry, octahedral coordination is accomplished by the ligation of the solvent molecule in solution, leading to reversible reduction processes of these complexes. Their redox potentials are observed in the range of −0.01 to 0.35 V and show a linear correlation between the reduction potentials and the Hammet constant of substitution groups on the salicylaldehyde moieties [85]. The pentacoordinated oxovanadium(V) complexes with the ligands derived from tris(hydroxylmethyl)aminomethane and salicylaldehyde derivatives (Fig. 1.24, **52**) also show reversible reduction to V(IV) complexes at −0.4 to −0.5 V versus Ag/AgCl [86].

Fig. 1.25
Dioxovanadium (V) complexes with tripodal ligands

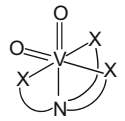

X: COO^-, py, NH_2, etc

53

Due to the high affinity of V(V) for the oxo ligand, dioxovanadium(V) complexes are also formed, which usually undergo irreversible reductions [83, 87, 88]. The reduction potential (E_{pc}) of the dioxovanadium(V) complex is not much different from that of the oxovanadium(IV) complex with the same ligand, indicating the strong electron-donating ability of oxo ligands [83, 87]. The irreversible reduction process should reflect the instability of dioxovanadium(IV) species where the basicity of the oxo ligand becomes strong enough to cause the protonation and successive ligand substitution reactions.

1.3.4 Chemical Redox Reactions of Vanadium Complexes

Vanadium complexes with high oxidation states are known to catalyze various oxidation reactions, such as the dehydrogenation of O-H and C-H bonds, oxygenation of aromatic compounds and sulfides, epoxidation, and oxidative coupling [89]. Recently, asymmetric oxidation reactions using complexes with chiral coordination environments have been developed [85, 90, 91]. Additionally, vanadium plays an important role in enzyme reactions. A characteristic, intriguing type of vanadium enzyme is the haloperoxidases, which catalyze the halogenation reaction using the halide and peroxo species. Generally, catalytic oxidations with vanadium complexes employ hydrogen peroxide or peroxo species as oxidants [92]. Thus, the redox reactions of peroxo species are at the center of the discussion of reaction mechanisms. In the catalytic cycles, vanadium complexes undergo complex redox reactions, including oxygen-transfer and hydrogen abstraction, as well as electron transfer.

Various synthetic models for haloperoxidases have been prepared, among which, the reaction mechanisms have been examined extensively using dioxovanadium(V) complexes with tripodal ligands (Fig. 1.25, **53**) [93]. Generally, the addition of acid accelerates the reaction rate, indicating activation of peroxo-vanadium species by protonation in the reaction. A simplified reaction mechanism is depicted in Fig. 1.26. The true reaction mechanism is more complicated because the oxidation of halide is oversimplified in this scheme, as well as the conversion of an oxo ligand to a peroxo ligand. Additionally, the reaction mechanism may be more complicated because several dioxovanadium(V) complexes have been reported to perform dehydrogenation reactions, to produce V(IV) species, under similar conditions. The dioxo- and oxoperoxovanadium(V) bpy complexes $[VO_2(bpy)_2]^+$ and

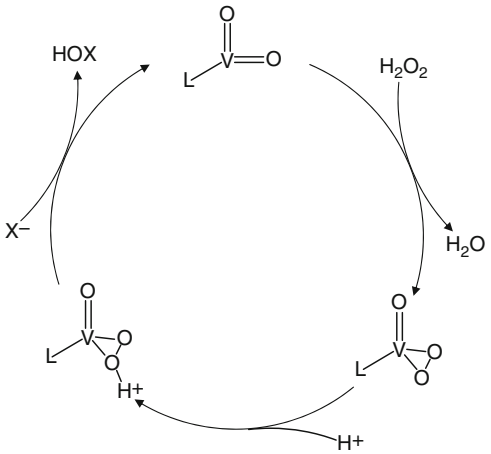

Fig. 1.26 Catalytic cycle of synthetic models of haloperoxidase

$[VO(O_2)(bpy)_2]^+$ produce $[V(IV)O(OH)(bpy)_2]^+$ in the reaction of *p*-hydroquinone by hydrogen abstraction, indicating the participation of vanadium(IV) complexes in the catalytic reactions [94]. Additionally, the dioxovanadium(V) complexes are known to undergo oxygen transfer reactions to triphenylphosphine, indicating that even V(III) species may be included in the reaction mechanisms in some cases. Clarification of such reaction mechanisms may enable the rational synthesis of effective vanadium catalysts.

References

1. Atkins P, Overton T, Rourke J, Weller M, Armstrong F (2006) Shriver & Atkins inorganic chemistry, 4th edn. Oxford University Press, Oxford
2. Fenton DE (1995) Biocoordination chemistry. Oxford University Press, Oxford
3. Elvington K, Gonzalez A, Pettersson L (1996) Speciation in vanadium bioinorganic systems. 2. An NMR, ESR, and potentiometric study of the aqueous H^+–vanadate–maltol system. Inorg Chem 35:3388–3393
4. Rehder D (2008) Bioinorganic vanadium chemistry. Wiley, Chichester
5. Choukroun R, Moumboko P, Chevalier S, Etienne M, Donnadieu B (1998) Cationic homoleptic vanadium(II), (IV), and (V) complexes arising from protonolysis of $[V(NEt)_4]$. Angew Chem Int Ed 37:3169–3172
6. Dubberley SR, Tyrell BR, Mountford P (2001) Tetrakis(dimethylamido)vanadium(IV). Acta Cryst C57:902–904
7. Song JI, Gambarotta S (1996) Preparation, characterization, and reactivity of a diamagnetic vanadium nitride. Chem Eur J 2:1258–1263
8. Komuro T, Matsuo T, Kawaguchi H, Tatsumi K (2005) Synthesis of a vanadium(III) tris(arylthiolato) complex and its reactions with azide and azo compounds: formation of a sulfenamide complex via cleavage of an azo N = N bond. Inorg Chem 44:175–177
9. Messerschmidt A, Wever R (1996) X-ray structure of a vanadium-containing enzyme: chloroperoxidase from the fungus *Curvularia inaequalis*. Proc Natl Acad Sci USA 93: 392–396

10. Messerschmidt A, Prade L, Wever R (1997) Implications for the catalytic mechanisms of the vanadium-containing enzyme chloroperoxidase from the fungus *Curvularia inaequalis* by X-ray structures of the native and peroxide form. Biol Chem 378:309–315
11. Addison AW, Rao TN, Reedijk J, Jacobus VR, Verschoor GC (1984) Synthesis, structure, and spectroscopic properties of copper(II) compounds containing nitrogen-sulfur donor ligands: the crystal and molecular structure of aqua[1,7-bis(N-methylbenzimidzol-2′-yl)-2,6-dithiaheptane]copper(II) perchlorate. J Chem Soc Dalton Trans 1349–1356
12. Baruah B, Rath SP, Chakravorty A (2004) A novel pentacoordinated dioxovanadium(V) salicylaldiminate: solvent specific crystallization of dimorphs with contrasting coordination geometries, ligand conformations and supramolecular architectures. Eur J Chem 9: 1873–1878
13. Cornman CR, Geiser-Bush KM, Rowley SP, Boyle PD (1997) Structural and electron paramagnetic resonance studies of the square pyramidal to trigonal bipyramidal distortion of vanadyl complexes containing sterically crowded Schiff base ligands. Inorg Chem 36:6401–6408
14. Wikete C, Wu P, Zampella G, De Giola L, Licini G, Rehder D (2007) Glycine-and sarcosine-based models of vanadium-dependent haloperoxidases in sulfoxygenation reactions. Inorg Chem 46:196–207
15. Santoni G, Licini G, Rehder D (2003) Catalysis of oxo transfer to prochiral sulfides by oxovanadium(V) compounds that model the active center of haloperoxidases. Chem Eur J 9:4700–4708
16. Hsu HF, Chu WC, Hung CH, Liao JH (2003) The first example of a seven-coordinate vanadium(III) thiolate complex containing the hydrazine molecule, an intermediate of nitrogen fixation. Inorg Chem 42:7369–7371
17. Groysman S, Goldberg I, Goldschmidt Z, Kol M (2005) Vanadium(III) and vanadium(V) amine tris(Phenolate) complexes. Inorg Chem 44:5073–5080
18. Aghabozorg H, Sadr-khanlou E (2007) 2,9-Dimethyl-1,10-phenanthrolinium dioxo(pyridine-2,6-dicarboxylato)vanadate(V) Monohydrate. Acta Cryst E63:m1753
19. Nakajima K, Tokida N, Kojima M, Fujita J (1992) Structures of two geometrical isomers of dioxo[(*S*)-*N*-salicylidene-3-aminopyrrolidine]vanadium(V). Bull Chem Soc Jpn 65:1725–1727
20. Santoni G, Rehder D (2003) Structural models for the reduced form of vanadate-dependent peroxidases: vanadyl complexes with bidentate chiral Schiff base ligands. J Inorg Biochem 98:758–764
21. Lorber C, Choukroun R, Donnadieu B (2003) Synthesis and crystal structure of unprecedented phosphine adducts of d^1-aryl imido–vanadium(IV) complexes. Inorg Chem 42:673–675
22. Stiefel EI, Eisenberg R, Rosenberg RC, Gray HB (1966) Characterization and electronic structures of six-coordinate trigonal-prismatic complexes. J Am Chem Soc 88:2956–2966
23. Kondo M, Minakoshi S, Iwata K, Shimizu T, Matsuzaka H, Kamigata N, Kitagawa S (1996) Crystal structure of a tris(dithiolene) vanadium(IV) complex having unprecedented D_{3h} symmetry. Chem Lett 25:489–490
24. Eisenberg R, Stiefel EI, Rosenberg RC, Gray HB (1966) Six-coordinate trigonal-prismatic complexes of first-row transition metals. J Am Chem Soc 88:2874–2876
25. Welch JH, Bereman RD, Singh P (1988) Synthesis and characterization of two vanadium complexes of the 1,2-dithiolene 5,6-dihydro-1,4-dithiin-2,3-dithiolate. Crystal structure of $[(C_4H_9)_4N][V(DDDT)_3]$. Inorg Chem 27:2862–2868
26. Stiefel EI, Dori Z, Gray HB (1967) Octahedral vs. trigonal-prismatic coordination. Structure of $(Me_4N)_2[V(mnt)_3]$. J Am Chem Soc 89:3353–3354
27. Cooper SR, Koh YB, Raymond KN (1982) Synthetic, structural, and physical studies of bis(triethylammonium) tris(catecholato)vanadate(IV), potassium bis(catecholato) oxovanadate(IV), and potassium tris(catecholato)vanadate(III). J Am Chem Soc 104:5092–5102
28. Branca M, Micera G, Dessi A, Sanna D, Raymond KN (1990) Formation and structure of the tris(catecholato)vanadate(IV) complex in aqueous solution. Inorg Chem 29:1586–1589

29. Cass ME, Gordon NR, Pierpont CG (1986) Catecholate and semiquinone complexes of vanadium. Factors that direct charge distribution in metal–quinone complexes. Inorg Chem 25:3962–3967
30. Kanamori K, Kusajima K, Yachi H, Suzuki H, Miyashita Y, Okamoto K (2007) Synthesis, x-ray structures, and solution properties of vanadium(III) and –(IV) complexes with *N*-(2-hydroxyphenyl)-*N*-(2-pyridylmethyl)amine. Bull Chem Soc Jpn 80:324–328
31. Morgenstern B, Steinhauser S, Hogetschweiler K, Garribba E, Micera G, Sanna D, Nagy L (2004) Complex formation of vanadium(IV) with 1,3,5-triamino-1,3,5-trideoxy-*cis*-inositol and related ligands. Inorg Chem 43:3116–3126
32. Drew RE, Einstein FWB (1972) The crystal structure of ammonium oxodiperoxoamminevanadate(V). Inorg Chem 11:1079–1083
33. Crans DC, Keramidas AD, Hoover-Litty H, Anderson OP, Miller MM, Lemoine LM, Pleasic-Williams S, Vandenberg M, Rossomando AJ, Sweet LJ (1997) Synthesis, structure, and biological activity of a new insulinomimetic peroxovanadium compound: bisperoxovanadium imidazole monoanion. J Am Chem Soc 119:5447–5448
34. Smatanová IK, Marek J, Švančárek P, Schwendt P (2000) Bis(tetra-n-butylammonium) bis[(mandelato)oxo(peroxo)vanadate(V)] mandelic acid solvate. Acta Cryst C56:154–155
35. (a) Towns RLR, Levenson RA (1972) Structure of the seven-coordinate cyano complex of vanadium(III). J Am Chem Soc 94:4345–4346. (b) Levenson RA, Towns RLR (1974) Crystal and molecular structure of potassium heptacyanovanadate(III) dihydrate. Inorg Chem 13: 105–109
36. Neumann R, Assael I (1989) Vanadium(V)/vanadium(III) redox couple in acidic organic media. Structure of a vanadium(III)-tetraethylene glycol pentagonal-bipyramidal complex $[[V(teg)(Br)_2]^+Br^-]$. J Am Chem Soc 111:8410–8413
37. Dutton JC, Fallon GD, Murray KS (1990) A macrocyclic binuclear vanadium(III) complex with di-μ-alkoxo bridging and pentacoordinate-bipyramidal metal co-ordination. X-ray crystal structure of $[V_2L(H_2O)_4][ClO_4]_4{\cdot}2H_2O$ (H_2L = 1,7,14,20-tetramethyl-2,6,15,19-tetraaza[7,7](2,6)-pyridinophane-4,7-diol). J Chem Soc Chem Commun 64–65
38. Stomberg R (1986) The crystal structure of potassium bis(oxalate)oxoperoxovanadate(V) hemihydrate, $K_3[VO(O_2)(C_2O_4)]{\cdot}½H_2O$, and potassium bis(oxalate)dioxovanadate(V) trihydrate, $K_3[VO_2(C_2O_4)_2]{\cdot}3H_2O$. Acta Chem Scand A40:168–176
39. Gyepes R, Pacigová S, Sivák M, Tatiersky J (2009) Experimental and computational evidence of solid-state anion–π and π–π interactions in $[VO(O_2)(L)(pa)]{\cdot}xH_2O$ complexes (L = picolinate, pyrazinate or quinolinate; pa = picolinamide). New J Chem 33:1515–1522
40. Szentivanyi H, Stomberg R (1983) The crystal structure of ammonium (2,2′-bipyridine) oxodiperoxovanadate(V) tetrahydrate, $NH_4[VO(O_2)_2(C_{10}H_8N_2)]{\cdot}4H_2O$, at –100°C. Acta Chem Scand A37:553–559
41. Castro SL, Martin JD, Christou G (1993) A new vanadium(V) persulfide complex: $(NEt_4)[VO(S_2)_2(bpy)]$. Inorg Chem 32:2978–2980
42. Al-Ani FT, Hughes DL, Pickett CJ (1988) Preparation, x-ray crystal structure, and properties of $[V(S_2)_2(terpy)]$: intramolecular coupling of the sulfide ligands of $[VS_4]^{3-}$. J Chem Soc Dalton Trans 1705–1707
43. Einstein FEB, Enwall E, Morris DM, Sutton D (1971) Crystal and molecular structure and vibrational spectra of the vanadium(V) oxide trinitrate–acetonitrile complex, $VO(NO_3)_3{\cdot}CH_3CN$. Inorg Chem 10:678–686
44. Kanamori K, Kameda E, Okamoto K (1996) Heptacoordinate vanadium(III) complexes containing a didentate sulfate ligand. X-ray structures of $[V_2(SO_4)_3\{N, N'$-bis(2-pyridylmethyl)-1,2-ethanediamine$\}_2]$ and $[V(SO_4)\{N, N, N', N'$-tetrakis(2-pyridylmethyl)-1,2-ethanediamine$\}]^+$ and their solution properties. Bull Chem Soc Jpn 69:2901–2909
45. Chatterjee M, Maji M, Ghosh S, Mak TCW (1998) Studies of V(III) complexes with selected α-N-heterocyclic carboxylato NO donor ligands: structure of a new seven-coordinated pentagonal bipyramidal complex containing picolinato ligands. J Chem Soc Dalton Trans 3641–3645
46. Okamoto K, Hidaka J, Fukagawa M, Kanamori K (1992) Structure of trisaqua (nitrilotriacetato)vanadium(III) tetrahydrate. Acta Cryst C48:1025–1027

47. Shimoi M, Saito Y, Ogino H (1991) Syntheses and crystal structures of seven-coordinate (ethylenediamine-*N, N, N′, N′*-tetraacetato)aquavanadate(III) complexes. Bull Chem Soc Jpn 64:2629–2634
48. Ogino H, Shimoi M, Saito Y (1989) Structural identification of the reactive vanadium(III) intermediate formed in the electron-transfer reactions of [*N′*-(2-hydroxyethyl)ethylenediamine-*N, N, N′*-triacetato]aquavanadium(III) complex ([V(hedtra)(H_2O)]) with halogenopentaamminecobalt(III) complex: x-ray crystal structure of [V(hedtra)(H_2O)]·$2H_2O$ and K[VO(hedtra)]·H_2O. Inorg Chem 28:3596–3600
49. Miyoshi K, Wang J, Mizuta T (1995) An x-ray crystallographic study on the molecular structures of seven-coordinate (ethylenediamine-*N, N, N′*-triacetato-*N′*-acetic acid)(aqua)-titanium(III) and -vanadium(III), [Ti^{III}(hedta)(H_2O)]·H_2O and [V^{III}(hedta)(H_2O)]·H_2O. Inorg Chim Acta 228:165–172
50. Kanamori K, Kyotoh A, Fujimoto K, Nagata K, Suzuki H, Okamoto K (2001) Syntheses, structures, and properties of vanadium(III) complexes with the hexadentate ligand, tetramethylenediamine-*N, N, N′, N′*-tetraacetate, *N, N′*-bis(2-pyridylmethyl)-1,2-ethanediamine-*N, N′*-diacetate, and *N, N′*-bis(2-pyridylmethyl)-1,3-propanediamine-*N, N′*-diacetate. Bull Chem Soc Jpn 74:2113–2118
51. Kanamori K, Ino K, Maeda H, Miyazaki K, Fukagawa M, Kumada J, Eguchi T, Okamoto K (1994) Relationship between oxo-bridged dimer formation and structure of vanadium(III) amino polycarboxylates. Inorg Chem 33:5547–5554
52. Kanamori K, Yamamoto K, Okayasu T, Matsui N, Okamoto K, Mori W (1997) Structure and magnetic properties of dinuclear vanadium(III) complexes with alkoxo bridge. Bull Chem Soc Jpn 70:3031–3040
53. Kanamori K, Okayasu T, Okamoto K (1995) Preparation and structure of dinuclear vanadium(III) complex triply bridged by three different groups. Chem Lett 24:105–106
54. Berry RE, Armstrong EM, Beddoes RL, Collison D, Ertok SN, Helliwell M, Garner CD (1999) The structural characterization of amavadin. Angew Chem Int Ed 38:795–797
55. Armstrong EM, Beddoes RL, Calviou LJ, Charnock JM, Collison D, Ertok N, Naismith JH, Garner CD (1993) The chemical nature of amavadin. J Am Chem Soc 115:807–808
56. Carrond MAAFdeCT, Duarte MTLS, Costa Pessoa J, Silva JAL, Fraústo da Silva JJR, Candida M, Vaz TA, Vilas-Boas LF (1988) Bis(*N*-hydroxyiminodiacetate)vanadate(IV), a synthetic model of amavadin. J Chem Soc Chem Commun 17:1158–1159
57. Won TJ, Barnes CL, Schlemper EO, Thompson RC (1995) Two crystal structures featuring the tetraperoxovanadate(V) anion and a brief reinvestigation of peroxovanadate equilibria in neutral and basic solution. Inorg Chem 34:4499–4503
58. Piovesana O, Cappuccilli G (1972) Eight-coordination. I. Dodecahedral vanadium(IV) complexes with sulfur-chelating ligands. Inorg Chem 11:1543–1550
59. Fanfani L, Nunzi A, Zanazzi PF, Zanzari AR (1972) The crystal structure of tetrakis(dithioacetato)vanadium(IV). Acta Cryst B28:1298–1302
60. Bonamico M, Dessy G, Fares V, Scaramuzza L (1974) Structural studies of eight-coordinate metal complexes. Part I. Crystal and molecular structures of tetrakis (phenylthioacetato)vanadium(IV) and tetrakis(dithiobenzoato)vanadium(IV). J Chem Soc Dalton Trans 1258–1263
61. Sendlinger SC, Nicholson JR, Lobkovsky EB, Hufman JC, Rehder D, Christou G (1993) Reactivity studies of mononuclear and dinuclear vanadium–sulfide–thiolate compounds. Inorg Chem 32:204–210
62. Duraj SA, Andras MT, Kibala PA (1990) Metal–metal bonds involving vanadium atoms. A facile synthesis of a novel divanadium tetrakis(dithioacetate) that contains two μ-η^2-S_2 bridges from bis(benzene)vanadium(0) and dithioacetic acid. Inorg Chem 29:1232–1234
63. Cotton FA, Wilkinson G, Bochmann M, Murillo C (1998) Advanced inorganic chemistry, 6th edn. Wiley, New York
64. Shaw MJ (2006) Vanadium electrochemistry. Encyclopedia of electrochemistry, vol 7a. Wiley, Weinheim, pp 357–381

65. Pampaloni G, Koelle U (1994) Chemical and electrochemical studies on metal carbonyl/cobaltocene Systems. J Organomet Chem 481:1–6
66. Elschenbroich C, Kroker J, Nowotny M, Behrendt A, Metz B, Harms K (1999) η^6-coordination of arsenine to titanium, vanadium, and chromium. Organometallics 18:1495–1503
67. Dobson JC (1989) Coordination chemistry and redox properties of polypyridyl complexes of vanadium(II). Inorg Chem 28:1310–1315
68. Ghosh P, Taube H, Hasegawa T, Kuroda R (1995) Vanadium(II) salts in pyridine and acetonitrile solvents. Inorg Chem 34:5761–5775
69. Holloway JDL, Geiger WE Jr (1979) Electron-transfer reactions of metallocenes. Influence of metal oxidation state on structure and reactivity. J Am Chem Soc 101:2038–2044
70. Ogino H, Nagata T, Ogino K (1989) Redox potentials and related thermodynamic parameters of (diaminopolycarboxylato)metal(III/II) redox couples. Inorg Chem 28:3656–3659
71. Sokolowski A, Adam B, Weyhermüller T, Kikuchi A, Hildenbrand K, Schnepf R, Hildebrandt P, Bill E, Wieghardt K (1997) Metal- vs. ligand-centered oxidations in phenolato−vanadium and− cobalt complexes: characterization of phenoxyl−cobalt(III) species. Inorg Chem 36:3702–3710
72. Hawkins CJ, Kabanos TA (1989) Synthesis and characterization of (catecholato)bis (β-diketonato)vanadium(IV) complexes. Inorg Chem 28:1084–1087
73. Klich PR, Daniher AT, Challen PR, McConville DB, Youngs WJ (1996) Vanadium(IV) complexes with mixed O, S donor ligands. Syntheses, structures, and properties of the anions tris(2-mercapto-4-methylphenolato)vanadate(IV) and bis(2-mercaptophenolato)oxovanadate(IV). Inorg Chem 35:347–356
74. Best SP, Ciniawsky SA, Humphrey DG (1996) Fourier-transform infrared study of short-lived highly reduced dithiolene complexes by potential-modulation spectroelectrochemical techniques. J Chem Soc Dalton Trans 2945–2949
75. Nawi MA, Riechel TL (1981) Electrochemical studies of vanadium(III) and vanadium(IV) acetylacetonate complexes in dimethylsulfoxide. Inorg Chem 20:1974–1978
76. Kabanos TA, Slawin AM, Williams DJ, Woollins JD (1990) The preparation and x-ray structure of $V(N_3S_2)$(dtbs)(phen)·$CHCl_3$ (dtbc = di-*t*-butylcatecholate, phen = phenanthroline). J Chem Soc Chem Commun 193–194
77. Michibata H, Kanamori K (1998) Selective accumulation of vanadium by ascidians from seawater. Advances in environmental science and technology, vol 30 (Vanadium in the environment, part 1), Wiley, NewYork, pp 217–249
78. Kitamura M, Yamashita K, Imai H (1976) Studies on the electrode processes of oxovanadium(IV). II. Electrolytic reduction of vanadyl acetylacetonate in acetonitrile solution at mercury electrode. Bull Chem Soc Jpn 49:97–100
79. Tsuchida E, Yamamoto K, Oyaizu K, Iwasaki N, Anson FC (1994) Electrochemical investigations of the complexes resulting from the acid-promoted deoxygenation and dimerization of (*N, N′*-ethylenebis(salicylideneaminato))oxovanadium(IV). Inorg Chem 33:1056–1063
80. Tsuchida E, Oyaizu K, Dewi EL, Imai T, Anson FC (1999) Catalysis of the electroreduction of O_2 to H_2O by vanadium–salen complexes in acidified dichloromethane. Inorg Chem 38: 3704–3708
81. Chatterjeea M, Ghosha S, Wub BM, Mak TCW (1998) A structural and electrochemical study of some oxovanadium(IV) heterochelate complexes. Polyhedron 17:1369–1374
82. Tasiopoulos AJ, Troganis AN, Evangelou A, Raptopoulou CP, Terzis A, Deligiannakis Y, Kabanos TA (1999) Synthetic analogues for oxovanadium(IV)–glutathione interaction: an EPR, synthetic and structural study of oxovanadium(IV) compounds with sulfhydryl-containing pseudopeptides and dipeptides. Chem Eur J 5:910–920
83. Tajika Y, Tsuge K, Sasaki Y (2005) Mononuclear oxovanadium complexes of tris(2-pyridylmethyl)amine. Dalton Trans 1438–1447
84. Asgedom G, Sreedhara A, Rao C, Kolehmainen E (1996) Monooxovanadium(V) mixed ligand complexes of Schiff bases and catecholates: synthesis, spectral and electrochemical characterization. Polyhedron 15:3731–3739

85. Nakajima K, Kojima K, Kojima M, Fujita J (1990) Preparation and characterization of optically active Schiff base-oxovanadium(IV) and -oxovanadium(V) complexes and catalytic properties of these complexes on asymmetric oxidation of sulfides into sulfoxides with organic hydroperoxides. Bull Chem Soc Jpn 63:2620–2630
86. Asgedom G, Sreedhara A, Rao C (1995) Oxovanadium(V) Schiff base complexes of trishydroxymethylaminomethane with salicylaldehyde and its derivatives: synthesis, characterization and redox reactivity. Polyhedron 14:1873–1879
87. Ghosh S, Nanda KK, Addison AW, Butcher RJ (2002) Mononuclear and mixed-valence binuclear oxovanadium complexes with benzimidazole-derived chelating agents. Inorg Chem 41: 2243–2249
88. Maurya MR, Kumar A, Abid M, Azam A (2006) Dioxovanadium(V) and μ-oxo bis[oxovanadium(V)] complexes containing thiosemicarbazone based ONS donor set and their antiamoebic activity. Inorg Chim Acta 359:2439–2447
89. Hirao T (1997) Vanadium in modern organic synthesis. Chem Rev 97:2707–2722
90. Bolm C, Bienewald F (1996) Asymmetric sulfide oxidation with vanadium catalysts and H_2O_2. Angew Chem Int Ed Engl 34:2640–2642
91. Takizawa S, Katayama T, Sasai H (2008) Dinuclear chiral vanadium catalysts for oxidative coupling of 2-naphthols via a dual activation mechanism. Chem Commun 35:4113–4122
92. Conte V, Floris B (2010) Vanadium catalyzed oxidation with hydrogen peroxide. Inorg Chim Acta 363:1935–1946
93. Pecoraro VL, Slebondnic C, Hamstra B (1998) Synthetic models for vanadium haloperoxidases. ACS symposium series, 711(Vanadium Compounds):157–167
94. Waidmann CR, DiPasquale AG, Mayer JM (2010) Synthesis and reactivity of oxo-peroxovanadium(V) bipyridine compounds. Inorg Chem 49:2383–2391

Part II
Hyper-Accumulators of Vanadium

Chapter 2
Amavadine, a Vanadium Compound in Amanita Fungi

José A.L. da Silva, João J.R. Fraústo da Silva, and Armando J.L. Pombeiro

Abstract This chapter is concerned with amavadine (also spelled as amavadin), a natural vanadium complex without the V=O bond, present in the fungus *Amanita muscaria* (L.:Fr.) Hook, which concentrates high levels of that metal (a capacity that is also known for a few other close *Amanita* fungi). The isolation, chemical synthesis and characterization of amavadine are reviewed, but its biological function remains unknown. However, the high stability constant of the complex, its redox behavior and ability to mediate the oxidation of some biological substrates support the possibility of a particular role (eventually concerning an enzyme) in the fungi, usually performed by other biomolecules, and biological functions of amavadine are suggested. The application of amavadine as a catalyst in chemical synthesis has been tested for some substrates, although under no biological conditions, and carboxylic acids, alcohols, ketones and halogenated compounds are obtained from oxidations of hydrocarbons catalyzed by very close models or a racemic mixture containing amavadine.

Keywords Amavadine • Amanita fungi • Catalase activity • Peroxidase activity • Oxidation of alkanes • Oxidation of thiols • Redox behavior • Catalysis • Electrocatalysis • Non-oxo vanadium(IV) complexes • Vanadium accumulation

2.1 Introduction

The unusual concentration of vanadium in living organisms was firstly reported 100 years ago in ascidians [1], but the nature of components where this metal occurs and their functions in some life forms (bacteria and eukaryotes) remained

J.A.L. da Silva (✉) • J.J.R. Fraústo da Silva • A.J.L. Pombeiro (✉)
Centro de Química Estrutural, Complexo I, Instituto Superior Técnico,
Technical University of Lisbon, Av. Rovisco Pais, Lisbon 1049-001, Portugal
e-mail: pcd1950@ist.utl.pt; pcd1950@ist.utl.pt; pombeiro@ist.utl.pt

H. Michibata (ed.), *Vanadium: Biochemical and Molecular Biological Approaches*,
DOI 10.1007/978-94-007-0913-3_2, © Springer Science+Business Media B.V. 2012

Fig. 2.1 *Amanita muscaria* collected at Melides (Portugal) (Courtesy from M. Moura)

unknown for a long time and possible applications of vanadium-biomolecules and their models are a matter of current interest.

Amavadine is a particular vanadium complex detected in a specific fungus named *Amanita muscaria* (L.:Fr.) Hook., see Fig. 2.1. The name *muscaria* derived from the word *musca*, fly in latin; this fungus is well-known as fly-agaric (it was used as an insecticide). The *A. muscaria* is widespread and a wind-dispersed ectomycorrhizal fungus with several distinct phylogenetic species. It was native from northern hemisphere in the temperate and boreal regions and is found in many countries of the southern hemisphere where it was introduced accidentally. Commonly is a symbiont with pine plantations, but is a host-generalist and occurs in association with various deciduous and coniferous trees [2].

The present review follows two others published on this specific subject. The first, as a paper, in 1989, was from one of us [3] and 6 years later, a chapter [4] appeared in a book on the bioinorganic chemistry of vanadium.

In the current text the main aspects to be commented concern the following topics: the accumulation of vanadium by some *Amanita* fungi, isolation and characterization of amavadine, its possible role and potential association with other biological elements or compounds and its applications in chemical synthesis of important industrial products, what has already generated some patents, such as [5].

The story of amavadine started in 1931 [6] found a remarkable accumulation of vanadium (120 ppm dry weight) in *A. muscaria*. Twelve years later [7] expanded Ter Meulen's surveys to various types of fungi, mostly from the genus *Amanita*, and concluded that *A. muscaria* was really exceptional among all the samples investigated due to the fact that its vanadium content could exceed 400 times the value normally detected in other species of the same genus. In a subsequent work it was shown that *A. muscaria* is not unique and high contents of vanadium were also

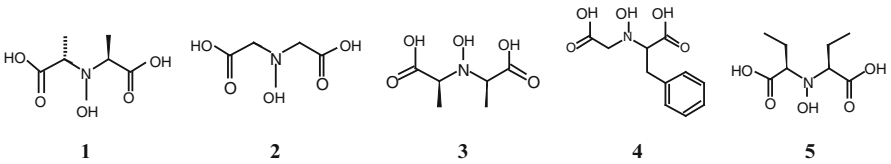

1 **2** **3** **4** **5**

Fig. 2.2 Amavadine ligand (**1**) and related ones

found in a few other *Amanita* (this genus has about 600 different species), *i.e.* the related *Amanita regalis* (Fr.:Fr.) Mich. [8] (or *A. muscaria* var. *umbrina* Fr. [9]), as well as in *Amanita velatipes* Atkinson [8, 10] or *Amanita gemmata* f. *amici* (Gill.) Gill., very close to *A. pantherina* (DC.:Fr.) Sécr. or to *A. muscaria* (L.:Fr.) Hook. [9].

The analyses of 22 chemical elements in 8 different species of *Amanita*, including the *A. muscaria*, revealed an unusual variation in composition of some elements, but mainly of vanadium [11]. The contents of this metal are similar in caps and stalks but its distribution is not homogeneous in the whole fruiting body, with usually has the highest concentration in the bulb [3, 12]. However, in environments richer in vanadium, an increase in this metal is apparently induced in *A. muscaria* specimens [12].

2.2 Isolation and Characterization of Amavadine from *Amanita muscaria* Fungus

Once ascertained the accumulation of vanadium in this fungus species, the following stage to appreciate the role of this metal in *A. muscaria* was the isolation and characterization of the biological compound. In 1972 [13], it was extracted with methanol from fresh samples of *A. muscaria* a vanadium containing compound which it was purified by different chromatographic procedures. These authors named that compound by *amavadine*, which was characterized by its stability up to 220°C (decomposition without melting point), using UV, IR and EPR spectroscopies, molecular weight and elemental composition. The EPR spectrum indicated the presence of vanadium in the oxidation state four and the analyses pointed to its natural ligand being the (S,S)-*N*-hydroxyimino-(2,2′)-dipropionic acid (**1**), see Fig. 2.2, (S,S-H_3HIDPA) [13, 14].

2.3 Synthetic Approaches to the Ligand, Its Models, the Complex Amavadine and Some Related Compounds

In 1973 [14] the ligand (in the protonated form), *N*-hydroxyimino-(2,2′)-dipropionic acid (**1**), was synthesized by reacting *N*-hydroxylamine with 2-bromoproprionic acid at basic pH. The obtained compound was converted to the acid form using

cationic chromatography. In 1986 [15] the same reaction was carried out at neutral pH and the ligand was precipitated by addition of a zinc acetate aqueous solution at pH 4 before its purification by cationic chromatography. The above two authors [16] proposed a procedure to isolate the ligand present in natural amavadine from the isomers resulting of the synthetic process, using chromatographic techniques and described in the same paper the preparation of the 2:1 vanadium(IV) complex by addition of a vanadyl [oxovanadium(IV) ion VO^{2+}] salt to the ligand in aqueous solution.

More recently, in 2005 [17], it was reported the first enantioselective synthetic approach of amavadine. The key-step is the synthesis of triflates (*trifluoromethane sulfonates*) of R-lactic acid ester followed by addition of hydroxylamine at very low temperatures. The last steps to obtain the ligand and the complex are similar to those used previously [15, 16].

Some model complexes of amavadine have been prepared, namely with the ligands (deprotonated forms) derived from *N*-hydroxyiminodiacetic acid (**2**) (H_3HIDA) [18], *meso-N*-hydroxyimino-2,2′-dipropionic acid (**3**) (R,S-H_3HIDPA) [19], *meso-N*-hydroxyimino-2,2′-dibutyric acid (R,S-H_3HIDBA) [20], or containing either a benzyl (**4**), a phenyl or an ethyl (**5**) instead the methyl group of the amavadine ligand, monoesters of the *N*-hydroxyimino-2,2′-dipropionic acid and three *N*-alkylated *N*-hydroxy amino acids [21], see Fig. 2.2.

2.4 Structural Characteristics of Amavadine

The structure of amavadine proposed initially in 1986 was a normal 1:2 complex of oxovanadium(IV) with 2,2′-(hydroxyimino)dipropionate, an hypothesis supported by a band at 980 cm^{-1} in the IR spectrum [16].

In 1984 [22], a comparison of the EPR spectra of fragments of frozen *A. muscaria* samples with those of the 2:1 oxovanadium(IV) complexes with some common amino acids (L-alanine, serine and cysteine) showed that these complexes were not appropriate amavadine models. Additionally, these authors observed that the amavadine was present in every part of the fungus and the parameters g_z, $g_{x,y}$, A_z and $A_{x,y}$ obtained from the EPR spectrum revealed that the natural complex had a distinct vanadium environment when compared with typical oxovanadium(IV) compounds.

An equivalent observation concerning the accurate models of amavadine had also been described in the studies [18, 23–25] of the oxovanadium(IV) complexes of polyaminocarboxylates ligands. The logarithms of the stability constant of the vanadium(IV) complexes with H_3HIDPA and H_3HIDA derived ligands (1:2) are 23.4 and 21.9 respectively, values unusual for this metal with the common polyaminocarboxylates ligands, as well as oddly higher than those of the complexes of other transition metals with the ligand of amavadine or its model with the H_3HIDA derived ligand. As a result of these discrepancies, the presence of the oxovanadium(IV) in amavadine became more and more doubtful and the structure initially proposed for this complex was considered inadequate.

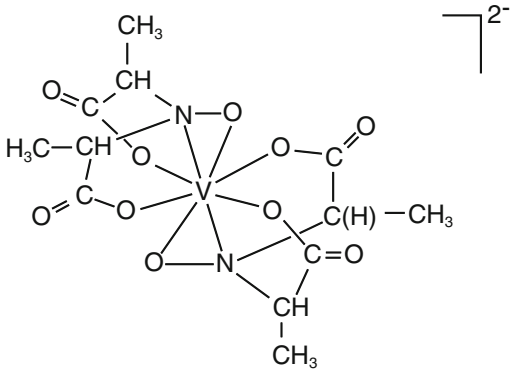

Fig. 2.3 Molecular structure of the amavadine complex

Alternatively, an unusual octa-coordinate structure with a bare vanadium(IV) complexed by two ligands was found out in 1987 [25] and 1988 [26], with the metal in a coordination environment constituted by two nitrogen and six oxygen donor atoms including two deprotonated hydroxyl groups of the hydroxyimino moieties of each ligand with the oxygen atom directly bound to the metal center. In this type of structure, supported by large-angle X-ray scattering (LAFS) experiments, the shortest V-O distance in the complex is longer than the usual length in an oxovanadium(IV) bond [25]. These results were independently confirmed on the basis of the X-ray crystal structure determination of the amavadine model complex with V(IV) coordinated by the synthetic ligand H_3HIDA in the deprotonated form [26].

In 1993, it was synthesized the stereochemical equivalent of the amavadine natural ligand and determined the structure of its vanadium(V) complex [27]. The optical, CD and ^{1}H and ^{13}C NMR spectra of the reduced form (with V^{4+}) of this complex and of the natural amavadine confirmed the identity of both complexes [27].

The structure of natural amavadine disclosed by X-ray diffraction analysis is a non-oxo vanadium(IV) complex with the basic form of the S,S-H_3HIDPA ligand, see Fig. 2.3, with a coordination sphere equivalent to that previously reported [25, 26]. The amavadine and its adequate models are remarkable examples of first-row transition metal complexes with a high coordination number [28].

Additionally, complexes of the ligands (in deprotonated forms) H_3HIDA, H_3HIDPA and R,S-H_3HIDBA with some metal ions of the groups 4, 5 and 6 were synthesized and analyzed by X-ray diffraction [19, 20, 29–34]. The V(IV) complex with R,S-H_3HIDPA (also in a basic form) was also reported [19].

In the obtained structures, only if the metals are in oxidation state four or five the hydroxyl of the hydroxyimino groups occur ionized and their oxygen atoms coordinated to the metal with a coordination number eight or nine [19, 20, 29, 31–34]. However, the Cr^{3+} complex has an octahedral geometry without coordination to the metal of the oxygen atom belonging to the hydroxyl group which in this case remains in the protonated form [30]. Crystals adequate to the determination of the

structure of vanadium complexes with other model ligands had not been achieved. It was also confirmed [21] that the absence of hydroxyimino and two carboxylic groups in the ligands leads to air-unstable vanadium(IV) complexes.

The complex of vanadium in the oxidation state four with metoxyiminodiacetate, $CH_3ON(CH_2COO^-)$, a ligand with a metoxy group (-OCH_3) instead of the hydroxyl (-OH) of the amavadine model with $HIDA^{3-}$, is a common oxovanadium(IV) compound [35] and not a deoxygenated vanadium(IV) as it occurs in ligands with the hydroxyimino group. In 2004, it was indicated [28] that the ligands with hydroxyimino and two carboxylate groups have hard donor N and O atoms that are able to donate enough electron density (σ and π) to the metal ion to neutralize its positive charge and additionally stabilize the non-oxo hard acceptor center of V(IV).

Comparisons of structural aspects of amavadine with those of model complexes have shown relevant similarities, except regarding the chiral characteristic of the biological molecule. The natural complex contains five chirality centers, one at vanadium and four at carbon atoms, and exhibits a S stereochemistry [36].

The oxidation of natural amavadine by a Ce(IV) salt results on a vanadium(V) complex and its characterization by COSY, NOE, ^1H, ^{13}C-NMR and CD spectroscopies confirmed an almost equal mixture of the Δ- and Λ-isomers of $[V(S,S\text{-HIDPA})_2]^-$ in the natural compound [37]. The analyses of amavadine by ^{51}V NMR spectroscopy present isotropic chemicals shifts less shielded than in other vanadium complexes, what may be a result of the absence of the V=O bond or of the unusual metal coordination number. Molecular orbital calculations using the discrete-variational-Xalpha method show a close similarity between the metal center of the amavadine with vanadium(IV) and the complexes with the oxovanadium(IV) core. The comparable character of the frontier orbitals elucidates the resemblance of these two types of complexes, which may explain why, for many years, amavadine was mistakenly thought as containing a VO^{2+} center [38–41].

2.5 Redox Behavior of Amavadine

The complexes $[VL_2]^{2-}$ (L = $HIDPA^{3-}$ or $HIDA^{3-}$) in aqueous medium at pH 7 undergo by cyclic voltammetry a single-electron reversible oxidation at ca. 0.8 V *versus* the standard H^+/H_2 electrode (a value close to that of the O_2/H_2O system); the difference between the oxidation potentials of these complexes is less than 0.1 V [42–45]. The reversibility of the oxidation process indicates that it does not affect markedly the molecular structure of the complexes. They appear to present the highest self-exchange rate constant to oxidation and reduction cross-reactions of the tested vanadium complexes [46, 47].

Both complexes [42–45] act as mediators in the oxidation in aqueous medium of thiolic compounds with carboxylic or ester groups, some with biological significance such as the cysteine (unique codified amino acid with a thiol group) and glutathione (the most relevant endogenous antioxidant occurring in cells, with various participations in metabolic reactions). The electrocatalytic behavior of

Scheme 2.1
Michaelis-Menten type mechanism of the electrocatalytic oxidation of thiols mediated by amavadine (the ligand is absent for clearness) (Adapted from [45])

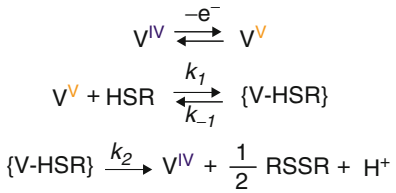

Scheme 2.2 Oxidation of hydrogen peroxide catalyzed by amavadine

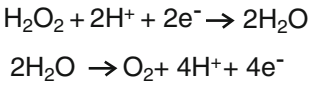

amavadine is not detected under similar conditions if the thiol group of cysteine is replaced by a hydroxyl or an alkylthioether, or if the carboxylic group is displaced by an amine, a methyl, a methylenethiol, a sulfonate or a hydroxide [44, 45]. However, the reactivity is maintained in the absence of the amino group of cysteine and the corresponding compound, mercaptoacetic acid, undergoes an electrocatalytic oxidation mediated by amavadine that is similar to that of the amino acid [44, 45].

Additionally, a Michaelis-Menten type of mechanism (usual for enzymes) was established by digital simulation methods of cyclic voltammetry [45] (Scheme 2.1) for the electrocatalytic oxidation reactions of these active thiolic compounds if mediated by an adequate model of amavadine, providing the synthesis of the corresponding disulfides. The mechanism involves a specific interaction between the substrate and the oxidized form of the mediator rather than a simple outer-sphere electron-transfer [45].

The electrochemical studies [42, 44] established also that the red vanadium(V) complexes formed upon oxidation of the corresponding bright blue compounds $[VL_2]^{2-}$ ($L = HIDPA^{3-}$ or $HIDA^{3-}$) are stable in some non-aqueous organic solvents, such as DMSO, DMF and acetone [44], but in aqueous solution they are unstable and revert to the air stable vanadium(IV) complexes [44]. In the presence of the biological oxidant H_2O_2, an acid solution (pH 2) of the blue complexes turns red, but reverts slowly to the original color and its final visible spectrum is analogous to the initial one [9]. The collection of the spectra discloses an isosbestic point that indicates a simple interconversion of the two oxidation states of the complex. This behavior can be repeated several times. At higher pH values (4.6 and 7) the initial and final spectra are also analogous but the addition of the equivalent amount of H_2O_2 originates a violet color solution resultant from partial oxidation of the V(IV) complex, which returns more rapidly to the original color than in more acidic solution [9]. In all the experiments, evolution of small gaseous bubbles rich in dioxygen was detected. These results suggest [9] a mechanism in which the V(IV) complex is first oxidized by H_2O_2 to the V(V) form, which then oxidizes water and returns quantitatively to the original V(IV) state (Scheme 2.2 for the overall catalyzed oxidation of hydrogen peroxide).

Apparently, the maximum efficiency of O_2 evolution is for the 1:1 complex/H_2O_2 ratio, but at less acidic pH the efficiency becomes more significant for higher proportions of H_2O_2 to $[V(HIDPA)_2]^{2-}$. It is noteworthy that slight acid soils correspond to the pH values of the *A. muscaria* habitats [2, 9].

2.6 Applications of Amavadine and Its Models on Catalysis

Amavadine models have been used as catalysts for the hydroxylation, oxygenation, peroxidative halogenation of alkanes and benzene [48], peroxidative oxygenation of benzene and mesitylene [49], and carboxylation of alkanes, both gaseous (methane [5, 50, 51], ethane [52] and propane [53]) and liquid (linear and cyclic C-5 and C-6) [54] ones. These reactions proceed under mild or moderate experimental conditions, to give the corresponding alcohols, ketones, organohalides or carboxylic acids (with one more carbon atom in the case of carboxylations), by involvement of radical mechanisms.

These reactions are not carried out in water, as the sole solvent, but the peroxidative oxidations are typically performed in mixed water/acetonitrile solution, using an aqueous H_2O_2 solution as oxidant (reaction 2.1).

$$\mathrm{RH} \xrightarrow[\text{Amavadine model}]{\mathrm{H_2O_2},\ \mathrm{H_2O/NCMe}} \mathrm{ROH} + \mathrm{R}_{(-\mathrm{H})} = \mathrm{O} \tag{2.1}$$

The best oxidant for the carboxylations is peroxydisulfate, $S_2O_8^{2-}$, and the reactions proceed in trifluoroacetic acid (TFA) at 80°C (reaction 2.2). However, this solvent can be replaced by the much more convenient and environmentally significant water/acetonitrile mixture, at a lower temperature (even 25°C) [55–58]. Nevertheless, the experimental constraints in these reactions concerning the oxidant used, the temperature values or the type of solvents, may not take place in natural biological environments of the fungi.

$$\mathrm{RH} + \mathrm{CO} \xrightarrow[\text{Amavadine model}]{\mathrm{S_2O_8^{2-}},\ \mathrm{TFA}} \mathrm{RCOOH} \tag{2.2}$$

The amavadine complex and its models, in the alkane carboxylation reactions, appear to be the most effective catalyst precursors so far reported for any alkane functionalization under mild/moderate conditions.

Additionally, the chiral properties of amavadine are expected to be valuable on asymmetric catalysis [17]. Preliminary results have appeared concerning the oxidation of thioanisole and alcohols, epoxidation of alcohols and cyanide addition to aldehydes, mediated by amavadine and its models [59].

2.7 Final Remarks – Possible Biological Role of Amavadine

The amounts of vanadium in the *A. muscaria* are determined by techniques which do not quantify the concentration of amavadine, neither its eventual occurrence with the metal in the oxidation state +5. These aspects still remain unknown and can be an obstacle to clarify the role of the amavadine in *A. muscaria*.

Generally, the metal accumulation involving specific ligands may concern (i) a protection against toxicity caused by the environmental conditions to the living organisms without mobility (what can be a benefit for passive defense against predators) or (ii) the synthesis of a transporter to a partner or to both species participating in symbiotic associations (*A. muscaria* is involved in this kind of partnership and its role could be supplying mineral salts and metabolites to host trees). Curiously, the fungus has the tendency to accumulate more significant levels of vanadium in the bulb [3, 12], the part of *A. muscaria* closer to its symbiotic partner, and the ligand of amavadine forms a very high stability constant complex with the vanadium(IV), what is a necessary condition for an efficient uptake of the metal from vanadium-poor environments [60]. Nevertheless, the anionic charge of the complex, in both four and five oxidation states of the metal, does not favor the crossing of the cellular membranes, in contrast with what occurs with another no-proteinaceous ligand, the siderophores, so important in uptake of iron.

The capacity of amavadine to occur in two different metal oxidation states supports other possible roles of this complex in *A. muscaria*. The minor structural differences between the oxidized and reduced forms of amavadine [27, 36, 44, 45] and the high value of the oxidation potential of this system can support a function of a specific system for electron-transfer, equivalent to blue copper-proteins (their values of redox potential are in some cases similar to that of the amavadine), as was previously suggested [60].

The ability of amavadine to act as an electron-transfer mediator in the oxidation of some biological thiols [42–45] can support a role of this biological molecule as a cofactor of oxidoreductases, a function mainly performed by other transition metals [61]. That electrocatalytic behavior of amavadine [45] and its reactivity toward H_2O_2 [9] suggest (see Scheme 2.3) that it can act either as a mediator for the oxidations of *e.g.* thiols, if present, or as a reducer of H_2O_2 and oxidant of the solvent, water, in fungi. The Michaelis-Menten type mechanism of the electrocatalytic oxidation of thiolic biological compounds mediated by amavadine also suggests that it can behave as an enzyme via an inner sphere process [45]. However, its action via an outer sphere type mechanism can not be ruled out in other oxidation reactions [62].

The negative charge of amavadine and its affinity to ammonium ion (compare with [26]) can suggest a strong interaction with amino acid residues with cationic side chains (such as lysine or arginine) or with the N-terminus of proteins, eventually interacting as a cofactor.

Peroxidases [9] are able to perform cross-linking of thiol groups in side chains of proteins in some higher plants as a defensive strategy in self-regeneration of

Scheme 2.3 Double behavior of amavadine (the ligand is absent for clearness) (Adapted from [9])

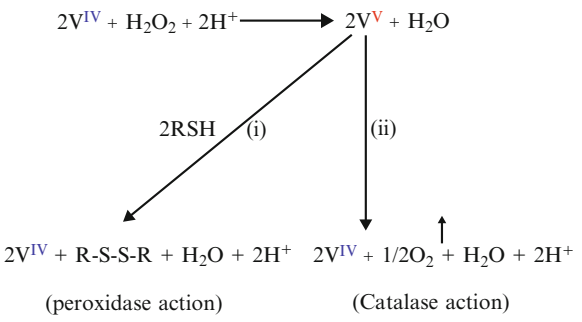

(i) Adequate biological thiol

(ii) In absence of biological thiols

damaged tissues [63], thus providing a supplementary protection against external microbial pathogens. This type of role is also admissible for amavadine [9].

Moreover, oxidative injury may be caused by excess of H_2O_2, and that effect can be deeply attenuated by the behavior of amavadine as a catalase (Scheme 2.3). This process, undertaken only by a simple complex, is not expected to be so efficient as in the case of an enzyme namely using ferric ion [64]. The relatively low level of iron in the fungus [65], usual metal in catalases and peroxidases [61], may justify the double behavior of amavadine presented in Scheme 2.3. Although these properties may be just coincidences, amavadine can have those roles, although not so efficiently as the iron based peroxidases and catalases [66], having into account its scarce occurrence in living organisms.

However, each ligated hydroxyimino group in amavadine is isoelectronic with the peroxo group and their possible analogies deserve to be further explored [50], namely concerning the reactivity of amavadine as a peroxidase [9] and a possible relationship with another relevant case of vanadium in biology, the V-haloperoxidases, occurring in several fungi and seaweeds [67]. The ability of amavadine and its models to catalyze the peroxidative halogenation of some organic substrates [48] needs also further investigation.

In 1993 we have suggested the possibility of the catecholic amino acid L-dopa (L-3,4-dihydroxyphenylalanine) behaving as a substrate of amavadine in an oxidative reaction [44] and it is known [68] the importance of that organic substrate in the biosynthesis of betalains (a pigment found in some plants which protects from destructive oxidative damage caused by radicals and occurs also in some higher fungi, such as *A. muscaria*). The enzymes involved in that synthesis were studied for this fungi, but the participation of amavadine as a biocatalyst in this reaction is not plausible since it is not active with similar compounds (such as catechol, gallic acid, phenol, thiophenol and tiron) [44].

Other issues, such as the following ones, also require answers to understand the role of amavadine. Why this complex occurs in *A. muscaria* or probably in a few other *Amanita* species? Which advantage gives that complex to these fungi

compared to others? The *A. muscaria* has a large habitat spreading and a relatively long standing life compared with other fungal species [69], and in its lamellae (where is present the genetic material necessary to the new generation of fungi) the concentration of vanadium appears to be relevant [70–72]. Is amavadine a contributor to these specificities?

The *A. muscaria*, including the var. *umbrina* (see above, Introduction), has a low iron amount [65] and concentrates significant levels of selenium [65, 71, 73] in contrast with other species in the *Amanita* genus. Iron has fundamental functions in biological systems, *e.g.* in electron-transfer and as a cofactor of enzymes (peroxidases, catalases) [61], which eventually can be performed by vanadium in specific cases. Selenium belongs to the same group of sulphur in the Periodic Table and its highest amounts in *A. muscaria* are in the lamellae [73], which also contain significant levels of vanadium. Are vanadium and selenium associated in the metabolism of this fungus? The analogies of the elements of the same periodic group suggest the possibility of selenium compounds, such as selenocysteine (the unique amino acid of selenium codified and structurally related with the also codified cysteine), to be activated by amavadine as an electron-transfer mediator in a process related to the abovementioned amavadine-mediated oxidation of thiols.

Another species of *Amanita*, in spite of belonging to a different section (at the immediate lower level of the subgenus in the taxonomic rank) of the *A. muscaria* [74], that contains low levels of iron and concentrates significant amounts of selenium [65], is the *Amanita lividopallescens* (Secr. ex Boud.) Kühner & Romagn. (1953) [or *Amanita malleata* (Piane *ex* Bon) Contu]. Is this fungus also an accumulator of vanadium? This is another matter that still needs further studies.

Hence, the biological role of amavadine is still a rather intriguing subject, although a number of attractive, but debatable, hypotheses can be put forward, such as those we are suggesting above, aiming to inspire further studies toward the eventual recognition of any of those (or other) possible functions of that fascinating natural bare vanadium complex.

Acknowledgments The authors are indebted to all co-authors cited in joint references, as well as to the Fundação para a Ciência e a Tecnologia (FCT) for partial financial support (pluriannual project PEst-OE/QUI/UI0100/2011).

References

1. Henze M (1911) Testings on the blood of ascidians I announcement – the vanadium compound of the blood corpuscles. Z Physiol Chem 72:494–501
2. Geml J, Tulloss RE, Laursen GA, Sazanova NA, Taylor DL (2008) Evidence for strong inter- and intracontinental phylogeographic structure in *Amanita muscaria*, a wind-dispersed ectomycorrhizal basidiomycete. Mol Phylogenet Evol 48:694–701
3. Fraústo da Silva JJR (1989) Vanadium in biology – the case of the *Amanita* toadstools. Chem Spec Bioavailab 1:139–150
4. Bayer E (1995) Amavadin, the vanadium compound of Amanitae. In: Sigel H, Sigel A (eds) Vanadium and its role for life, metal ions in biological systems, vol 31. Marcel Dekker, New York, pp 407–421

5. Pombeiro AJL, Fraústo da Silva JJR, Fujiwara Y, Silva JAL, Reis PM, Palavra AMF Catalyst system and process for direct one-pot conversion of methane into acetic acid under relatively mild conditions, comprises vanadium complex, peroxodisulfate salt and trifluoroacetic acid. WO 2004/037416 A2. May 6, 2004
6. Ter Meulen H (1931) Regarding the distribution of the molybdene in nature. Rec Trav Chim Pays-Bas 50:491–504
7. Bertrand D (1943) Le vanadium chez les champignons et plus spécialement chez les amanite. Bull Soc Chim Biol 25:194–197
8. Meisch H-U, Reinle W, Schmitt JA (1979) High vanadium content in mushrooms is not restricted to the fly agaric (*Amanita muscaria*). Z Naturforsch 66:620–621
9. Matoso CMM, Pombeiro AJL, da Silva JJR Fraústo, da Silva MFCG, da Silva JAL, Baptista-Ferreira JL, Pinho-Almeida F (1998) A possible role for amavadine in some *Amanita* fungi. In: Tracey AS, Crans DC (eds) Vanadium compounds – chemistry, biochemistry and therapeutic applications, American chemical society symposium series no. 711. American Chemical Society, Washington, DC, pp 241–247, Chapter 18, and references therein
10. Koch E, Kneifel H, Bayer E (1987) Occurrence of amavadin in mushrooms of the genus *Amanita*. Z Naturforsch 42c:873–878
11. Vetter J (2005) Mineral composition of basidiomes of *Amanita* species. Mycol Res 109: 746–750
12. Falandysz J, Kunito T, Kubota R, Lipka K, Mazur A, Falandysz JJ, Tanabe S (2007) Selected elements in fly agaric *Amanita* muscaria. J Environ Sci Health A 42:1615–1623, and references therein
13. Bayer E, Kneifel H (1972) Isolation of amavadin, a vanadium compound occurring in *Amanita muscaria*. Z Naturforsch 27b:207–207
14. Kneifel H, Bayer E (1973) Determination of the structure of the vanadium compound, amavadine, from fly agaric. Angew Chem Int Ed 12:508–508
15. Koch E, Kneifel H, Bayer E (1986) Synthesis of new complexons – N-hydroxy-alpha, alpha′-iminodipropionic-hydroxyiminodiacetic and N-hydroxyiminodiacetic acid. Z Naturforsch 41b:359–362
16. Kneifel H, Bayer E (1986) Stereochemistry and total synthesis of amavadin, the naturally-occurring vanadium compound of *Amanita-muscaria*. J Am Chem Soc 108:3075–3077
17. Hubregtse T, Neeleman E, Maschmeyer T, Sheldon RA, Hanefeld U, Arends IWCE (2005) The first enantioselective synthesis of the amavadin ligand and its complexation to vanadium. J Inorg Biochem 99:1264–1267
18. Anderegg G, Koch E, Bayer E (1987) N-hydroxy-α, α′-iminodipropionic and N-hydroxyiminodiacetic acid as complexing agents and an example for selective coordination of the vanadyl ion VO2+ in amavadine. Inorg Chem Acta 127:183–188
19. Hubregtse T, Kooijman H, Spek AL, Maschmeyer T, Sheldon RA, Arends IWCE, Hanefeld U (2007) Study on the isomerism in meso-amavadin and an amavadin analogue. J Inorg Biochem 101:900–908
20. Smith PD, Berry RE, Harben SM, Beddoes RL, Helliwell M, Collison D, Garner CD (1997) New vanadium-(IV) and -(V) analogues of amavadin. J Chem Soc Dalton Trans 1997: 4509–4516
21. Hubregtse T, Hanefeld U, Arends IWCE (2007) Stabilizing factors for vanadium(IV) in amavadin. Eur J Org Chem 2007:2413–2422
22. Gillard RD, Lancashire RJ (1984) Electron-spin resonance of vanadium in *Amanita muscaria*. Phytochemistry 23:179–180
23. Felcman J, Fraústo da Silva JJR, Vaz MCTA (1984) Metal-complexes of N-hydroxy-imino-di-α-propionic acid and related ligands. Inorg Chim Acta 93:101–108
24. Bemski G, Felcman J, Fraústo da Silva JJR, Moura I, Moura JJG, Vaz MCTA, Vilas-Boas LF (1986) Amavadine, an oxovanadium(IV) complex of N-hydroxy-imino-α, α′-dipropionic acid. In: Xavier AV (ed) Frontiers in bioinorganic chemistry. VCH Verlagsgesellaschaft, Weinheim, pp 97–105

25. Bayer E, Koch E, Anderegg G (1987) Amavadin, an example for selective binding of vanadium in nature – studies of its complexation chemistry and a new structural proposal. Angew Chem Int Engl 26:545–546
26. Carrondo MAAFdeCT, Duarte MTLS, Costa Pessoa J, Silva JAL, Fraústo da Silva JJR, Vaz MCTA, Vilas-Boas LF (1988) Bis-(N-hydroxy-iminodiacetate)vanadate(IV), a synthetic model of "amavadin". J Chem Soc Chem Commun 1988:1158–1159
27. Armstrong EM, Beddoes RL, Calviou LJ, Charnock JM, Collison D, Ertok N, Naismith JH, Garner CD (1993) The chemical nature of amavadin. J Am Chem Soc 115:807–808
28. Paine TK, Weyhermuller T, Slep LD, Neese F, Bill E, Bothe E, Wieghardt K, Chaudhuri P (2004) Nonoxovanadium(IV) and oxovanadium(V) complexes with mixed O, X, O-donor ligands (X = S, Se, P, or PO). Inorg Chem 43:7324–7338
29. Yadav HS, Armstrong EM, Beddoes RL, Collison D, Garner CD (1994) The molybdenum analog of amavadin. J Chem Soc Chem Commun 1994:605–606
30. Galvão AM, Levi E, Pombeiro AJL, Guedes da Silva MFC, Silva JAL, Fraústo da Silva JJR (1995) Modelos da amavadina – estudos com o complexo de crómio(III) com hida. In: 2nd conference on inorganic chemistry of the Portuguese Chemical Society, Monte Real-Portugal, CP22, pp 91–92
31. Harben SM, Smith PD, Beddoes RL, Collison D, Garner CD (1997) Eight-coordinate [bis(oxyiminodiacetate)titanium(IV)]$^{2-}$ and nine-coordinate [bis(oxyiminodiacetate) aquazirconium(IV)]$^{2-}$; variation in coordination mode in amavadin-like complexes. Angew Chem Int Engl 36:1897–1898
32. Harben SM, Smith PD, Helliwell M, Collison D, Garner CD (1997) The synthesis, structure and nuclear magnetic resonance properties of some titanium relatives of amavadin: [Δ-Ti(R, R-hidpa)2]2-, [Δ, Λ-Ti(R, R-hidpa)2]2- and [Δ, Λ-Ti(hida)2]2- [H3hidpa = 2,2′-(hydroxyimino)dipropionic acid, H3hida = N-hydroxyiminodiacetic acid]. J Chem Soc Dalton Trans 1997:4517–4523
33. Smith PD, Harben SM, Beddoes RL, Helliwell M, Collison D, Garner CD (1997) Synthesis and structures of niobium(V) and tantalum(V) analogues of amavadin: [M(hida)2]- (M=Nb-V or Ta-V, H3hida equals hydroxyimino-diacetic acid) and [Nb(R, R-hidpa)2]- [H3hidpa=2,2′-(hydroxyimino)-dipropionic acid]. J Chem Soc Dalton Trans 1997:685–691
34. Smith PD, Cooney JJA, McInnes EJL, Beddoes RL, Collison D, Harben SM, Helliwell M, Mabbs FE, Mandel A, Powell AK, Garner CD (2001) New molybdenum(V) analogues of amavadin and their redox properties. J Chem Soc Dalton Trans 2001:3108–3114
35. Carrondo MAAFD, Duarte MTLS, Silva JAL, daSilva JJRF (1991) The crystal and molecular-structure of N, N′-bipyridyl, N-methoxy iminodiacetate oxovanadium(IV). Polyhedron 10:73–77
36. Berry RE, Armstrong EM, Beddoes RL, Collison D, Ertok SN, Helliwell M, Garner CD (1999) The structural characterization of amavadin. Angew Chem Int Engl 38:795–797
37. Armstrong EM, Collison D, Ertok N, Garner CD (1999) NMR studies on natural and synthetic amavadin. Conference Information: XXXIst Colloquium Spectroscopicum Internationale, 05–10 Sept 1999 Ankara, Turkey Talanta 53 (2000) Spl. Issue SI 75–87
38. Armstrong EM, Collison D, Deeth RJ, Garner CD (1995) Discrete variational Xα studies of the electronic-structure of amavadin. J Chem Soc Dalton Trans 1995:191–195
39. Remenyi C, Munzarova ML, Kaupp M (2005) Comparative density-functional study of the electron paramagnetic resonance parameters of amavadin. J Phys Chem B 109:4227–4233
40. Geethalakshmi KR, Waller MP, Buhl M (2007) The presumption of innocence? A DFT-directed verdict on oxidized amavadin and vanadium catecholate complexes. Inorg Chem 46: 11297–11307
41. Ooms KJ, Bolte SE, Baruah B, Choudhary MA, Crans DC, Polenova T (2009) ^{51}V solid-state NMR and density functional theory studies of eight-coordinate non-oxo vanadium complexes: oxidized amavadin. Dalton Trans 2009:3262–3269
42. Nawi MA, Riechel TL (1987) The electrochemistry of amavadine, a vanadium natural product. Inorg Chim Acta 136:33–39

43. Thackrey RD, Riechel TL (1988) Mediators for the oxidation of glutathione and other biological thiols. J Electroanal Chem 245:131–143
44. Fraústo da Silva JJR, Guedes da Silva MFC, Silva JAL, Pombeiro AJL (1993) Redox properties of the amavadine models $[V(hida)_2]^{2-}$ and $[V(hidpa)_2]^{2-}$ and their electroinduced reactivity toward activated-thiols and activated-phenols. In: Pombeiro AJL, McCleverty JA (eds) Molecular electrochemistry of inorganic, bioinorganic and organometallic compounds. Kluwer Academic, Dordrecht, pp 411–415
45. Guedes da Silva MFC, Silva JAL, Fraústo da Silva JJR, Pombeiro AJL, Amatore C, Verpeaux J-N (1996) Evidence for a Michaelis-Menten type mechanism in the electrocatalytic oxidation of mercaptopropionic acid by an amavadine model. J Am Chem Soc 118:7568–7573
46. Lenhardt JM, Baruah B, Crans DC, Johnson MD (2006) Self-exchange electron transfer in high oxidation state non-oxo metal complexes: amavadin. Chem Commun 44:4641–4643
47. Lenhardt JM, Baruah B, Crans DC, Johnson MD (2009) Electron transfer in non-oxovanadium(IV) and (V) complexes: kinetic studies of an amavadin model. Conference Information: 6th international symposium on chemistry and biological chemistry of vanadium, Lisbon, Portugal, 17–19 July 2009, Pure Appl Chem 81:1241–1249
48. Reis PM, Silva JAL, da Silva JJRF, Pombeiro AJL (2000) Amavadine as a catalyst for the peroxidative halogenation, hydroxylation and oxygenation of alkanes and benzene. Chem Commun 2000:1845–1856
49. Reis PM, Silva JAL, da Silva JJRF, Pombeiro AJL (2004) Peroxidative oxidation of benzene and mesitylene by vanadium catalysts. J Mol Catal A Chem 224:189–195
50. Reis PM, Silva JAL, Palavra AF, da Silva JJRF, Kitamura T, Fujiwara Y, Pombeiro AJL (2003) Single-pot conversion of methane into acetic acid in the absence of CO and with vanadium catalysts such as amavadine. Angew Chem Int Engl 42:821–823
51. Kirillova MV, Kuznetsov ML, Reis PM, da Silva JAL, da Silva JJRF, Pombeiro AJL (2007) Direct and remarkably efficient conversion of methane into acetic acid catalyzed by amavadine and related vanadium complexes. A synthetic and a theoretical DFT mechanistic study. J Am Chem Soc 129:10531–10545
52. Kirillova MV, Kuznetsov ML, da Silva JAL, da Silva MFC, da Silva JJRF, Pombeiro AJL (2008) Amavadin and other vanadium complexes as remarkably efficient catalysts for one-pot conversion of ethane to propionic and acetic acids. Chem Eur J 14:1828–1842
53. Kirillova MV, da Silva JAL, da Silva JJRF, Palavra AF, Pombeiro AJL (2007) Highly efficient direct carboxylation of propane into butyric acids catalyzed by vanadium complexes. Adv Synth Catal 349:1765–1774
54. Reis PM, Silva JAL, Palavra AF, da Silva JJRF, Pombeiro AJL (2005) Vanadium-catalyzed carboxylation of linear and cyclic C-5 and C-6 alkanes. J Catal 235:333–340
55. Pombeiro AJL, Kirillova MV, Kirillov AM, Silva JAL, Fraústo da Silva JJR method for the conversion, under mild conditions and in aqueous medium, of gaseous and liquid alkanes into carboxylic acids. WO/2008/088234-A1. July 24, 2008
56. Kirillova MV, Kirillov AM, Kuznetsov ML, Silva JAL, da Silva JJRF, Pombeiro AJL (2009) Alkanes to carboxylic acids in aqueous medium: metal-free and metal-promoted highly efficient and mild conversions. Chem Commun 2009:2353–2355
57. Kirillova MV, Kirillov AM, Pombeiro AJL (2009) Metal-free and copper-promoted single-pot hydrocarboxylation of cycloalkanes to carboxylic acids in aqueous medium. Adv Synth Catal 351:2936–2948
58. Kirillova MV, Kirillov AM, Pombeiro AJL (2010) Mild, single-pot hydrocarboxylation of gaseous alkanes to carboxylic acids in metal-free and copper-promoted aqueous systems. Chem Eur J 16:9485–9493
59. Hubregtse T (2007) Structural investigations of amavadin-based vanadium complexes. D Phil thesis, Technical University of Delft, The Netherlands
60. Carrondo MAAFD, Duarte MTLS, Silva JAL, Fraústo daSilva JJRF (1992) An X-ray study of the complex anion bis(N-hydroxy-iminodiacetate) vanadate(IV) – a model for vanadium containing biological compound. Struct Chem 3:113–119

61. Fraústo da Silva JJR, Williams RJP (2001) The biological chemistry of the elements – the inorganic chemistry of life, 2nd edn. Clarendon, Oxford
62. Crans DC, Smee JJ, Gaidamauskas E, Yang L (2004) The chemistry and biochemistry of vanadium and the biological activities exerted by vanadium compounds. Chem Rev 104: 8499–902
63. Durner J, Klessig DF (1995) Inhibition of ascorbate peroxidase by salicylic-acid and 2,6-dichloroisonicotinic acid, 2 inducers of plant defense responses. Proc Natl Acad Sci USA 92:11312–11316
64. Cotton FA, Wilkinson G (1966) Advanced inorganic chemistry – a comprehensive text, 2nd edn. Interscience, New York
65. Borovicka J, Randa Z (2007) Distribution of iron, cobalt, zinc and selenium in macrofungi. Mycol Prog 6:249–259
66. Williams RJP, Fraústo da Silva JJR (1996) The natural selection of the chemical elements. Oxford University Press, Oxford
67. Almeida M, Humanes M, Melo R, Silva JA, da Silva JJRF, Vilter H, Wever R (1998) Saccorhiza polyschides (phaeophyceae; phyllariaceae) a new source for vanadium-dependent haloperoxidases. Phytochemistry 48:229–239
68. Strack D, Vogt T, Schliemann W (2003) Recent advances in betalain research. Phytochemistry 62:247–269
69. Molina R, Trappe JM (1982) Patterns of ectomycorrhizal host specificity and potential among pacific northwest conifers and fungi. For Sci 28:423–458
70. Bertrand D (1950) The biochemistry of vanadium. Am Mus Nat Hist Bull 94:403–456
71. Watkinson JH (1964) Selenium-accumulating plant of humid regions – *Amanita muscaria*. Nature 202:1239–1240
72. Meisch H-U, Schmitt JA, Reinle W (1978) Heavy-metals in higher fungi. 3. vanadium and molybdenum. Z Naturforsch 33c:1–6
73. Stijve T (1977) Selenium content of mushrooms. Z Lebensm Unters Forsch 164:201–203
74. Drehmel D, Moncalvo JM, Vilgalys R (1999) Molecular phylogeny of *Amanita* based on large-subunit ribosomal DNA sequences: implications for taxonomy and character evolution. Mycologia 91:610–618

Chapter 3
High Levels of Vanadium in Ascidians

Hitoshi Michibata and Tatsuya Ueki

Abstract Henze's discovery of high levels of vanadium in an ascidian was not only a trigger for research in vanadium science, but also aroused great interest in the question of how such extraordinarily high levels of vanadium could be accumulated and what the role of vanadium in ascidians could possibly be. Many investigators, including inorganic, catalytic, and applied chemists, as well as physiological, molecular, and pharmaceutical biologists have been involved in this interdisciplinary problem. In this review, we not only trace the history of vanadium research, but also describe recent advances in our understanding of the field from several viewpoints: the determination of high levels of vanadium, the identification of vanadium-accumulating blood cells, the energetics of vanadium accumulation, the sulfate transport system, the redox mechanism of vanadium, and the possible physiological roles of vanadium in ascidians.

Keywords Ascidian • Vanadium • Hyper-accumulation • Redox • Metal-binding proteins

3.1 Introduction

The discovery of vanadium compounds in ascidian blood cells dates back to 1911 when the German physiologist Martin Henze discovered high levels of vanadium in an ascidian collected from the Bay of Naples [1]. It is no exaggeration to say that Henze's discovery was a catalyst for research in vanadium science, which has involved not only inorganic, catalytic, and applied chemistry, but also physiological,

H. Michibata (✉) • T. Ueki
Department of Biological Science, Graduate School of Science, Hiroshima University, 1-3-1 Kagamiyama, Higashihiroshima 739-8526, Japan
e-mail: hmichi@hiroshima-u.ac.jp; ueki@hiroshima-u.ac.jp

H. Michibata (ed.), *Vanadium: Biochemical and Molecular Biological Approaches*,
DOI 10.1007/978-94-007-0913-3_3,

molecular, and pharmaceutical biology. From 1903 to 1921, Henze was the head of the chemistry department at the Stazione Zoologica di Napoli, which was founded in March 1872 by Anton Dohrn, a fervent defender of Darwin's theory of evolution by natural selection. Dohrn dedicated his life to collecting facts and ideas in support of Darwinism [2].

Henze's discovery concerning ascidians attracted considerable interest because of the extraordinarily high levels of vanadium, which had not been reported in any other organism, and the possible role of vanadium as an oxygen carrier, it possibly being a third prosthetic group in respiratory pigments, the others being iron and copper. Although it was later demonstrated that vanadium does not play such a role, interest continued in the ascidians because of their evolutionary position between vertebrates and invertebrates, in the subphylum Urochordata. Ascidian juveniles have a notochord during the larval stage prior to metamorphosis, during which they accumulate high levels of vanadium. Following a series of Henze's studies [1, 3–5], Callifano & Caselli isolated from ascidian blood cells a vanadium-complex that they designated "haemovanadin" [6]. Bielig et al. [7], examining the biochemistry of haemovanadin, reported that haemovanadin was a complicated complex consisting of vanadium, sulfuric acid, protein and organic ligands, with a gross composition of $[C_{16}H_{19}N_3O_{12}]VO$.

3.2 Thermal Neutron Activation Analysis

Many analytical chemists and physiologists looked for not only vanadium, but also niobium, chromium, tantalum, tungsten, and titanium, employing a variety of analytical methods such as spectrocolorimetry, emission spectrometry, and atomic absorption spectrometry. However, direct comparisons could not be made with the data obtained because of varying sensitivity and precision of the methods used and because the data were reported variously, in terms of dry weight, wet weight, ash weight, and protein amount.

The most sensitive method for determining vanadium in those days was thermal neutron activation analysis, which is the method we used at the start of our studies. Seven species belonging to the suborder Phlebobranchia and eight species belonging to the suborder Stolidobranchia were analyzed for vanadium content. Samples were irradiated with thermal neutrons in the TRIGA MARK II nuclear reactor at Rikkyo University. Species belonging to the suborder Phlebobranchia were shown to have a higher vanadium content than those in the suborder Stolidobranchia. Of the ascidian tissues examined, blood cells contained the highest amounts of vanadium [8]. The highest concentration of vanadium (350 mM) was found in the blood cells of *Ascidia gemmata*, belonging to the suborder Phlebobranchia [9]. Levels of iron and manganese, determined simultaneously, did not vary much between the members of the two suborders (Table 3.1).

Table 3.1 Concentrations of vanadium in the tissues of several ascidians (mM)

Species	Tunic	Mantle	Branchial sac	Serum	Blood cells
Phlebobranchia					
Ascidia gemmata	N.D.	N.D.	N.D.	N.D.	347.2
A. ahodori	2.4	11.2	12.9	1.0	59.9
A. sydneiensis	0.06	0.7	1.4	0.05	12.8
Phallusia mammillata	0.03	0.9	2.9	N.D.	19.3
Ciona intestinalis	0.003	0.7	0.7	0.008	0.6
Stolidobranchia					
Styela plicata	0.005	0.001	0.001	0.003	0.003
Halocynthia roretzi	0.01	0.001	0.004	0.001	0.007
H. aurantium	0.002	0.002	0.002	N.D.	0.004

The vanadium content in each tissue was quantitatively determined mainly by neutron-activation analysis [8, 9]
N.D. not determined

3.3 Identification of Vanadocytes

Ascidian blood cells (coelomic cells) are morphologically classified into 9–11 different types, grouped into six categories: hemoblasts, lymphocytes, leukocytes, vacuolated cells, pigment cells, and nephrocytes [10]. The vacuolated cells are classified into at least four types: morula cells, signet ring cells, compartment cells, and small compartment cells. Among them, morula cells had been thought to be the vanadium-accumulating cells, the so-called "vanadocytes" [11–15].

At the end of the 1970s, with the increasing availability of scanning transmission electron microscopes equipped with an energy-dispersing X-ray detector, it became possible to determine which cell type was the true vanadocyte. An Italian group first reported that it was not the morula cells, but rather the granular amoebocytes, signet ring cells, and compartment cells that emitted the X-rays characteristic of vanadium. Thus, identification of the true vanadocytes became a high priority matter to researchers concerned with the mechanism by which vanadium was accumulated in ascidians. Using density gradient centrifugation to isolate specific types of blood cells and using thermal neutron activation analysis to quantify vanadium in isolated subpopulations of blood cells, we showed that vanadium was accumulated in the signet ring cells of *Ascidia ahodori* [16]. In *Phallusia mammillata*, analysis with the chelating reagent 2,2-bipyridine, which is known to complex with vanadium in the +3 oxidation state, revealed that many types of blood cells, including signet ring cells, vacuolated amoebocytes, bivacuolated cells, and type-II compartment cells, were stained brown, indicating the presence of vanadium [17]. We also found evidence of vanadium in the signet ring cells of *Phallusia nigra* by transmission X-ray microscopy at the Synchrotron Radiation Center of Ritsumeikan University, Kyoto, Japan [18].

However, using the above methods it was not possible to obtain direct evidence of vanadium localization in vanadocytes. What could provide direct evidence for the location of vanadium was the scanning X-ray microscope installed at the

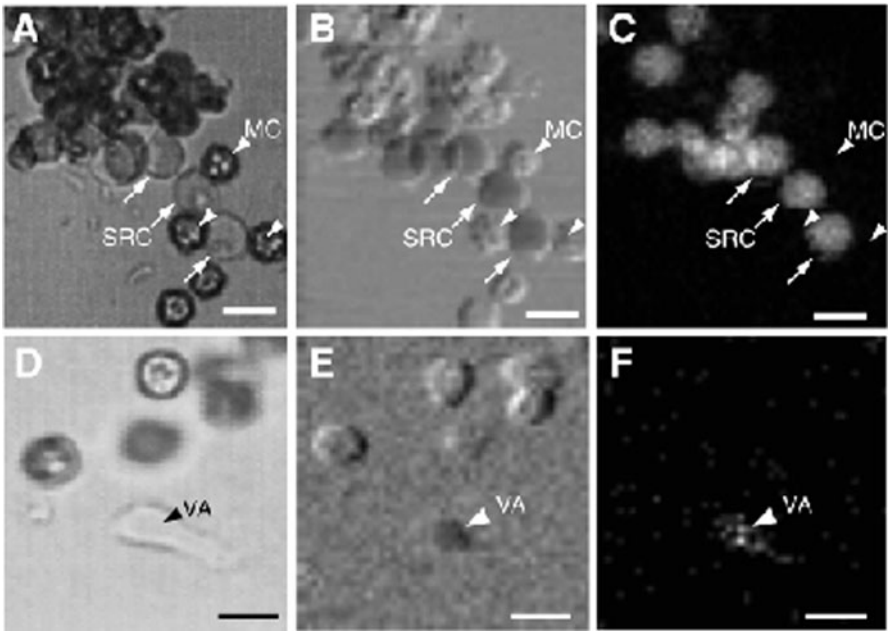

Fig. 3.1 *Phallusia mammillata* blood cells observed by differential interference contrast optical microscopy (**a**, **d**) and X-ray microscopy in the transmission mode (**b**, **e**) and fluorescence mode for vanadium (**c**, **f**). Photographs **a**–**c** are from the same field of view; photographs **d**–**f** are from another field. Vanadium is accumulated in signet ring cells (SRC, shown by *arrows*) and a vacuolated amoebocyte (VA, shown by *arrowheads* in **d**–**f**), but not in morula cells (MC, shown by *arrowheads* in **a**–**c**). Each scale bar = 10 mm (Reproduced from reference [21]. Copyright 2002 Zoological Society of Japan)

ESRF in the ID 21 beam line. This microscope is dedicated to X-ray imaging and spectromicroscopy in the 0.2–7 keV range, in both absorption and fluorescence modes [19, 20]. Because X-ray microscopy in this energy range is useful for observing hydrated specimens up to 10 μm thick, we used this technology to successfully visualize vanadium in living ascidian blood cells. The vanadium image obtained by integrating the fluorescence signal in only the vanadium window clearly showed that the signet ring cells and vacuolated amoebocytes contained vanadium, but the morula cells and compartment cells did not [21]. This study provided conclusive evidence that the true vanadocytes were the signet ring cells (Fig. 3.1).

3.4 Oxidation State of Vanadium

In seawater, the average concentration of vanadium is approximately 35 nM and the oxidation state of vanadium ions dissolved in seawater is the +5 oxidation state [22, 23]. When vanadium ions are taken in by ascidians, most of them are

reduced to the +3 oxidation state (V^{III}) via the +4 oxidation state (V^{IV}). Henze [1] first suggested that the blood cells of *P. mammillata* contained vanadium in the +5 oxidation state (V^{V}). Later, Lybing [24], Bielig et al. [25], Boeri and Ehrenberg [26] and Webb [27] reported the +3 oxidation state of vanadium in ascidians. Thereafter, studies using noninvasive physical methods, such as EPR, EXAFS, XAS, NMR, and SQUID, revealed that the intracellular oxidation state of vanadium is predominantly in the +3 oxidation state, with a small amount in the +4 oxidation state [28–31]. However, as mentioned above, ascidians have at least 9–11 different types of blood cells. The above physical methods were applied to whole blood cells, but not to isolated vanadocytes. Thus, we reexamined, using noninvasive EPR, the oxidation state of vanadium in fractionated vanadocytes of *Ascidia gemmata* under a reducing atmosphere. The results confirmed that 97.6% of the vanadium ions were in the +3 oxidation state with small amounts (2.4%) of V^{IV} ions [32].

3.5 Vanadium Reducing Agents

When vanadium ions are reduced to V^{III}, some reducing agent(s) must participate in the process. Several candidates for the reduction of vanadium in ascidian blood cells were proposed: tunichromes, a class of hydroxy-DOPA containing tripeptides [33], GSH, H_2S, NADPH, DTT [34], and thiols, such as cysteine [35].

As described later in detail, it is highly probable that NADPH and glutathione act as intrinsic reducing agents in ascidian blood cells. The enzymes of the pentose phosphate pathway, which is known to produce two molecules of NADPH per cycle, were identified in ascidian blood cells and shown to localize exclusively to the vanadocytes [36–39]. The enzymes identified were 6-PGDH (EC1.1.1.44), G6PDH (EC1.1.1.49), TKL (EC2.2.1.1), and GP (EC2.4.1.1). Glutathione was also reported to be localized in the vanadocytes, with a concentration estimated to be in the mM range [40]. Based on their redox potentials, these agents can reduce V^{V} to V^{IV} but cannot reduce V^{IV} to V^{III}. Thus, other agents are required for the reduction of V^{IV} to V^{III}.

Several reducing agents that may be involved in the reduction of V^{IV} to V^{III} have been discussed [41]. Among the biologically relevant molecules that may be reducing agents are cysteine complexes. Ascidian blood cells contain aliphatic sulfonic acids, such as cysteic acid, an oxidation product of cysteine [35], and cysteine methyl ester has been reported to reduce V^{IV} to V^{III} with the assistance of EDTA and EDTA-like ligands of aminopolycarboxylate in water [41, 42]. The reduction of V^{IV} to V^{III} by cysteine methyl ester was found to be aided by glycylhistidine and glycylaspartic acid [41]. Additionally, cleavage of the disulfide bonds of Vanabin2 resulted in the reduction of V^{V} to V^{IV} [40]. Thus, cysteine complexes are likely to participate in the reduction. To completely elucidate the electron transfer cascade from NADPH to vanadium ions, the unknown reductant involved in the reduction of V^{IV} to V^{III} must be clarified (Fig. 3.2).

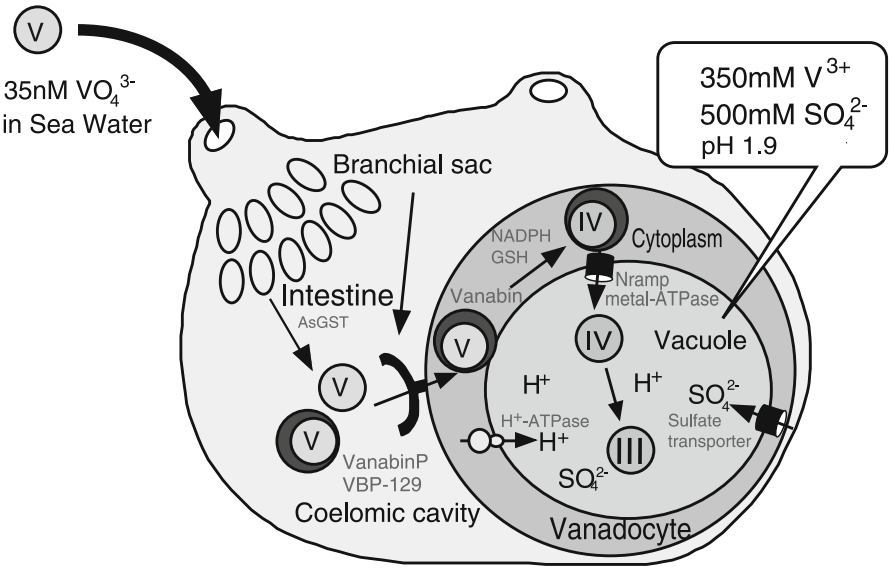

Fig. 3.2 Schematic representation of vanadium accumulation and reduction in ascidians. The concentration of vanadium in the +5 oxidation state is only 35 nM in seawater; in contrast, the highest concentration of vanadium in ascidian blood cells is 350 mM [9], and the concentration of sulfate is 500 mM [62]. The vacuole interior is maintained at an extremely low pH (1.9) by H^+-ATPases [9, 48]. In this environment, almost all of the vanadium accumulated is reduced to V^{III} via V^{IV} [32]. The first step in vanadium uptake may occur at a branchial sac or digestive organ (intestine), where glutathione-S-transferase was identified as a major vanadium carrier protein [91]. We discovered vanadium-binding proteins, designated Vanabins, in the blood plasma and cytoplasm of vanadocytes [68–69, 73, 75]. The pentose phosphate pathway, which produces NADPH, was shown to be localized in the cytoplasm by in vitro experiments, and NADPH has been found to reduce V^V to V^{IV} [36–39]. A metal-ATPase that might be involved in vanadium transport has been found in the vacuolar membrane

3.6 Energetics of Accumulation

In addition to reporting a high level of vanadium, Henze [1] also reported extreme acidity in ascidian blood cells. The mysterious fact that the cells containing high levels of vanadium show extremely low pH has attracted the interest of investigators. The chemical species of vanadium are dependent on pH and the redox potential [43]. Thus, the pH values in ascidian blood cells are of interest to researchers in the vanadium sciences. In the 1980s, it became controversial whether ascidian blood cells have a low pH; some investigators insisted that the intracellular pH was neutral on the basis of measurements made by an improved transmembrane equilibrium using ^{14}C-labeled methylamine and on the basis of the ^{31}P chemical shift observed using NMR [44]. Nevertheless, this unusual phenomenon has attracted the interest of investigators because of the possible role of a highly acidic environment in changing or maintaining the redox potential.

Table 3.2 Correlation between the vanadium concentration and pH in ascidian blood cells

Species	Vanadium concentration (mM)	pH
A. gemmata	350	1.86
A. ahodori	60	2.67
A. sydneiensis samea	13	4.20

The vanadium content in each tissue was quantitatively determined mainly by neutron-activation analysis [8, 9]. pH values were measured by both a microelectrode and ESR under anaerobic conditions and converted into $[H^+]$ [9]

In our studies, we focused on this phenomenon from the perspective of the energetics of vanadium accumulation. In *Ascidia gemmata*, in which the signet ring cells contain the highest concentration of vanadium known (350 mM), the vacuolar pH (1.86) is also the lowest [9]. In *A. ahodori*, in which the signet ring cells contain 60 mM vanadium, the vacuolar pH is 2.67, and in *A. sydneiensis samea*, in which the signet ring cells contain 13 mM vanadium, the vacuolar pH is 4.20 [9]. Thus, a comparative analysis of the intracellular levels of vanadium versus pH values in the signet ring cells (vanadocytes) of three different species suggests a correlation between a high level of vanadium and a low pH (i.e., a higher concentration of protons) (Table 3.2).

V-ATPases are proton pumps that play an important role in pH homeostasis in various intracellular organelles, including clathrin-coated vesicles, endosomes, lysosomes, Golgi-derived vesicles, multivesicular bodies, and chromaffin granules, which belong to the central vacuolar system [45–47]. V-ATPases create electrochemical gradients between the plasma and vacuolar membranes. These proton gradients are used to drive secondary transport processes. In ascidian blood cells, the steep proton gradient is thought to be the energy source for the accumulation of vanadium ions, which, at maximum accumulation, exhibit a 10^7-fold concentration gradient across the membrane.

Immunocytological analysis revealed that V-ATPases are localized in the vacuolar membranes of vanadocytes. Additionally, a specific inhibitor of V-ATPases, bafilomycin A_1, inhibits the proton pump in vanadocyte vacuoles, resulting in neutralization of the vacuolar contents [48]. Thus, V-ATPases were ascertained to function in vanadocytes. V-ATPases are composed of many subunits that are clustered into a membrane-associated domain (V_0 domain) and a peripherally associated domain (V_1 domain). Subunit C of the V-ATPases was reported to play an important role in the regulation of V-ATPases; when isolated cDNA encoding subunit C was expressed in the corresponding pH-sensitive budding yeast mutant *vma5*, which is normally viable only in a low pH medium, the transformed yeast mutant could grow in a neutral pH medium [49], suggesting it may have acquired the ability to acidify its intracellular contents. As a follow-up to this study, a functional assay to examine whether protons concentrated by V-ATPases are linked to the accumulation of vanadium should be conducted.

In the vacuoles of vanadocytes, almost all vanadium ions are reduced to V^{III} [32]. In such an environment, the possibility cannot be excluded that hydrolysis of the coordinating water molecules contributes to the extremely low pH.

3.7 Sulfate Ions

The co-existence of high levels of both vanadium and sulfate ions has attracted investigators since Henze first discovered this unusual phenomenon [1]. Considerable amounts of sulfate and sulfur compounds have been reported to be associated with vanadium in ascidian blood cells [5, 30, 35, 50–61]. We reported that the blood cells of the most vanadium-rich ascidian, *A. gemmata*, contain 350 mM vanadium, and that 97% of this vanadium is reduced to V^{III} [32]. Raman spectroscopy revealed that the ratio of the levels of sulfate and vanadium in blood cells from *A. gemmata* is approximately 1.5, which is the expected value if sulfate ions are present as the counterions of vanadium ions in the +3 oxidation state [62]. In *A. sydneiensis samea*, the ratio was 2.2 (86 mM sulfate vs. 38 mM V^{III}) in the blood cell fraction without giant cells [63]. This value is within an appropriate range for the existence of sulfate as counter ions, although the ratio is beyond the expected ratio of 1.5. In another ascidian, *A. ceratodes*, X-ray absorption spectrometry of whole blood cells in comparison with inorganic models revealed the V^{III}: sulfate ratios to be 1.0:1.1 and 1.9:1.0 in two specimens; however, the combined concentration of sulfate and sulfonate (SO_3^-) ions was sufficient to balance the ionic charge [30]. Together, these results support the hypothesis that sulfate ions are actively accumulated in ascidian blood cells and their concentration is sufficient to balance the charges in the vacuoles of vanadocytes.

Kinetic studies of sulfate transport and the metabolic pathways of sulfate incorporation have been examined in various living organisms [64], and several genes involved in these processes, including *SUL1*, *SUL2*, *MET3*, *MET4*, and *MET6*, have been isolated. Assimilated sulfate is first reduced to sulfite using reducing equivalents produced by the oxidation of NADPH and is then used in the synthesis of organic sulfur metabolites (mostly cysteine, methionine, and *S*-adenosylmethionine) in a process that requires considerable amounts of NADPH. The reduction of sulfate to sulfide proceeds via adenylation, which lowers the electropotential of sulfate so that it can be reduced to sulfite and sulfide by means of NADPH oxidation [65, 66]. The correlation between high levels of sulfate ions assimilated in the vacuole and the expression of enzymes involved in the pentose-phosphate pathway in the cytoplasm of vanadocytes is noteworthy [67].

To identify cDNA encoding a sulfate transporter from blood cells of *A. sydneiensis samea*, a PCR using degenerate primers corresponding to the conserved region among known sulfate transporters was performed. The deduced amino acid sequence of one of the representative cDNAs encoding a putative sulfate transporter had striking similarities to Slc13-type sulfate transporters from

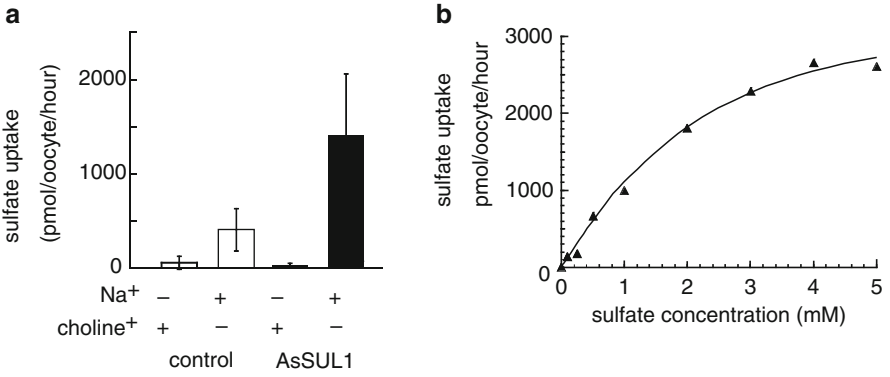

Fig. 3.3 *As*SUL1 expression in Xenopus oocytes. (**a**) Na^+ dependency of sulfate uptake by AsSUL1. The initial sulfate concentration was 1 mM. (**b**) Kinetic properties of *As*SUL1. Sulfate uptake was measured with increasing concentrations of sulfate in the presence of (^{35}S) sulfate in uptake buffer containing 100 mM NaCl. The K_m and V_{max} of *As*SUL1 were 1.75 mM and 2,500 pmol/oocyte/h, respectively (Reproduced from reference [63]. Copyright 2009 Elsevier B.V.)

various organisms [63]. The putative protein product was calculated to possess 12 transmembrane domains and a C-terminal signature sequence, which are also common characteristics of the Slc13 family. Thus, the corresponding gene was designated *A. sydneiensis samea* sulfate transporter 1 (*As*SUL1). The isolated *As*SUL1 cDNA was used for a transport assay using the *Xenopus* oocyte expression system. The *Xenopus* oocyte expressing *As*SUL1 was observed to take up about threefold higher amounts of SO_4^{2-} in the presence of Na^+ than that of the control [63]. Thus, it was concluded that *As*SUL1 encoded a protein of the Slc13 family of Na^+-dependent sulfate transporters. The significance of the co-existence of high levels of vanadium and sulfate ions in the vacuoles of ascidian vanadocytes should be clarified as a next step (Fig. 3.3).

3.8 Vanabins: Vanadium-Binding Proteins

Although it stands to reason that some proteins must participate in the accumulation process of vanadium in ascidians, no protein had been reported until we first identified a vanadium-associated protein from the vanadium-rich ascidian, *A. sydneiensis samea* [68]. When a homogenate of blood cells was applied to a DEAE-Sephacel anion-exchange column, one major peak containing both vanadium and proteins was obtained. Resolved by SDS-PAGE, the peak included at least two major proteins with apparent molecular masses of 12.5 and 15 kDa, and a minor 16-kDa protein. Using immunoscreening or PCR, cDNAs encoding 12.5 and 15 kDa proteins were identified [69]. Recombinant proteins, designated as Vanabin1 and Vanabin2, of these two independent but related cDNAs, were shown to bind, respectively, 10

and 20 V^{IV} ions, with dissociation constants (K_d) of 2.1×10^{-5} and 2.3×10^{-5} M [69]. The binding of V^{IV} (VO^{2+}) to these Vanabins was inhibited by the addition of Cu^{2+} ions, but not by Mg^{2+} or MoO_4^{2-} ions. The conserved motif of the Vanabins can be described as the consensus sequence {C}−{X2–5}−{C}. The minor 16-kDa protein band was revealed to correspond to sequence variants of Vanabin2 [70]. Vanabins are rich in charged residues, such as arginine (3/87 and 5/91 in Vanabin1 and Vanabin2, respectively), aspartate (6/87 and 6/91), glutamate (2/87 and 7/91), and lysine (12/87 and 14/91), whereas metallothioneins are rich in serine and lysine. By a mutagenesis study, two regions where positively charged amino acids are gathered have recently been reveled to be responsible for V^{IV} binding [71]. The mechanism of metal selectivity in Vanabins has not been determined, although the effects of acidic pH on selective metal binding and on the secondary structure of Vanabin2 was studied so far [72]. Vanabin2 was shown to selectively bind V^{IV}, Fe^{3+}, and Cu^{2+} ions under acidic conditions. In contrast, Co^{2+}, Ni^{2+}, and Zn^{2+} ions were bound at pH 6.5 but not at pH 4.5. Changes in pH had no detectable effect on the secondary structure of Vanabin2 under acidic conditions, as determined by CD spectroscopy [72]. Additionally, EST analysis of vanadocytes revealed that two other novel Vanabins, designated as Vanabin3 and Vanabin4, have primary structures that are similar to those of Vanabin1 and Vanabin2, bind qualitatively to V^{IV} ions, and are expressed in vanadocytes [73, 74]. These Vanabins, Vanabin1–4, were shown to be localized in the cytoplasm of vanadocytes (Fig. 3.4).

Although vanadium ions are supposedly taken up from seawater through the branchial sac or alimentary canal, transferred to the coelom, and concentrated in vanadocytes, it is not known if carrier proteins are involved in the transport of vanadium from the coelomic fluid (blood plasma) into the vanadocytes. Using IMAC, we identified several vanadium-associated proteins in the coelomic fluid (blood plasma) and cloned the cDNA for the major protein. Sequence analysis indicates that this protein is a novel Vanabin, which we have designated "VanabinP" (Vanabin in plasma) [75]. RT-PCR analysis and *in situ* hybridization indicated that the VanabinP gene was transcribed in some cell types localized to peripheral connective tissues of the alimentary canal, muscle, blood cells, and a portion of the branchial sac. Recombinant VanabinP bound a maximum of 13 V^{IV} ions per molecule with a K_d of 2.8×10^{-5} M. These results suggest that VanabinP is produced in several types of cell, including blood cells, and is immediately secreted into the blood plasma, where it functions as a V^{IV} carrier.

A better understanding of the functions of Vanabins and the mechanism of vanadium accumulation in ascidians requires high-quality 3D structures of the proteins in the presence and absence of vanadium ions. We reported the solution structure of Vanabin2 by multidimensional NMR experiments [75]. Vanabin2 is composed of 91 amino acids, including 18 cysteines. The electrospray ionization (ESI) mass spectrum of Vanabin2 showed a deconvoluted molecular mass of 10,467 Da, which is 18 mass units lower than the expected molecular mass of the protein in which all of the cysteine residues are reduced. Indeed, the complete reduction of Vanabin2 by DTT caused the molecular weight (at 10,485 Da) to increase by 18 mass units, indicating that all 18 cysteine residues of Vanabin2

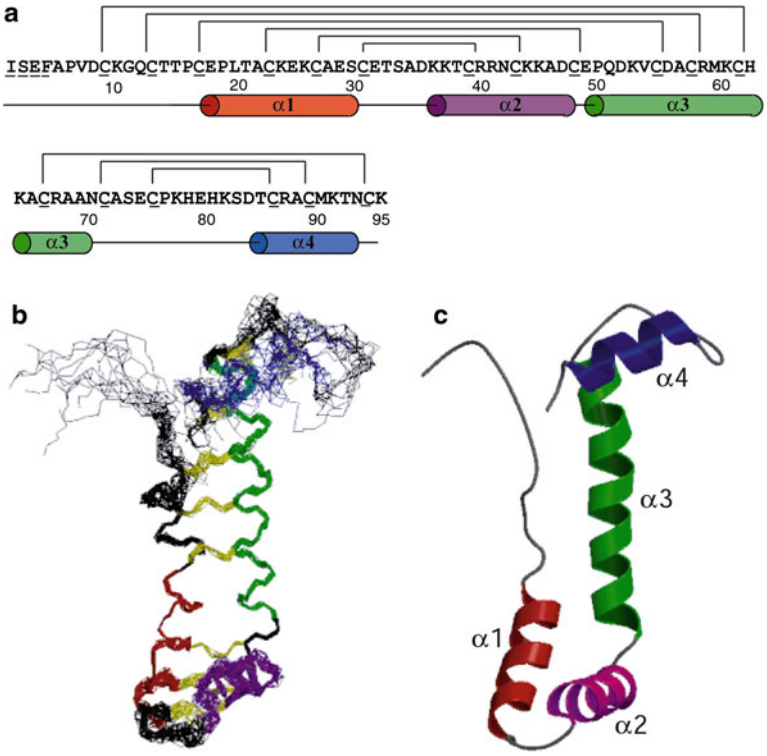

Fig. 3.4 Structure of Vanabin2 from **a**. sydneiensis samea. (**a**) Amino acid sequence of Vanabin2. The amino-terminal tag is *italicized*. Disulfide bond pairings, as determined by the CYANA calculation, are indicated at the *top* of the sequence. The secondary structure elements of Vanabin2 are indicated at the *bottom* of the sequence and are colored correspondingly in all panels. (**b**) The final ten structures superposed over the backbone heavy atoms of residues 18–70. The side chains of the half-cysteine residues are shown as *yellow lines*. (**c**) Ribbon representation of a single structure in the same orientation as in panel **b** (Reproduced from reference [76]. Copyright 2005 American Chemical Society)

are involved in intramolecular disulfide bonds [76]. Thus, the NMR study was carried out under nonreducing conditions. The structural analysis revealed a novel bow-shaped conformation, with four α-helices connected by nine disulfide bonds. No structural homolog has been reported to date. The ^{15}N-HSQC perturbation experiments of Vanabin2 indicate that V^{IV} ions, which are exclusively localized on the same face of the molecule, are coordinated by amine nitrogens derived from amino acid residues, such as lysines, arginines, and histidines, as suggested by the EPR results [77].

Structural modeling of Vanabins 1, 3, and 4, based on the NMR data of Vanabin2, resulted in fairly homologous structures, whereas the modeled structure of VanabinP differed from that of Vanabin2, especially in the long loop domain between the third and fourth helices. Generally, metal-binding proteins can interact with

other metal-binding proteins and proteins, such as membrane metal transporters, membrane anchor proteins, or metal-reducing/oxidizing proteins [78]. Thus, using the Far Western blotting method, several proteins that interact with Vanabins were obtained. Among these, Vanabin interacting protein 1 (VIP1) was shown to be localized in the cytoplasm of vanadocytes and to clearly interact with Vanabins 1–4, but not with VanabinP, based on two hybrid analyses [79]. To determine whether ascidian species other than *A. sydneiensis samea* have Vanabin-like genes, we searched for the genes in a database and found five groups of cDNAs that encoded Vanabin-like proteins in another ascidian, *Ciona intestinalis* [80]. The genes encoding *C. intestinalis* Vanabins, *Ci*Vanabin1 to *Ci*Vanabin5, were clustered in an 8.4-kb genomic region. All the *C. intestinalis* Vanabins were cysteine-rich, and the repetitive pattern of cysteines closely resembled that of *A. sydneiensis samea* Vanabins. Using immobilized metal ion affinity chromatography (IMAC), we found that a recombinant protein of at least one of the *C. intestinalis* Vanabins (*Ci*Vanabin5) bound to V^{IV} ions [80].

3.9 Vanabin as Vanadium Reductase

Vanabin2 is a rare protein with nine disulfide bonds per molecule. The fully oxidized disulfide bonds were observed on polyacrylamide gels at a position corresponding to 14 kDa. When exposed to concentrations of more than 0.6 mM DTT and 10 mM 2-ME, Vanabin2 migrated to a position corresponding to 20 kDa with a concomitant disappearance of the isoellipticity points in the CD spectra, suggesting that the disulfide bonds of Vanabin2 were reduced and cleaved [40]. The treatment of Vanabin2 with an intrinsic reducing reagent, 1–4 mM GSH, which corresponds to the intrinsic concentrations in vanadocytes, resulted in mild migration, indicating that Vanabin2 was partially reduced.

On the other hand, thiol–disulfide exchange reactions are known to be involved in many cellular activities, such as protein folding and unfolding [81], regulation of transcription factor activity [82], activity of ribonucleotide reductase [83], maintenance of redox potentials [84], responses against oxidative stress caused by metal ions [85], and metal transfer from metalloproteins to metal-depleted enzymes (metallochaperone activity) [86] in a manner analogous to phosphorylation/dephosphorylation reactions catalyzed by protein kinases and phosphatases.

We examined whether thiol–disulfide exchange reactions in Vanabin2 were involved in reduction of V^{V} to V^{IV} [40]. EPR spectrometry was performed to detect VO^{2+} (V^{IV}) species, which exhibit a typical signal consisting of eight-line manifolds. Within 24 h after addition of 10 μM Vanabin2 to a reaction mixture containing 10 mM V^{V} and 2 mM GSH at room temperature, a large signal due to V^{IV} was observed. In contrast, when 2 mM GSH was added to a 10 mM V^{V} solution without Vanabin2, only a slight increase in EPR signal intensity was observed after a 24 h incubation. Based on these results, we concluded that Vanabin2 acts as a vanadium reductase.

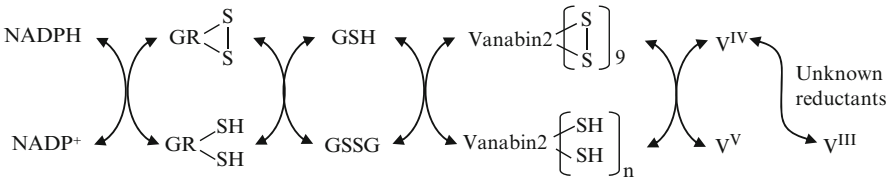

Fig. 3.5 A possible cascade for the thiol-disulfide exchange reactions conjugated with NADPH, GR (glutathione reductase), GSH, Vanabin2, and vanadium ions (Reproduced from reference [40]. Copyright 2009 Elsevier B.V.)

Due to the inherent difficulty of rapidly monitoring by EPR the reduction of V^V by Vanabin2, activity of the reductase was instead measured using a coupled NADPH oxidation assay with reduction of GSSG catalyzed by glutathione reductase (GR) [40]. As a negative control, the first assay determined that little NADPH was oxidized by 2 mM GSH and 0.25 U/mL GR in the absence of Vanabin2 and V^V ions. When 4 μM Vanabin2 was added to the assay system, NADPH was slightly oxidized. When 0.1–2.5 mM V^V was added to 2 mM GSH and 0.25 U/mL GR, the levels of oxidized NADPH increased slightly with increasing V^V concentration. Finally, addition of both Vanabin2 and V^V to 2 mM GSH and 0.25 U/mL GR increased the amount of oxidized NADPH markedly with increasing V^V concentration, reaching saturation at 1.5 mM V^V. The V_{app} and K_{app} values for Vanabin2-catalyzed V^V reduction were 1.15 mol-NADPH/min/mol-Vanabin2 and 0.51 mM, respectively. Thus, Vanabin2 is a novel vanadium reductase, because partial cleavage of its disulfide bonds by GSH results in the reduction of V^V to V^{IV}.

Vanabin2 forms a possible electron transfer cascade from the electron donor, NADPH, via GR, GSH, and Vanabin2 to the acceptor vanadium ions conjugated through thiol–disulfide exchange reactions [40] (Fig. 3.5). In this cascade, electrons are ultimately transferred from the donor NADPH to the acceptor vanadium ions. In this model, reduction of V^V to V^{IV} occurs via thiol–disulfide exchange reactions of Vanabin2. The resulting disulfides are converted to thiols by reduced GSH and the oxidized GSSG is then re-reduced by GR [87, 88]. The resulting disulfides of GR are reduced to thiols by NADPH [87, 88], which may be linked to the pentose-phosphate pathway. We are currently in the process of confirming the intrinsic existence of the components, such as glutaredoxin. The situation in ascidians is complicated, however, by the fact that V^{IV} is further reduced to V^{III}.

3.10 Other Proteins Involved in Vanadium Accumulation

Several proteins that are probably involved in vanadium accumulation and the redox process have already been isolated from a vanadium-rich ascidian, *A. sydneiensis samea*, including a V-ATPase [48, 49, 89], chloride channel [90], enzymes of the

pentose-phosphate pathway [36–39], glutathione transferase [91, 92], VBP-129 [93], and *As*Nramp [94]. In this section we briefly describe the last three proteins recently isolated.

Seawater containing plankton as food is taken by ascidians through their branchial siphon and branchial sac into the digestive tract, which consists of a narrow tube commencing with the opening of the esophagus at the base of the branchial sac. The molecular mechanisms underlying the uptake of vanadium from seawater in the ascidian digestive system had not been investigated. Thus, using a V^{IV}-chelating column, we investigated whether there were vanadium-binding proteins in the ascidian digestive system. Consequently, vanadium-binding proteins with striking homology to GSTs, designated *As*GST-I and *As*GST-II, were isolated [91]. The recombinant *As*GST-I formed a dimer, exhibited GST activity, and was able to bind both V^{IV} (VO^{2+}) and V^{V} ($VO_4{}^{3-}$). *As*GST-I bound approximately 16 vanadium ions per dimer as either V^{IV} or V^{V}, with K_d values of 1.8×10^{-4} and 1.2×10^{-4} M, respectively. *As*GST-I also bound Fe^{3+} and Cu^{2+} with high affinity, in the order $Cu^{2+} > VO^{2+} > Fe^{3+}$, and it bound Co^{2+}, Ni^{2+}, and Zn^{2+} with low affinity [92]. The expression levels of *As*GSTs are exceptionally high in the digestive system relative to the other major organs and tissues, as determined by immunoblotting. Because *As*GSTs may be among the first molecules involved in the influx of vanadium ions through the digestive system, it is important to understand them in analyzing the first step of the ten million-fold vanadium-accumulating process in ascidians.

Vanadium ions taken in through the branchial sac and digestive tract must be discharged into the body cavity where the blood plasma is filled. At least two vanadium-binding proteins, VanabinP [75] and VBP-129 [93], have been isolated from ascidian plasma. VBP-129, designated as a vanadium-binding protein consisting of 129 amino acid residues, was identified in blood plasma of the vanadium-rich ascidian *A. sydneiensis samea*. Although VBP-129 mRNA was transcribed in all tissues examined, the VBP-129 protein was exclusively localized in the blood plasma and muscle cells of this ascidian. It bound not only VO^{2+} but also Fe^{3+}, Co^{2+}, Cu^{2+}, and Zn^{2+}; on the other hand, a truncated form of VBP-129, designated VBP-88, bound only Co^{2+}, Cu^{2+} and Zn^{2+}. In a pull-down assay, an interaction between VanabinP and VBP-129 occurred both in the presence and absence of VO^{2+}. These results suggest that VBP-129 and VanabinP function cooperatively as metallochaperones in ascidian blood plasma [93].

As previously mentioned, Vanabins1–4 were shown to be localized in the cytoplasm of vanadocytes. Thus, some membrane metal transporter(s) seem to be necessary to transport vanadium ions into the cytoplasm through the membrane. Because the Nramp/DCT family of membrane metal transporters is known to transport a broad range of divalent cations (Fe^{2+}, Cu^{2+}, Zn^{2+}, Mn^{2+}, Cd^{2+}, Co^{2+}, Ni^{2+}, Pb^{2+}) across the membrane using a proton gradient as the motive force, localization of a homolog of the Nramp/DCT family in the membrane of ascidian vanadocytes was examined, using immunological methods. Consequently, a cDNA encoding a protein closely related to the Nramp family of proteins was cloned from the cDNA library of *A. sydneiensis samea* blood cells. We found that the product

of this gene, *As*Nramp, was localized on the vacuolar membrane and operated as an antiporter of VO^{2+} ions and H^+ ions. In contrast, a rat homolog of Nramp/DCT, rDCT1, could not transport VO^{2+} under any of the conditions examined [94]. The results of this study indicated that *As*Nramp was a $VO^{2+} \cdot H^+$ antiporter expressed on the vacuolar membrane of vanadocytes. These findings support the proposed model, holding that a proton electrochemical gradient generated by V-ATPase is the driving force for V^{IV} transport from the cytoplasm into the vacuole. These results will be reported in detail as an original paper.

Several other pathways may exist that function together. Another possible mechanism for VO^{2+} transport into the vacuole is a P_{1B}-type ATPase, *As*HMA1, which we have already cloned from blood cells of *A. sydneiensis samea* and the metal selectivity and transport activity of which we have examined (Ueki et al. unpublished data).

3.11 Possible Role of Vanadium in Ascidians

Our final objective is to clarify the physiological function of vanadium in ascidian blood cells. As described in Sect. 3.9, thiol–disulfide exchange reactions in Vanabin2 are involved in the reduction of V^V to V^{IV}. Vanabin2 may act as an electron carrier in an electron transfer cascade from the electron donor, NADPH, to the acceptor vanadium ions, via GR, GSH, and Vanabin2, which both conjugates and reduces the vanadium ions through thiol–disulfide exchange reactions. Thus, ascidians may accumulate the metal ions as a source of oxidizing energy that can drive redox reactions in blood cells or in other tissues.

One approach to identifying the physiological function of vanadium is the comprehensive study of the effect of vanadium on gene expression. A draft genome of the ascidian species *Ciona intestinalis* has been read and inferred to contain approximately 16,000 protein-coding genes [95]. This species accumulates vanadium to a concentration of 0.6 mM in its blood cells [8] and is a model organism for the study of vanadium accumulation. cDNAs for transcripts of 13,464 genes have been characterized and compiled as the "*Ciona intestinalis* Gene Collection Release I" [96, 97], and a custom oligo-based DNA microarray is available [98]. We have performed a study to identify genes regulated by excess vanadium ions, using DNA microarrays (Kume et al. unpublished data). Among 39,523 gene-specific probes on the microarray slide, 550 spots were up-regulated and 820 spots were down-regulated by treatment with 1 mM V^{IV} or V^V ions for 24 h, suggesting that the overall change in gene expression was similar between V^{IV}- and V^V-treated individuals. Vanabins, subunits of V-ATPase, and several metal transporters were up-regulated. Among the major metabolic pathways, expression of enzymes in the glutathione-related pathway, such as glutaredoxin, thioredoxin reductase, peroxiredoxin, and sulfiredoxin was affected by treatment with V^V or V^{IV}. The results will be reported in detail as an original paper.

Another comprehensive approach to identify the function of vanadium in ascidians could be a mutational analysis to find a mutant strain that cannot accumulate vanadium. In *C. intestinalis*, such an approach is available by using transposon mutagenesis [99–101].

3.12 Outlook

It has been a century since the first finding that ascidian species contain high levels of vanadium and sulfate ions by Henze [1, 3–5]. Since then, various hypotheses about the functional role of vanadium have been proposed, but most of them are not supported by sufficient evidence. From the middle of the 1990s, many genes and proteins have been shown to be involved in the process of accumulating and reducing vanadium in ascidians. Vanabins are one family of such genes and proteins found only in vanadium-rich ascidians and are thought to be the key molecule in this process. In our model, Vanabins participate in an electron transfer cascade, in which electrons are transferred from the donor (NADPH) to the acceptor (vanadium ions), via GR, GSH, and Vanabin2, which acts as a vanadium-reducing enzyme via thiol-disulfide exchange reactions, which, in turn, may accelerate the accumulation of vanadium (Fig. 3.5). Our recent comprehensive studies, such as DNA microarray experiments, have suggested that various genes and proteins participate in redox systems via thiol-disulfide exchange reactions (submitted). We hope that the role of vanadium in ascidians will be clarified in the near future.

References

1. Henze M (1911) Unterschungen über das Blut der Ascidien. I. Mitteilung. Die Vanadiumverbindung der Bluktkörperchen. Hoppe Seyler Z Physiol Chem 72:494–501
2. Fantini B (2000) The “Stazione Zoologica Anton Dohrn” and the history of embryology. Int J Dev Biol 44:523–535
3. Henze M (1912) Unterschungen über das Blut der Ascidien. II. Mitteilung. Hoppe Seyler Z Physiol Chem 79:215–228
4. Henze M (1913) Über das Vorkommen freier Schwefelsäure im Mantel von *Ascidia mentula*. Hoppe Seyler Z Physiol Chem 88:345–346
5. Henze M (1932) Über das Vanadiumchromogen des Ascidienblutes. Hoppe Seyler Z Physiol Chem 213:125–135
6. Califano L, Caselli P (1948) Ricerche sulla emovanadina. I. Dimostrazione di una proteina. Publ Staz Zool Napoli 21:261–271
7. Bielig HJ, Jost E, Pfleger K, Rummel W (1961) Sulfataufnahme bei *Phallucia mammillata* Cuvier. Verteilung und Schicksal von Sulfat-und Aminosäure-Schwefel im Blut (Untersuchumgen über Hämovanadin, VI). Hoppe-Seyler’s Z Physiol Chem 325:132–145
8. Michibata H, Terada T, Anada N, Yamakawa K, Numakunai T (1986) The accumulation and distribution of vanadium, iron, and manganese in some solitary ascidians. Biol Bull 171: 672–681

9. Michibata H, Iwata Y, Hirata J (1991) Isolation of highly acidic and vanadium-containing blood cells from among several types of blood cells in Ascidiidae species by density-gradient centrifugation. J Exp Zool 257:306–313
10. Wright RK (1981) Urochordata. In: Ratcliffe NA, Rowley AF (eds) Invertebrata blood cells, vol 2. Academic, London, pp 565–626
11. Webb DA (1939) Observations on the blood of certain ascidians, with special reference to the biochemistry of vanadium. J Exp Biol 16:499–523
12. Endean R (1960) The blood cells of ascidian, *Phallusia mammillata* (Heller). Q J Microsc Sci 107:177–197
13. Kalk M (1963) Cytoplasmic transmission of a vanadium compound in a tunicate oocyte, visible with electronmicroscopy. Acta Embryol Morph Exp 6:289–303
14. Kalk M (1963) Cytoplasmic transmission of a vanadium compound in a tunicate oocyte, visible with electron microscopy. Acta Embryol Morph Exp 6:289–303
15. Kustin K, Levine DS, McLeod GC, Curby WA (1976) The blood of *Ascidia nigra*: blood cell frequency distribution, morphology, and the distribution and valence of vanadium in living blood cells. Biol Bull 150:426–441
16. Michibata H, Hirata J, Uesaka M, Numakunai T, Sakurai H (1987) Separation of vanadocytes: determination and characterization of vanadium ion in the separated blood cells of the ascidian, *Ascidia sydneiensis samea*. J Exp Zool 244:33–38
17. Nette G, Scippa S, Genovese M, de Vincentiis M (1999) Cytochemical localization of vanadium(III) in blood cells of ascidian *Phallusia mammillata* Cuvier, and its relevance to hematic cell lineage determination. Comp Biochem Biophys Part C 122:231–237
18. Takemoto K, Yamamoto A, Michibata H, Uyama T, Ueki T, Ikeda S, Kihara H (2000) Observation of blood cells of the ascidian, *Phallusia nigra*, with X-ray microscope. Mem SR Center Rit- sumeikan Univ 2000:71–77
19. Susini J, Barrett R (1996) The X-ray microscopy facility project at the ESRF. In: Thieme J, Schmahl G, Umbach E (eds) X-ray microscopy and spectromicroscopy. Springer, Wuerzburg, pp I45–I54
20. Susini J, Barrett R, Kaulich B, Oestreich S, Salomé M (2000) The X- ray microscopy facility at the ESRF: a status report. In: Meyer-Ilse W, Warwick T, Attwood D (eds) X-ray microscopy. Proceeding of the sixth international conference. American Institute of Physics, Melville, pp 19–26
21. Ueki T, Takemoto K, Fayard B, Salome M, Yamamoto A, Kihara H, Susini J, Scippa S, Uyama T, Michibata H (2002) Scanning x-ray microscopy of living and freeze-dried blood cells in two vanadium-rich ascidian species, *Phallusia mammillata* and *Ascidia sydneiensis samea*. Zool Sci 19:27–35
22. Cole PC, Eckert JM, Williams KL (1983) The determination of dissolved and particular vanadium in sea water by X-ray fluorescence spectrometry. Anal Chim Acta 153:61–67
23. Collier RW (1984) Particular and dissolved vanadium in the North Pacific Ocean. Nature 309:441–444
24. Lybing S (1953) The valence of vanadium in hemolysates of blood from *Ascidia obliqua*. Alder Arkiv Kemi 6:261–269
25. Bielig HJ, Bayer E, Califano L, Wirth L (1954) The vanadium-containing blood pigment. II. Hemovanadin, a sulfate complex of trivalent vanadium. Publ Staz Zool Napoli 25:26–66
26. Boeri E, Ehrenberg A (1954) On the nature of vanadium in vanadocytes hemolysate from ascidians. Arch Biochem Biophys 50:404–416
27. Webb DA (1956) The blood of tunicates and the biochemistry of vanadium. Publ Staz Zool Napoli 28:273–288
28. Tullius TD, Gillum WO, Carlson RM, Hodgson KO (1980) Structural study of the vanadium complex in living ascidian blood cells by X-ray absorption spectrometry. J Am Chem Soc 102:5670–5676
29. Dingley AL, Kustin K, Macara IG, McLeod GC (1981) Accumulation of vanadium by tunicate blood cells occurs via a specific anion transport system. Biochim Biophys Acta 649:493–502

30. Frank P, Carlson RM, Hodgson KO (1986) Vanadyl ion EPR as a non-invasive probe of pH in intact vanadocytes from *Ascidia ceratodes*. Inorg Chem 25:470–478
31. Lee S, Kustin K, Robinson WE, Frankel RB, Spartalian K (1988) Magnetic properties of tunicate blood cells. I. *Ascidia nigra*. Inorg Biochem 33:183–192
32. Hirata J, Michibata H (1991) Valency of vanadium in the vanadocytes of *Ascidia gemmata* separated by density-gradient centrifugation. J Exp Zool 257:160–165
33. Bruening RC, Oltz EM, Furukawa J, Nakanishi K, Kustin K (1985) Isolation and structure of tunichrome B-1, a reducing blood pigment from the tunicate *Ascidia nigra* (Linnaeus). J Am Chem Soc 107:5298–5300
34. Ryan DE, Grant KB, Nakanishi K, Frank P, Hodgson KO (1996) Reactions between vanadium ions and biogenic reductants of tunicates: spectroscopic probing for complexation and redox products in vitro. Biochemistry 35:8651–8661
35. Frank P, Hedman B, Carlson RMK, Tyson TA, Roe AL, Hodgson KO (1987) Large reservoir of sulfate and sulfonate residues within plasma cells from Ascidia ceratodes, revealed by X-ray absorption near-edge structure spectrometry. Biochemistry 26:4975–4979
36. Uyama T, Yamamoto K, Kanamori K, Michibata H (1998) Glucose-6-phosphate dehydrogenase in the pentose phosphate pathway is localized in vanadocytes of the vanadium-rich ascidian, *Ascidia sydneiensis samea*. Zool Sci 15:441–446
37. Uyama T, Kinoshita T, Takahashi H, Satoh N, Kanamori K, Michibata H (1988) 6-Phosphogluconate dehydrogenase is a 45-kDa antigen recognized by S4D5, a monoclonal antibody specific to vanadocytes in the vanadium-rich ascidian, *Ascidia sydneiensis samea*. J Biochem 124:377–382
38. Uyama T, Ueki T, Suhama Y, Kanamori K, Michibata H (1998) A 100-kDa antigen recognized by a newly prepared monoclonal antibody specific to the vanadocytes of the vanadium-rich ascidian, *Ascidia sydneiensis samea*, is glycogen phosphorylase. Zool Sci 15:815–821
39. Ueki T, Uyama T, Yamamoto K, Kanamori K, Michibata H (2000) Exclusive expression of transketolase in the vanadocytes of the vanadium-rich ascidian, *Ascidia sydneiensis samea*. Biochim Biophys Acta 1494:83–90
40. Kawakami N, Ueki T, Amata Y, Kanamori K, Matsuo K, Gekko K, Michibata H (2009) A novel vanadium reductase, Vanabin2, forms a possible cascade involved in electron transfer. Biochim Biophys Acta 1794:674–679
41. Islam MK, Tsuboya C, Kusaka H, Aizawa S, Ueki T, Michibata H, Kanamori K (2007) Reduction of vanadium(V) to vanadium(IV) by NADPH, and vanadium(IV) to vanadium(III) by cysteine methyl ester in the presence of biologically relevant ligands. Biochim Biophys Acta 1770:1212–1218
42. Kanamori K, Kinebuchi Y, Michibata H (1997) Reduction of vanadium(IV) to vanadium(III) by cysteine methyl ester in water in the presence of aminopolycarboxylates. Chem Lett 26: 423–424
43. Baes CF, Mesmer RE (1976) The hydrolysis of cations. Wiley Ineterscience, New York, pp 197–210
44. Hawkins CJ, Kott P, Pary DL, Swinehart JH (1983) Vanadium content and oxidation state related to ascidian phylogeny. Comp Biochem Physiol 76B:555–558
45. Forgac M (1989) Structure and function of vacuolar class of ATP-driven proton pumps. Physiol Rev 69:765–796
46. Forgac M (1992) Structure, function and regulation of the coated vesicle V-ATPase. J Exp Biol 172:155–169
47. Nelson N (1992) Structure and function of V-ATPases in endocytic and secretory organelles. J Exp Biol 172:149–153
48. Uyama T, Moriyama Y, Futai M, Michibata H (1994) Immunological detection of a vacuolar-type H^+-ATPase in vanadocytes of the ascidian *Ascidia sydneiensis samea*. J Exp Zool 270:148–154
49. Ueki T, Uyama T, Kanamori K, Michibata H (2001) Subunit C of the vacuolar-type ATPase from the vanadium-rich ascidians, *Ascidia sydneiensis samea*, rescued the pH sensitivity of yeast *vma5* mutants. Mar Biotechol 3:316–321

50. Levine EP (1961) Occurrence of titanium, vanadium, chromium, and sulfuric acid in the ascidian *Eudistoma ritteri*. Science 133:1352–1353
51. Botte L, Scippa S, de Vincentiis M (1979) Content and ultrastructural localization of transitional metals in ascidian ovary. Dev Growth Differ 21:483–491
52. Botte L, Scippa S, de Vincentiis M (1979) Ultrastructural localization of vanadium in the blood cells of Ascidiacea. Experientia 35:1228–1230
53. Scippa S, Botte L, Zierold K, de Vincentiis M (1982) Ultrastructure and X-ray microanalysis of blood cells of *Ascidia malaca*. Acta Zool (Stockholm) 63:121–131
54. Scippa S, Botte L, Zierold K, de Vincentiis M (1985) X-ray microanalytical studies on cryofixed blood cells of the ascidian *Phallusia mammillata.* I. Elemental composition of morula cells. Cell Tissue Res 239:459–461
55. Scippa S, Zierold K, de Vincentiis M (1988) X-ray microanalytical studies on cryofixed blood cells of the ascidian *Phallusia mammillata.* II. Elemental composition of the various blood cell types. J Submicrosc Cytol Pathol 20:719–730
56. Bell MV, Pirie BJS, McPhail DB, Goodman BA, Falk-Petersen IB, Sargent JR (1982) Contents of vanadium and sulphur in the blood cells of *Ascidia mentula* and *Ascidiella aspersa*. J Mar Biol Ass UK 62:709–716
57. Pirie BJS, Bell MV (1984) The localization of inorganic elements, particularly vanadium and sulphur, in haemolymph from the ascidians *Ascidia mentula* (Müller) and *Ascidiella aspersa* (Müller). J Exp Mar Biol Ecol 74:187–194
58. Lane DJW, Wilkes SL (1988) Localization of vanadium, sulphur and bromine within the vanadocytes of *Ascidia mentula* Müller: a quantitative electron probe X-ray microanalytical study. Acta Zool (Stockholm) 69:135–145
59. Frank P, Hedman B, Carlson RMK, Hodgson KO (1994) Interaction of vanadium and sulfate in blood cells from the tunicate *Ascidia ceratodes*: observations using X-ray absorption edge structure and EPR spectroscopies. Inorg Chem 33:3794–3803
60. Frank P, Hedman B, Hodgson KO (1999) Sulfur allocation and vanadium – sulfate interactions in whole blood cells from the tunicate *Ascidia ceratodes*, investigated using X-ray absorption spectrometry. Inorg Chem 38:260–270
61. Anderson DH, Swinehart JH (1991) The distribution of vanadium and sulfur in the blood cells, and the nature of vanadium in the blood cells and plasma of the ascidian, *Ascidia ceratodes*. Comp Biochem Physiol 99A:585–592
62. Kanamori K, Michibata H (1994) Raman spectroscopic study of the vanadium and sulphate in blood cells homogenates of the ascidian, *Ascidia gemmata*. J Mar Biol Ass UK 74:279–286
63. Ueki T, Furuno N, Xu Q, Nitta Y, Kanamori K, Michibata H (2009) Identification and biochemical analysis of a homolog of a sulfate transporter from a vanadium-rich ascidian *Ascidia sydneiensis samea*. Biochim Biophys Acta 1790:1295–1300
64. Thomas D, Surdin-Kerjan Y (1997) Metabolism of sulfur amino acids in *Saccharomyces cerevisiae*. Microbiol Mol Biol Rev 61:503–532
65. De Meio RM (1975) Sulfate activation and transfer. In: Greenberg DM (ed) Metabolism of sulfur compounds, vol VII, Metabolic pathway. Academic, New York, pp 287–358
66. Siegel LM (1975) Biochemistry of the sulfur cycle. In: Greenberg DM (ed) Metabolism of sulfur compounds, vol VII, Metabolic pathway. Academic, New York, pp 217–286
67. Michibata H, Ueki T (2010) Advances in research on the accumulation, redox behavior, and function of vanadium in ascidians. Biomol Concept 1:97–107
68. Kanda T, Nose Y, Wuchiyama J, Uyama T, Moriyama Y, Michibata H (1997) Identification of a vanadium-associated protein from the vanadium-rich ascidian, *Ascidia sydneiensis samea*. Zool Sci 14:37–42
69. Ueki T, Adachi T, Kawano S, Aoshima M, Yamaguchi N, Kanamori K, Michibata H (2003) Vanadium-binding proteins (vanabins) from a vanadium-rich ascidian *Ascidia sydneiensis samea*. Biochim Biophys Acta 1626:43–50
70. Ueki T, Satake M, Kamino K, Michibata H (2008) Sequence variation of Vanabin2-like vanadium-binding proteins in blood cells of the vanadium-accumulating ascidian *Ascidia sydneiensis samea*. Biochim Biophys Acta 1780:1010–1015

71. Ueki T, Kawakami N, Toshishige M, Matsuo K, Gekko K, Michibata H (2009) Characterization of vanadium-binding sites of the vanadium-binding protein Vanabin2. Biochim Biophys Acta 1790:1327–1333
72. Kawakami N, Ueki T, Matsuo K, Gekko K, Michibata H (2006) Selective metal binding by Vanabin2 from the vanadium-rich ascidian, *Ascidia sydneiensis samea*. Biochim Biophys Acta 1760:1096–1101
73. Yamaguchi N, Kamino K, Ueki T, Michibata H (2004) Expressed sequence tag analysis of vanadocytes in a vanadium-rich ascidian, *Ascidia sydneiensis samea*. Mar Biotechnol (NY) 6:165–174
74. Yamaguchi N, Amakawa Y, Yamada H, Ueki T, Michibata H (2006) Localization of vanabins, vanadium-binding proteins, in the blood cells of the vanadium-rich ascidian *Ascidia sydneiensis samea*. Zool Sci 23:909–915
75. Yoshihara M, Ueki T, Watanabe T, Yamaguchi N, Kamino K, Michibata H (2005) VanabinP, a novel vanadium-binding protein in the blood plasma of an ascidian, *Ascidia sydneiensis samea*. Biochim Biophys Acta 1730:206–214
76. Hamada T, Asanuma M, Ueki T, Hayashi F, Kobayashi N, Yokoyama S, Michibata H, Hirota H (2005) Solution structure of Vanabin2, a vanadium(IV)-binding protein from the vanadium-rich ascidian *Ascidia sydneiensis samea*. J Am Chem Soc 127:4216–4222
77. Fukui K, Ueki T, Ohya H, Michibata H (2003) Vanadium-binding protein in a vanadium-rich ascidian *Ascidia sydneiensis samea*: CW and pulsed EPR studies. J Am Chem Soc 125: 6352–6353
78. O'Halloran TV, Culotta VC (2000) Metallochaperones, an intracellular shuttle service for metal ions. J Biol Chem 275:25057–25060
79. Ueki T, Shintaku K, Yonekawa Y, Takatsu N, Yamada H, Hamada T, Hirota H, Michibata H (2007) Identification of vanabin-interacting protein 1 (VIP1) from blood cells of the vanadium-rich ascidian *Ascidia sydneiensis samea*. Biochim Biophys Acta 1770:951–957
80. Trivedi S, Ueki T, Yamaguchi N, Michibata H (2003) Novel vanadium-binding proteins (Vanabins) identified in cDNA libraries and the genome of the ascidian *Ciona intestinalis*. Biochim Biophys Acta 1630:64–70
81. Doig AJ, Williams DH (1991) Is the hydrophobic effect stabilizing or destabilizing in proteins? The contribution of disulphide bonds to protein stability. J Mol Biol 217:389–398
82. Shelton MD, Chock PB, Mieyal JJ (2005) Glutaredoxin: role in reversible protein s-glutathionylation and regulation of redox signal transduction and protein translocation. Antioxid Redox Signal 7:348–366
83. Holmgren A (1989) Thioredoxin and glutaredoxin systems. J Biol Chem 264:13963–13966
84. Åslund F, Berndt KD, Holmgren A (1997) Redox potentials of glutaredoxins and other thiol–disulfide oxidoreductases of the thioredoxin superfamily determined by direct protein–protein redox equilibria. J Biol Chem 272:30780–30786
85. Chrestensen CA, Starke DW, Mieyal JJ (2000) Acute cadmium exposure inactivates thioltransferase glutaredoxin, inhibits intracellular reduction of protein–glutathionyl–mixed disulfides, and initiates apoptosis. J Biol Chem 275:26556–26565
86. Lin Y-F, Yang J, Rosen BP (2007) ArsD residues Cys12, Cys13, and Cys18 form an As(III)-binding site required for arsenic metallochaperone activity. J Biol Chem 282:16783–16791
87. Mukhopadhyay R, Shi J, Rosen BP (2000) Purification and characterization of ACR2p, the *Saccharomyces cerevisiae* arsenate reductase. J Biol Chem 275:21149–21157
88. Lu J, Chew E-H, Holmgren A (2007) Targeting thioredoxin reductase is a basis for cancer therapy by arsenic trioxide. Proc Natl Acad Sci USA 104:12288–12293
89. Ueki T, Uyama T, Kanamori K, Michibata H (1998) Isolation of cDNAs encoding subunits *A* and *B* of the vacuolar-type ATPase from the vanadium-rich ascidian, *Ascidia sydneiensis samea*. Zool Sci 15:823–829
90. Ueki T, Yamaguchi N, Michibata H (2003) Chloride channel in vanadocytes of a vanadium-rich ascidian *Ascidia sydneiensis samea*. Comp Biochem Physiol B Biochem Mol Biol 136:91–98

91. Yoshinaga M, Ueki T, Yamaguchi N, Kamino K, Michibata H (2006) Glutathione transferases with vanadium-binding activity isolated from the vanadium-rich ascidian *Ascidia sydneiensis samea*. Biochim Biophys Acta 1760:495–503
92. Yoshinaga M, Ueki T, Michibata H (2007) Metal binding ability of glutathione transferases conserved between two animal species, the vanadium-rich ascidian *Ascidia sydneiensis samea* and the schistosome *Schistosoma japonicum*. Biochim Biophys Acta 1770:1413–1418
93. Yoshihara M, Ueki T, Yamaguchi N, Kamino K, Michibata H (2008) Characterization of a novel vanadium-binding protein (VBP-129) from blood plasma of the vanadium-rich ascidian *Ascidia sydneiensis samea*. Biochim Biophys Acta 1780:256–263
94. Ueki T, Furuno N, Michibata H (2011) A novel vanadium transporter of the *Nramp* family expressed at the vacuole of vanadium-accumulating cells of the ascidian *Ascidia sydneiensis samea*. Biochim Biophys Acta 1810:457–464
95. Dehal P, Satou Y, Campbell RK, Chapman J, Degnan B, De Tomaso A, Davidson B, Di Gregorio A, Gelpke M, Goodstein DM, Harafuji N, Hastings KE, Ho I, Hotta K, Huang W, Kawashima T, Lemaire P, Martinez D, Meinertzhagen IA, Necula S, Nonaka M, Putnam N, Rash S, Saiga H, Satake M, Terry A, Yamada L, Wang HG, Awazu S, Azumi K, Boore J, Branno M, Chin-Bow S, DeSantis R, Doyle S, Francino P, Keys DN, Haga S, Hayashi H, Hino K, Imai KS, Inaba K, Kano S, Kobayashi K, Kobayashi M, Lee BI, Makabe KW, Manohar C, Matassi G, Medina M, Mochizuki Y, Mount S, Morishita T, Miura S, Nakayama A, Nishizaka S, Nomoto H, Ohta F, Oishi K, Rigoutsos I, Sano M, Sasaki A, Sasakura Y, Shoguchi E, Shin-i T, Spagnuolo A, Stainier D, Suzuki MM, Tassy O, Takatori N, Tokuoka M, Yagi K, Yoshizaki F, Wada S, Zhang C, Hyatt PD, Larimer F, Detter C, Doggett N, Glavina T, Hawkins T, Richardson P, Lucas S, Kohara Y, Levine M, Satoh N, Rokhsar DS (2002) The draft genome of *Ciona intestinalis*: insights into chordate and vertebrate origins. Science 298:2157–2167
96. Satou Y, Kawashima T, Kohara Y, Satoh N (2003) Large scale EST analyses in *Ciona intestinalis*: its application as Northern blot analyses. Dev Genes Evol 213:314–318
97. Satou Y, Yamada L, Mochizuki Y, Takatori N, Kawashima T, Sasaki A, Hamaguchi M, Awazu S, Yagi K, Sasakura Y, Nakayama A, Ishikawa H, Inaba K, Satoh N (2002) A cDNA resource from the basal chordate *Ciona intestinalis*. Genesis 33:153–154
98. Sasaki A, Satoh N (2007) Effects of 5-aza-2′-deoxycytidine on the gene expression profile during embryogenesis of the ascidian *Ciona intestinalis*: a microarray analysis. Zool Sci 24:648–655
99. Hozumi A, Kawai N, Yoshida R, Ogura Y, Ohta N, Satake H, Satoh N, Sasakura Y (2010) Efficient transposition of a single Minos transposon copy in the genome of the ascidian *Ciona intestinalis* with a transgenic line expressing transposase in eggs. Dev Dyn 239:1076–1088
100. Sasakura Y, Awazu S, Chiba S, Satoh N (2003) Germ-line transgenesis of the Tc1/mariner superfamily transposon Minos in *Ciona intestinalis*. Proc Natl Acad Sci USA 100:7726–7730
101. Sasakura Y, Oogai Y, Matsuoka T, Satoh N, Awazu S (2007) Transposon mediated transgenesis in a marine invertebrate chordate: *Ciona intestinalis*. Genome Biol 8(Suppl 1):S3

Chapter 4
Hyper-Accumulation of Vanadium in Polychaetes

Daniele Fattorini and Francesco Regoli

Abstract The present chapter summarizes our current knowledge on vanadium accumulation in polychaetes, with special emphasis on tube-dwelling fan worms of the Sabellidae family. Some of these species exhibit the unusual capability to hyperaccumulate vanadium at levels several order of magnitude higher than those commonly found in most aquatic organisms. Concentrations higher than 5,000 and 10,000 μg/g were measured in branchial crowns of *Pseudopotamilla occelata* and *Perkinsiana littoralis* respectively, stored in vacuoles of the epithelial cells. These tissues appear as feather-like filaments, typically expanded for filter-feeding and respiration activities, while the rest of the body remain protected inside the tube. Feeding trials suggested that the elevated levels of vanadium in branchial filaments of sabellids can act as chemical deterrents against predation in more exposed tissues. A similar function, recently proposed also for the elevated levels of arsenic in branchial crowns of *Sabella spallanzanii* suggest that hyperaccumulation of toxic metals is a common antipredatory strategy for branchial crowns of sabellid polychaetes, which often results unpalatable for consumers.

Keywords Vanadium • Marine organisms • Polychaetes • Sabellidae • Branchial crowns • Hyper-accumulation • Subcellular distribution • Biological functions • Chemical defenses • Anti-predatory strategy

4.1 Introduction

Vanadium constitutes more than 0.01% of the earth's crust, but its accumulation in form of ores or minerals is considered generally rare; inorganic compounds with oxidation states III, IV and V are largely dispersed in various environmental

D. Fattorini • F. Regoli (✉)
Dipartimento di Scienze della Vita e dell'Ambiente, Università Politecnica delle Marche, Via Ranieri (Montedago) 65, Ancona 60131, Italy
e-mail: d.fattorini@univpm.it; f.regoli@univpm.it

H. Michibata (ed.), *Vanadium: Biochemical and Molecular Biological Approaches*,
DOI 10.1007/978-94-007-0913-3_4,

matrices like soils, water basins and atmosphere [1, 2]. Mean levels of vanadium in the oceans usually range between 1 and 3 μg/L, corresponding to an average vanadate concentration of about 30 nM, which makes this element one of the more distributed in water column, only lower than molybdenum (about 100 nM), but largely more abundant than iron (less than 1 nM). Concentrations of vanadium in seawater can vary widely rising up to about 30 μg/L [3], and vent-derived iron oxides have been shown to scavenge vanadium, thus contributing to modulate its concentration and cycling in the ocean [4].

Despite the environmental relevance of vanadium in **aquatic systems**, the bioaccumulation dynamics of this metal have been not intensively investigated. Data on tissue concentrations are available only for a limited number of species around the world and the potential biological function of this element has been often debated. With the notable exception of tunicates (see Chap. 3), vanadium concentrations in tissues of **marine organisms** are generally in the order of ng/g, rarely up to the μg/g. Nonetheless, an unusual variability to accumulate vanadium has been reported for polychaetes with levels ranging from less than one to thousands of μg/g in some species [5–7]. Particularly high concentrations of vanadium in specific tissues of certain polychaetes may reflect a more general feature to hyperaccumulate toxic metals [6, 8–10]. In this light, the present chapter reviews our knowledge on vanadium concentrations in marine organisms (excluding tunicates), with particular emphasis to polychaetes and the potential biological role of this element in such species.

4.2 Vanadium Bioaccumulation in Marine Organisms

Various authors agree that vanadium is one of the less investigated metals in tissues of living, especially marine, animals [7, 11–13]. During the last 30 years, concentrations of vanadium have been characterized in approximately 100 organisms distributed among algae, bivalves, cephalopods, crustaceans, echinoderms, fishes and cetaceans (Table 4.1). A similar lack of data could be partly due to the limited interaction of this element with biological functions [2, 14, 15]; beside the typical vanadium containing proteins (vanabins) of tunicates [15–22], this element is required by the vanadate-dependent haloperoxidases, which catalyse the halogenation of organic substrates in the presence of inorganic halide by peroxide via specific intermediates [2, 14]. In addition, tissue concentrations of vanadium in aquatic species are often close to detection limits of most conventionally adopted analytical methods making this element not always suitable for routine analyses [7, 12, 13, 23].

Among available data, vanadium content in several green and brown **algae** from the Red Sea ranged from about 0.1 to 1 μg/g, and up to 3 μg/g only in the phaeophyceae *Padina boryana* [24]. Higher values were reported in the Antarctic red algae *Phyllophora antarctica*, where vanadium concentration ranged from about 5 to 10 μg/g in different sampling areas (Table 4.1) [12].

Table 4.1 Vanadium concentrations reported in tissues of various marine organisms including algae, bivalves, cephalopods, crustaceans, echinoderms, fishes and cetaceans

Taxa	Location	Species	Tissue	V μg/g (d.w.)	Ref.
Algae	Red Sea, Saudi Arabia	*Acanthophora najadiformis*	Whole algae	1.06	[24]
		Caulerpa racemosa	Whole algae	0.65	
		Cladophora heteronema	Whole algae	0.43	
		Cystoseira myrica	Whole algae	0.99	
		Digenea simplex	Whole algae	1.37	
		Enteromorpha clathrata	Whole algae	0.90	
		Halimeda opuntia	Whole algae	0.54	
		Hypnea musciformis	Whole algae	0.32	
		Laurencia obtusa	Whole algae	0.32	
		Padina boryana	Whole algae	2.96	
		Sargassum subrepandum	Whole algae	0.11	
		Turbinaria triquetra	Whole algae	0.16	
	Cape Evans (Antarctica)	*Phyllophora antarctica*	Whole algae	5.44 ± 0.11	[12]
	Terra Nova Bay (Antarctica)	*Phyllophora antarctica*	Whole algae	10.0 ± 0.1	
Bivalves	Oganawa Bay, Japan	*Mytilus coruscus*	Soft tissues	0.12 ± 0.01	[11]
	Tanesashi Bay, Aomori, Japan	*Mytilus galloprovincialis*	Soft tissues	0.20 ± 0.30	
	Tona Bay, Miyagi, Japan	*Mytilus galloprovincialis*	Soft tissues	0.62 ± 0.20	
	Galicia, Spain	*Cardium edule*	Soft tissues	5.14 ± 0.14	[25]
		Ensis ensis	Soft tissues	3.75 ± 0.22	
		Mytilus galloprovincialis	Soft tissues	2.73 ± 0.12	
		Venerupis rhomboides	Soft tissues	2.93 ± 0.03	
	Poland	*Mytilus edulis*	Soft tissues	0.96–1.36	[26]
	French seashore	*Crassostrea gigas*	Soft tissues	0.50–2.70	[27]
		Mytilus edulis	Soft tissues	0.60–4.10	
	Terra Nova Bay (Antarctica)	*Adamussium colbecki*	Soft tissues	1.00 ± 0.30	[23]
	Terra Nova Bay (Antarctica)	*Adamussium colbecki*	Soft tissues	1.43 ± 0.23	[7]
		Yoldia eightsii	Soft tissues	2.51 ± 0.18	
	Cape Evans (Antarctica)	*Laternula elliptica*	Digestive gland	17.5 ± 0.11	[12]
			Soft tissues	1.71 ± 0.11	
	Terra Nova Bay (Antarctica)	*Laternula elliptica*	Digestive gland	6.63 ± 0.11	
			Soft tissues	2.24 ± 0.11	

(continued)

Table 4.1 (continued)

Taxa	Location	Species	Tissue	V μg/g (d.w.)	Ref.
	Venezuelan coasts	*Tivela mactroides*	Soft tissues	0.50–6.13	[28]
	Adriatic sea (Mediterranean)	*Mytilus galloprovincialis*	Soft tissues	0.50–7.47	[29]
Cephalopods	French coast, English Channel	*Eledone cirrhosa*	Digestive gland	3.3 ± 0.5	[32]
			Whole tissues	1.0 ± 0.2	
	French coast, English Channel	*Octopus vulgaris*	Digestive gland	4.5 ± 1.0	[31]
			Whole tissues	0.7 ± 0.1	
	Galicia, Spain	*Sepia officinalis*	Whole tissues	0.95 ± 0.12	[25]
	French coast, English Channel	*Sepia officinalis*	Digestive gland	5.0 ± 1.3	[32]
			Whole tissues	0.7 ± 0.2	
	Seine river Bay, France	*Sepia officinalis*	Digestive gland	3.3 ± 0.1	[33]
			Whole tissues	0.5 ± 0.2	
	New Caledonia	*Nautilus macromphalus*	Digestive gland	8.8 ± 2.0	[34]
Crustaceans	Al-Saflyah, Qatar	*Penaeus semisulcatus*	Soft tissues	0.071 ± 0.009	[35]
	Messaied, Qatar	*Penaeus semisulcatus*	Soft tissues	0.531 ± 0.104	
	Ras Laffan, Qatar	*Penaeus semisulcatus*	Soft tissues	0.114 ± 0.017	
	Kuwait	*Macrophthalmus depressus*	soft tissues	0.52–2.30	[36]
	Baffin Bay (Greenland)	*Calanus hyperboreus*	Soft tissues	0.11 ± 0.02	[37]
		Mysis oculata	Soft tissues	0.14 ± 0.05	
		Themisto libellula	Soft tissues	0.12 ± 0.05	
	Mekong Delta, South Vietnam	*Macrobrachium equidens*	Soft tissues	0.72 ± 0.43	[38]
		Macrobrachium rosenbergii	Soft tissues	0.37 ± 0.19	
		Macrobrachium sp.	Soft tissues	0.54 ± 0.37	
		Metapenaeus tenuis	Soft tissues	0.11	
	Galicia, Spain	*Cancer pagurus*	Soft tissues	3.54 ± 0.12	[25]
		Palaemon elegans	Soft tissues	2.14 ± 0.16	
		Panaeus kerathurus	Soft tissues	2.04 ± 0.12	

(continued)

Table 4.1 (continued)

Taxa	Location	Species	Tissue	V μg/g (d.w.)	Ref.
Echinoderms	Cape Evans (Antarctica)	*Odontaster validus*	Soft tissues	1.87 ± 0.11	[12]
		Odontaster validus	Arms	0.52 ± 0.01	
	Cape Evans (Antarctica)	*Sterechinus neumayeri*	Soft tissues	2.25 ± 0.11	
		Odontaster validus	Soft tissues	1.88 ± 0.11	
		Odontaster validus	Arms	0.47 ± 0.01	
		Sterechinus neumayeri	Soft tissues	2.41 ± 0.11	
Fish	Al-Saflyah, Qatar	*Sphyraena jello*	Muscle	0.032 ± 0.003	[35]
		Siganus canaliculatus	Muscle	0.024 ± 0.004	
		Rhabdosargus sarbo	Muscle	0.029 ± 0.006	
		Platycephalus indicus	Muscle	0.011 ± 0.003	
		Nematalosa nasus	Muscle	0.023 ± 0.006	
		Lethrinus nebulosus	Muscle	0.021 ± 0.004	
		Gnathanodon speciosus	Muscle	0.042 ± 0.007	
		Epinephelus tauvina	Muscle	0.014 ± 0.004	
		Crenidens crenidens	Muscle	0.031 ± 0.005	
		Siganus canaliculatus	Muscle	0.083 ± 0.011	
		Scomberoides commersonnianus	Muscle	0.087 ± 0.022	
		Rhabdosargus sarbo	Muscle	0.073 ± 0.019	
		Platycephalus indicus	Muscle	0.069 ± 0.017	
		Lethrinus nebulosus	Muscle	0.135 ± 0.026	
		Gnathanodon speciosus	Muscle	0.077 ± 0.023	
		Gerres oyena	Muscle	0.091 ± 0.014	
		Epinephelus tauvina	Muscle	0.232 ± 0.043	
		Crenidens crenidens	Muscle	0.091 ± 0.013	
	Ras Laffan, Qatar	*Sphyraena jello*	Muscle	0.039 ± 0.014	
			Spleen	0.74 ± 0.01	
		Scomberoides commersonnianus	Muscle	0.041 ± 0.009	
		Nematalosa nasus	Muscle	0.036 ± 0.011	
		Lethrinus nebulosus	Muscle	0.053 ± 0.011	
		Gnathanodon speciosus	Muscle	0.031 ± 0.006	
		Gerres oyena	Muscle	0.047 ± 0.009	
		Epinephelus tauvina	Muscle	0.064 ± 0.006	

(continued)

Table 4.1 (continued)

Taxa	Location	Species	Tissue	V μg/g (d.w.)	Ref.
Fish	Azerbaijan, Caspian Sea	*Neogobius melanostomus*	Muscle	0.048 ± 0.027	[39]
		Clupeonella delicatula	Muscle	0.064 ± 0.031	
	Iran, Caspian Sea	*Rutilus frisii*	Muscle	0.012 ± 0.005	
		Rutilus caspicus	Muscle	0.016 ± 0.008	
		Clupeonella delicatula	Muscle	0.012 ± 0.006	
	Kazakhstan, Caspian Sea	*Rutilus caspicus*	Muscle	0.025 ± 0.014	
		Neogobius fluviatilis	Muscle	0.026 ± 0.006	
	Turkmenistan, Caspian Sea	*Rutilus caspicus*	Muscle	0.019 ± 0.002	
		Neogobius sp.	Muscle	0.017 ± 0.009	
	Mekong Delta, South Vietnam	*Puntioplites proctozysron*	Muscle	0.36	[38]
		Polynemus paradiseus	Muscle	0.39 ± 0.11	
		Pisodonophis boro	Muscle	0.23	
		Parambassis wolffii	Muscle	0.20	
		Glossogobius aureus	Muscle	0.98 ± 0.33	
		Eleotris melanosoma	Muscle	0.95	
		Cynoglossus sp.	Muscle	0.85	
		Cyclocheilichthys armatus	Muscle	0.57	
		Clupeoides sp.	Muscle	0.38	
	Galicia, Spain	*Solea solea*	Muscle	1.17 ± 0.06	[25]
		Merluccius merluccius	Muscle	0.82 ± 0.05	
		Lepidorhombus whiffiagonis	Muscle	1.25 ± 0.08	
	Cape Evans (Antarctica)	*Trematomus bernacchii*	Muscle	0.05 ± 0.01	[12]
	Terra Nova Bay (Antarctica)	*Trematomus bernacchii*	Muscle	1.16 ± 0.11	
			Gonad	1.59 ± 0.11	
			Liver	1.23 ± 0.11	
Cetaceans	Adriatic Sea, Italy	*Grampus griseus*	Kidney	0.10	[13]
			Liver	0.09	
			Muscle	0.04	
		Tursiops truncatus	Kidney	0.04–0.23	
			Liver	0.44–0.53	
			Muscle	0.04	
	Ligurian Sea, Italy	*Ziphius cavirostris*	Kidney	3.71	
			Liver	0.04	
			Muscle	0.03	

(continued)

Table 4.1 (continued)

Taxa	Location	Species	Tissue	V μg/g (d.w.)	Ref.
	Sicily Channel, Italy	*Grampus griseus*	Heart	0.09	
			Kidney	0.15	
			Liver	0.12	
			Lung	0.09	
		Physeter macrocephalus	Heart	0.67	
			Kidney	0.25	
			Liver	0.35	
			Lung	0.31	
			Muscle	0.09	
		Stenella coeruleoalba	Heart	0.08–0.23	
			Kidney	0.12–0.28	
			Liver	0.07–0.86	
			Lung	0.15–1.28	
			Muscle	0.06–0.61	
Cetaceans	Sicily Channel, Italy	*Tursiops truncatus*	Heart	0.14–0.28	[13]
			Kidney	0.13–0.92	
			Liver	0.25–0.52	
			Lung	0.09–0.28	
			Muscle	0.12–0.36	
		Ziphius cavirostris	Kidney	10.83	
			Lung	5.65	
			Muscle	0.97	
	Tyrrhenian Sea, Italy	*Physeter macrocephalus*	Kidney	0.09	
			Liver	0.13	
			Muscle	0.07	
		Stenella coeruleoalba	Kidney	6.71	
			Liver	0.16–0.50	
			Muscle	0.04–2.02	
		Tursiops truncatus	Kidney	0.06–0.12	
			Liver	0.03–0.41	
			Muscle	0.05–0.20	
		Ziphius cavirostris	Kidney	0.02	
			Muscle	0.05	
	Arctic Sea, Alaska	*Balaena mysticetus*	Liver	0.32–4.80	[40]
		Delphinapterus leucas	Liver	0.12–0.76	
	Atlantic Ocean	*Delphinapterus leucas*	Liver	0.04–0.08	[41]
		Lagenorhynchus acutus	Liver	0.04–0.24	
		Phocoena phocoena	Liver	0.04–0.08	

(continued)

Table 4.1 (continued)

Taxa	Location	Species	Tissue	V μg/g (d.w.)	Ref.
	Brazilian coasts	*Pontoporia blainvillei*	Liver	0.04–0.22	[42]
		Stenella attenuata	Liver	0.20–0.27	
	Japanese costs	*Stenella coeruleoalba*	Liver	0.01–0.28	[43]

Concentrations are expressed as μg/g dry weight (single values or mean values ± standard deviations, as given in original references)

Levels measured in tissues of various **bivalves** from temperate areas, were generally between 0.5 and 5 μg/g [7, 11, 23, 25, 26] with limited increases observed in oysters and mussels from French coast after restricted contamination episodes (about 0.5–4 μg/g) [27]. Similar ranges were measured in the Antarctic species *Adamussium colbecki* and *Yoldia eightsii* [7], while in the soft-shelled clam *Laternula elliptica* the vanadium concentrations were higher, especially in the digestive gland, from about 6 to 17 μg/g (Table 4.1) [12]. The absence of an extended database on vanadium in bivalve tissues and the limited knowledge on the influence of both temporal or geographical variability, preclude a mechanistic or environmental interpretation of the differences between various species. In this respect natural oscillations were shown to drastically modulate the vanadium concentrations in the soft tissues of the clam *Tivela mactroidea* from the Venezuelan coast, with values seasonally ranging from 0.5 to more than 6 μg/g [28]. Similarly, marked seasonal fluctuations of vanadium content were also observed in tissues of the Mediterranean mussel, *Mytilus galloprovincialis*, from the Adriatic sea (from about 0.5 to 7.5 μg/g) [29]; such changes could be ascribed to both environmental and biological factors, including the phytoplanctonic bloom in late winter, which has an important role in transferring metals from the water column to filter-feeding organisms, and the phase of reproductive cycle with development of gonadic tissues which have a lower accumulation capability [29, 30].

Vanadium in whole tissues of **cephalopods**, including *Octopus vulgaris*, *Elodone cirrhosa* and *Sepia officinalis* is usually lower than 1 μg/g, while more elevated levels (3 μg/g) have been observed in *Nautilus macromphalus* from the New Caledonia [25, 31–34]. All these species exhibited higher concentrations in digestive tissues (approximately 3–9 μg/g), suggesting the diet and trophic transfer as probably the more important source for vanadium in these marine organisms.

Also **crustaceans** generally exhibited low levels of vanadium in their tissues, from less than 0.1 to 0.5 μg/g in various species from Qatar, Kuwait, Vietnam and Greenland [35–38]; levels of approximately 2–3 μg/g were measured in the soft tissues of crab (*Cancer pagurus*) and shrimps (*Palaemon elegans* and *Panaeus kerathurus*) from the Galician coasts in Spain [25].

The only available data for vanadium in **echinoderms** have been reported by Grotti et al. [12]: approximately 2 μg/g were detected in the soft tissues of the Antarctic species *Odontaster validus* and *Sterechinus neumayeri* from Cape Evans and Terra Nova Bay, and lower concentrations (about 0.5 μg/g) in their arms.

In general these results seems to confirm a certain tendency of some Antarctic marine invertebrates to concentrate slightly higher levels of vanadium compared to temperate organisms [7, 12, 23].

Overall the review of literature data on invertebrates highlight a variability of vanadium concentrations distributed in three orders of magnitude (from about 0.1 to more than 10 μg/g). However, our actual knowledge is still too limited to clarify if this variability is related to species-specific or biological features, environmental and climate conditions, geographical characteristics or geochemical anomalies, to cite a few. All the investigated taxonomic groups are represented by a very little sample size (a dozen of species as maximum), and a more extended database would be necessary to characterize biological and environmental factors affecting vanadium bioavailability and accumulation in aquatic organisms.

Among aquatic vertebrates, approximately 40 different **fish** species from Qatar and the Caspian Sea exhibited values not exceeding 0.1 μg/g in the muscle fillets, with a median value of approximately 0.05 μg/g (Table 4.1) [35, 39]. Slightly more elevated levels of vanadium have been measured in muscle of fish from the Mekond Delta in the Southern Vietnam, with values ranging from approximately 0.2 to 1.0 μg/g [38]; this area is characterized by increasing population and agricultural activities which might have influenced trace metal bioavailability for organisms inhabiting these areas [38]. However, values of approximately 1 μg/g were also measured in muscle of *Lepidorhombus whiffiagonis*, *Merluccius merluccius* and *Solea solea* from unpolluted areas of Galicia (Spain) [25], suggesting that the specific regional characteristics can modulate vanadium bioavailability in fish tissue. Vanadium content in other fish tissues were available for liver and gonads of the Antarctic *T. bernacchii* [12] and for the spleen of *Sphyraena jello* from the Qatar [35], representing a too limited dataset for any comparison (Table 4.1).

An interesting historical report of trace metal concentrations, including vanadium, has been reported for several organs (heart, kidney, liver, lung and muscle) of various cetacean specimens accidentally stranded along the Italian coasts (Table 4.1) [13]. The overall results did not reveal any significant differences as a function of the geographical area, the species or the analyzed organ; concentrations in muscle and liver tissue, (the most abundant sampled organs), ranged from about 0.04 to 1.3 μg/g, while slightly more elevated concentrations were observed in the kidney of several specimens of *Ziphius cavirostris* and *Stenella coeruleoalba* (4–10 μg/g), and in the lung of a single individual of *Z. cavirostris* from the Sicily Channel (about 5 μg/g). These results were generally in agreement with those reported for other **cetaceans** in open oceans with mean vanadium liver content from 0.01 to 4.80 μg/g [40–43].

4.3 Vanadium Bioaccumulation in Polychaetes

The characterization of vanadium content in **polychaetes** tissues is limited to a few species around the world (Fig. 4.1). The overall data reveal an elevated variability with values distributed among six order of magnitude, from less than 0.1

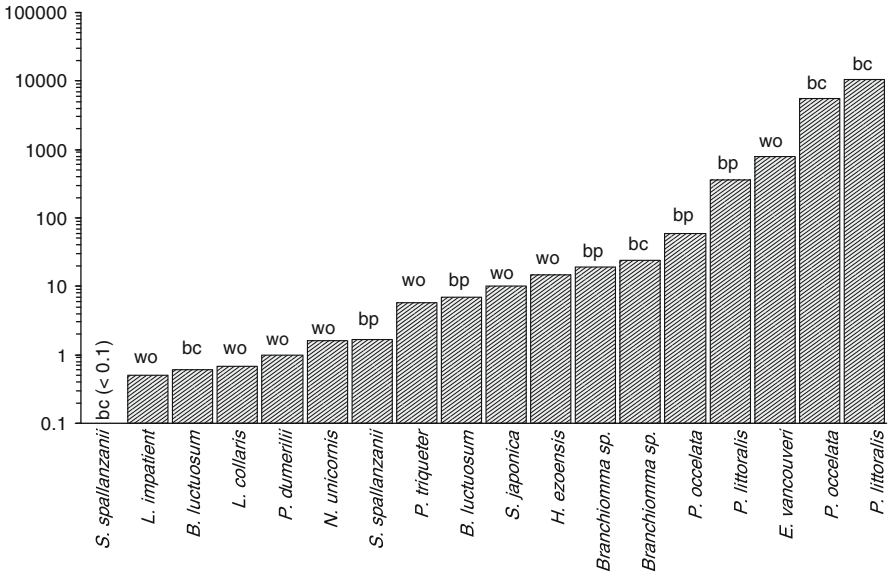

Fig. 4.1 Vanadium concentrations in tissues of various polychaete species. Values are given as μg/g (d.w.) and represent the highest levels measured in each species as given in original reference [5–7]. The y-axis was log transformed to better show the great variability of data (*br* branchial crown, *bp* body portion, *wo* whole organism)

to more than 10,000 μg/g. Polychaetes from the Mediterranean, including species from the family Eunicidae (*Lysidice collaris*, *Nematonereis unicornis*), Lumbrineridae (*Lumbrineris impatient*), Nereididae (*Platynereis dumerilii*), **Sabellidae** (*Branchiomma luctuosum*, *S. spallanzanii*) and Serpulidae (*Pomatoceros triqueter*), exhibited concentrations ranging between 0.5 and 7 μg/g [7], while values from 10 to 15 μg/g have been measured in the Mediterranean sabellid *Branchiomma* sp., and in *Sabellastarte japonica* and the serpulid *Hydroides ezoensis* from Japan [6]. Nonetheless, contrasting with the generally limited bioaccumulation of vanadium in marine organisms, some polychaetes contain unusually elevated tissue levels of this element, which appear a widespread, but not constant feature within sabellid species [7].

The sabellid *Eudistylia vancouveri* was the first marine worm characterized in terms of capability to accumulate vanadium from the environment [5]. This polychaete is a tube dwelling species of approximately 25–30 cm in length, generally forming large colonies attached to rocks or to other hard substrates, in shallow waters and up to 20 m depth [44, 45]; it is a very common species from South California to the British Columbia, Vancouver Island and Alaska. In the early 1980s this species was proposed as potential bioindicator of trace metal pollution due its ability to concentrate elements such as copper, titanium and, especially, vanadium at a significantly higher rate than observed in mussels, *Mytilus edulis*, from the same areas [5, 44, 45]. In particular, concentrations of vanadium ranged

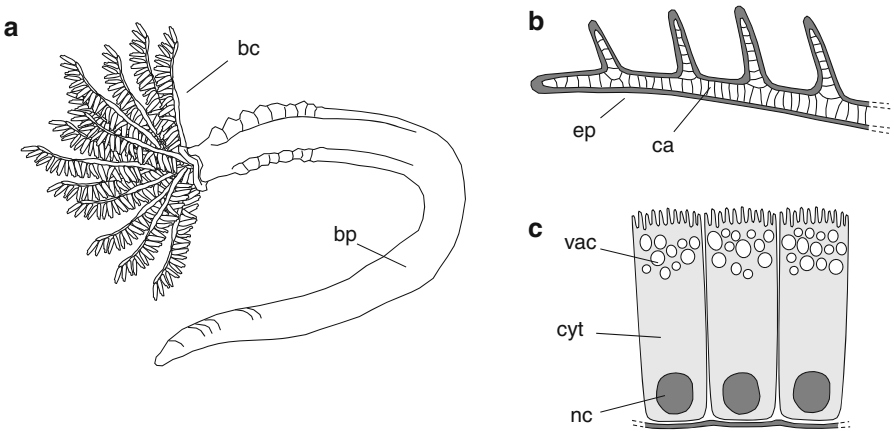

Fig. 4.2 (**a**) schematic representation of a generic sabellid polychaete without its self-constructed muddy or sandy tube. This marine worms possess branchial crown (*bc*) representing feather-like filaments involved in filter-feeding and respiration activities; the body portion (*bp*) is a well separated anatomical structure protected inside the tube. Branchial filaments are constituted by a series of radioles (**b**) with an internal cartilaginous structure (*ca*) covered by an outer epithelial layer (*ep*); the latter is formed by a single layer of cylindrical cells (**c**) with large vacuoles (*vac*) in apical position in the cytoplasm (*cyt*) and *oval-shaped* nucleus (*nc*) in the base of the cell

from about 90 to almost 800 μg/g in the whole tissues of *E. vancouveri* collected along a pollution gradient [5]. These results, much higher than those normally observed in marine species (with the exception of tunicates), allowed to indicate *E. vancouveri* as the first reported vanadium hyperaccumulator organism, although mechanisms and sites of storages remained to be elucidated.

Similar characteristics of vanadium **hyperaccumulation** have been then reported in another sabellid polychaete, *Pseudopotamilla occelata* [6, 46]. This is a widely distributed species in the Pacific Ocean, mainly inhabiting shallow coastal waters of the East Sea from Russia to China and Japan, commonly found in numerous colonies aggregated to hard substrates [47]. Specimens of 15 cm in length live inside a self constructed tube, formed by sand particles and mucus, that provide protection to body tissues, while the branchial crowns, composed by two opposing half circles of bipinnate radioles, are typically expanded outside the tube for filter-feeding and respiration activities (Fig. 4.2). Specimens of *P. occelata* from Sanriku coast, North-eastern Japan, were show to concentrate extremely high levels of vanadium in branchial crowns, ranging from 3,000 to over 7,000 μg/g, values approximately 100 fold higher than those measured in the rest of body tissues (up to 50 μg/g) [46].

The analyses of **subcellular distribution** revealed that 90% of vanadium body burden was concentrated into the bipinnate radioles, which represent only the 7% of the whole polychaete weight. The metal was mainly localized in the epithelial layer covering the internal cartilaginous-like structures of the branchial filaments which contain fibrous proteins, sulfonated mucopolysaccharides, and

matrix components [48]; it occurred with an ionic trivalent (III) state in a highly symmetrical octahedral coordination, and soluble form [46]. An additional investigation combining transmission and scanning electron microscopy techniques, with X-ray microanalysis on epithelial cells of branchial filaments highlighted the presence of large vacuoles in the apical portion of the cytoplasm opposite to oval-shaped nuclei (Fig. 4.2) [6]. The X-ray microanalyses indicated the highest content of vanadium inside the vacuole formations, although the metal did not appear to be uniformly distributed in the epithelium; concentrations inside the vacuoles were estimated to be more than 6,000 μg/g on a wet weight basis, corresponding to about 30,000 μg/g dry weight [6].

This intracellular distribution of vanadium has homologies with that reported for ascidians, where this element is concentrated mainly within vacuoles of the signet ring cells, the so-called vanadocytes [17, 19–21]. The accumulation and storage of vanadium in ascidians is modulated by a group of vanadium-associated proteins (now vanabins), initially identified in blood cells of *Ascidia sydneiensis samea* as two major proteins of 12.5 and 15.0 kDa and a minor peptide of 16 kDa [21]. The family of vanabins now includes five closely related small proteins, and novel vanadium-binding proteins, not homologous to vanabins have been isolated in ascidian blood cells including VBP129, AsGST-I and AsGST-II with a striking homology to glutathione S-transferases [15, 49]. These proteins have been shown to bind vanadium accumulated from seawaters and to reduce it in the cytosol from V(V) to V(IV) in the presence of glutathione (GSH), glutathione reductase and an electron transfer cascade from NADPH [15, 20, 22]. The V(IV) would thus be transported into vacuoles and further reduced to V(III) by unknown reductants. A similar mechanism for vanadium reduction and accumulation within vacuoles could be suggested also for sabellid polychaetes. In fact polyclonal antibodies against ascidian vanadium binding proteins, recognized the same antigen in the epithelial cells of branchial crowns of *P. occelata*; the presence a group of vanadium binding proteins in the polychaete tissues could also explain the storage of this element in the +3 oxidation state within vacuoles by *P. occelata* [6, 46, 50].

Hyperaccumulation of vanadium has been recently reported in another sabellid polychaete, *Perkinsiana littoralis*. This fan worm (about 15 cm in length) is a typical species in the Antarctic and sub-Antarctic areas and, as the previously described sabellids (Fig. 4.2), it lives on hard substrates inside a self produced muddy tube protecting the body tissues, while the filter feeding branchial crowns are extended outside [51]. This species has been characterized for the content of several trace metals in body tissues and branchial crowns [7]. With the exception of As, Cd and V, concentrations of trace elements in tissues of *P. littoralis* were similar to those measured in other sabellid species including *E. vancouveri*, *P. occelata*, *P. littoralis* and the Mediterranean *Sabella spallanzanii* (Table 4.2) [5–7, 46, 52–54]. Significant differences were found in the distribution of trace metals levels between tissues of *P. littoralis*, with most of the analyzed elements, including Ag, Al, Co, Cr, Cu, Hg, Pb, Se and V being higher in branchial crowns than in the body tissue (Table 4.2). The elevated levels of cadmium in body tissue of *P. littoralis* (up to 30 μg/g) were associated to the naturally enhanced bioavailability of this metal in the Antarctic

Table 4.2 Concentrations of trace metals in tissues of marine sabellids

	P. littoralis [ref. 7]		*E. vancouveri* [ref. 5]	*P. occelata* [ref. 6]		*S. spallanzanii* [ref. 52–54]	
	Body tissue	Branchial crown	Whole worm	Body tissue	Branchial crown	Body tissue	Branchial crown
Ag	1.46 ± 0.31	15.2 ± 4.2	–	–	–	–	–
Al	50.1 ± 10.8	169 ± 26	–	60 ± 31	180 ± 52	–	–
As	23.6 ± 5.2	21.7 ± 4.5	12.4–17.0	–	–	47.5 ± 19.1	1,036 ± 136
Ba	4.55 ± 0.71	1.27 ± 0.51	–	–	–	–	–
Cd	27.9 ± 4.6	0.81 ± 0.35	–	–	–	1.5–3.0	0.1–0.5
Co	0.25 ± 0.08	0.41 ± 0.06	–	–	–	–	–
Cr	0.14 ± 0.05	0.87 ± 0.17	–	–	–	0.9–1.3	0.5–0.9
Cu	7.36 ± 2.27	26.3 ± 5.4	10–26	4.3 ± 0.7	8.0 ± 3.9	10–24	7.0–30
Fe	110 ± 48	119 ± 7	271–1,574	160 ± 46	300 ± 59	2,400–3,900	1,400–3,900
Hg	0.03 ± 0.01	0.14 ± 0.03	–			–	–
Mn	14.2 ± 1.7	5.83 ± 1.3	9.9–21.7	7.7 ± 2.7	14.5 ± 3.4	3.5–8.9	3.2–11.7
Ni	4.54 ± 1.64	4.39 ± 2.72	0.61–1.08	–	–	1.5–2.6	1.1–2.5
Pb	0.38 ± 0.1	1.75 ± 0.57	3.2–21.3	–	–	1.4–2.0	0.8–1.8
Se	7.51 ± 1.4	21 ± 3.7	–	–	–	–	–
Sr	–	–	–	52 ± 21	34 ± 16	–	–
Ti	–	–	72.5 ± 2.13	–	–	–	–
V	357 ± 67	10,461 ± 1,801	94–786	60 ± 25	5,500 ± 1,800	1.71 ± 0.775	< 0.07
Zn	167 ± 29	89.9 ± 9.6	96–193	71 ± 8	200 ± 89	40–43	54–70

Values are expressed as μg/g (d.w.) and represent the mean levels (± standard deviations) or the range obtained in various specimens, as given in original references contributors [5–7, 52, 54]

Table 4.3 Subcellular distribution of vanadium in branchial crowns of the Antarctic fan worm *P. littoralis* [7]

	Fraction	Distribution (%)		Tissue	Distribution (%)	
Subcellular	H	52.1 ± 3.4%	→	Epithelium	95.7 ± 0.6%	*Enzymatic*
Fractions	ML	8.8 ± 1.4%		Cartilage	4.4 ± 0.3%	*Digestion of H*
	m	2.3 ± 0.4%				
	cyt	36.7 ± 2%				
	↓					
Cytosolic	<3 kDa	21.2 ± 1.4%				
Fractions	3–10 kDa	45.3 ± 2.9%				
	10–30 kDa	16.2 ± 1.8%				
	>30 kDa	17.1 ± 0.9%				

Values are given as percentage contribution of various fractions to the total content of vanadium. Fractions include the heavy pellet (H); mitochondria and lysosomes (ML); microsomes (m); and cytosol (cyt). The latter fraction was subdivided according to molecular weight of proteins. The heavy fraction (H) was enzymatically digested and subdivided in the epithelium and the cartilaginous-likes structure (see text for further details)

region of Terra Nova Bay, characterized by local upwelling phenomena which are responsible for the high concentrations of cadmium in tissues of marine organisms [55]. In general, the different tissue distribution of trace elements in *P. littoralis* was similar to that obtained in *P. ocellata*, with higher concentrations in the radioles [6], while more limited differences between branchial crowns and the body portions were observed in *S. spallanzanii* [52].

Particularly elevated concentrations of vanadium were measured in **branchial crowns** of *P. littoralis*, with mean levels raising up to 10,000 μg/g, 30 fold higher than in the thoracic portion of the organism (>300 μg/g) [7]. Similarly to *P. occelata*, more than 80% of the total vanadium body burden was concentrated in tissues which represent less than 10% of the weight of the animals. Additional similarities between *P. occelata* and *P. littoralis* were shown in the intracellular localization of the vanadium within branchial filaments. Differential centrifugation on homogenates of *P. littoralis* branchial crowns allowed to separate four different fractions [7]: the heavy pellet (H), containing heterogeneous components, inorganic granular concretions, nuclei, cellular debris, and undisrupted tissues; the mitochondria and lysosomes (ML) enriched fraction; the microsomes (m); and the cytosol (cyt). The latter fraction was further separated in soluble and protein components by microconcentration devices with molecular cut-off at 3, 10, and 30 kDa, while the H pellet was subjected to an enzymatic digestion to separate the cartilaginous-like structures from the epithelium (Fig. 4.2) of branched feeding tentacles [7].

More than 50% of vanadium was associated to the heavy pellet (H), 35% to cytosol (cyt), and 10% to mitochondria and lysosomes (ML). Within the H fraction, the separation of the cartilaginous-like structures by the enzymatic digestion allowed to demonstrate that the metal was mostly present (>95%) in epithelial tissues (Table 4.3), in agreement with results obtained in *P. occelata* concentrating vanadium in vacuoles of the epithelial cells [6, 7]. In the cytosolic

fraction of *P. littoralis*, 45% of vanadium was bound to proteins with a molecular weight interval of 3–10 kDa, the remaining being uniformly distributed between soluble compounds (<3 kDa), and in proteins with molecular weight of 10–30 and >30 kDa. (Table 4.3) [7]. These results could corroborate the hypothesis that low molecular weight vanadium binding proteins, similar to those described for ascidians, modulate transport, **biotransformation** and storage of vanadium in polychaete tissues.

4.4 Potential Biological Function of Vanadium in Polychaetes

The presence of extremely elevated levels of vanadium in specific tissues or cells of some polychaetes may suggest a **biological role** for this element. Several polychaetes have been shown to accumulate elevated concentrations of different metals in their tissues [6, 8, 9] and various hypotheses have been made, still representing a stimulating field of investigation. Since the early 1980s, an antipredatory mechanism was hypothesized for the presence of elevated copper levels (600–1,100 μg/g) in the gills of the terebellid *Melinna palmata* [8], while copper or zinc halogens observed in jaws of some nereids, have been related to both a structural function and a first defence against bacteria [56, 57]. An antibacterial activity has been also proposed for the capability of some polychaete species to concentrate cadmium by specific binding proteins [10, 58].

The hyperaccumulation of vanadium in branchial crowns of the sabellid *P. ocellata* has been interpreted as a mechanism to facilitate the oxygen absorption on the surface of bipinnate radioles, or to maintain it when the worm is withdrawn into the tube [6, 46]. This hypothesis was supported by the similarity of *P. occelata* with ascidians in terms of vanadium chemical speciation and presence of antigens for the same vanadium binding protein isolated in *A. sydneiensys samea* [50]. However, an oxygen binding function of vanadium is less convincing to explain the elevated concentrations in branchial crowns of *P. littoralis*; the high levels of dissolved oxygen in cold Antarctic seawater guarantee an elevated adsorption for tissues through diffusion, as also indicated by the loss of haemoglobin in several Antarctic fish species [55]. In addition, data for other sabellids from both the Mediterranean and Japan clearly demonstrate that not all these organisms possess the capability to concentrate vanadium in the filter-feeding branchial filaments [6, 7].

On the other hand, sabellids commonly occur in areas of high consumer activity playing a critical role in several trophic interactions [59–61]. Although chemical defences against consumers have been poorly investigated in sabellid worms, these organisms likely rely on both deterrence and avoidance to persist in predator-rich environments [62, 63]. A recent investigation on defensive traits of several polychaetes species revealed that various sabellids from Caribbean and temperate western Atlantic, including *Bispira brunnea*, *Bispira variegata*, *Anamobaea orstedii*, *Branchiomma nigromaculata*, *Branchiomma* sp., *Megalomma* sp., *Sabellastarte magnifica* and *Sabella* sp., all had unpalatable branchial crowns, and two of these

species also had unpalatable bodies [62]. The compounds potentially responsible for these effects were not identified, but the different palatability of branchial crowns and body portions would indicate that most sabellids possess more efficient antipredatory defences in tissues exposed to consumers, a characteristic reported only for a limited number of marine invertebrates which, through the differential allocation of chemical deterrents, are able to change the palatability of exposed and protected tissues [63].

A chemical **antipredatory strategy** has been associated to the elevated concentrations of arsenic reported as a quite typical characteristic for several polychaetes, and often associated with the presence of moderately toxic compounds, quite unusual for the majority of marine organisms which accumulate this element as organic, nontoxic molecules like arsenobetaine or arsenocholine [64–66]. The Mediterranean fan worm *S. spallanzanii*, was shown to contain exceptionally high levels of arsenic in branchial crowns (up to 1,500 μg/g), approximately 20-fold greater than in body portions [9, 53, 54, 66] representing an interesting similitude with the distribution of vanadium in tissues of *P. occelata* and *P. littoralis* [6, 7]. The predominant chemical form of arsenic observed in *S. spallanzanii* was dimethylarsinic acid (DMA), a moderately toxic compound which the sabellid can synthesize by methylation of inorganic arsenic accumulated from abiotic matrices (i.e. sediments and the water column), or demethylating more complex arsenocompounds normally assumed from phytoplankton through diet [67]. The deterring function of arsenic in more vulnerable tissues of *S. spallanzanii* was corroborated by the evidence that the branchial crowns of this polychaete were unpalatable for the white seabream *Diplodus sargus sargus* which consumed without hesitation the body tissues of the sabellid [54, 67].

A similar defensive role was proposed also for the marked accumulation of vanadium in branchial crowns of *P. littoralis* which were always vigorously rejected by the Antarctic emerald rock cod *T. bernacchii* after tasting the tissues [7]; this effect was not observed in the same fish which, immediately after branchial crowns, were offered a new control food or body tissues of the polychaetes. Investigations on Antarctic ecology demonstrated that chemical defences have evolved in numerous species, and more than 300 natural products, usually produced as secondary metabolites, have been isolated primarily from sponges, cnidarians, molluscs, ascidians, and, to a lesser extent, from other invertebrates and seaweeds [59, 68]. In addition to the high incidence of predation, the Antarctic benthos is mostly exposed to the pressure of mobile macroinvertebrates which reduce the deterrent relevance of physical devices, like structural skeletal elements, well known in tropical environments where fish grazing predominates.

Although several Antarctic marine invertebrates use natural products as **chemical defences** against predation, fouling, overgrowth, and bacteria [60], such metabolites seem quite uncommon in polychaetes; besides mycosporine-like amino acids with ultraviolet protection, only a bromophenolic compound has been described in two species of the genus *Thelepus* (Terebellidae) [68, 69]. In this respect, sabellid worms might have the ability to hyperaccumulate trace elements (like As and V) instead of natural products as chemical defences against predation in more exposed

tissues, an hypothesis strongly supported by the similitude between *S. spallanzanii* and *P. littoralis*. The future characterization of trace metals content (including vanadium) in branchial crowns of other unpalatable sabellids would be useful to evaluate whether such capability can be considered a typical feature of these worms. Certainly, the reasons behind the possibility for different sabellid species to hyperaccumulate different metals is actually unknown, remaining a stimulating hypothesis for future investigations.

References

1. Butler A (1998) Acquisition and utilization of transition metal ions by marine organisms. Science 281:207–209
2. Rehder D (2003) Biological and medicinal aspects of vanadium. Inorg Chem Commun 6: 604–617
3. Sepe A, Ciaralli L, Ciprotti M, Giordano R, Funari E, Costantini S (2003) Determination of cadmium, chromium, lead and vanadium in six fish species from the Adriatic Sea. Food Addit Contam 20:543–552
4. Trefry JH, Metz S (1989) Role of hydrothermal precipitates in the geochemical cycling of vanadium. Nature 342:531–533
5. Popham JD, D'Auria JM (1982) A new sentinel organism for vanadium and titanium. Mar Pollut Bull 13:25–27
6. Ishii T, Otake T, Okoshi K, Nakahara M, Nakamura R (1994) Intracellular localization of vanadium in the fan worm Pseudopotamilla occelata. Mar Biol 121:143–151
7. Fattorini D, Notti A, Nigro M, Regoli F (2010) Hyperaccumulation of vanadium in the Antarctic polychaete *Perkinsiana littoralis* as a natural chemical defense against predation. Environ Sci Pollut Res Int 17:220–228
8. Gibbs PE, Bryan GW, Ryan KP (1981) Copper accumulation by the polychaete *Melinna palmata*: an antipredation mechanism? J Mar Biol Assoc UK 61:707–722
9. Fattorini D, Notti A, Halt MN, Gambi MC, Regoli F (2005) Levels and chemical speciation of arsenic in polychaetes: a review. Mar Ecol 26:255–264
10. Sandrini JZ, Regoli F, Fattorini D, Notti A, Ferreira Inácio A, Linde-Arias AR, Laurino J, Bainy ACS, Marins LFF, Monserrat JM (2006) Short-term responses to cadmium exposure in the estuarine polychaete *Laeonereis acuta* (polychaeta, Nereididae): subcellular distribution and oxidative stress generation. Environ Toxicol Chem 25:1337–1344
11. Fukushima M, Suzuki H, Saito K, Chatt A (2008) Vanadium levels in marine organisms of Onagawa Bay in Japan. Environ Monit Assess 141:329–337
12. Grotti M, Soggia F, Lagomarsino C, Dalla Riva S, Goessler W, Francesconi KA (2008) Natural variability and distribution of trace elements in marine organisms from Antarctic coastal environments. Antarctic Sci 20:39–51
13. Bellante A, Sprovieri M, Buscaino G, Salvagio Manta D, Buffa G, Di Stefano V, Bonanno A, Barra M, Patti B, Giacoma C, Mazzola S (2009) Trace elements and vanadium in tissues and organs of species of cetaceans from Italian coasts. Chem Ecol 25:311–323
14. Bashirpoor M, Schmidt H, Schulzke C, Rehder D (1997) Models for vanadate-dependent haloperoxidases: vanadium complexes with 0_4N-Donor Sets. Chem Ber 130:651–657
15. Kawakami N, Ueki T, Amata Y, Kanamori K, Matsuo K, Gekko K, Michibata H (2009) A novel vanadium reductase, Vanabin2, forms a possible cascade involved in electron transfer. Biochim Biophys Acta 1794:674–679
16. Michibata H, Hirata J, Uesaka M, Numakunai T, Sakurai H (1987) Separation of vanadocytes: determination and characterization of vanadium ion in the separated blood cells of the ascidian, *Ascidia ahodori*. J Exp Zool 244:33–38

17. Michibata H, Hirose H, Sugiyama K, Ookubo Y, Kanamori K (1990) Extraction of a vanadium-binding substance (vanadobin) from the blood cells of several ascidian species. Biol Bull Mar Biol Lab Woods Hole 179:140–147
18. Michibata H, Terada T, Anada N, Yamakawa K, Numakunai T (1986) The accumulation and distribution of vanadium, iron and manganese in some solitary ascidians. Biol Bull Mar Biol Lab Woods Hole 171:672–681
19. Michibata H, Uyama T (1990) Extraction of vanadium-binding substances (vanadobin) from a subpopulation of signet ring cells newly identified as vanadocytes in ascidians. J Exp Zool 254:132–137
20. Michibata H, Uyama T, Ueki T, Kanamori K (2002) Vanadocytes, cells hold the key to resolving the highly selective accumulation and reduction of vanadium in ascidians. Microsc Res Tech 56:421–434
21. Kanda T, Nose Y, Wuchiyama J, Uyama T, Moriyama Y, Michibata H (1997) Identification of a vanadium-associated protein from the vanadium-rich ascidian, *Ascidia sydneiensis samea*. Zool Sci 14:37–42
22. Ueki T, Adachi T, Kawano S, Aoshima M, Yamaguchi N, Kanamori K, Michibata H (2003) Vanadium-binding proteins (vanabins) from a vanadium-rich ascidian *Ascidia sydneiensis samea*. Biochim Biophys Acta 1626:43–50
23. Minganti V, Capelli R, De Pellegrini R (1998) The concentrations of Pb, Cd, Cu, Zn, and V in Adamussium colbecki from Terra Nova Bay (Antarctica). Int J Environ Anal Chem 71: 257–263
24. El-Naggar MEE, Al-Amoudi OA (1989) Heavy metal levels in several species of marine algae from the Red Sea of Saudi Arabia. JKAU Sci 1:5–13
25. Lavilla I, Vilas P, Bendicho C (2008) Fast determination of arsenic, selenium, nickel and vanadium in fish and shellfish by electrothermal atomic absorption spectrometry following ultrasound-assisted extraction. Food Chem 106:403–409
26. Protasowicki M, Dural M, Jaremek J (2008) Trace metals in the shells of blue mussels (*Mytilus edulis*) from the Poland coast of Baltic sea. Environ Monit Assess 141:329–337
27. Chiffoleau JF, Chauvaud L, Amouroux D, Barats A, Dufour A (2004) Nickel and vanadium contamination of benthic invertebrates following the "Erika" wreck. Aquat Living Resour 17:273–280
28. Alfonso JA, Azócar JA, LaBrecque JJ, Benzo Z, Marcano E, Gómez CV, Quintal M (2005) Temporal and spatial variation of trace metals in clams *Tivela mactroidea* along the Venezuelan coast. Mar Pollut Bull 50:1713–1744
29. Fattorini D, Notti A, Di Mento R, Cicero AM, Gabellini M, Russo A, Regoli F (2008) Seasonal, spatial and inter-annual variations of trace metals in mussels from the Adriatic Sea: a regional gradient for arsenic and implications for monitoring the impact of off-shore activities. Chemosphere 72:1524–1533
30. Regoli F (1998) Trace metals and antioxidant enzymes in gills and digestive gland of the Mediterranean mussel *Mytilus galloprovincialis*. Arch Environ Contam Toxicol 34:48–63
31. Miramand P, Guary JC (1980) High concentrations of some heavy metals in tissues of the Mediterranean Octopus. Bull Environ Contam Toxicol 24:738–788
32. Miramand P, Bentley D (1992) Concentration and distribution of heavy metals in tissues of two cephalopods, *Eledone cirrhosa* and *Sepia officinalis*, from the French coast of the English Channel. Mar Biol 114:407–414
33. Miramand P, Bustamante P, Bentley D, Kouéta N (2006) Variation of heavy metal concentrations (Ag, Cd, Co, Cu, Fe, Pb, V and Zn) during the life cycle of the common cuttlefish *Sepia officinalis*. Sci Total Environ 361:132–143
34. Bustamante P, Grigioni S, Boucher-Rodoni R, Caurant F, Miramand P (2000) Bioaccumulation of 12 trace elements in the tissues of the nautilus *Nautilus macromphalus* from New Caledonia. Mar Pollut Bull 40:688–696
35. Abdel-Moati MAR, Nasir NA (1997) Bioaccumulation of chromium, nickel, lead and vanadium in some commercial fish and prawn from Qatari waters. Qatar Univ Sci J 17:195–203

36. Bu-Olayan AH, Subrahmanyam MNV (1998) Trace metal concentrations in the crab *Macrophthalmus depressus* and sediments on the Kuwait coast. Environ Monit Assess 53:297–304
37. Campbell LM, Norstrom RJ, Hobson KA, Muir DCG, Backus S, Fisk AT (2005) Mercury and other trace elements in a pelagic Arctic marine food web (Northwater Polynya, Baffin Bay). Sci Total Environ 351:247–263
38. Ikemoto T, Tu NPC, Okuda N, Iwata A, Omori K, Tanabe S, Tuyen BC, Takeuchi I (2008) Biomagnification of trace elements in the aquatic food web in the Mekong Delta, South Vietnam using stable carbon and nitrogen isotope analysis. Arch Environ Contam Toxicol 54:504–515
39. Anan Y, Kunito K, Tanabe S, Mitrofanov I, Aubrey DG (2005) Trace element accumulation in fishes collected from coastal waters of the Caspian Sea. Mar Pollut Bull 51:882–888
40. Mackey EA, Becker PR, Demiralp R, Greenberg RR, Koster BJ, Wise SA (1996) Bioccumulation of vanadium and other trace metals in liver of Alaskan cetaceans and pinnipeds. Arch Environ Contam Toxicol 30:503–512
41. Mackey EA, Demiralp R, Becker PR, Greenberg RR, Koster BJ, Wise SA (1995) Trace element concentrations in cetacean liver tissues archived in the National Marine Mammal Tissue Bank. Sci Total Environ 175:25–41
42. Kunito T, Nakamura S, Ikemoto T, Anan Y, Kubota R, Tanabe S, Rosas CW, Fillmann G, Readman JW (2004) Concentration and subcellular distribution of trace elements in liver of small cetaceans incidentally caught along the Brazilian coast. Mar Pollut Bull 49:574–587
43. Agusa T, Nomura K, Kunito T, Anan Y, Iwata H, Miyazaki N, Tatsukawa R, Tanabe S (2008) Interelement relationship and age-related variation of trace element concentrations in liver of striped dolphins (*Stenella coeruleoalba*) from Japanese coastal waters. Mar Pollut Bull 57: 807–815
44. Young JS, Adee RR, Piscopo I, Buschbom RL (1981) Effects of copper on the sabellid polychaete. Eudistylia vancouveri. II. Copper accumulation and tissue injury in the branchial crown. Arch Environ Contam Toxicol 10:87–104
45. Young JS, Buschbom RL, Gurtisen JM, Joyce SP (1979) Effects of copper on the sabellid polychaete. Eudistylia vancouveri: I. Concentration limits for copper accumulation. Arch Environ Contam Toxicol 8:97–106
46. Ishii T, Nakai I, Numako C, Okoshi K, Otake T (1993) Discovery of a new vanadium accumulator, the fan worm *Pseudopotamilla occelata*. Naturwissenschaften 80:268–270
47. Bagaveeva EV, Zvyagintsev AY (2000) The introduction of polychaetes *Hydroides elegans* (Haswell), *Polydora limicola* (Annenkova), and *Pseudopotamilla occelata* (Moore) to the Northwestern part of the East Sea. Ocean Res 22:25–36
48. Cole AG, Hall BK (2004) The nature and significance of invertebrate cartilages revisited: distribution and histology of cartilage and cartilage-like tissues within the Metazoa. Zoology 107:261–273
49. Yoshihara M, Ueki T, Yamaguchi N, Kamino K, Michibata H (2008) Characterization of a novel vanadium-binding protein (VBP-129) from blood plasma of vanadium-rich ascidian *Ascidia sydneiensis samea*. Biochim Biophys Acta 1780:256–263
50. Uyama T, Nose Y, Wuchiyama J, Moriyama Y, Michibata H (1997) Finding of the same antigens in the polychaete, *Pseudopotamilla occelata*, as those in the vanadium-rich ascidian, *Ascidia sydneiensis samea*. Zool Sci 14:43–47
51. Giangrande A, Gambi MC (1997) The genus *Perkinsiana* (Polychaeta, Sabellidae) from Antarctica, with descriptions of the new species *P. milae* and *P. borsibrunoi*. Zool Scripta 26:267–278
52. Bocchetti R, Fattorini D, Gambi MC, Regoli F (2004) Trace metal concentrations and susceptibility to oxidative stress in the polychaete *Sabella spallanzanii* (Gmelin) (Sabellidae): potential role of antioxidants in revealing stressful environmental conditions in the Mediterranean. Arch Environ Contam Toxicol 46:353–361
53. Fattorini D, Bocchetti R, Bompadre S, Regoli F (2004) Total content and chemical speciation of arsenic in the polychaete *Sabella spallanzanii*. Mar Environ Res 58:839–843

54. Fattorini D, Regoli F (2004) Arsenic speciation in tissues of the Mediterranean polychaete *Sabella spallanzanii*. Environ Toxicol Chem 23:1881–1887
55. Bargagli R (2005) Antarctic ecosystems. Environmental contamination, climate change and human impact. Springer, Berlin
56. Lichtenegger HC, Schöberl T, Bartl MH, Waite H, Stucky GD (2002) High abrasion resistance with sparse mineralization: copper biomineral in worm jaws. Science 298:389–392
57. Lichtenegger HC, Schöberl T, Ruokolainen JT, Cross JO, Heald SM, Birkedal H, Waite JH, Stucky GD (2003) Zinc and mechanical prowess in the jaws of *Nereis*, a marine worm. P Natl Acad Sci USA 100:9144–9149
58. Nejmeddine A, Dhainaut-Courtois N, Baert JL, Sautière P, Fournet B, Boulenguer P (1988) Purification and characterization of a cadmium-binding protein from *Nereis diversicolor* (Annelida, Polychaeta). Comp Biochem Physiol C 89:321–326
59. McClintock JB, Baker BJ (1997) A review of the chemical ecology of Antarctic marine invertebrates. Am Zool 37:329–342
60. McClintock JB, Baker BJ (2001) Marine chemical ecology, Marine science series. CRC, Boca Raton
61. Paul VJ, Puglisi MP, Ritson-Williams R (2006) Marine chemical ecology. Nat Prod Res 23:153–180
62. Kicklighter CE, Hay ME (2006) Integrating prey defensive traits: contrasts of marine worms from temperate and tropical habitats. Ecol Monogr 76:195–215
63. Kicklighter CE, Hay ME (2007) To avoid or deter: interactions among defensive and escape strategies in sabellid worms. Oecologia 151:161–173
64. Fattorini D, Alonso-Hernandez CM, Diaz-Asencio M, Munoz-Caravaca A, Pannacciulli FG, Tangherlini M, Regoli F (2004) Chemical speciation of arsenic in different marine organisms: importance in monitoring studies. Mar Environ Res 58:845–850
65. Fattorini D, Notti A, Regoli F (2006) Characterization of arsenic content in marine organisms from temperate, tropical, and polar environments. Chem Ecol 22:405–414
66. Ventura-Lima J, Fattorini D, Notti A, Monserrat JM, Regoli F (2010) Bioaccumulation patterns and biological effects of arsenic in aquatic organisms. In: Gosselin JD, Fancher IM (eds) Environmental health risks: lead poisoning and arsenic exposure. Nova Science Publishers Inc., New York, Chapter 6. ISBN 978-1-60741-781-1
67. Notti A, Fattorini D, Razzetti EM, Regoli F (2007) Bioaccumulation and biotransformation of arsenic in the Mediterranean polychaete *Sabella spallanzanii*: experimental observations. Environ Toxicol Chem 26:1186–1191
68. Avila C, Taboada S, Nuñez-Pons L (2008) Antarctic marine chemical ecology: what is next? Mar Ecol 29:1–71
69. Goerke H, Emrich R, Weber K, Duchene JC (1991) Concentrations and localization of brominated metabolites in the genus *Thelepus* (Polychaeta, Terebellidae). Comp Biochem Physiol B 99:203–206

Part III
Enzymatic Roles of Vanadium

Chapter 5
Structure and Function of Vanadium Haloperoxidases

Ron Wever

Abstract Vanadium haloperoxidases contain the bare metal oxide vanadate as a prosthetic group and differ strongly from the heme peroxidases in substrate specificity and molecular properties. The substrates of these enzymes are limited to halides and sulfides, which in the presence of hydrogen peroxide are converted into hypohalous acids or sulfoxides, respectively. Several seaweeds contain iodo- and bromoperoxidases and their direct or indirect involvement in the production of the huge amounts of brominated, iodinated compounds and the formation of I_2 in the marine environment will be reviewed. Vanadium chloroperoxidases occur in a group of common terrestrial fungi and are probably involved in the degradation of plant cell walls and breakdown of the leaf cuticle. The natural presence of high-molecular-weight chloro-aromatics in the environment is probably be due to the activity of these enzymes. Based upon several X-ray structures of the enzymes and detailed kinetics a molecular mechanism is proposed and discussed in detail. As will be shown the metal oxide in the active site binds hydrogen peroxide in a side-on fashion and acts as a Lewis acid allowing nucleophilic attack of an incoming halide and formation of HOX. The surprising evolutionary relationship between the bacterial and mammalian acid phosphatases that hydrolyze phosphate monoesters and the vanadium haloperoxidases will be shown.

Keywords Vanadium iodoperoxidases • Vanadium bromoperoxidases • Vanadium chloroperoxidase • Steady-state kinetics • X-ray structures • Active site structures • Mutants • Sulfoxidation • Acid phosphatases • Halometobolites • Biological importance • Environmental significance • Atmospheric chemistry

R. Wever (✉)
Van 't Hoff Institute for Molecular Sciences, University of Amsterdam, Science Park 904, Amsterdam 1098 XH, The Netherlands
e-mail: r.wever@uva.nl

H. Michibata (ed.), *Vanadium: Biochemical and Molecular Biological Approaches*,
DOI 10.1007/978-94-007-0913-3_5, © Springer Science+Business Media B.V. 2012

5.1 Introduction

Vanadium is the second most abundant metal in seawater at a concentration of about 35 nM [1] and universally [2] distributed in the soil. The metal oxide is the prosthetic group in the vanadium haloperoxidases from seaweeds and in a group of fungi, the dematiaceous hyphomycetes. Vilter [3] was the first to demonstrate evidence for the involvement of vanadium in the vanadium-dependent haloperoxidase. He showed that the bromoperoxidase isolated from *Ascophyllum nodosum* was inactivated by dialysis at pH 3.8 in phosphate buffer containing EDTA and that the enzyme was reactivated by vanadate in suitable buffers. Subsequently it was demonstrated [4, 5] that vanadate was the prosthetic group in the bromoperoxidase and that since phosphate is a structural and electronic analogue of vanadate it replaces vanadate in the enzyme [5, 6]. The vanadium chloroperoxidases with similar enzymatic and kinetic properties as the bromoperoxidases were detected a few years later in a family of terrestrial fungi [7, 8]. The oxidation state of the metal in the native form of the haloperoxidases is vanadium V that upon reduction is converted into the catalytically inactive IV state. As a d^1 metal ion, vanadium IV has a single electron that is strongly coupled to the ^{51}V nucleus ($I = 7/2$). This redox state of the metal can easily be detected by EPR since it gives rise to an EPR signal of either 8 or 2 sets of 8 overlapping lines. This technique allows the detection of relatively low concentrations of these enzymes [9]. Unfortunately at this redox state the enzyme is inactive. Unlike heme peroxidases the UV-VIS spectra of these vanadium enzymes show only a modest absorption in the optical spectra around 315 nm due to the bound cofactor.

Haloperoxidases catalyze the two-electron oxidation of halides (Cl^-, Br^-, I^-) by H_2O_2 to hypohalous acids:

$$H_2O_2 + H^+ + X^- \rightarrow HOX + H_2O \tag{5.1}$$

In fact this reaction can be regarded as an oxygen-transfer reaction from the peroxide to the halide ion. These hypohalous acids or related halogenating intermediates, such as OX^-, X_3^- and X^+ are released from the active site during turnover and they may act nonspecifically on a variety of organic compounds (RH) that are susceptible for electrophilic attack resulting in the production of a diversity of halogenated compounds (RX).

$$HOX + R - H \rightarrow RX + H_2O \tag{5.2}$$

In the absence of a nucleophilic acceptor a reaction may also occur between HOX and H_2O_2 resulting in the formation of singlet oxygen.

$$HOX + H_2O_2 \rightarrow {}^1O_2 + H_2O + HX \tag{5.3}$$

The historical nomenclature convention of the vanadium haloperoxidases is based on the most electronegative halide oxidized by these enzymes. Chloroperoxidases catalyze the oxidation of Cl^- and Br^- and I^-, bromoperoxidases catalyze only the oxidation of Br^- and I^- and iodoperoxidases [10] are specific for iodide oxidation. However the distinction between the haloperoxidases is somewhat arbitrary since a bromoperoxidase may also oxidize chloride albeit with a low specificity constant.

5.2 Occurrence, Biological Function of Vanadium Iodo- and Bromoperoxidases and Impact of the Halogenated Products on the Environment

A striking array of iodinated and brominated products produced by natural sources is found in the biosphere and in particular the marine environment is a rich source. A majority of these products are probably formed by the enzymatic activity of the enzyme family of vanadium bromo- and iodoperoxidases. Iodo- and bromoperoxidases have been found in red and brown macro-algae from all over the world [11–13] and also in marine diatom cultures [14]. In the green macro-alga *Ulvella lens* probably also a vanadium dependent enzyme is present [15].

5.2.1 Brominated Compounds

Macro-algae and phytoplankton produce huge amounts of bromoform and other volatile brominated compounds [16] and oxidative stress as well as UV light result in the release of these compounds by seaweeds. Estimates [16] give a global annual source strength of 2.2 10^{11} g $CHBr_3$ by macro-algae. The brominated compounds are ventilated to the atmosphere and may reach the lower region of the stratosphere in which they may play a natural role in the regulation of the ozone concentration [17] and references therein]. Thus, macro-algae have a dominant role in producing bromoform and other volatile brominated compounds that plays a role in the breakdown of ozone in tropo- and lower stratosphere [18, 19]. However, there are other natural sources of these halogenated compounds as well as evidenced [19] by halogen mediated ozone destruction over the biological active tropical Atlantic Ocean. Halogenated compounds are produced as shown [14] by marine diatoms that occur in all oceans. Also bromoform in the Artic Ocean [20, 21] appears to originate from phytoplankton. In some seaweed species the iodo- and bromoperoxidases are extracellularly located [22–25]. When these and other seaweeds are triggered by changes in the environment such as stress and light they produce not only HOBr [22, 25, 26] but also a variety of volatile brominated compounds [27–30]. It is well documented [31] that plant when exposed to stress

such as wounding, pathogenic attack and light generate reactive oxygen species and H_2O_2. The vanadium bromoperoxidase will convert this rapidly into HOBr.

HOBr has a direct antimicrobial and virucidal effect [32, 33] and as shown [26] the oxidized halogen species produced by the marine alga *L. digitata* deactivate homoserine lactones. These lactones are important communication signals between bacteria and as a result of deactivation biofilm formation and fouling by bacteria and fungi of the surface of the seaweeds is prevented. Thus, oxidized halogens produced by the extra cellular peroxidase not only control biofouling by a bactericidal mechanism but also interfere with bacterial signaling systems.

A question that has not yet clearly been answered is how formation of HOBr by bromoperoxidases is linked to the formation of these volatile halogenated compounds. At least two mechanisms are operational. Theiler et al. [34] have proposed that HOBr generated by seaweeds reacts with ketoacids in the seaweeds. These compounds are susceptible to halogenation; the halogenated ketoacids formed are unstable and decay via the haloform reaction to a mixture of mono-, di-, and tribrominated compounds. Indeed as shown [15] incubation of oxaloacetate with BPO/hydrogen peroxide/Br^- leads to formation of $CHBr_3$ and CH_2Br_2. Alternatively it has been proposed [22] that HOBr produced by these seaweeds and which diffuses into the seawater reacts in an abiotic process with dissolved organic matter naturally present in seawater. The brominated compounds are unstable and decay again leading to the formation of bromoform and other compounds. This process occurs also when drinking water containing organic matter is exposed to HOCl or HOBr [35].

5.2.2 Iodine and Iodinated Compounds

The brown seaweeds of the genus *Laminaria* (kelp) are the most efficient iodine accumulators among all living species and accumulate up to 1% of their dry weight of this halogen. In coastal regions Laminariales are the major contributor to the iodine flux from the oceans through the production of volatile iodocarbons. The iodoperoxidases that are found in these seaweed species play not only a prime role in the production of iodine and iodocarbons [36] but also in the accumulation of iodide. Phylogenetic analyses [37] indicate that these vanadium IPO's shares a close common ancestor with brown algal vanadium-dependent bromoperoxidases. As discussed in more detail later the most striking difference in the active site of vanadium IPO is the presence of an alanine, instead of an invariant serine that is present in both in vanadium CPO and vanadium BPO.

Exposure to UV light and stress of *L. digitata* induces an efflux of volatile iodocarbons and bursts of molecular iodine I_2 [38–40] and there is a strong relation to the H_2O_2 released by this alga as well. It is likely that the observed bursts are a consequence of the known stress-induced production of H_2O_2 in *L. digitata.* These results strongly support the model [41] that direct biogenic emission of I_2 by algae

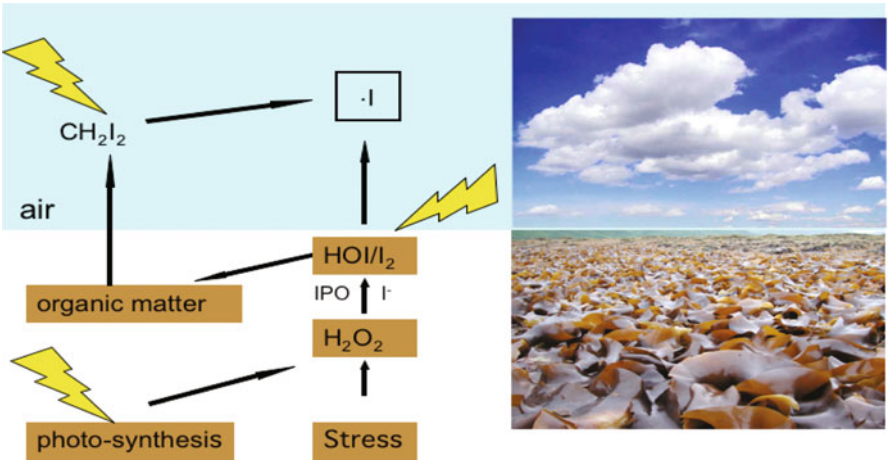

Fig. 5.1 Events occurring when seaweed is exposed to stress or light. An oxidase is triggered by stress signals e.g. low tide, rain or damage of the seaweed and produces hydrogen peroxide. Apparently during photosynthesis also hydrogen peroxide is generated. The iodoperoxidase converts this into reactive HOI, which is either converted into I_2 or it reacts directly with organic matter in seawater. The formed iodinated compounds ventilate to the atmosphere, are photolyzed by UV light and iodine radicals I^- are generated. The iodine radicals react further in the atmosphere and lead to particle formation that acts as condensation nuclei for coastal cloud formation. A major emission flux of I_2 from the algae to the atmosphere also, which are directly photolysed leading iodine radicals

is a very important natural process in the marine boundary layer, that impacts the tropospheric photochemistry both on regional and global scales. Iodine mediated coastal particle formation also occurs which is driven by emission of molecular iodine I_2 by macro algal species under stress conditions at low tide. Particle formation strongly correlates with IO produced at high concentrations following photolysis of I_2 and subsequent rapid reaction with O_3. These particles grow to larger size and these particles should be able to act as cloud condensation nuclei at reasonable atmospheric super saturations. Indeed, iodocarbons and iodine containing particles produced in coastal areas by seaweeds provide condensation nuclei for coastal cloud formation [42–44]. A recent study [45] shows that other seaweed species also emit I_2 when stressed for example by low tide. Further this study confirms that condensable particle forming gases derive from the photochemical oxidation of I_2 emitted by these plants. Figure 5.1 gives a simplified picture of the processes that may occur and are triggered by the activity of the seaweeds.

The physiological function of the production of these iodinated compounds by these seaweeds is not clear and here is considerable debate as to the role of the iodoperoxidases in the Laminaria species and the involvement in iodide accumulation. Kupper et al. proposed [46] that iodide accumulation in kelp constitutes an extra cellular protection against oxidative stress such as O_3 in air or H_2O_2 [47] generated under stress conditions by these plants. However, the O_3 concentrations

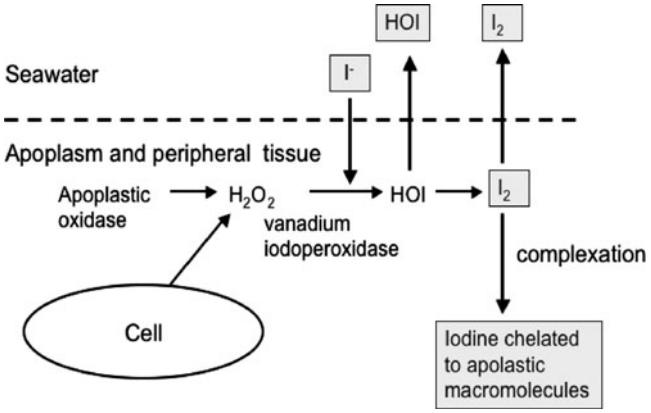

Fig. 5.2 Mechanism of iodine uptake according to [48] and adapted. Iodide in seawater (0.3 μM) diffuses into the peripheral tissue were it is oxidized by the vanadium iodoperoxidases to I_2. This inorganic species becomes bound to apoplastic macromolecules and accumulates. These macromolecules are conceivably charged polysaccharides, which are abundant in these seaweeds

in air are likely to be low. It is also possible that by using the hydrogen peroxide generated the vanadium iodoperoxidases act as a chemical defense system against invading (micro) organisms.

The accumulation and distribution of iodine in these brown algae has been the subject of many studies [46] and references therein] and has led to various mechanisms and considerable debate. Micro chemical imaging studies of iodine distribution in *L. digitata* and careful fixation procedures have recently shown [48] that the distribution of iodine shows a huge, decreasing gradient from the meristoderm to the apoplasm with very high levels in the external cell layers. The meristoderm contains about 80% of the total iodine content and the peripheral tissue is therefore the main storage compartment of iodine and means that iodine is easily accessible and can be mobilized for potential antioxidant activities and chemical defense. Interestingly also the highest contents of bromine are also detected in the peripheral tissue. The results also suggested that iodine is mainly chelated as labile inorganic species by apoplastic molecules e.g. sulfated polysaccharides or protein like molecules. On the basis of these results a modified hypothesis (Fig. 5.2) for the mechanism of iodine uptake was proposed.

An apolastic oxidase which is activated by light or stress produces hydrogen peroxide which oxidizes iodide from seawater to a yet undefined oxidation state and after which the iodine species become bound to apolastic macromolecules or alternatively diffuse into seawater and the environment. It would have been nice to have data as well about the distribution of the vanadium iodoperoxidase. This could have led to a better understanding of the role of the iodoperoxidases and maybe also of the systems that are involved in the generation of hydrogen peroxide.

5.3 Presence and Biological Function of Vanadium Chloroperoxidases

Fungi belonging to the dematiaceous hyphomycetes that were isolated from plant material and soils collected in Death Valley were shown to contain haloperoxidase activity that could function at more elevated pH and temperature [49, 50]. Some years later it was shown [7] that the non-heme chloroperoxidase produced by the fungus *Curvularia inaequealis* also contains vanadate as the prosthetic group in the enzyme. The vanadium enzyme is produced in the secondary growth phase, when nutrients become limiting. In the group of the dematiaceous hyphomycetes several species produce vanadium haloperoxidases (e.g. *Drechslera biseptata*, *D. subpapendorfii*, *Embellisia didymospora, Ulocladium chartarum* [8, 51] and *Botrytis cinera* [52]). Many of these hyphomycetes are phytopathogenic and/or grow on decaying plant material. To date no halogenated metabolites have been reported to be formed by these organisms directly and it has been proposed that physiological role of the vanadium chloroperoxidase is an oxidative attack mechanism on the lignocellulose in cell walls of plants or the cuticle layer on the leaves of plant [53]. The oxidative degradation will facilitate penetration of the fungal hyphen into the host to reach nutrients in the cell. It is very likely that HOCl generated by fungal species in soils reacts with organic matter resulting in the formation of organohalogens. Since chloroperoxidase-producing fungi are ubiquitous in decaying lignocellulose and plant debris and occur widely in nature these enzymes are responsible in the natural production of high-molecular-weight chloro-aromatics and in lignin breakdown [54]. Because lignin is the earth's most abundant aromatic substance chlorolignin produced by this route and humus derived from it are probably significant components of the global chlorine cycle [55].

Recently it has become clear that haloperoxidases are not the only class of enzymes that are able to incorporate halogens in complex organic molecules. The iron (II)- and a-oxoglutarate -dependent halogenases [56] are able to specifically chlorinate specific compounds by a Cl-Fe(IV)-oxo species through 'rebound' of a chloride radical, analogous to the hydroxyl radical rebound mechanism postulated for heme and non-heme hydroxylases. The FADH2 halogenases chlorinate specific compounds by formation of an enzyme-bound chloronium intermediate that is targeted via a protein tunnel to the region of the bound substrate. These classes of enzymes will not be discussed here but see [57] for details.

5.4 Haloperoxidase Activity Assays

Classical heme peroxidase substrates such as guaiacol, *o*-dianisidine and benzidine are not oxidized by haloperoxidases and other non-standard assays should be used. The activity of the bromo- and chloroperoxidases is routinely determined using scavengers reacting with the very reactive intermediates HOCl or HOBr [58] and

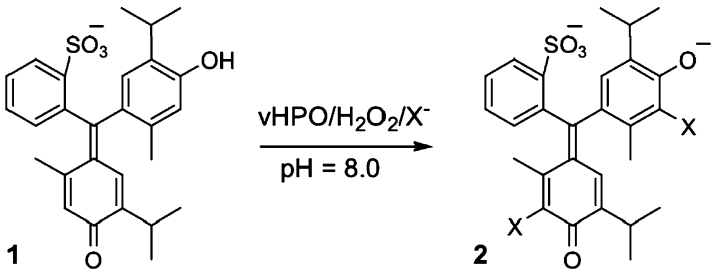

Fig. 5.3 Bromination of iodination of thymol blue (1). At pH 8 there is marked color change due a shift in the pKa upon halogenation of the dye, the dihalogenated compound (2) has a deep blue color with an absorbance maximum at 620 nm

that result in marked changes in absorbance. A quantitative assay to determine the halogenating activity of these enzymes is the bromination or chlorination of monochlorodimedone [59]. This compound is a 1,3 diketone with an activated carbon atom that is brominated or chlorinated by HOX or X_2 to the dihalogenated compound. This reaction is monitored spectrophotometrically at 290 nm and the loss of absorbance of monochlorodimedone ($\varepsilon = 20{,}000\ M^{-1}\ cm^{-1}$) is recorded. This assay can not be used to measure iodoperoxidase activity due to the poor reactivity of oxidized iodine species towards monochlorodimedone, high instability of the iodinated product and formation of I_3^- that also strongly absorbs in the UV region. In general iodoperoxidase activity is measured by spectrophotometric detection of triiodide.

The MCD formation is quantitative with respect to H_2O_2 consumption but only at neutral or slightly alkaline pH values. At higher pH values a competing reaction with hydrogen peroxide occurs resulting in the formation of dioxygen Eq. 5.3. This competing reaction results in singlet oxygen formation and a decrease in the rate of bromination or chlorination of monochlorodimedone [60]. This decrease in rate should be taken into account when the activity measurements are carried at higher pH values. In fact the vanadium chloroperoxidase has been used as a highly efficient catalyst for the production of singlet oxygen and the enzyme is 10^3–10^4 times faster than the molybdate- peroxide system [61]. The halogenation of phenol red is an alternative assay. This test may only been used for qualitative purpose due to poly-halogenation of the dye [62]. However the bromination of the dye results in a marked color change, which also allows visual screening of haloperoxidase activity of large numbers of samples. This assay has been used in high-throughput screening of mutant libraries of vanadium chloroperoxidase [63]. Also the dye thymol blue may acts as a scavenger for HOBr. The kinetic parameters obtained [58] are essentially the same as that reported [59] using monochlorodimedone. Thymol blue has also a high reactivity towards HOI formed and it has been used in the steady-state kinetic analysis [58] of the oxidation of I^- by vanadium bromoperoxidase from *A. nodosum*.

Figure 5.3 illustrates the reaction and the results show that this method is quantitative and superior to the standard I_3^- assay.

The vanadium iodoperoxidases oxidize iodide to HOI according to Eq. 5.4 and the HOI formed reacts further to I_2 (Eq. 5.5).

$$H_2O_2 + I^- \rightarrow HOI + H_2O \tag{5.4}$$

$$HOI + I^- + H^+ \rightarrow I_2 + H_2O \tag{5.5}$$

$$I_2 + I^- \leftrightarrow I_3^- \tag{5.6}$$

The triiode formation is the result of reversible complexation of I_2 with I^- according to Eq. 5.6. This method when used [36] in an assay is not free from intrinsic problems and due the value of the equilibrium constant of Eq. 5.6 iodoperoxidase activity can only be measured quantitatively at iodide concentrations higher than 20 mM. Also a reaction occurs between HOI and H_2O_2 at pH values > 6.5 [58] and thus reported values for K_m and V_{max} should be treated with caution. To date the synthesis of iodinated organic compounds by vanadium iodoperoxidases has not been reported.

5.4.1 Steady-State Kinetics of Bromoperoxidases

Detailed steady-state kinetic studies on the oxidation of bromide by vanadium bromoperoxidases have been carried out, which suggested a bi-bi ping-pong two substrate mechanism in which hydrogen peroxide first binds to the active site followed by halide oxidation. The kinetic mechanisms for the bromoperoxidases from various sources appear to be very similar [59, 60]. Only slight inhibition of these enzymes by high concentrations of H_2O_2 (120–400 mM) was observed [60]. Thus vanadium bromoperoxidases are very resistant towards oxidative inactivation [61]. By contrast most heme peroxidases would be completely destroyed by these concentrations of H_2O_2.

Evidence that hydrogen peroxide reacts only with a deprotonated group in the enzyme with a p*Ka* of 5.7–6.7 was obtained from measurement of the log K_m value for H_2O_2 as a function of pH. This log K_m decreased linearly with increasing pH but levels off above pH 6. The second-order rate constant that was derived for the binding of hydrogen peroxide to the bromoperoxidase from the specificity constant [62] is $2.5 \times 10^6\ M^{-1}\ s^{-1}$ at pH > 6. In contrast the *Km* for bromide is hardly affected by pH [59]. Table 5.1 gives values of the kinetic constants of the various haloperoxidases.

5.4.2 Steady State Kinetics of the Iodide Oxidation by Iodo- and Bromoperoxidases

A careful analysis carried out by [58] showed that the oxidation of I^- by the vanadium bromoperoxidase from A. nodosum occurs also by an ordered two-substrate

Table 5.1 Kinetic parameters of the oxidation of I^-, Br^- and Cl^- catalyzed by vanadium iodo bromo- and chloroperoxidases

		X^-			H_2O_2		
Enzyme	pH	K_m (μM)	k_{cat} (s^{-1})	k_{cat}/K_m (M^{-1} s^{-1})	K_m (μM)	k_{cat} (s^{-1})	k_{cat}/K_m (M^{-1} s^{-1})
IPO (*L. digitata*) I^- oxidation [37]	6.2	2.5×10^3	462	1.8×10^5	n.d.	n.d	n.d
VBPO (L. *digitata*) I^- oxidation [37]	6.3	1.8×10^4	38	2.1×10^3	n.d.	n.d.	n.d.
VBPO (*A. nodosum*) I^- oxidation [58]	8.0	1.8×10^2	75	4.2×10^5	n.d.	n.d.	n.d.
VBPO (*A. nodosum*) Br^- oxidation [59]	4.5	3.4×10^3	278	8.2×10^4	1,100	278	2.5×10^5
	5.2	5.1×10^3	166	3.2×10^4	162	166	1.0×10^6
	6.6	9.3×10^3	113	1.2×10^4	42	113	2.7×10^6
	7.9	1.8×10^4	50	2.8×10^3	22	50	2.3×10^6
VCPO Br^- oxidation [63, 64]	4.2	<5	253	$>5.1 \times 10^7$	90	250	2.6×10^6
	5.2	9	248	2.8×10^7	35	203	5.8×10^6
	6.3	7	37	5.3×10^6	<5	33	6.6×10^6
	8.0	120	1	8.3×10^3	<5	1	$>2 \times 10^5$
VCPO Cl^- oxidation [65, 66]	5.0	1.1×10^3	23	2.0×10^4	49	183	3.7×10^6
	6.3	1.0×10^4	7.3	7.1×10^2	2.6	152	5.8×10^6
	8.0	1.1×10^5	n.d.	n.d.	n.d.	n.d.	n.d.
VCPO alkaline mutant Br— oxidation [63]	5.0	n.d.	575	n.d.	n.d.	n.d.	n.d.
	8.0	3.1×10^3	100	3.2×10^4	16	100	6.2×10^6
VCPO alkaline mutant Cl^- oxidation [63]	5.0	n.d.	36	n.d.	n.d.	n.d.	n.d.

n.d – not determined

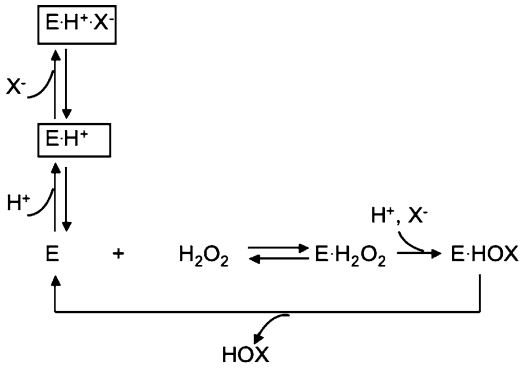

Scheme 5.1 Simplified reaction mechanism of the vanadium peroxidases based on enzyme kinetics. The enzyme species in boxes represent inhibited forms of the enzymes. For Cl^- oxidation a proton is needed a since the K_m for Cl^- is strongly pH dependent whereas protonation is not needed for Br^- oxidation by either bromoperoxidase or chloroperoxidase

mechanism. The K_m value for I^- of 0.18 mM is about 100-fold smaller than that found for bromide oxidation by the same enzyme and conditions. The k_{cat} value of 75 s^{-1} for iodide oxidation is similar to that found for bromide oxidation at the same pH.

Table 5.1 gives a summary of some of the kinetic constants of the iodo-, bromo- and of the chloroperoxidase that will be discussed later.

These early kinetic studies suggested the presence of a peroxo-intermediate. The primary reaction products of the enzyme-mediated peroxidation of bromide appear to be Br_3, Br_2 or HOBr. Although HOBr is probably the first oxidized identity this is difficult to prove since different bromine species may be present that are in rapid equilibrium [59]. It was not possible to demonstrate specificity with regard to bromination of various organic nucleophilic acceptors for the enzyme from the brown seaweed *A. nodosum*. This suggests a mechanism in which the enzyme releases a diffusible halogen intermediate into the seawater. This brown seaweed produces simple halohydrocarbons such as CH_2Br_2 and $CHBr_3$ that are probably the result of the enzymatically generated HOBr with organic matter in seawater or ketoacids in the seaweed. A brominated surface tryptophane is found in the enzyme from *A. nodosum* that is the result from free diffusion of the HOBr species generated by the enzyme during turnover [67]. Single molecule fluorescence microscopy also gave evidence for a specific bromination. By this technique it was possible to study the diffusion behavior of bromonium species produced by a vanadium peroxidase from the fungus *Curvularia verruculosa* [68]. Under steady-state conditions hypobromite was able to diffuse over 800 nm in the bulk solution before it reacted with organic substrates. Scheme 5.1 gives a simplified model for the reaction mechanism of the enzyme.

In addition to the simple volatile brominated compounds produced mostly by brown seaweed other seaweed species contain more elaborate and complex brominated compounds such as halogenated sequiterpenes. In this case there may be a more specific interaction between organic substrate and an enzyme bound halogenating intermediate. Vanadium bromoperoxidases isolated from marine red algae (species of *Laurencia, Plocamium, Corallina*) convincingly catalyze [69, 70]

the asymmetric bromination and cyclization of a terpenoid precursor (E)-(+) – nerolidol, producing single diastereoisomers that are also found in red algae. These vanadium bromoperoxidases produce bromonium ions or equivalents in the active site that brominates one face of the terminal olefin that docks within the active site cavity in a specific orientation. Surprisingly cyclic terpenes are only formed in mixtures of water and organic solvents. When the organic solvent is deleted only halohydrines are formed due to a competing reaction with water. This raises the question as to the formation of the cyclic terpenes under physiological conditions.

As will be discussed bromoperoxidases from *A. nodosum* and *Corallina officinalis* catalyze sulfoxidation of aromatic sulfides enantioselectively. This suggests specific binding of organic molecules possibly close to or at the active site of this enzyme as well.

5.4.3 Properties of the Prosthetic Group in Bromoperoxidase

When the vanadium bromoperoxidase from *A. nodosum* is exposed to phosphate buffers containing EDTA at low pH the enzymatic activity is rapidly lost. In phosphate buffers at neutral pH the enzyme also inactivates but more slowly, however, in Tris buffers the enzyme remains active for months. Complete recovery of the enzymatic activity is possible by incubation of the apo-enzyme at neutral pH with orthovanadate (HVO_4^{2-}) [3]. This reconstitution by vanadate was taken as early evidence that vanadate is present in the active site. Indeed the X-ray structures of vanadium bromoperoxidases confirmed that vanadate is indeed the prosthetic group in these enzymes [71, 72]. Vanadate binds strongly to apo-bromoperoxidase with K_d values of 35–55 nM. These values are close to the concentration of vanadate in seawater of 35 nM [1]. Thus, no additional enzyme system is required to incorporate vanadate in the enzyme. Also molybdate may be incorporated in the active site of the bromoperoxidase, however, the enzyme reconstituted with molybdate is inactive [9]. The purified enzyme only displays weak bands at 300–330 nm in the optical absorption spectrum [73]. These bands diminish in intensity when H_2O_2 is added and the original intensity is restored by addition of bromide. This was taken as the first direct indication for the existence of an enzyme-peroxide intermediate in line with the steady state kinetic studies.

When substrates are added to the bromoperoxidase or during turnover the vanadium (IV) or (III) states are not observed by EPR [9] or by K-edge X-ray absorption studies [74]. Thus and since also the reduced enzyme is inactive, the redox state of the metal during turnover remains vanadium (V). Hence it has been proposed that vanadium binds and activated hydrogen peroxide by acting as a Lewis acid [9]. In this metal-assisted mechanism electron density from the bound peroxide is withdrawn in such a way that the nucleophilic halide reacts with this activated peroxide intermediate to yield hypohalous acid. These spectroscopic methods have not only yielded insight into the mechanism but also valuable structural data were obtained. EXAFS studies [74, 75] showed that the geometry of the metal oxide

bound in the active site was five-coordinate. The multiple scattering effects from outer atoms of a group pointed to a histidine ligated to the vanadate. An ESEEM study [76] of the reduced enzyme showed the presence of nitrogen atoms in the direct coordination sphere of the metal oxide. The X-ray structure of the vanadium bromoperoxidase from *A. nodosum* [71] confirmed these findings.

5.4.4 Kinetic and Optical Properties of Vanadium Chloroperoxidases

Although expression of active recombinant bromoperoxidases has been reported it is not straightforward due to the formation of inactive inclusion bodies that have to be solubilized and subsequent activation of the enzyme [77, 78]. In contrast cloning and expression of vanadium chloroperoxidase is fairly easy. The enzyme has both been expressed in the yeast *Saccharomyces cerevisiae* [79] and in *E.coli* [63]. Activation of the recombinant apo-form of the enzyme is easily achieved by addition of vanadate to either the growth medium or the isolated apo-enzymes. Most soils contain a high concentration (100 ppm) of vanadium is and since the affinity of the apochloroperoxidase for vanadate is high the amount of vanadium is not a limiting factor in the conversion of the apo-enzyme into the holo-enzyme. Further low concentrations of H_2O_2 increase the affinity of the apo-enzyme for vanadate at least 200-fold. This is due to the formation of pervanadate that binds the active site with a dissociation constant of less than 5 nM [80].

The substrate inhibited Bi Bi ping-pong mechanism of the chloroperoxidase [7, 65, 66] resembles those of the vanadium bromoperoxidases . The chloroperoxidase exhibits a pH profile similar to vanadium bromoperoxidases although the optimal pH of 4.5–5.0 is at a lower pH value. The enzyme is inhibited at lower pH values by chloride in a competitive way whereas at higher pH values normal Michaelis-Menten kinetics is observed. As in the bromoperoxidases the log K_m for hydrogen peroxide decreases with increasing pH and very low values of less than 5 μM are observed. In contrast as shown in Fig. 5.4 the log K_m for chloride increases linearly with pH.

This demonstrates that protons are involved in binding and activation of substrates [66, 81]. The enzyme reacts first with peroxide to form a peroxo-intermediate after which a chloride ion and a proton react resulting in the formation of an enzyme-HOCl intermediate. This intermediate decays in a rate-determining step to enzyme and free HOCl. The linear dependency of the log K_m for hydrogen peroxide on pH suggests that like the bromoperoxidase an ionizable group is involved in the binding of hydrogen peroxide. Hydrogen peroxide is unable to bind when this group is protonated. The linear dependence of the log K_m for chloride on pH shows that for binding of chloride to occur, protonation of a group is essential. However protonation of this group is clearly not essential for bromide oxidation. Both the K_m for bromide of the native bromoperoxidase from *A. nodosum* and the vanadium

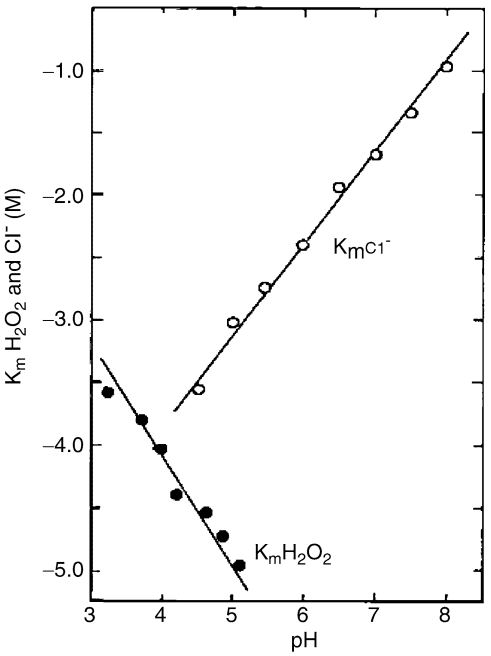

Fig. 5.4 Log K_m for chloride and hydrogen peroxide as a function of pH. Figure was constructed from data published in [7, 65]

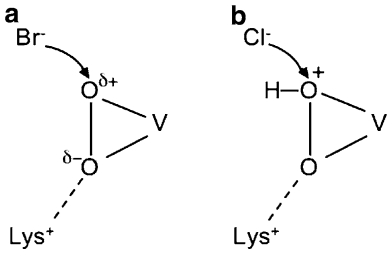

Scheme 5.2 Protonation state of the side-on bound peroxide that is attacked by the incoming halide. (**a**) less oxidizing non-protonated form of the side-on bound hydrogen peroxide. (**b**) strongly oxidizing protonated form

chloroperoxidase oxidizing bromide are hardly dependent upon pH. Thus it has been proposed [66, 81] that chloride oxidation requires protonation of the peroxo-complex in the active site as confirmed by model studies [82] and DFT calculations [83] that suggested the necessity of protonation of the peroxo- state for chloride oxidation on each turnover. Scheme 5.2 illustrates the proposal.

A similar band in the near UV (316 nm) as observed in the optical spectrum of vanadium bromoperoxidase [73] is present in the chloroperoxidase [80], which is not found in the apo-enzyme. The intensity of the band at 316 nm decreases upon addition of hydrogen peroxide but a weak band is formed at 480 nm. Chloride restores the original spectrum. This has allowed monitoring the pre-steady state binding of peroxide to the enzyme and made it also possible to study the reaction of the peroxo-intermediate with the second substrate chloride.

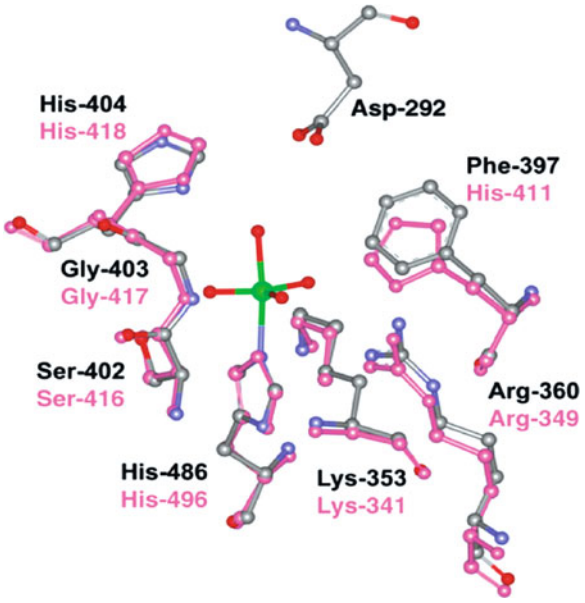

Fig. 5.5 Active sites of VCPO from *C. inaequalis* (*grey*) and VBPO from *A. nodosum* (*pink*) have been superimposed to demonstrate the similar geometries. Active site residue labels correspond to VCPO (*top*) and VBPO (*bottom*) (From [84]. Reproduced with permission of the American Chemical Society)

The first order rate constant for the binding of hydrogen peroxide to the enzyme at pH 5 was 0.8×10^5 M^{-1} s^{-1}. At higher pH values the reaction between enzyme and peroxide was too fast to be measured. This increase in rate constant may relate to the decrease in K_m for peroxide at higher pH values (see Fig. 5.5). It was also possible to study the rate of chloride oxidation by the peroxo-intermediate using a sequential stopped flow [80]. The first-order rate constant of 7.0 s^{-1} is similar in magnitude to the k_{cat} obtained from steady-state kinetics.

The UV-VIS spectra of several mutants have been obtained [80, 81] and the UV spectra together with the known X-ray data [85] confirm that amino acid residue in the active site contribute to the optical spectrum in the near UV. The crystal structure of the His496Ala mutant shows that tetrahedral vanadate is present in the active site but not bound to this histidine [85]. The optical spectrum [81] of this mutant lacks the feature at 315 nm indicating that the V-N bond is crucial for the observed spectrum.

The optical absorption spectra including the effect of peroxide addition, change of pH and mutation of active site residues are in line with TD-DFT and quantum mechanical calculations [86]. In the native enzyme a His496 $p \rightarrow V$ 3d transition dominates, whereas in the peroxide form a peroxide $p^* \rightarrow V$ 3d CT transition found at 480 nm is most intense. On the basis of analogy to well-studied inorganic imidazole-peroxovanadate complexes this band was already attributed [80] to a

peroxo- to vanadium charge-transfer band. Thus by using reliable models of active sites in chloroperoxidase the observed spectral features can be calculated theoretically.

The bromoperoxidase activity of chloroperoxidase has also been studied [64]. The chloroperoxidase has much larger very oxidation efficiency for bromide (K_m about 10 μM) than the bromoperoxidase, which has a K_m for bromide at pH 5.2 of 5.1 mM. The k_{cat} at pH 5 is about 250 s^{-1}. This value is similar to that of the bromoperoxidase from *A. nodosum*. The chloroperoxidase is strongly inhibited by excess bromide and hardly any activity is observed at 100 mM bromide. Interestingly the vanadium peroxidase that was isolated [87] from the lichen *Xanthoria parietina* that grows on rocks and stones also has a very small value (28 μM) for the K_m for bromide. This enzyme was also inhibited strongly by excess bromide. It is conceivable therefore that this enzyme is also a vanadium chloroperoxidase. However, chloroperoxidase activity has not been tested.

Table 5.1 shows that the specificity constants for the reaction of hydrogen peroxide with the peroxidases and mutants are nearly the same in all cases and not affected by pH. These specificity constants correspond [59] to the lower limits of the bimolecular rate constant of the binding of peroxide to the vanadate and this means that the protein environment in the active site does not control the reaction of peroxide with vanadate. In contrast the specificity constants for the reaction with the halides vary 1000-fold. This suggests that in line with the oxidation-reduction potentials of the halides the halide reactivity is driven by chemical reactivity of the peroxo-vanadium intermediate rather than molecular recognition in a binding pocket [58].

5.5 Sulfoxidation and Other Oxidation Reactions

In the absence of halide the vanadium haloperoxidases are capable of catalyzing the enantioselective sulfoxidation of organic sulfides [88, 89]. The bromoperoxidase from the red seaweed *C. pilulifera* produces the S-enantiomer of methyl phenyl sulfoxide (55% e.e.) whereas the bromoperoxidase from the brown seaweed *A. nodosum* produces the R-enantiomer of this sulfide (96% e.e.) [89, 90]. Organic sulfides that structurally resemble indenes and also small sulfides, possessing a *cis*- positioned carboxyl group with respect to the sulfur atom, are rapidly converted to the corresponding sulfoxides with selectivities exceeding 95% e.e. The oxygen of the peroxide is directly transferred to the sulfide in a selective manner, strongly suggesting that the aromatic sulfide binds near or at the active site with a relatively high K_m value > 1.5 mM [89]. Compared to the brominating activity of the bromoperoxidase from *A. nodosum* (166 s^{-1}). The k_{cat} value for the sulfoxidation reactions (1 min^{-1}) is low. This enzyme also catalyzes the sulfoxidation of racemic non-aromatic cyclic thioethers with kinetic resolution [91]. In contrast to the vanadium bromoperoxidases the chloroperoxidase was observed to mediate the formation of only racemic sulfoxides [90]. The highly reactive chloroperoxidase

peroxo intermediate probably directly abstracts an electron from the substrate. A positively charged sulfur radical is subsequently formed which migrates from the enzyme and is subsequently non-enzymatically converted into a sulfoxide.

Surprisingly, the recombinant vanadium chloroperoxidase from the fungus C*urvularia inaequalis* catalyzes the oxidation of 2,2′-azino-bis(3-ethylbenzthiazoline-6-sulfonic acid) (ABTS), a classical chromogenic heme peroxidase substrate. The enzyme mediates the oxidation of ABTS in the presence of hydrogen peroxide with a turnover frequency of 11 s^{-1} at pH 4.0 and has a K_m for ABTS of approximately 35 μM [92]. Also the industrial sulfonated azo dye Chicago Sky Blue 6B was bleached by recombinant vanadium chloroperoxidase in the presence of hydrogen peroxide. No further studies on this bleaching reaction have been reported.

5.6 Stability of Bromo and Chloroperoxidases

The bromo and chloroperoxidases are remarkable stable [23, 73, 87, 93–95]. In particular the chloroperoxidase is highly resistant towards elevated temperatures; the midpoint temperatures determined from thermal denaturation curves of the chloroperoxidase range from 82°C to 90°C [65]. Detergents such as SDS or water miscible organic solvents e.g. ethanol or dioxane have little effect on activity. The vanadium chloroperoxidase also remains fully active and is stable in micro-emulsions containing 10% non-ionic surfactant [96]. Oxidative agents such as H_2O_2 at concentrations in the M range, HOCl and singlet oxygen have little effect on the activity of the chloroperoxidase [61]. In comparison to heme peroxidases the vanadium haloperoxidases are unique and the ability of the enzymes to handle the oxidative substrate and product are related to the nature of the active site. This stability is a requirement for the potential application of the vanadium peroxidase as (industrial) biocatalyst in organic synthesis, their use in disinfection formulations [33, 97] and as bleaching enzymes [63].

5.7 X-Ray Structures of Vanadium Bromoperoxidases

Three X-ray structures of bromoperoxidases have been determined, the homodimeric structure of the enzyme from the brown seaweed *A. nodosum* [71] and those of the red seaweeds *Corallina pilulifera* and *C. officinalis* [72]. The enzymes from the red seaweeds crystallize as dodecamers and the structures are made up of 6 homo-dimers. The subunit in the bromoperoxidases from *Cor. officinalis* [98] measures approximately 85 × 56 × 55 Å in size. Twelve subunits are arranged within a 23 cubic point group symmetry. The vanadate-binding site is located at the bottom of the active site cleft, which is about 20 Å deep and 14 Å wide. The active site cleft is formed predominantly from residues of two different subunits in the dimer. These subunits are intertwined and this suggests that the subunit by itself will show no

activity and that reconstitution of activity of a recombinant enzyme is a difficult process. It is possible to superimpose the secondary structure of the vanadium chloroperoxidase [99] from the fungus *Curvularia inaequalis* on the *Corallina* bromoperoxidase dimer. Many of the a-helices of each chloroperoxidase domain are structurally equivalent [98] to the a-helices in the *Corallina* bromoperoxidase dimer.

5.8 Active Site of Vanadium Bromoperoxidase from *A. Nodosum* and Chloroperoxidase from *Curvularia inaqualis*

Most of the amino acid residues in the active site of the haloperoxidases are conserved. Figure 5.5 illustrates the active site in the bromoperoxidase from *A. nodosum* [71] in pink and also that of the vanadium chloroperoxidase from *Curvularia inaequalis* [99] in grey.

In the bromoperoxidase from *A. nodosum* vanadium is bound as orthovanadate on the N-terminal side of a four-helix bundle and the vanadium metal is the center of a trigonal bipyramid with three equatorial oxo ligands, one oxygen in the axial position and a covalent linkage to the $N^{\varepsilon 2}$ of His486. The positively charged amino acids, including Lys341, Arg349 and Arg480 form a kind of a positively charged cage, which compensates the negative charge of the oxygen atoms in the equatorial plane. There are hydrogen bonds of the Ser416 and Gly417 to the bound vanadate. The axial oxygen atom forms a hydrogen bond with the $N^{\varepsilon 1}$ of the distal His418, which is a conserved catalytic residue in vanadium peroxidases. As in the enzyme from *Cor. officinalis* amino acid residues from both monomers contribute to the substrate access channel of each active center.

Both a 2.1 Å crystal structure of native chloroperoxidase and of recombinant chloroperoxidase at 1.66 Å resolution has been reported [85, 99, 100]. The enzyme molecule crystallizes as a monomer and has an overall cylindrical shape (not shown) with a length of about 80 Å and a diameter of 55 Å. The protein fold is mainly α-helical with two four-helix bundles as the main structural motifs. In contrast to the vanadium bromoperoxidase from *A. nodosum* there are no disulfide bridges in the chloroperoxidase. The vanadium-binding center is located on top of the second four-helix bundle and orthovanadate is bound in the same way as in the bromoperoxidases. Three oxygen atoms form a plane and the fourth oxygen is found at the apex. It is hydrogen bonded to the nitrogen $N^{\varepsilon 1}$ of His404. The $N^{\varepsilon 2}$ atom from His496 ligates directly to the metal. Again the negative charge of the vanadate group is compensated by hydrogen bonds to three positively charged residues (Arg360, Arg490, Lys353). Further, the vanadate forms hydrogen bonds with a glycine (Gly403) and a serine residue (Ser402). There is also a histidine residue (His404) close to and hydrogen bonded to the apical hydroxyl moiety of the vanadate that may act as an acid/base group in catalysis. Two water molecule

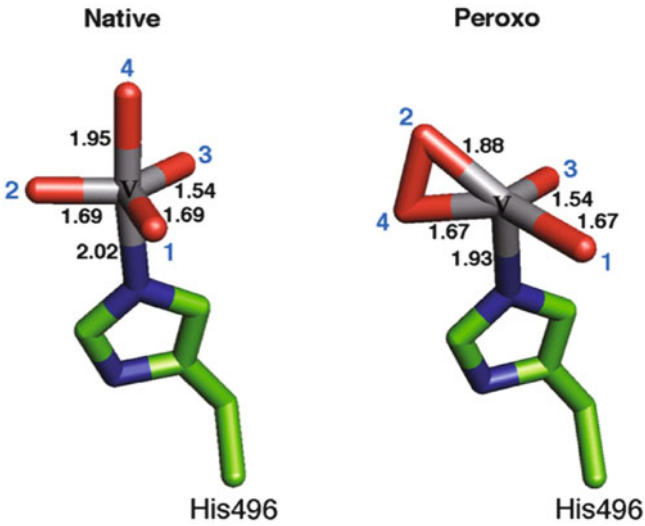

Fig. 5.6 Suggested location of the V–O and V–N distances obtained from the vanadium K-edge EXAFS recorded for native VCPO (*left*) after the addition of H_2O_2 (peroxo- intermediate) (*right*), on the basis of the coordination numbers determined by protein crystallography for crystals obtained at pH 8.0 [99]. PDB VCPO (Wildtype): 1idq, resolution 2.03 Å at pH 8.0. PDB PeroxoVCPO (wildtype): 1idu, resolution 2.24 Å and pH 8.0. The vanadium centre (V) is shown in grey and the oxygens (*red*, labeled 1, 2, 3 and 4) and nitrogens (*blue*) are labeled based on [99] (Reproduced with permission from [101])

hydrogen bonded to the His 404 are also present in the chloroperoxidase [99]. As Fig. 5.6 shows the active sites of the two enzymes are structurally nearly superimposable.

X-ray structures are not yet available for a vanadium iodoperoxidase. However, the full-length cDNA has been obtained [37] for the iodoperoxidase from *L. digitata* and phylogenetic analyses indicated that this iodoperoxidase shares a close common ancestor with brown algal vanadium-dependent bromoperoxidases. A three-dimensional structure model of the iodoperoxidase active site and comparisons with those of other vanadium- dependent haloperoxidases revealed [37] a striking difference in the catalytic region of iodoperoxidase. Instead of an invariant serine in vanadium bromo- and chloroperoxidase an alanine residue (Ala481) is present at the same position (Fig. 5.6). This substitution results in the loss of one of the hydrogen bonds involving the negatively charged oxygen atoms of the vanadate cofactor in vanadium chloro and bromoperoxidase.

Recently [101] vanadium K-edge X-ray Absorption Spectra were reported for the native and peroxo-forms of vanadium chloroperoxidase from *Curvularia inaequalis* at pH 6.0. The Extended X-ray Absorption Fine Structure (EXAFS) regions provided a refinement of crystallographic data. As shown in Fig. 5.6 vanadium is coordinated in the native enzyme to two oxygen atoms at 1.69 Å, another oxygen atom at 1.93 Å and the nitrogen of an imidazole group at 2.02 Å. Further one short

V-O bond (1.54 Å) is present. In addition to H bonds oxygen atom 1 and 2 have electrostatic interaction with the positively charged residues Arg360 and Arg489 and Lys353 (O2). The EXAFS data [74] on the vanadium bromoperoxidase from *A. nodosum* and the X ray structure of this enzyme [71] also show one short V=O bond. Reduction of the chloroperoxidase with dithionite has a clear influence on the spectrum, showing a change from vanadium (V) to vanadium (IV).

5.9 Structure of the Peroxo-Intermediate of Vanadium Chloroperoxidase

By incubating native crystals in mother liquor containing peroxide and shock freezing these in cryobuffer it was possible to obtain the X-ray structure of the important catalytic peroxo-intermediate [99]. The peroxide is bound side-on with a distance of 1.47 Å between the two peroxide oxygen atoms O2 and O4. The resulting coordination geometry is that of a distorted tetragonal pyramid with only four oxygen atoms and one nitrogen atom. According to the X-ray data there are several changes in the hydrogen-bonding network when peroxide is bound. His404 is no longer bonded to any of the vanadate oxygens, but there are still two water molecules in the active site. Lys353 forms a hydrogen bond to one of the peroxide oxygens. The EXAFS study [102] gives a refinement of the X-ray structure, although it should be kept in mind that the X-rays structure was obtained at pH 8 and the EXAFS study was carried out at pH 6. As Fig. 5.6 shows a short V=O bond of 1.54 Å is still present, another V-O bond at 1.67 Å and the side-on bound peroxide involves V-O bonds of 1.67 and 1.88 Å to oxygen atoms 2 and 4, respectively. Oxygen atom 2 is more exposed to the solvent, whereas oxygen 4 is more buried in the protein cavity [63] and is hydrogen bonded to Lys 353. This Lys 353 polarizes the oxygen-oxygen bond and is very important in catalysis. Indeed mutation to an alanine [81] has a profound effect on the catalytic activity. Considering the location of oxygen 2 in the active site it is likely that at this atom nucleophilic attack by halide occurs. The shorter V-N bond observed in the peroxo-form with respect to the native enzyme is in line with the previously reported [80] stronger binding of peroxo vanadate to the enzyme.

5.10 Molecular Mechanism of Vanadium Haloperoxidases and Difference in Reactivity Between Iodo-, Bromo-, and Chloroperoxidase

Based on the effect of mutations of the active site residues and kinetic data the following mechanism arises for the chloroperoxidase. By the Lewis acid properties of the metal ion electron density is withdrawn from the bound peroxide assisted by

the two positively charged arginine residues (Arg490 and Arg360). The conserved Lys353 that forms a hydrogen bond to one of the oxygen atoms further polarizes and activates the bound peroxide. One of the oxygen atoms of the peroxide is protonated to allow oxidation chloride ion (c.f. Fig. 5.4). After formation of the peroxide intermediate the next step in catalysis is the nucleophilic attack of the halide on the electrophilic hydrogen peroxide (oxygen 2 in Fig. 5.6) and breaking the peroxide bond, resulting in formation of HOX or XO^-. All mutations of the active site residues result in kinetically crippled [64, 66, 80, 81] mutants. Most or all of the chloroperoxidase activity is lost, however, some mutants retain some bromoperoxidase activity.

Detailed structural data are available now and in principle it should be possible to explain the difference in reactivity between the vanadium iodo-, bromo- and chloroperoxidases and the effects of mutations on the activity. A prominent difference in the active site architecture of the chloroperoxidase and the iodo- and bromoperoxidases is the presence of a second histidine in the iodo- and bromoperoxidase, a residue that in chloroperoxidase is a phenylalanine. Since chloride is more easily oxidized than bromide and bromide more easily oxidized than iodide it has been suggested [63, 71, 81] that the histidine in bromoperoxidase accepts the proton from the bound peroxide and in this way reduces the oxidative strength of the bound peroxide and the reactivity of the peroxidase. This decrease in reactivity may also explain why vanadium chloroperoxidase is strongly inhibited [103] by the nucleophilic inhibitor azide whereas the bromoperoxidase is only weakly inhibited by azide. When by site-directed mutagenesis the Phe397 in chloroperoxidase was replaced by a histidine it was observed [66] that the specificity constant for the oxidation of chloride decreases 100-fold. However, the specificity constant for bromide oxidation decreased also10-fold and further the mutant rapidly inactivated during turnover. Thus the difference in oxidizing ability between the two enzymes is not simply due to a single residue but apparently more factors are involved. An attempt was also made to induce chlorinating activity in the bromoperoxidase from *C. pulilifera* by mutating the Arg397 in this bromoperoxidase to a tryptophane that is present in chloroperoxidase. Indeed chlorinating activity was observed [104], however, the reported K_m value for chloride of about 700 mM is 100-fold higher than that of native chloroperoxidase. No satisfactory explanations have been offered for these observations and the factors that are important in tuning the reactivity of the haloperoxidases are not fully understood.

The active site of bromoperoxidase differs from the iodoperoxidase by the presence of serine instead of an alanine residue. The absence of the polar serine residue in the iodoperoxidase from *L. digitata* lowers the charge neutralization of the vanadate cofactor in its peroxo state and this may be the reason [37, 58] why the peroxo-vanadate in the iodoperoxidase is less capable of oxidizing highly electronegative halides. In this context the observation is important that a significant decrease in the chloride oxidation occurs when the Ser402 in vanadium chloroperoxidase is mutated to an alanine residue [66]. This mutation abolishes oxidation of the most electronegative halide, i.e. chloride, while maintaining still 20% oxidizing activity of bromide. Finally it should be noted the access cavity in

vanadium iodoperoxidase is wide and open compared to the small deep channel to the active site in chloroperoxidase. This feature may affect the reactivity of the peroxo-intermediate to halides [105] as well. This exposed site may also explain why an acid phosphatase that has essentially the same active site as the chloroperoxidase [79] and in which vanadate is substituted has only a very low brominating activity [106]. This phosphatase has a very accessible active site [107, 108].

Driven by potential application of the chloroperoxidase in antifouling paints a directed evolution study [63] was carried out to improve the brominating activity of the vanadium chloroperoxidase from *C. inaequalis* at mildly alkaline pH. Two rounds of random mutagenesis were carried out, followed by saturation mutagenesis at a hot-spot position. A triple mutant was created by rational combination of positive mutants. This final triple mutant had an activity that was the highest ever measured for vanadium haloperoxidases. At pH 8 it showed an increase in the k_{cat} from 1 to 100 s^{-1} and at pH 5 a fivefold higher brominating activity was found (k_{cat} 575 s^{-1}). Also the chlorinating activity at pH 5 was doubled to 36 s^{-1}. The K_m values for the substrates increased somewhat but overall the specificity constants k_{cat}/K_m for bromide and chloride were increased (Table 5.1). The mutants were in the first and second coordination sphere of the vanadate cofactor and the effect on the steady-state kinetic parameters confirm that fine-tuning of residues Lys353 and Phe397 and changes in the electrostatic potential in the active site are very important.

5.10.1 Theoretical Calculations on the Nature of the Vanadate Cofactor

A detailed molecular picture of the catalytic mechanism of the haloperoxidases requires understanding of the structure of the vanadate cofactor, its protonation state, protonation state of the peroxo intermediate and the relevant interactions between vanadate and surrounding amino acids. The present accuracy of the X-ray data does not allow an assignment of these protonation states and hydrogen bonding networks. Several theoretical investigations have therefore been performed on vanadium complexes that model the native VCPO and on the enzyme itself. However, it should be kept in mind that the theoretical calculations up to now are based upon the X-ray data and the more accurate distances obtained by EXAFS have not been taken into account yet.

DFT calculations [109] resulted in a doubly protonated vanadate with an axial hydroxo ligand and one hydroxo group in the equatorial plane. The same conclusion was reached in a time-dependent DFT study [110] as well as in a QM/MM study [111]. A solid-state ^{51}V-NMR study on VCPO in combination with DFT calculations of the NMR observables using a series of small models [84] concluded this picture. The importance of including the protein environment into the QM models was also shown [107] which again led to a minimum with two protons, but now in the form of an axially bound water ligand. The ^{51}V-NMR chemical shifts

[101] were remodeled [112] using QM/MM-optimized models of the complete protein and systematically increasing the size of the QM region. It was concluded that the resting state of the cofactor is either the proposed doubly protonated vanadate or a triply protonated state in which there is an axially bound water and an equatorial hydroxide. These studies converge on the scenario in which the resting state of the enzyme can be described as doubly protonated trigonal bipyramidal vanadate with at least one hydroxyl group in the apical position. The second proton can be assigned to any of the equatorial oxygen atoms or to the apical oxygen forming a bound water molecule. According to [113] and based on quantum mechanics/molecular mechanics evaluations of ground state properties, UV-VIS spectra and NMR chemical shifts the most likely ground state configuration of vanadate in vanadium chloroperoxidase is an axially bound water molecule that is stabilized by a hydrogen bond to His404. Mutation experiments already showed that the mutant His404Ala was strongly impaired in its activity and ability to bind vanadate. Further water molecules that are present in the crystallographic structure are very important in explaining the spectral and NMR data. These computational studies and the studies of the effect of mutations on the enzymatic activity and structure show clearly that the enzyme has a very complex hydrogen-bonding network around the cofactor. Two water molecules also participate in this but whether they have a possible role in tuning the activity is not clear. Thus the factors that are important in tuning the reactivity are not fully understood but it is unlikely that halide specificity is due to a selective halide binding effect. In this respect it should be noted that the existence of halide binding pocket is doubtful. Haloperoxidases are inhibited by excess halide and if a halide is found in the active site of these enzymes [114] it may present binding to an inhibitory site. The ability to oxidize halides most likely relates to the action of amino acid residues on the peroxo-intermediate in or in close vicinity of the active site and the resulting hydrogen bonding network.

5.11 Bacterial Vanadium Enzymes

Thus far vanadium haloperoxidases have only been found in eukaryotes but they may also be present in prokaryotes. Three putative homologous genes that are present in the 43-kb napyradiomycin biosynthetic cluster found in marine sediment derived actinomycetes [115] show sequences that correspond to the active site residues of the vanadium haloperoxidases but also to the acid phosphatases. Heterologous expression of this biosynthetic cluster in bacterial host resulted in the synthesis of chlorinated meroterpenoids. This observation was taken as evidence that bacteria also contain vanadium enzymes. However, an alignment (Fig. 5.7) of the active site region of the vanadium chloroperoxidase with corresponding parts in the NapH1, NapH3 en NapH4 region show clearly that the active site residue His404 is lacking and replaced by either a serine residue (NapH1 and NapH4) or a phenylalanine at this position.

```
NapH1          ATFEPLIAAWHHKRIYDAVRPVTAVRHVYGNRKIRAWGGVGMGTVDDIRASEWSSYLPVG 419
NapH4          ATFDTLIAAWGYKRKYEAVRPITAVRHVYGNRKIRAWGGVGMGTVDDIRANEWAGYLPVG 414
NapH3          ARFDSLIAAWHHKRAYDTVRPFSAVRHVYGSKPVTAWGGPGKGTVESIPADEWTGYLPVG 332
VCPO           ACTDAGIFSWKEKWEFEFWRPLSGVRDDGRPD-----HGDPFWLTLGAPATNTNDIPFKP 395
                            *      *

NapH1          DHPEYPSGSTSLCSATSQAARRYFESDELDWTINYKAGSTVVEPGITPGKDLSIHIPTWT 479
NapH4          DHPEYPSGSTTVGSAASQAARRFFDSDDLNWEFDFEVGKSIVEPGITPVENVRVSFPTWT 474
NapH3          NHPEYPSGFTTLIAAQAQAARSFLGDDVLNWTHAFPAGSGQREPGAVPASDLELTWATWT 392
VCPO           PFPAYPSGHATFGGAVFQMVRRYYNGRVGTWKDDEPDNIAIDMMISEELNGVNRDLRQPY 455
                     ***

NapH1          DFTR-------------------------TCGNSRVWGGVHFQTTVDRT----------- 503
NapH4          DFNK-------------------------RCAYSRVDGGVHFKKTVERS----------- 498
NapH3          DFEN-------------------------DCATSRVWAGAHFTKTAETS----------- 416
VCPO           DPTAPIEDQPGIVRTRIVRHFDSAWELMFENAISRIFLGVHWRFDAAAARDILIPTTTKD 515
                                              *     *
```

Fig. 5.7 Alignment of the sequences of NapH1, NapH4, NapH3 and vanadium chloroperoxidase. Conserved residues in bold. *, Active site residues involved in hydrogen bonds and binding the vanadate cofactor. Clustal W was used for the phylogenic analysis

Considering the importance of this residue in catalysis [81] it is unlikely that all these genes code for an active haloperoxidase and may have another function e.g. as discussed below as phosphatases.

5.12 Active Site Similarity of Haloperoxidases and Acid Phosphatases

The three regions providing the metal-anion binding site in the vanadium enzymes show [116–118] a high similarity to stretches that are present in a large group of acid phosphatases that were previously considered unrelated. Based on this sequence similarity and the structural and electronic homology with phosphate, it was concluded that the architecture of the active sites in the two classes of enzymes is very similar. Indeed the X-ray structure of the acid phosphatase [107] from *Escherichia blattae* and that [108] of *Salmonella enterica* confirmed the remarkable similarity of the residues binding vanadate in the vanadium enzymes and phosphate in the phosphatases. Not only the phosphatases from bacteria contain this motif for the active site but it is wide spread in nature and include for example the membrane-bound glucose-6-phosphatase, an enzyme involved in regulation of glucose levels in the blood of mammals and the large family of lipid phosphohydrolases [118].

Since the same supra-molecular environment is present in the two classes of enzymes, it is likely that they exhibit dual enzymatic activities. Indeed when vanadate was removed from the active site of the vanadium chloroperoxidase from *C. inaequalis* it exhibited phosphatase activity [79]. However, the phosphatase activity with *p*-nitrophenyl phosphate (*p*NPP) is low probably due to the deeply buried active site in the protein that is not easily accessible for substrates. The low turnover allowed pre-steady state-studies on the phosphatase activity of both on both native

chloroperoxidase and mutants [81] and to obtain details of the mechanism. A rather stable phospho-intermediate is formed in which His496 acting as a nucleophile reacts with the phosphate group. By incubating apo-chloroperoxidase crystals with *p*-nitrophenylphosphate and subsequent flash cooling of the crystals it was possible to trap the phospho-intermediate intermediate and obtain a high resolution X-ray structure [119]. It consists of a metaphosphate anion PO_3^- covalently bound via its phosphorous atom to the $N^{\varepsilon 2}$ atom of the His 496 with a water molecule in the position for a nucleophilic attack on the phosphorus.

When vanadate is substituted in the active site of acid phosphates they exhibit bromoperoxidase activity and enantioselective sulfoxidation activity. Thus, the analogy between these classes of enzymes includes both structural and catalytic aspect. However, the turnover values of 3–30 min^{-1} are much lower than of native bromoperoxidase from *A. nodosum.* When vanadate is substituted in the phosphatase phytase sulfoxidation and bromoperoxidase activity is observed also [120]. However, phytase does not belong to the class of acid phosphatases and active site of phytase has an architecture that differs from the acid phosphatases. The phosphatases have very different physiological functions and are found in species varying from *E. coli* to humans. Since phosphate and phosphate metabolizing enzymes entered evolution at an early stage and in which oxygen and hydrogen peroxide were not yet present, it seems likely that vanadate was coined by nature to become the prosthetic group in the vanadium enzymes in a more recent period and thus these enzymes have evolved from the phosphatases.

References

1. Butler A (1998) Acquisition and utilization of transition metal ions by marine organisms Butler. Science 281:207–210
2. Lagerkvist BJ, Oskarsson A (2007) Vanadium. In: Nordberg GF, Fowler BA, Nordberg M, Friberg L (eds) Handbook on the toxicology of metals, 3rd edn. Academic, San Diego, pp 905–924
3. Vilter H (1984) Peroxidases from phaeophyceae- a vanadium (V) dependent peroxidase from *Ascophyllum nodosum*. Phytochemistry 23:1387–1390
4. Wever R, Plat H, DeBoer E (1985) Isolation procedure and some properties of the bromoperoxidase from the seaweed *Ascophyllum nodosum*. Biochim Biophys Acta 830:181–186
5. De Boer E, van Kooy Y, Tromp MGM, Plat H, Wever R (1986) Bromoperoxidase from *Ascophyllum nodosum*: a novel class of enzymes containing vanadium as a prosthetic group? Biochim Biophys Acta 869:48–53
6. De Boer E, Tromp MGM, Plat H, Krenn GE, Wever R (1986) Vanadium (V) as an essential element for haloperoxidase activity in marine brown algae: purification and characterization of a vanadium (V)-containing bromoperoxidase from *Laminaria saccharina*. Biochim Biophys Acta 872:104–115
7. VanSchijndel JWPM, Vollenbroek EGM, Wever R (1993) The chloroperoxidase from the fungus *Curvularia inaequalis*; a novel vanadium enzyme. Biochim Biophys Acta 1161: 249–256
8. Vollenbroek EGM, Simons LH, van Schijndel J, Barnett P, Balzar M, Dekker H, van der Linden C, Wever R (1995) Vanadium chloroperoxidases occur widely in nature. Biochem Soc Trans 23:267–271

9. De Boer E, Boon K, Wever R (1988) Electron paramagnetic resonance studies on conformational states and metal ion exchange properties of vanadium bromoperoxidase. Biochemistry 27:1629–1635
10. Colin C, Leblanc C, Wagner E, Delage L, Leize-Wagner E, van Dorsselaer A, Kloareg B, Potin P (2003) The brown algal kelp *Laminaria digitata* features distinct bromoperoxidase and iodoperoxidase activities. J Biol Chem 278:23545–23552
11. Wever R, Hemrika W (2001) Vanadium haloperoxidases. In: Messerschmidt A, Hubert R, Poulos T, Wieghardt K (eds) Handbook of metalloproteins. Wiley, Chichester, pp 1417–1428
12. Suthiphongchai T, Boonsiri P, Panijpan B (2008) Vanadium-dependent bromoperoxidases from *Gracilaria* algae. J Appl Phycol 20:271–278
13. Wever R, Tromp MGM, Van Schijndel JWPM, Vollenbroek E (1993) Bromoperoxidases: their role in the formation of HOBr and bromoform by seaweeds. In: Oremland RD (ed) Biogeochemistry of global change. Chapman and Hall, New York, pp 811–824
14. Moore RM, Webb M, Tokarczyk R, Wever R (1996) Bromoperoxidase and iodoperoxidase enzymes and production of halogenated methanes in marine diatom culture. J Geophys Res 101:20899–20908
15. Ohshiro T, Nakano S, Takahashi Y, Suzuki M, Izumi Y (1999) Occurrence of bromoperoxidase in the marine green macro-alga, *Ulvella lens*, and emission of volatile brominated methane by the enzyme. Phytochemistry 52:1211–1215
16. Carpenter LJ, Liss PS (2000) On temperate sources of bromoform and other reactive organic bromine gases. J Geophys Res 105:20539–20547
17. Simpson WR, von Glasow R, Riedel K, Anderson P, Ariya P, Bottenheim J, Burrows J, Carpenter LJ, Friess U, Goodsite ME, Heard D, Hutterli M, Jacobi HW, Kaleschke L, Neff B, Plane J, Platt U, Richter A, Roscoe H, Sander R, Shepson P, Sodeau J, Steffen A, Wagner T, Wolff E (2007) Halogens and their role in polar boundary-layer ozone depletion. Atmos Chem Phys 7:4375–4418
18. Read KA, Mahajan AS, Carpenter LJ, Evans MJ, Faria BVE, Heard DE, Hopkins JR, Lee JD, Moller SJ, Lewis AC, Mendes L, McQuaid JB, Oetjen H, Saiz-Lopez A, Pilling MJ, Plane JMC (2008) Extensive halogen-mediated ozone destruction over the tropical Atlantic Ocean. Nature 453:1232–1235
19. Itoh N, Shinya M (1994) Seasonal evolution of bromomethanes from coralline algae (Corallinaceae) and its effect on atmospheric chemistry. Mar Chem 45:95–103
20. Dyrssen D, Fogelqvist E (1981) Bromoform concentrations of the Artic Ocean in the Svalbard area. Oceanol Acta 43:313–317
21. Krysell M (1999) Bromoform in the Nansen Basin in the Arctic Ocean. Mar Chem 33: 187–197
22. Wever R, Tromp MGM, Krenn BE, Marjani A, van Tol M (1991) Brominating activity of the seaweed *Ascophyllum nodosum* – impact on the biosphere. Environ Sci Technol 25:446–449
23. Almeida M, Filipe S, Humanes M, Maia MF, Melo R, Severino N, da Silva JAL, da Silva JJRF, Wever R (2001) Vanadium haloperoxidases from brown algae of the Laminariaceae family. Phytochemistry 57:633–642
24. Krenn BE, Tromp MGM, Wever R (1989) The brown alga *Ascophyllum nodosum* contains 2 different vanadium bromoperoxidases. J Biol Chem 264:19287–19292
25. Almeida MG, Humanes M, Melo R, Silva JA, Frausto Da Silva JJR, Wever R (2000) Purification and characterisation of vanadium haloperoxidases from the brown alga *Pelvetia canaliculata*. Phytochemistry 54:5–11
26. Borchardt SA, Allain EJ, Michels JJ, Stearns GW, Kelly RF, Mccoy WF (2001) Reaction of acetylated homoserine lactone signaling molecules with oxidized halogen antimicrobials. Appl Environ Microbiol 67:3174–3179
27. Sauvageau C (1926) Sur quelques algues floridée renformant du brome a l'etat libre. Bull Stat Biol D'Arcachon 23:1–23
28. Mtolera MSP, Collen J, Pedersen M, Ekdahl A, Abrahamsson K, Semesi AK (1996) Stress-induced production of volatile halogenated organic compounds in *Eucheuma denticulatum* (Rhodophyta) caused by elevated pH and high light intensities. Eur J Phycol 31:89–95

29. Bondu S, Cocquempot B, Deslandes E, Morin P (2008) Effects of salt and light stress on the release of volatile halogenated organic compounds by Solieria chordalis: a laboratory incubation study. Bot Mar 51:485–492
30. Nightingale PD, Malin G, Liss PS (1995) Production of chloroform and other low- molecular weight halocarbons by some species of macro algae. Limnol Oceanogr 40:680–689
31. Apel K, Hirt H (2004) Reactive oxygen species: metabolism, oxidative stress an signal transduction. Ann Rev Plant Biol 55:373–399
32. Hansen EH, Albertsen L, Schafer T, Johansen C, Frisvad JC, Molin S, Gram L (2003) Curvularia haloperoxidase: antimicrobial activity and potential application as a surface disinfectant. Appl Environ Microbiol 69:4611–4617
33. Renirie R, Dewilde A, Pierlot C, Wever R, Hober D, Aubry J-M (2008) Bactericidal and virucidal activity of the alkalophilic P395DL241VT343A mutant of vanadium chloroperoxidase. J Appl Microbiol 105:264–270
34. Theiler R, Cook JC, Hager LP, Siuda JF (1978) Halohydrocarbon synthesis by bromoperoxidase. Science 202:1094–1096
35. Jaworske DA, Helz GR (1985) Rapid consumption of bromine oxidants in river and estuarine waters. Environ Sci Technol 19:1188–1191
36. Leblanc C, Colin C, Cosse A, Delage L, La Barre S, Morin P, Fievet B, Voiseux C, Ambroise Y, Verhaeghe E, Amouroux D, Donard O, Tessier E, Potin P (2006) Iodine transfers in the coastal marine environment: the key role of brown algae and of their vanadium-dependent haloperoxidases. Biochemie 88:1773–1785
37. Colin C, Leblanc C, Michel G, Wagner E, Leize-Wagner E, Dorsselaer V, Potin P (2005) Vanadium-dependent iodoperoxidases in *Laminaria digitata*, a novel biochemical function diverging from brown algal bromoperoxidases. J Biol Inorg Chem 10:156–166
38. Palmer CJT, Anders L, Carpenter LJ, Küpper FC, McFiggans G (2005) Iodine and halocarbon response of *Laminaria digitata* to oxidative stress and links to atmospheric new particle production. Environ Chem 2:282–290
39. Laturnus F, Svensson T, Wiencke C, Öberg G (2004) Ultraviolet radiation affects emission of ozone-depleting substances by marine macroalgae: results from a laboratory incubation study. Environ Sci Technol 38:6605–6609
40. Dixneuf S, Ruth AA, Vaughan S, Varma RM, Orphal J (2009) The time dependence of molecular iodine emission from *Laminaria digitata*. Atmos Chem Phys 9:823–829
41. Saiz-Lopez A, Plane JMC, McFiggans G, Williams PI, Ball SM, Bitter M, Jones RL, Hongwei C, Hoffmann T (2006) Modeling molecular iodine emissions in a coastal marine environment: the link to new particle formation. Atmos Chem Phys 6:883–895
42. O'Dowd D, Jimenez JL, Bahreini R, Flagan RC, Seinfeld JH, Hämeri K, Pirjola L, Kulmala M, Jennings GS, Hoffmann T (2002) Marine aerosol formation from biogenic iodine emissions. Nature 417:632–636
43. McFiggans G, Coe H, Burgess R, Allan J, Cubison M, Alfarra MR, Saunders R, Saiz-Lopez A, Plane JMC, Wevill DJ, Carpenter LJ, Rickard AR, Monks PS (2004) Direct evidence for coastal iodine particles from Laminaria macroalgae – linkage to emissions of molecular iodine. Atmos Chem Phys 4:701–713
44. McFiggans G, Bale CSE, Ball SM, Beames JM, Bloss WJ, Carpenter LJ et al (2010) Iodine-mediated coastal particle formation: an overview of the reactive halogens in the marine boundary layer (RHaMBLe) Roscoff coastal study. Atmos Chem Phys 10:2975–2999
45. Ball SM, Hollingsworth AM, Humbles J, Leblanc C, Potin P, McFiggans G (2010) Spectroscopic studies of molecular iodine emitted into the gas phase by seaweed. Atmos Chem Phys 10:6237–6254
46. Kupper FC, Carpenter LJ, McFiggans GB, Palmer CJ, Walte TJ, Boneberg EM, Woitsch S, Weiller M, Abela R, Grolimund D, Potin P, Butler A, Luther GW, Kroneck PMH, Meyer-Klaucke W, Feiters MC (2008) Iodide accumulation provides kelp with an inorganic antioxidant impacting atmospheric chemistry. Proc Natl Acad Sci USA 105:6954–6958
47. Manley SL (2002) Phytogenesis of halomethanes: a product of selection or a metabolic accident? Biogeochemistry 60:163–180

48. Verhaeghe EF, Fraysse A, Guerquin-Kern JL, Wu TD, Deves G, Mioskowski C, Leblanc C, Ortega R, Ambroise Y, Potin P (2008) Microchemical imaging of iodine distribution in the brown alga *Laminaria digitata* suggests a new mechanism for its accumulation. J Biol Inorg Chem 13:257–269
49. Hunter-Cevera JC, Sotos LS (1986) Screening for new enzyme in nature: haloperoxidase production by Death Valley dematiaceous hyphomyctes. Microb Ecol 12:121–127
50. Hunter JC, Belt A, Sotos LS, Fonda ME (1990) Fungal chloroperoxidase method. US Patent 4,937,192
51. Barnett P, Hemrika W, Hl D, Muijsers AO, Renirie R, Wever R (1998) Isolation, characterization, and primary structure of the vanadium chloroperoxidase from the fungus *Embellisia didymospora*. J Biol Chem 273:23381–23387
52. Bar-Nunn N, Shcolnick S, Mayer AM (2002) Presence of a vanadium dependent peroxidase in *Botrytis cinerea*. FEMS Microbiol Lett 217:121–124
53. Barnett P, Kruitbosch DL, Hemrika W, Dekker HL, Wever R (1997) The regulation of the vanadium chloroperoxidase from Curvularia inaequalis. Biochim Biophys Acta 1352:73–84
54. Bengtson P, Bastviken D, de Boer W, Öberg G (2009) Possible role of reactive chlorine in microbial antagonism and organic matter chlorination in terrestrial environments. Environ Microbiol 11:1330–1339
55. Ortiz-Bermúdez P, Hirth KC, Srebotnik E, Hammel KE (2007) Chlorination of lignin by ubiquitous fungi has a likely role in global organochlorine production. Proc Natl Acad Sci USA 104:3895–3900
56. Fujimori DG, Walsh CT (2007) What is new in enzymatic halogenations. Curr Opin Chem Biol 11:553–560
57. Wagner C, El Omari M, Konig G (2009) Biohalogenation: nature's way to synthesize halogenated metabolites. J Nat Prod 72:540–553
58. Verhaeghe E, Buisson D, Zekri E, Leblanc C, Potin P, Ambroise Y (2008) A colorimetric assay for steady state analysis of iodo- and bromoperoxidase activities. Anal Biochem 379:60–65
59. De Boer E, Wever R (1988) The reaction mechanism of the novel vanadium-bromoperoxidase, a steady-state kinetic analysis. J Biol Chem 263:12326–12332
60. Soedjak HS, Walker JV, Butler A (1995) Inhibition and inactivation of vanadium bromoperoxidase by the substrate hydrogen peroxide and further mechanistic studies. Biochemistry 34:12689–12696
61. Renirie R, Pierlot C, Aubry JM, Hartog AF, Schoemaker HE, Alsters PL, Wever R (2003) Vanadium chloroperoxidase as a catalyst for hydrogen peroxide disproportionation to singlet oxygen in mildly acidic environment. Adv Synth Catal 345:849–858
62. De Boer E, Plat H, Tromp MGM, Wever R, Franssen MCR, van der Plas HC, Meijer EM, Schoemaker HE (1987) Vanadium containing bromoperoxidase: an example of an oxidoreductase with high operational stability in aqeous and organic media. Biotechnol Bioeng 30:607–610
63. Hasan Z, Renirie R, Kerkman R, Ruijssenaars HJ, Hartog AF, Wever R (2006) Laboratory-evolved vanadium chloroperoxidase exhibits 100-fold higher halogenating activity at alkaline pH; catalytic effects from first and second coordination sphere mutations. J Biol Chem 281:9738–9744
64. Hemrika W, Renirie R, Macedo-Ribeiro S, Messerschmidt A, Wever R (1999) Heterologous expression of the vanadium-containing chloroperoxidase from *Curvularia inaequalis* in *Saccharomyces cerevisiae* and site-directed mutagenesis of the active site residues His496, Lys353, Arg360 and Arg490. J Biol Chem 274:23820–23827
65. VanSchijndel JWPM, Barnett P, Roelse J, Vollenbroek EGM, Wever R (1994) The stability and steady state kinetics of vanadium chloroperoxidase from the fungus *Curvularia inaequalis*. Eur J Biochem 22:151–157
66. Tanaka N, Hasan Z, Wever R (2003) Kinetic characterization of the active site mutants Ser402Ala and Phe397His of vanadium chloroperoxidase from the fungus Curvularia inaequalis. Inorg Chem Acta 356:288–296

67. Feiters MC, Leblanc C, Kupper FC, Meyer-Klaucke W, Michel G, Potin P (2005) Bromine is an endogenous component of a vanadium bromoperoxidase. J Am Chem Soc 127: 15340–15341
68. Martínez VM, De Cremer G, Roeffaers MBJ, Sliwa M, Mukulesh M, De Vos DE, Hofkens J, Sels BF (2008) Exploration of single molecule events in a haloperoxidase and its biomimic: localization of halogenation activity. J Am Chem Soc 130:13192–13193
69. Carter-Franklin JN, Butler A (2004) Vanadium bromoperoxidase-catalyzed biosynthesis of halogenated marine natural products. J Am Chem Soc 126:15060–15066
70. Butler A, Carter-Franklin JN (2004) The role of vanadium bromoperoxidase in the biosynthesis of halogenated marine natural products. Nat Prod Rep 21:180–188
71. Weyand M, Hecht HJ, Kiess M, Liaud MF, Vilter H, Schomburg D (1999) X-ray structure determination of a vanadium-dependent haloperoxidase from *Ascophyllum nodosum* at 2.0 Å resolution. J Mol Biol 293:595–611
72. Isupov MN, Dalby AR, Brindley AA, Izumi Y, Tanabe T, Murshudov GN, Littlechild JA (2000) Crystal structure of dodecameric vanadium-dependent bromoperoxidase from the red algae *Corallina officinalis*. J Mol Biol 299:1035–1049
73. Tromp MGM, Olafsson G, Krenn BE, Wever R (1990) Some structural aspects of vanadium bromoperoxidase from *Ascophyllum nodosum*. Biochim Biophys Acta 1040:192–198
74. Arber JM, De Boer E, Garner CD, Hasnain SS, Wever R (1989) Vanadium K-Edge X-ray absorption spectroscopy of bromoperoxidase from Ascophyllum nodosum. Biochemistry 28:7968–7973
75. Carrano CJ, Mohan M, Holmes SM, Delarosa R, Butler A, Charnock JM, Garner CD (1994) Oxovanadium (V) alkoxy chlorocomplexes of the hydridotripyrozolyl-borates as models for the binding-site in bromoperoxidase. Inorg Chem 33:646–655
76. De Boer E, Keijzers CP, Klaasen AAK, Reijerse EJ, Collison D, Garner CD, Wever R (1998) N-14-coordination to $VO2^{+}$ in reduced vanadium bromoperoxidase, an electron spin echo study. FEBS Lett 235:93–97
77. Ohshiro T, Hemrika W, Aibara T, Wever R, Izumi Y (2002) Expression of the vanadium-dependent bromoperoxidase gene from a marine macro-alga Corallina pilulifera in *Saccharomyces cerevisiae* and characterization of the recombinant enzyme. Phytochemistry 60:595–601
78. Coupe EE, Smyth MG, Fosberry A, Hall RM, Littlechild JA (2007) The dodecameric vanadium-dependent haloperoxidase from the marine algae *Corallina officinalis*: Cloning, expression, and refolding of the recombinant enzyme. Protein Expr Purif 52:265–272
79. Hemrika W, Renirie R, Dekker HL, Barnett P, Wever R (1997) From phosphatases to vanadium peroxidases: a similar architecture of the active site. Proc Natl Acad Sci USA 94:2145–2149
80. Renirie R, Hemrika W, Piersma SR, Wever R (2000) Cofactor and substrate binding to vanadium-chloroperoxidase determined by UV-VIS spectroscopy and evidence for high affinity for pervanadate. Biochemistry 39:1133–1141
81. Renirie R, Hemrika W, Wever R (2000) Peroxidase and phosphatase activity of active-site mutants of vanadium chloroperoxidase from the fungus *Curvularia inaequalis*, implications for the catalytic mechanism. J Biol Chem 275:11650–11657
82. Smith TS, Pecoraro VL (2002) Oxidation of organic sulfides by vanadium haloperoxidase model complexes. Inorg Chem 41:6754–6760
83. Zampella G, Fantucci PVL, De Gioia L (2005) Reactivity of Peroxo Forms of the Vanadium Haloperoxidase Cofactor. A DFT investigation. J Am Chem Soc 127:953–960
84. Pooransingh-Margolis N, Renirie R, Hasan Z, Wever R, Vega AJ, Polenova T (2006) ^{51}V Solid-state magic angle spinning NMR spectroscopy of vanadium chloroperoxidase. J Am Chem Soc 128:5190–5208
85. Macedo-Ribeiro S, Hemrika W, Renirie R, Wever R, Messerschmidt A (1999) X-ray crystal structures of active site mutants of the vanadium-containing chloroperoxidase from the fungus *Curvularia inaequalis*. J Biol Inorg Chem 4:209–219

86. Borowski T, Szczepanik W, Chruszcz M, Broclawik E (2004) First-principle calculations for the active centers in vanadium-containing chloroperoxidase and its functional models: geometrical and spectral properties. Int J Quantum Chem 99:864–875
87. Plat H, Krenn BE, Wever R (1987) The bromoperoxidase from the lichen *Xanthoria parietina* is a novel vanadium enzyme. Biochem J 248:277–279
88. Andersson M, Willetts A, Allenmark S (1997) Asymmetric sulfoxidation catalyzed by a vanadium-containing bromoperoxidase. J Org Chem 62:8455–8458
89. Ten Brink HB, Tuynman A, Dekker HL, Hemrika W, Izumi Y, Oshiro T, Schoemaker HE, Wever R (1998) Enantioselective sulfoxidation catalyzed by vanadium peroxidases. Inorg Chem 37:6780–6784
90. Ten Brink HB, Schoemaker HE, Wever R (2001) Sulfoxidation mechanism of vanadium bromoperoxidase from *Ascophyllum nodosum*. Eur J Biochem 268:132–138
91. Ten Brink HB, Holland HL, Schoemaker HE, Van Lingen H, Wever R (1999) Probing the scope of the sulfoxidation activity of vanadium bromoperoxidase from *Ascophyllum nodosum*. Tetrahedron Asym 10:4563–4572
92. Ten Brink HB, Dekker HL, Schoemaker HE, Wever R (2000) Oxidation reactions catalyzed by vanadium chloroperoxidase from *Curvularia inaequalis*. J Inorg Biochem 80:91–98
93. Sheffield DJ, Harry T, Smith AJ, Rogers LJ (1993) Purification and characterization of the vanadium bromoperoxidase from the macroalga *Corallina officinalis*. Phytochemistry 32:21–26
94. Zhang B, Cao X, Chenf X, Wu P, Xiao T, Zhang W (2010) Efficient purification with high recovery of vanadium bromoperoxidase from *Corallina officinalis*. Biotechnol Lett. doi:10.1007/s10529-010-0454-y
95. Garcia-Rodriguez E, Ohshiro T, Aibara T, Izumi Y, Littlechild J (2005) Enhancing effect of calcium and vanadium ions on thermal stability of bromoperoxidase from *Corallina pilulifera*. J Biol Inorg Chem 10:275–282
96. Renirie R, Pierlot C, Wever R, Aubry JM (2008) Singlet oxygenation in microemulsion catalyzed by vanadium chloroperoxidase. J Mol Catal B Enzym 56:259–264
97. Hoogenkamp MA, Crielaard W, Ten Cate JM, Wever R, Hartog AF, Renirie R (2009) Antimicrobial activity of vanadium chloroperoxidase on planktonic *Streptococcus mutans* cells and *Streptococcus mutans* biofilms. Caries Res 43:334–338
98. Littlechild J, Garcia-Rodriguez E, Dalby A, Isupov M (2002) Structural and functional comparisons between vanadium haloperoxidase and acid phosphatase enzymes. J Mol Recognit 15:291–296
99. Messerschmidt A, Prade L, Wever R (1997) Implications for the catalytic mechanism of the vanadium-containing enzyme chloroperoxidase from the fungus *Curvularia inaequalis* by X-ray structures of the native and peroxide form. Biol Chem 378:309–315
100. Messerschmidt A, Wever R (1996) X-ray structure of a vanadium-containing enzyme: chloroperoxidase from the fungus *Curvularia inaequalis*. Proc Natl Acad Sci USA 93: 392–396
101. Renirie R, Charnock JM, Garner CD, Wever R (2010) Vanadium K-edge XAS studies on the native and peroxo forms of vanadium chloroperoxidase from Curvularia inaequalis. J Inorg Biochem 104:657–664
102. Tanaka N, Wever R (2004) Hydroxyalamine, hydrazine and azide inhibition and phosphate inactivation of vanadium chloroperoxidase from the fungus *Curvularia inaequalis*. J Inorg Biochem 98:625–630
103. Kravitz JY, Pecoraro VL, Carlson HA (2005) Quantum mechanics calculation of the vanadium dependent chloroperoxidase. J Chem Theory Comput 1:1265–1274
104. Ohshiro T, Littlechild J, Garcia-Rodriguez E, Isupov MN, Iida Y, Kobayashi T, Izumi Y (2004) Modification of halogen specificity of a vanadium-dependent bromoperoxidase. Protein Sci 13:1566–1571
105. Pacois LF, Galvez O (2010) Active site, catalytic cycle, and iodination reactions of vanadium iodoperoxidase: a computational study. J Chem Theory Comput 6:1738–1752

106. Tanaka N, Dumay V, Liao Q, Lange AJ, Wever R (2002) Bromoperoxidase activity of vanadate-substituted acid phosphatases from *Shigella flexneri* and *Salmonella enterica* ser. *typhimurium*. Eur J Biochem 269:2162–2167
107. Ishikawa K, Mihara Y, Gondoh K, Suzuki E, Asano Y (2000) X-ray structures of a novel acid phosphatase from *Escherichia blattae* and its complex with the transition-state analog molybdate. EMBO J 19:2412–2423
108. Makde RD, Mahajan SK, Kumar V (2007) Structure and mutational analysis of the PhoN protein of *Salmonella typhimurium* provide insight into mechanistic details. Biochemistry 46:2079–2090
109. Zampella G, Fantucci P, Pecoraro VL, De Gioia L (2006) Insight into the catalytic mechanism of vanadium haloperoxidases. DFT investigation of vanadium cofactor reactivity. Inorg Chem 45:7133–7143
110. Bangesh M, Plass W (2005) TD-DFT studies on the electronic structure of imidazole bound vanadate in vanadium containing haloperoxidases (VHPO). J Mol Struct Theochem 725: 163–175
111. Raugei S, Carloni P (2006) Structure and function of vanadium haloperoxidases. J Phys Chem B 110:3747–3758
112. Waller MP, Buhl M, Geethalakshmi KR, Wang DQ, Thiel W (2007) V-51 NMR chemical shifts calculated from QM/MM models of vanadium chloroperoxidase. Chem Eur J 13: 4723–4732
113. Zhang Y, Gascón J (2008) QM/MM investigation of structure and spectroscopic properties of a vanadium-containing peroxidase. J Inorg Biochem 102:1684–1690
114. Littlechild J, Garcia-Rodriguez E, Isupov M (2009) Vanadium containing bromoperoxidase – insights into the enzymatic mechanism using X-ray crystallography. J Inorg Biochem 103: 617–621
115. Winter JM, Moffitt MC, Zazopoulos E, McAlpine JB, DorresteinPC MBS (2007) Molecular basis for chloronium-mediated meroterpene cyclization: cloning, sequencing, and heterologous expression of the napyradiomycin biosynthetic gene cluster. J Biol Chem 282: 16362–16368
116. Neuwald AF (1997) An unexpected structural relationship between integral membrane phosphatases and soluble haloperoxidases. Protein Sci 6:1764–1767
117. Stukey J, Carman GM (1997) Identification of a novel phosphatase sequence motif. Protein Sci 6:469–472
118. Brindley DN, Waggoner DW (1998) Mammalian lipid phosphate phosphohydrolases. J Biol Chem 273:24281–24284
119. Macedo-Ribeiro S, Renirie R, Wever R, Messerschmidt A (2008) Crystal structure of a trapped phosphate intermediate in vanadium apochloroperoxidase catalyzing a dephosphorylation reaction. Biochemistry 47:929–934
120. Van de Velde F, Arends IWCE, Sheldon RA (2000) Biocatalytic and biomimetic oxidations with vanadium. J Inorg Biochem 80:81–89

Chapter 6
Bioinspired Catalytic Bromination Systems for Bromoperoxidase

Toshiyuki Moriuchi and Toshikazu Hirao

Abstract The oxidative bromination of arenes is induced by a vanadium catalyst in the presence of a bromide salt and a Brønsted acid or a Lewis acid under molecular oxygen, which provides an eco-friendly bromination method as compared with a conventional bromination one with bromine. This catalytic bromination can be applied to the bromination of alkenes and alkynes to give the corresponding *vic*-dibromides. Use of aluminium halide as a Lewis acid in place of a Brønsted acid is demonstrated to provide a more practical protocol for the oxidative bromination. From ketones, α-bromination products are obtained. $AlBr_3$ is found to serve as both a bromide source and a Lewis acid for the smooth bromination reaction.

Keywords Vanadium bromoperoxidase • Vanadium catalyst • Oxidative bromination • Molecular oxygen • Brønsted acid • Lewis acid

6.1 Introduction

The bromination of organic compounds is regarded as one of the most fundamental reactions in organic synthesis, providing important precursors for various transformations. Conventional bromination reaction requires hazardous and toxic elemental bromine. To avoid this, an alternative environmentally friendly method is a necessary requirement. Considerable efforts have been focused on developing an efficient bromination method by using a bromide ion as a bromide source instead of bromine [1, 2]. In these methods, the bromination reaction proceeds by utilizing generation of a bromonium-like species through total two-electron oxidation of a bromide ion. As an oxidant, hydrogen peroxide [3], oxone® [4], cerium(IV)

T. Moriuchi (✉) • T. Hirao (✉)
Department of Applied Chemistry, Graduate School of Engineering, Osaka University, Yamada-oka, Suita, Osaka 565-0871, Japan
e-mail: moriuchi@chem.eng.osaka-u.ac.jp; hirao@chem.eng.osaka-u.ac.jp

H. Michibata (ed.), *Vanadium: Biochemical and Molecular Biological Approaches*,
DOI 10.1007/978-94-007-0913-3_6,

ammonium nitrate (CAN) [5], sodium periodate [6], lead tetraacetate [7], and Selectfluor® [8] have been shown to induce oxidative bromination of alkenes and alkynes in the presence of bromide salts such as alkali metal bromide or Bu_4NBr (Scheme 6.1a).

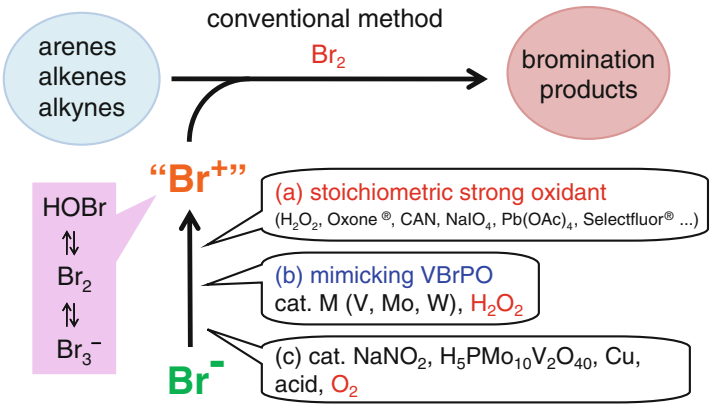

Scheme 6.1 Development of synthetic methods for bromination

On the other hand, the biochemical roles of vanadium have gained growing interest from both biological and chemical perspectives, which is related to the insulinnomimetic ability of vanadium compounds and the presence of vanadium as an essential constituent in certain haloperoxidases and nitrogenases [9–17]. Haloperoxidases are enzymes that catalyze the oxidation of halide ions by using H_2O_2 as the oxidant [18–22]. Haloperoxidases have received much attention because of their capability to halogenate a range of organic compounds. These enzymes are classified into three groups as Fe Heme containing, vanadium containing, and metal free haloperoxidases. Vanadium bromoperoxidase (VBrPO) [23–26], a naturally occurring enzyme found in marine algae, catalyzes two-electron oxidation of the bromide ion in the presence of H_2O_2, leading to a bromonium-like species. VBrPO has been demonstrated to induce the catalytic bromination of organic compounds [10, 25–28]. In the reaction path, an oxo-peroxo species generated from a dioxo vanadium and hydrogen peroxide is considered to be an active species [14, 16]. The oxidative bromination reaction induced by a vanadium catalyst and H_2O_2, mimicking the catalytic activity of VBrPO has attracted much attention (Scheme 6.1b) [27, 29–42]. Other metals including tungsten [43] or molybdenum [44] complexes have been found to work as a bromination catalyst in the presence of stoichiometric hydrogen peroxide. These systems, however, require a stoichiometric amount of a strong oxidant to generate the bromonium-like species. From the view point of green chemistry perspective, molecular oxygen is regarded as the best candidate for oxidants. Some oxidative bromination reactions under molecular oxygen as a terminal oxidant in place of a strong oxidant have been reported, developing the more advanced catalytic systems rather than the enzyme

(Scheme 6.1c). $NaNO_2$ has been shown to serve as a catalyst in the presence of aqueous HBr to induce the bromination of arenes and aryl ketones under molecular oxygen (by Liu and Liang et al.) [45], alkenes and alkynes under air (by Iskra et al.) [46]. This chapter summarizes the catalytic oxidative bromination reaction by using a vanadium catalyst, a bromide salt, and a Brønsted acid or a Lewis acid under molecular oxygen.

6.2 Vanadium-Catalyzed Oxidative Bromination Promoted by Brønsted Acid with Molecular Oxygen

To develop an efficient catalytic system for the bromination reaction, oxidation of the bromide ion based on vanadium redox ability has been focused on. A high valent vanadium is expected to oxidize the bromide ion to a bromonium-like species in the presence of an acid because the vanadium is known to have the stronger oxidation capability in the presence of an acid. A low valent vanadium thus formed could be reoxidized by molecular oxygen. The combination of the redox properties of a vanadium catalyst and molecular oxygen is envisioned to provide an environmentally acceptable catalytic system in oxidative bromination. On the basis of this concept, the oxidative bromination reaction induced by vanadium catalyst, bromide ion, and Brønsted acid under molecular oxygen has been investigated.

The oxidative bromination reaction of 1,3,5-trimethoxybenzene with 5 mol% of NH_4VO_3, 300 mol% of Bu_4NBr, and 300 mol% of trifluoroacetic acid (TFA) in 1,4-dioxane under atmospheric oxygen proceeds at 80 °C to allow the formation of the monobromination product (Table 6.1, entry 1) [47]. The use of *p*-toluenesulfonic acid monohydrate ($PTS{\cdot}H_2O$) instead of TFA under the identical conditions shows a 20% decrease in the yield (entry 2). The similar yield is observed with $NaVO_3$ as compared with the ammonium counterpart (entry 3). V_2O_5 is found to be less effective than NH_4VO_3 (entry 4). $VO(acac)_2$ and $VOSO_4$ give the similar NMR yields to NH_4VO_3 (entries 5 and 6). WO_3, which is known to catalyze the oxidative bromination with H_2O_2 [43], does not serve as a catalyst (entry 7). The oxo metal complexes including $TiO(acac)_2$, $MoO_2(acac)_2$, and MnO_2, display no promising results (entries 8–10). Acetonitrile, dimethylformamide, acetic acid, and dimethoxyethane are found to be less effective than 1,4-dioxane. Among various conditions examined, the reaction with 5 mol% of NH_4VO_3, Bu_4NBr (300 mol%), and TFA (300 mol%) in 1,4-dioxane at 80 °C is superior (method A).

The oxidative bromination reaction of a variety of arenes, alkenes, and alkynes undergoes smoothly by using this catalytic system [47]. Some selected results are listed in Table 6.2. The bromination reaction of the phenol derivatives, such as 2,6-xylenol and resorcinol, using method A leads to the monobrominated compounds regioselectively in the similar yields (entries 1 and 2). This bromination reaction can be applied to the bromination of alkenes. In the case of styrene, the reaction proceeds smoothly at a high conversion rate, even at room temperature, in

Table 6.1 Bromination reaction under atmospheric oxygen[a]

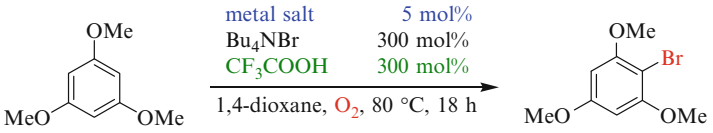

entry	metal salt	NMR yield (%)
1	NH_4VO_3	80[b]
2[c]	NH_4VO_3	62
3	$NaVO_3$	77
4	V_2O_5	53
5	$VO(acac)_2$	74
6	$VOSO_4$	75
7	WO_3	0
8	$TiO(acac)_2$	0
9	$MoO_2(acac)_2$	2
10	MnO_2	5

[a]Conditions: 0.4 mmol of 1,3,5-trimethoxybenzene, 5 mol% NH_4VO_3, 300 mol% Bu_4NBr, 300 mol% TFA, 1.5 mL of solvent, under O_2
[b]Isolated yield
[c]PTS·H_2O was used in place of TFA

the presence of 1 mol% of NH_4VO_3 and 200 mol% of PTS·H_2O and Bu_4NBr in acetonitrile (method C). The bromination reaction of α-methylstyrene gives 33% of the dibromide and 62% of the bromohydrin regioselectively (entry 4). On the other hand, using 5 mol% NH_4VO_3, 900 mol% Bu_4NBr, and 900 mol% TFA in 1,4-dioxane at 80 °C (method B), only the bromohydrin is produced in 60% yield (entry 3). In the case of *trans*-β-methylstyrene, the ketone is obtained in addition to the *erythro*-dibromo and bromohydrin compounds (entry 5). The bromination reaction of *cis*-β-methylstyrene leads to the *threo*-dibromide together with small amounts of the *erythro* isomer, bromohydrin, and ketone (entry 6). Starting from the styrene derivatives, the regioisomeric bromohydrins and ketones are not formed. Dibromides are produced in the reaction of aliphatic alkenes by using method B. Allylbenzene and 1-decene are converted to the dibromides in 94% and 97% yields, respectively (entries 7 and 8). In the case of 5-hexene-1-ol, the dibromide is obtained in 94% yield, with the hydroxyl group intact (entry 9). Moreover, the present catalytic system can be applied to the bromination of alkynes. The bromination reaction of 1-phenylpropyne and 1,4-dimethoxy-2-butyne provides only the *trans*-1,2-dibromoalkenes in 98% and 77% yields, respectively (entries 10 and 11).

Table 6.2 Bromination reaction of arenes, alkenes, and alkynes

entry	substrate	method	products, isolated yields (%)					
1	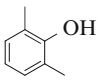	A	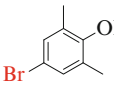	73				
2	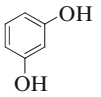	A	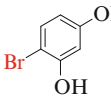	72				
3		B		0		60		
4[b]		C		33		62		
5[b]		C		59		18		15
6[b]		C		51[c]		17		11
7		B	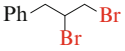	94				
8		B	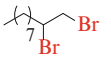	97				
9		B	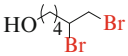	94				
10		B		94				
11	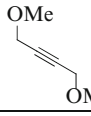	B	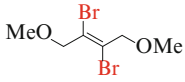	77				

Method A: 0.4 mmol of substrate, 5 mol% NH_4VO_3, 300 mol% Bu_4NBr, 300 mol% TFA, 1.5 mL of 1,4-dioxane, under O_2, 80 °C, 18 h. **Method B**: 0.4 mmol of substrate, 5 mol% NH_4VO_3, 900 mol% Bu_4NBr, 900 mol% TFA, 1.5 mL of 1,4-dioxane, under O_2, 80 °C, 12 h. **Method C**: 0.4 mmol of substrate, 1 mol% NH_4VO_3, 200 mol% Bu_4NBr, 200 mol% PTS·H_2O, 1.5 mL of acetonitrile, under O_2, room temperature, 6 h

[a]NMR yield

[b]Together with the *erythro* isomer (9%)

The amount of the catalyst can be successfully reduced to 1 mol%, although a longer reaction time is required (Table 6.3, entry 1) [47]. Furthermore, the bromination reaction proceeds well, even under air, in the presence of 600 mol% of Bu_4NBr and TFA to give 70% of the bromination compound **1a** (entry 2). The bromination depends on the amounts of the bromide source and acid. Use of 900 mol% of the bromide source and acid leads to the dibromide **1b** in 70% yield with the concomitant monobromo compound **1a** in 28% yield (entry 3). When a catalytic amount of TFA is used, the bromination yield is reduced significantly

Table 6.3 Bromination reaction using alternative conditions

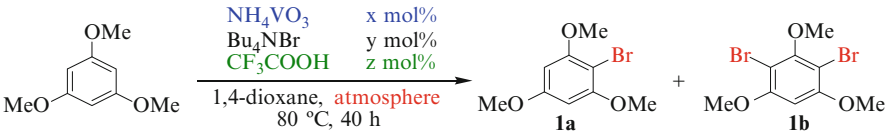

entry	X (mol%)	Y (mol%)	Z (mol%)	atmosphere	NMR yields (%)	
					1a	**1b**
1	1	300	300	O_2	65	0
2	5	600	600	air	70	0
3	5	900	900	O_2	28	70
4	5	300	30	O_2	14	0
5	5	300	300	Ar	7	0
6	300	900	900	Ar	quant.	0

(entry 4). Moreover, this bromination is not effectively performed under argon conditions (entry 5), although the desired compound is obtained quantitatively by using of excess amounts of NH_4VO_3, Bu_4NBr, and TFA, even under argon atmosphere (entry 6). These results indicate that the presence of acid and molecular oxygen is essential for an efficient catalytic bromination reaction.

In the case of α-methylstyrene, the catalyst loading can be successfully reduced to 0.01 mol% in the gram-scale reaction, as shown in Scheme 6.2, indicating an extremely high efficiency of the catalyst and versatility of the reaction [47].

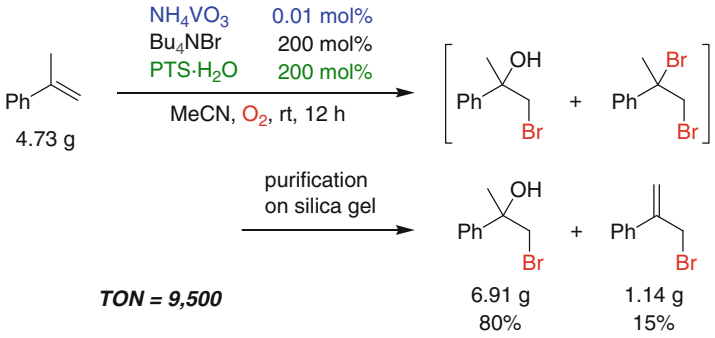

Scheme 6.2 Gram-scale catalytic bromination reaction

Oxidative bromination reactions induced by metal catalysts under molecular oxygen as a terminal oxidant have been reported by few groups (Scheme 6.1). Newmann et al. have performed the bromination reaction by using cat. $H_5PMo_{10}V_2O_{40}$ with tetraglyme under HBr and air bubbling Eq. 6.1 [48]. Copper-catalyzed bromination through one-electron oxidation of substrates has been reported, although adaptable substrates are limited (by Gusevskaya et al., Eq. 6.2) [49]. Regioselective

copper-catalyzed bromination of arenes with molecular oxygen has been demonstrated by Stahl et al. Eq. 6.3 [50].

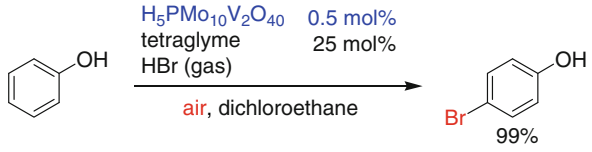

(6.1)

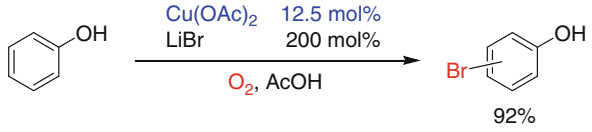

(6.2)

(6.3)

6.3 Vanadium-Catalyzed Oxidative Bromination Promoted by Lewis Acid with Molecular Oxygen

6.3.1 Vanadium-Catalyzed Oxidative Bromination Promoted by $AlCl_3$ with Molecular Oxygen

In the previous section, oxidative bromination reaction by using a combination of ligand-free inexpensive NH_4VO_3 with Bu_4NBr and a Brønsted acid such as TFA or PTS·H_2O under molecular oxygen is demonstrated. In this system, excess amounts of protic acid are required to obtain the bromination compound efficiently. The use of a Lewis acid in place of a Brønsted acid is considered to provide the more practical bromination reaction system as follows: (1) Expanding of the substrate adaptability without using protic acid. (2) Improvement of reactivity by controlling the Lewis acidity. (3) Enantioselective bromination induced by chiral Lewis acid. In this section, the development of the catalytic oxidative bromination system by using NH_4VO_3 catalyst, Bu_4NBr, and $AlCl_3$ as a Lewis acid under molecular oxygen is described.

The bromination reaction of 1,3,5-trimethoxybenzene in the presence of 5 mol% of NH_4VO_3, 120 mol% of Bu_4NBr, and 120 mol% of $AlCl_3$ as a Lewis acid in 1,4-dioxane at 80 °C for 18 h under molecular oxygen proceeds well to give the monobromide **1a** in 92% yield (Table 6.4, entry 1) [51, 52]. The bromination in

Table 6.4 Bromination reaction by using various conditions[a]

entry	acid	solvent	temp. (°C)	NMR yields (%)	
				1a	**1b**
1	$AlCl_3$	1,4-dioxane	80	92[b]	0
2	$AlCl_3$	1,4-dioxane	25	45	0
3	$AlCl_3$	toluene	25	54	0
4	$CuCl_2$	1,4-dioxane	80	87	0
5	$ZnCl_2$	1,4-dioxane	80	12	0
6	$FeCl_3$	1,4-dioxane	80	0	0
7	$CoCl_3$	1,4-dioxane	80	0	0
8	$BF_3{\cdot}OEt_2$	1,4-dioxane	80	48	0
9[c]	$AlCl_3$	1,4-dioxane	80	0	quant.[b]
10[c]	TFA	1,4-dioxane	80	80[b]	0

[a]Conditions: 0.5 mmol of 1,3,5-trimethoxybenzene, 5 mol% NH_4VO_3, acid, Bu_4NBr, 1.5 mL of solvent, under O_2, 18 h
[b]Isolated yield
[c]300 mol% Bu_4NBr and acid were used

other solvents, such as toluene, acetonitrile, dimethoxyehane, and dichloroethane results in a slightly decreased yield. Using 1,4-dioxane or toluene as a solvent, the bromination reaction undergoes even at room temperature in a moderate yield (entries 2 and 3). When $CuCl_2$ or $BF_3{\bullet}OEt_2$ is used instead of $AlCl_3$, the bromination product **1a** is obtained in a lower yield (entries 4 and 8). $ZnCl_2$, $FeCl_3$, and $CoCl_2$ are less or not effective as a Lewis acid (entries 5–7). In the presence of 300 mol% of Bu_4NBr and 300 mol% of $AlCl_3$, the dibromide **1b** is obtained in a quantitative yield (entry 9). The use of 300 mol% of TFA instead of $AlCl_3$ leads to the formation of only 80% of the monobromide **1a** (entry 10), indicating that $AlCl_3$ exhibits the higher efficiency than TFA.

The bromination reaction of other substrates by using the cat. $NH_4VO_3/Bu_4NBr/AlCl_3/O_2$ system in 1,4-dioxane at 80 °C for 18 h under molecular oxygen (method A) is shown in Table 6.5 [51, 52]. The monobromination of 2,6-dimethylphenol proceeds without the formation of the benzyl bromide (entry 1). 3-Hydroxyphenol undergoes mono- or dibromination reaction to give **3a** or **3b** in a high yield in the presence of 120 or 400 mol% of $AlCl_3$ and Bu_4NBr, respectively (entries 2 and 3). The bromination reaction of alkenes by using 1,2-dimethoxyethane as a solvent at a lower temperature (method B) provides only the desired *vic*-dibromide in a high

Table 6.5 Bromination reaction by using cat. $NH_4VO_3/AlCl_3/Bu_4NBr/O_2$ system

entry	substrate	conditions[a,b]	product, isolated yield (%)
1		A, 120	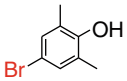 **2a,** 95
2	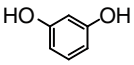	A, 120	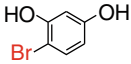 **3a,** 95
3		A, 400	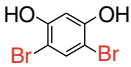 **3b,** 98
4		B, 400	 **4c,** 99
5	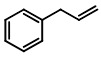	B, 400	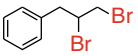 **5c,** 95
6	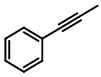	A, 400	 **6d,** quant.
7	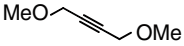	A, 400	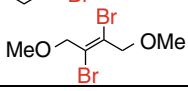 **7d,** 86

[a]Method, amount of Bu_4NBr and $AlCl_3$ (mol%)
[b]**Method A**: 0.5 mmol of substrate, 5 mol% NH_4VO_3, Bu_4NB and $AlCl_3$, 1.5 mL of 1,4-dioxane, under O_2, 80 °C, 18 h. **Method B**: 0.5 mmol of substrate, 5 mol% NH_4VO_3, Bu_4NBr and $AlCl_3$, 1.5 mL of dimethoxyethane, under O_2, 50 °C, 18 h

yield. 1-Decene or allylbenzene is converted to the corresponding dibromide **4c** or **5c** in 99% or 95% yield, respectively (entries 4 and 5). Both aromatic and aliphatic alkynes undergo the selective *vic*-dibromination by using method A, as exemplified by the conversion of 1-phenyl-1-propyne and 1,4-dimethoxy-2-butyne to the *trans*-dibromides **6d** and **7d** in quantitative and 86% yields, respectively (entries 6 and 7). This stereoselectivity suggests the involvement of a bromonium-like species as an intermediate for *anti*-bromination.

6.3.2 *Vanadium-Catalyzed Oxidative Bromination Promoted by $AlBr_3$ with Molecular Oxygen*

On the basis of the above-mentioned results in the Sect. 3.1, $AlBr_3$ is expected to serve as both a bromide source and a Lewis acid. Actually, the bromination reaction of 1,3,5-trimethoxybenzene with 5 mol% of NH_4VO_3 and 120 mol% of $AlBr_3$ under molecular oxygen leads to the quantitative formation of the dibromide **1b** (Table 6.6, entry 1) [52]. This result indicates that two bromides of $AlBr_3$ are able to participate as a bromide source. When the amount of $AlBr_3$ is reduced to 50 mol%,

Table 6.6 Bromination of 1,3,5-trimethoxybenzene by using cat. $NH_4VO_3/AlBr_3/O_2$ system[a]

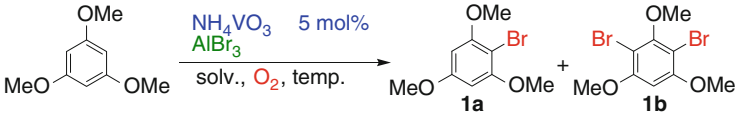

entry	$AlBr_3$ (mol%)	solvent	temp. (°C), time (h)	NMR yields (%)	
				1a	**1b**
1	120	1,4-dioxane	80, 4	0	quant.[b]
2	50	1,4-dioxane	80, 4	92[b]	0
3	50	ether	25, 18	99[b]	0
4	120	ether	25, 18	0	98[b]
5[c]	50	ether	25, 18	0	0
6[d]	50	ether	25, 18	3	0

[a]Conditions: 0.5 mmol of 1,3,5-trimethoxybenzene, 5 mol% NH_4VO_3, $AlBr_3$, 1.5 mL of solvent, under O_2
[b]Isolated yield
[c]Absence of NH_4VO_3
[d]Reaction under argon

the monobromide **1a** is selectively obtained in a high yield (entry 2). The effects of solvent, reaction temperature, and time are screened. Although 1,4-dioxane, dimethoxyethane, and MeCN are found to require heating for the bromination reaction, the high reactivity is observed in ether even at room temperature. Under these conditions, the use of 50 or 120 mol% of $AlBr_3$ give the mono- or dibromide in almost quantitative yield, respectively (entries 3 and 4). The results obtained from the reaction in the absence of NH_4VO_3 or molecular oxygen indicate that the vanadium catalyst and molecular oxygen are essential for the transformation (entries 5 and 6).

The applicability for the bromination reaction is investigated by using NH_4VO_3 catalyst and $AlBr_3$ under molecular oxygen either in 1,4-dioxane at 80 °C (method C) or in ether at room temperature (method D), as shown in Table 6.7 [52]. In both conditions, the bromination of phenol derivative proceeds well to afford the mono- or dibromide in a high yield by selecting appropriate conditions. With the present bromination system, a simple aromatic compound like anisole is subjected to the monobromination to afford **10a**. Moreover, phenol derivatives bearing the electron-withdrawing groups are brominated smoothly in high yields. Starting from 4-halophenols, dihalogenated products **11a** and **12a** are obtained. The bromination of phenol derivatives bearing the formyl or methoxycarbonyl group results in the formation of the monobromide **13a** or **14a**. In these cases, the further oxidation of the aldehyde moiety or decomposition of the ester moiety is not observed. In the bromination of TBS-protected *o*-cresol, the TBS group is survived to give only the 4-brominated product **15a**. This oxidative bromination of alkenes and alkynes leads to the formation of the corresponding dibromides by using 5 mol% of NH_4VO_3 together with $AlBr_3$ (method E), although the presence of the additional bromide

Table 6.7 Bromination of arenes, alkenes, and alkynes by using cat. $NH_4VO_3/AlBr_3/O_2$ system

substrate	conditions[a,b]	product, isolated yield (%)	
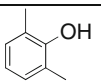	C, 60, 8	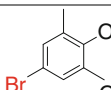	**2a**, 94
	D, 60, 18		95
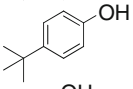	C, 60, 8	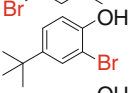	**8a**, 98
	D, 110, 18	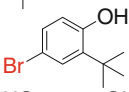	**9a**, 99
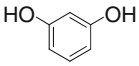	C, 40, 8	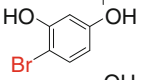	**3a**, 80
	C, 80, 8	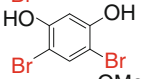	**3b**, 66
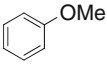	C, 120, 8	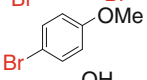	**10a**, 96
	C, 120, 8	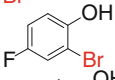	**11a**, 95
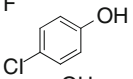	D, 110, 18	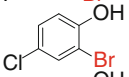	**12a**, 97
	C, 60, 8	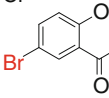	**13a**, 86[c]
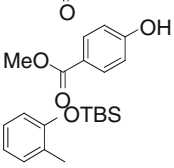	C, 110, 18	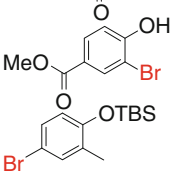	**14a**, quant.
	D, 120, 18		**15a**, quant.
	E, 120, 18	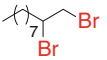	**4c**, 99[d,e] 76[e,f]
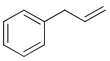	E, 120, 18	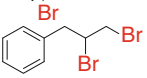	**5c**, 93[d,e]
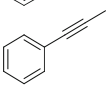	E, 120, 18	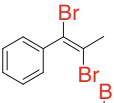	**6d**, 98[d]
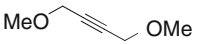	E, 120, 18	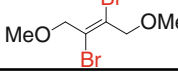	**7d**, 97[d]

[a]Method, amount of $AlBr_3$ (mol%), time (h)

[b]**Method C**: 0.5 mmol of substrate, 5 mol% NH_4VO_3, $AlBr_3$, 1.5 mL of 1,4-dioxane, under O_2, 80 °C. **Method D**: 0.5 mmol of substrate, 5 mol% NH_4VO_3, $AlBr_3$, 1.5 mL of ether, under O_2, rt. **Method E**: 0.5 mmol of substrate, 5 mol% NH_4VO_3, 120 mol% $AlBr_3$, 1.5 mL of MeCN, under O_2, 80 °C

[c]Together with 3-bromosalicylaldehyde (11%)

[d]120 mol% Bu_4NBr was used as an additive

[e]Reaction was conducted at 50 °C. [f] 1,000 mol% KBr was used as an additive

Table 6.8 Bromination of ketones by using cat. $NH_4VO_3/AlBr_3/O_2$ system[a]

substrate	$AlBr_3$ (mol%)	product, yield (%)	
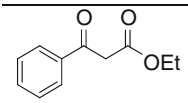	55	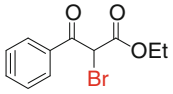	**16e**, 95
	110	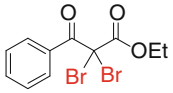	**16f**, 98
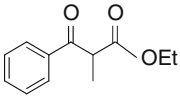	55	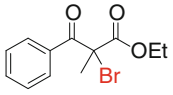	**17e**, 96
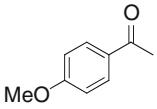	55	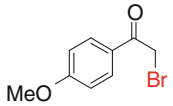	**18e**, 52[b,c]
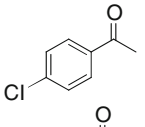	55	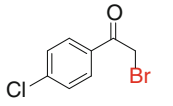	**19e**, 70[b,d]
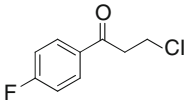	55	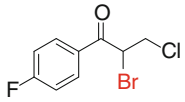	**20e**, 72[b]

[a]Conditions: 0.5 mmol of substrate, 5 mol% NH_4VO_3, $AlBr_3$, 1.5 mL of MeCN, under O_2, 80 °C, 18 h
[b]NMR yield
[c]Together with dibromide (45%)
[d]Together with dibromide (27%)

salt is required. The bromination reaction of 1-decene proceeds well to afford the dibromide **4c** in 99% yield at 50 °C. The less expensive KBr can be effective as a bromide source. Allylbenzene undergoes the selective *vic*-dibromination to give 1,2-dibromo-3-phenylpropane **5c** in 93% yield, without formation of the benzyl bromide. The selective *anti*-dibromination of aromatic and aliphatic alkynes such as 1-phenylpropyne and 1,4-dimethoxy-2-butyne is observed by using method E at 80 °C to give the *trans*-dibromides **6d** and **7d** in high yields, respectively.

Moreover, the oxidative bromination using cat. $NH_4VO_3/AlBr_3/O_2$ system can be applied to the α-bromination of ketones by method E (Table 6.8) [52]. β-Keto esters such as ethyl benzoylacetate undergo the bromination reaction to mono- or dibromination products **16e** and **16f** depending on the amount of $AlBr_3$. Substitution at α-position leads to the formation of the monobromination product **17e**. The α-bromination of monoketones is also carried out. 4′-Methoxyacetophenone is brominated to give the monobromide **18e** together with the dibromide. Bromination of 4′-chloroacetophenone affords the monobromide **19e** as a major product. Starting from 3-chloro-4′-fluoropropiophenone, the trihalide **20e** is obtained.

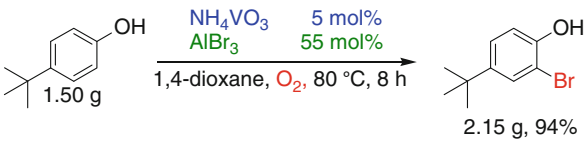

Scheme 6.3 Gram-scale catalytic bromination reaction

Notably, a gram-scale practical reaction is successfully carried out to give the bromination product in a high yield, as exemplified by the monobromination of 4-*tert*-butylphenol to the monobromide in 94% isolated yield (Scheme 6.3) [52].

6.4 Conclusions

The bromination reaction of various arenes, alkenes, alkynes, and ketones without use of a strong oxidant is performed by a vanadium catalyst in the presence of a bromide salt and a Brønsted acid or a Lewis acid under molecular oxygen. Use of aluminium halide as a Lewis acid in place of a Brønsted acid is demonstrated to provide a more versatile and practical method for selective bromination of wide ranging substrates. $AlBr_3$ is found to serve as both a bromide source and a Lewis acid to induce the smooth bromination. The oxidation of a bromide anion is considered to proceed to generate a bromonium-like species by the combination of vanadium catalyst and a Lewis acid without using a stoichiometric strong oxidant or protic acid. This methodology is more advantageous as a catalytic system than vanadium bromoperoxidase (VBrPO) requiring hydrogen peroxide as an oxidant. Through these studies, the present catalytic oxidative bromination reaction system based on vanadium redox properties is found to provide a new synthetic methodology for the bromination. This methodology has many advantages such as use of a commercially available inexpensive ligand-free vanadium catalyst and molecular oxygen as a terminal oxidant, which provides environmentally acceptability.

References

1. Eissen M, Lenoir D (2008) Electrophilic bromination of alkenes: environmental, health and safety aspects of new alternative methods. Chem Eur J 14:9830–9841
2. Podgoršek A, Zupan M, Iskra J (2009) Oxidative halogenation with “green” oxidants: oxygen and hydrogen peroxide. Angew Chem Int Ed 48:8424–8450
3. Ho T-L, Gupta BG Balaram, Olah GA (1977) Synthetic methods and reactions; 39. Phase transfer catalyst promoted halogenation of alkenes with hydrohalic acid/hydrogen peroxide. Synthesis 676–677
4. Dieter RK, Nice LE, Velu SE (1996) Oxidation of α, β-enones and alkenes with oxone and sodium halides: a convenient laboratory preparation of chlorine and bromine. Tetrahedron Lett 37:2377–2380

5. Nair V, Panicker SB, Augstine A, George TG, Thomas S, Vairamani M (2001) An efficient bromination of alkenes using cerium(IV) ammonium nitrate (CAN) and potassium bromide. Tetrahedron 57:7417–7422
6. Dewkar KG, Narina VS, Sudalai A (2003) $NaIO_4$-mediated selective oxidative halogenation of alkenes and aromatics using alkali metal halides. Org Lett 5:4501–4504
7. Muathen HA (2004) Mild oxidative bromination of alkenes and alkynes with zinc bromide and lead tetraacetate. Synth Commun 34:3545–3552
8. Ye C, Shreeve MJ (2004) Structure-dependent oxidative bromination of unsaturated C−C bonds mediated by selectfluor. J Org Chem 69:8561–8563
9. Rehder D (1991) The bioinorganic chemistry of vanadium. Angew Chem Int Ed Engl 30: 148–167
10. Butler A, Walker JV (1993) Marine haloperoxidases. Chem Rev 93:1937–1944
11. Fraústo da Silva JJR, Williams RJP (1993) The biological chemistry of the elements. Clarendon Press, Oxford
12. Sigel H, Sigel A (1995) Vanadium and its role in life, vol 31, Metal ions in biological systems. Marcel Dekker Inc., New York
13. Tracey AS, Crans DC (1998) Vanadium compounds: chemistry, biochemistry, and therapeutic applications. ACS symposium series no. 711. American Chemical Society, Washington, DC
14. Rehder D (1999) The coordination chemistry of vanadium as related to its biological functions. Coord Chem Rev 182:297–322
15. Thompson KH, McNeill JH, Orvig C (1999) Vanadium compounds as insulin mimics. Chem Rev 99:2561–2572
16. Crans DC, Smee JJ, Gaidamauskas E, Yang L (2004) The chemistry and biochemistry of vanadium and the biological activities exerted by vanadium compounds. Chem Rev 104: 849–902
17. Kustin K, Costa Pessoa J, Crans DC (2007) Vanadium: chemistry: the versatile metal. ACS symposium series no. 974. American Chemical Society, Washington, DC
18. Butler A (1999) Mechanistic considerations of the vanadium haloperoxidases. Coord Chem Rev 187:17–35
19. Littlechild J (1999) Haloperoxidases and their role in biotransformation reactions. Curr Opin Chem Biol 3:28–34
20. Littlechild J, Garcia-Rodrguez E, Dalby A, Isupov M (2003) Structural and functional comparisons between vanadium haloperoxidase and acid phosphatase enzymes. J Mol Recognit 15:291–296
21. Ligtenbarg AGJ, Hage R, Feringa BL (2003) Catalytic oxidations by vanadium complexes. Coord Chem Rev 237:89–101
22. Plass W (2009) Vanadium haloperoxidases as supramolecular hosts: synthetic and computational models. Pure Appl Chem 81:1229–1239
23. Butler A, Baldwin AH (1997) Vanadium bromoperoxidase and functional mimics. Struct Bond 89:109–132
24. Littlechild J, Garcia-Rodrguez E (2003) Structural studies on the dodecameric vanadium bromoperoxidase from *Corallina* species. Coord Chem Rev 237:65–76
25. Butler A, Carter-Franklin JN (2004) The role of vanadium bromoperoxidase in the biosynthesis of halogenated marine natural products. Nat Prod Rep 21:180–188
26. Hartung J, Dumont Y, Greb M, Hach D, Köhler SH, Časný M, Rehder D, Vilter H (2009) On the reactivity of bromoperoxidase I (*Ascophyllum nodosum*) in buffered organic media: formation of carbon bromine bonds. Pure Appl Chem 81:1251–1264
27. Martinez JS, Carroll GL, Tschirret-Guth RA, Altenhoff G, Little RD, Butler A (2001) On the regiospecificity of vanadium bromoperoxidase. J Am Chem Soc 123:3289–3294
28. Carter-Franklin JN, Parrish JD, Tschirret-Guth RA, Little RD, Butler A (2003) Vanadium haloperoxidase-catalyzed bromination and cyclization of terpenes. J Am Chem Soc 125: 3688–3689
29. de la Rosa RI, Clague MJ, Butler A (1992) A functional mimic of vanadium bromoperoxidase. J Am Chem Soc 114:760–761

30. Conte V, Di Furia F, Moro S, Rabbolini S (1996) A mechanistic investigation of bromoperoxidases mimicking systems. Evidence of a hypobromite-like vanadium intermediate from experimental data and ab initio calculations. J Mol Catal A Chem 113:175–184
31. Colaps GJ, Hamstra BJ, Kampf JW, Pecoraro VL (1996) Functional models for vanadium haloperoxidase: reactivity and mechanism of halide oxidation. J Am Chem Soc 118: 3469–3478
32. Nica S, Pohlmann A, Plass W (2005) Vanadium(V) oxoperoxo complexes with side chain substituted *N*-salicylidene hydrazides: modeling supramolecular interactions in vanadium haloperoxidases. Eur J Inorg Chem 2005:2032–2036
33. Bhattacharjee M (1992) Activation of bromide by vanadium pentoxide for the bromination of aromatic hydrocarbons: reaction mimic for the enzyme bromoperoxidase. Polyhedron 11:2817–2818
34. Conte V, Di Furia F, Moro S (1994) Mimicking the vanadium bromoperoxidases reactions: mild and selective bromination of arenes and alkenes in a two-phase system. Tetrahedron Lett 35:7429–7432
35. Dinesh CU, Kumar R, Pandey B, Kumar P (1995) Catalytic halogenation of selected organic compounds mimicking vanadate-dependent marine metalloenzymes. J Chem Soc Chem Commun 611–612
36. ten Brink HB, Tuynman A, Dekker HL, Hemrika W, Izumi Y, Oshiro T, Schoemaker HE, Wever R (1998) Enantioselective sulfoxidation catalyzed by vanadium haloperoxidases. Inorg Chem 37:6780–6784
37. Bora U, Bose G, Chaudhuri MK, Dhar SS, Gopinath R, Khan AT, Patel BK (2000) Regioselective bromination of organic substrates by tetrabutylammonium bromide promoted by V_2O_5—H_2O_2: an environmentally favorable synthetic protocol. Org Lett 2:247–249
38. Rothenberg G, Clark JH (2000) Vanadium-catalysed oxidative bromination using dilute mineral acids and hydrogen peroxide: an option for recycling waste acid streams. Org Process Res Dev 4:270–274
39. Maurya MR, Saklani H, Agarwal S (2004) Oxidative bromination of salicylaldehyde by potassium bromide/H_2O_2 catalysed by dioxovanadium(V) complexes encapsulated in zeolite–Y: a functional model of haloperoxidases. Catal Commun 5:563–568
40. Greb M, Hartung J, Köhler F, Ŝpehar K, Kluge R, Csuk R (2004) The (schiff base)vanadium(V) complex catalyzed oxidation of bromide — a new method for the in situ generation of bromine and its application in the synthesis of functionalized cyclic ethers. Eur J Org Chem 2004: 3799–3812
41. Khan AT, Goswami P, Choudhury LH (2006) A mild and environmentally acceptable synthetic protocol for chemoselective α-bromination of β-keto esters and 1,3-diketones. Tetrahedron Lett 47:2751–2754
42. Moriuchi T, Yamaguchi M, Kikushima K, Hirao T (2007) An efficient vanadium-catalyzed bromination reaction. Tetrahedron Lett 48:2667–2670
43. Sels B, De Vos D, Buntinx M, Pierard F, Kirsch-De Mesmaeker A, Jacobs P (1999) Layered double hydroxides exchanged with tungstate as biomimetic catalysts for mild oxidative bromination. Nature 400:855–857
44. Conte V, Di Furia F, Moro S (1996) Synthesis of brominated compounds. A convenient molybdenum- catalyzed procedure inspired by the mode of action of haloperoxidases. Tetrahedron Lett 37:8609–8612
45. Zhang G, Liu R, Xu Q, Ma L, Liang X (2006) Sodium nitrite-catalyzed oxybromination of aromatic compounds and aryl ketones with a combination of hydrobromic acid and molecular oxygen under mild conditions. Adv Synth Catal 348:862–866
46. Podgoršek A, Eissen M, Fleckenstein J, Stavber S, Zupan M, Iskra J (2009) Selective aerobic oxidative dibromination of alkenes with aqueous HBr and sodium nitrite as a catalyst. Green Chem 11:120–126
47. Kikushima K, Moriuchi T, Hirao T (2009) Vanadium-catalyzed oxidative bromination reaction under atmospheric oxygen. Chem Asian J 4:1213–1216

48. Newmann R, Assael I (1988) Oxybromination catalysed by the heteropolyanion compound $H_5PMo_{10}V_2O_{40}$ in an organic medium: selective *para*-bromination of phenol. J Chem Soc Chem Commun 1285–1287
49. Menini L, Parreira LA, Gusevskaya EV (2007) A practical highly selective oxybromination of phenols with dioxygen. Tetrahedron Lett 48:6401–6404
50. Yang L, Lub Z, Stahl SS (2009) Regioselective copper-catalyzed chlorination and bromination of arenes with O_2 as the oxidant. Chem Comm 6460–6462
51. Kikushima K, Moriuchi T, Hirao T (2010) Oxidative bromination reaction using vanadium catalyst and aluminum halide under molecular oxygen. Tetrahedron Lett 51:340–342
52. Kikushima K, Moriuchi T, Hirao T (2010) Vanadium-catalyzed oxidative bromination promoted by Brønsted acid or Lewis acid. Tetrahedron 66:6906–6911

Part IV
Medicinal Functions of Vanadium

Chapter 7
Vanadium Effects on Bone Metabolism

Susana B. Etcheverry, Ana L. Di Virgilio, and Daniel A. Barrio

Abstract Vanadium compounds are present in trace amounts in living organisms. In mammals, once absorbed from the gastrointestinal tract, they distribute among tissues and storage mainly in liver, kidney and bone. Vanadium compounds in pharmacological doses exert interesting effects as insulin enhancers, antitumoral and osteogenic agents. This review deals with the more relevant information about the osteogenic effects of vanadium compounds. Their actions on the different components of hard tissue and bone related cells in culture are summarized. Besides, the putative mechanism of action and the effects on in vivo models are also discussed.

Keywords Vanadium • Osteoblasts • Mechanism of action • Cytotoxicity • Genotoxicity

7.1 Introduction

Vanadium is a trace element present in biological systems, both in plants and animals. In vertebrates, it enters the organism mainly by the digestive and respiratory tracts through food and inhalation, respectively [1, 2]. Once absorbed, it distributes

S.B. Etcheverry (✉)
Cátedra de Bioquímica Patológica, Facultad de Ciencias Exactas,
Universidad Nacional de La Plata, 47 y 115 (1900), La Plata, Argentina

CEQUINOR (UNLP-CONICET), 47 y 115 (1900), La Plata, Argentina
e-mail: etcheverry@biol.unlp.edu.ar

A.L. Di Virgilio • D.A. Barrio
Cátedra de Bioquímica Patológica, Facultad de Ciencias Exactas,
Universidad Nacional de La Plata, 47 y 115 (1900), La Plata, Argentina
e-mail: aldivirgilio@biol.unlp.edu.ar; barrio@biol.unlp.edu.ar

H. Michibata (ed.), *Vanadium: Biochemical and Molecular Biological Approaches*,
DOI 10.1007/978-94-007-0913-3_7,

among tissues and accumulates in different organs, being the greater quantities of vanadium detected in liver, kidney and especially in bone [2].

While vanadium essentiality has been established in lower forms of life and also in higher plants, convincing evidence to support an essential role for this element in humans is still lacking [3].

Although ubiquitous in air, soil, water, and food supply, vanadium is generally found in nanogram or microgram quantities, which makes it difficult to measure. Its role as an essential element in humans remains uncertain due in part to the lack of symptoms associated to its deficiency in man and to the scarce methods strictly suitable to assure the absolute absence of this trace element in vanadium free diets for experimental animal models. However, there is scientific consensus on the putative biochemical role for vanadium compounds in living organisms [4].

In animal models and human beings, pharmacologic amounts of vanadium (i.e., 10–100 times normal intake) affect cholesterol and triglyceride metabolism, stimulate glucose oxidation and glycogen synthesis in the liver [5].

Vanadium's primary mode of action is as a cofactor that enhances or inhibits enzymes. The inhibition of the activity of Na^+-K^+-ATPase by vanadate was the first effect of vanadium thoroughly investigated and reported in the literature [6], but currently, many other biological and pharmacological actions have been described for vanadium derivatives [7]. The role of vanadium in regulation of intracellular signaling pathways converts it in a possible therapeutic agent to be use in the treatments of a number of diseases. Different metabolic alterations for carbohydrates, lipids and proteins are markers for Diabetes mellitus. Besides, the disease is also characterized for a group of chronic complications which diminish the quality of life of diabetic patients and, finally, cause their death. Patients with Diabetes mellitus, mainly type 1 diabetic patients develop higher rates of bone resorption and turnover which convey to a decrease bone mineral density compared with healthy controls. Recently, Diabetes mellitus has been shown to be associated with osteoporosis [8, 9]. Several mechanisms seem to underlay bone alteration process in diabetic patients. Both, micro and macro angiopathies cause a decrease of blood flow especially in highly vascularised tissues. As a consequence, different metabolic changes take place in these tissues, including bone. For instance, it is probably that the synthesis and function of anabolic factors for bone development would decrease and, also highly concentrations of advanced glycation end (AGE) products can be formed in the constituents of the extracellular matrix (ECM). Among these components, collagen is one of the more affected proteins which cause a great impact in bone formation and functions [10]. Recently, some vanadium compounds have been reported in the literature as osteogenic agents due to their actions on bone related cells and on collagen formation. Besides, from a chemical point of view, it is well known the possible replacement of phosphorous by vanadium in the apatite lattice of bone tissue [11–14]. This review addresses and summarizes the osteogenic effects of vanadium compounds both *in vitro* and *in vivo* models as well as on cell regulatory processes that can be considered as putative mechanisms of action for these compounds. Besides, the possible mechanisms of adverse side effects derived from the vanadium administration are also briefly commented.

7.2 Hard Tissue

Bone is a dynamic tissue that is constantly being reshaped by osteoblasts, which build bone, and osteoclasts, which resorb bone. Osteoclasts and osteoblasts are instrumental cells in controlling the amount of bone tissue in vertebrates.

Osteoblasts are mononucleate cells responsible for bone formation. The origin of these cells is depicted in Fig. 7.1. Osteoblasts derive from osteoprogenitor cells located in the periosteum and the bone marrow. Progenitor osteoblastic cells are immature cells that express the crucial regulatory transcription factor Cbfa1/Runx2. Osteoprogenitors differentiate under the influence of growth factors, in particular the bone morphogenetic proteins (BMPs) [15]. Moreover, other growth factors including fibroblast growth factor (FGF), platelet-derived growth factor (PDGF) and transforming growth factor beta (TGF-β) may promote the proliferation and differentiation of osteoblast precursors and potentially induce the mineralization process (osteogenesis). Mature osteoblasts are highly specialized cells which synthesize the major constituents of the osteoid, that is the unmineralized, organic extracellular matrix (ECM), which is composed mainly of Type I collagen and noncollagenous proteins. Osteoblasts are also responsible for mineralization of the osteoid. In fact, the mature osteoblasts promote the formation of the biological hydroxyapatite, the main hard tissue mineral phase component. These cells also regulate their content of mineral ions through the activity of different enzymes such as alkaline phosphatase (ALP) which is anchored in the osteoblastic membranes and plays a key role in the mineralization process. Aside from ALP, the organic matrix exerts a great degree of crystallographic control over the nucleation and growth of mineral particles.

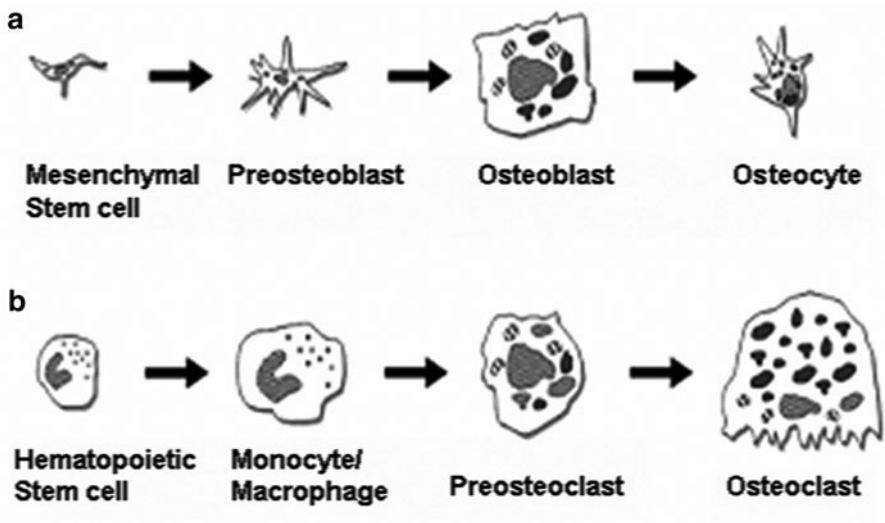

Fig. 7.1 Schematic origin of osteoblasts and osteoclasts

In the different steps of mineralization, type I collagen, the predominant protein in the ECM of bone and teeth, plays a key role [16]. Osteoblasts that are trapped in the bone matrix become osteocytes. They cease to generate osteoid and mineralized matrix, and instead act in a paracrine manner on active osteoblasts.

The other relevant cells in hard tissues are the osteoclasts. They remove bone tissue through a process known as bone resorption. Osteoclasts are multinucleate cells formed by the fusion of cells of the monocyte-macrophage cell line (Fig. 7.1).

Osteoclasts are characterized by high expression of tartrate resistant acid phosphatase (TRAP) and cathepsin K [17].

7.3 Vanadium Compounds Interactions with Hard Tissue Components

7.3.1 With Hydroxyapatite

Hydroxyapatite is the major mineral component of the mineral phase of bones and hard tissues in mammals. It is thermodynamically more stable than other minerals which form during the development of the mineralization process. Hydroxyapatite is synthesized *via* intermediate precursors such as amorphous calcium phosphate (ACP), octacalcium phosphate, or dicalcium phosphate dehydrate [18–20].

The chemical nature and the open lattice of hydroxyapatite promote substitution events both for cations and anions (Fig. 7.2, Taken from reference [21]).

The most common substitutions involve carbonate, fluoride and chloride for hydroxyl groups, while defects can also exist resulting in deficient hydroxyapatite. The substitution and the vacancy effects are very important since these processes in the apatite lattice contribute to a greater solubility of this phase and in consequence, favor its behavior as an ion reservoir. Physiologically, the mineralization process takes place with a non random distribution. It occurs inside **matrix vesicles** (MVs) which are extracellular, membrane-invested particles selectively located at sites of initial calcification in cartilage, bone, and predentin [22].

Matrix vesicle biogenesis occurs by polarized budding and pinching-off of vesicles from specific regions of the outer plasma membranes of differentiating growth plate chondrocytes. The first crystals of apatite bone mineral are formed within the MVs [16]. This is followed by propagation of hydroxyapatite into the ECM and its deposition between collagen fibrils.

When vanadium is absorbed in vertebrates, it distributes among different tissues and is storage mainly in bone [23].

The skeletal retention and bone effects of vanadium are of particular research interest [24]. Vanadate ions can be incorporated into hydroxyapatite lattice possibly for its analogy to phosphate [25, 26]. For these reasons, special attention was focused on the interaction of vanadium species with hydroxyapatite and with some components of the ECM such as chondroitin sulfate A, N-acetyl-D-galactosamine

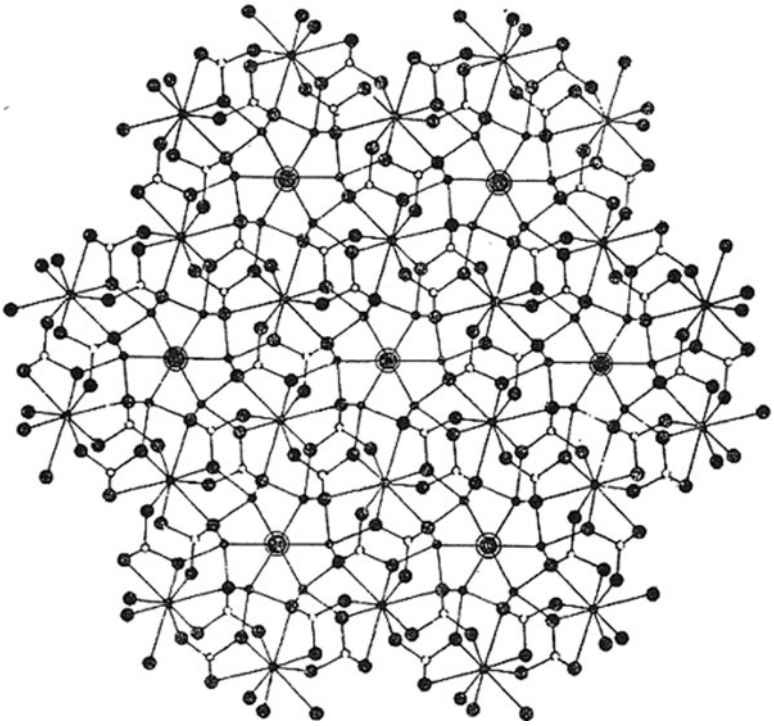

Fig. 7.2 Hydroxyapatite lattice. Taken from reference [21]

and D-Glucuronic acid. The structural and spectroscopic effects of the incorporation of VO_4^{3-} in the hydroxyapatite lattice were investigated as a model for the process of incorporation of vanadium in bone [27]. The substitution of PO_4^{3-} by VO_4^{3-} is facilitated for the structural behavior of the hydroxyapatite lattice which lends itself for substitution. Nevertheless, it is required that the apatite would be in an amorphous form for the incorporation of vanadate to be accomplished since it could not be observed when the apatite lattice is in the crystalline state. The incorporation of small quantities of VO_4^{3-} in the PO_4^{3-} sites produces only slight distortions in the macroscopic and microscopic structure of the mineral phase of bones. This fact could be determined by X-ray diffraction studies of substituted hydroxyapatite powder samples. Based on these results, it can be assumed that bone has an active role in the detoxification process when the organisms are exposed to high vanadium concentrations, comparable to that known for other toxic trace elements that can be also incorporated in bone. On the contrary, the substitution of calcium by other cations in the hydroxyapatite lattice affects these bonds more strongly [28, 29]. Besides, it was also demonstrated that VO^{2+} could not be incorporated into the apatite lattice although it is strongly adsorbed on its surface [30]. All together these studies showed that hydroxyapatite is a good model to study the incorporation of vanadium in bone.

7.3.2 With ECM Components

To continue with the understanding of the effects of vanadium species on hard tissues we investigated the interactions of vanadium with chondroitin sulfate A (CSA), an acid mucopolysaccharide present in connective tissue and other mineralized systems [31]. Results from different spectroscopic determinations suggested the coordination of oxovanadium(IV) to the carboxylate group and the glycosidic oxygen of the D-glucuronate moieties [32]. These results are relevant for the interaction of VO^{2+} with collagen, a system in which interactions of oxovanadium(IV) with nitrogen has been clearly established [33, 34].

7.3.3 With Bone Cells in Culture

The relevance of vanadium in bone tissue arises from the studies performed to establish the essentiality of this element in animals and human beings [23, 35].

As bone is quantitatively the main tissue for vanadium storage bone accumulation is twice than the accumulation in kidney and tenfold the liver accumulation [36] it is worthy to try to understand the effects of vanadium compounds in bone related cells. Cells in culture are a useful system to investigate many different biological events. In particular, considering the biology and biochemistry of hard tissues, it is interesting to thoroughly study events such as cell proliferation, differentiation and mineralization, as well as the intracellular mechanisms by which vanadium derivatives exert their biological actions.

In particular, we have studied the effects of vanadium compounds in two osteoblast-cell lines of murine origin Fig. 7.3. [37–40].

MC3T3E1 osteoblasts are derived from mouse calvaria. These cells display the features of typical fibroblasts [41].

MC3T3E1 cell line is a model of preosteoblasts that can differentiate to mature osteoblasts in culture. The different maturation stages of this cell line *in vitro* resemble that of the physiological process *in vivo* (proliferation, differentiation and mineralization), providing an adequate system for biological studies referred to bone tissues.

In the proliferative stage, MC3T3E1 cells do not express a great level of alkaline phosphatase (ALP) specific activity. After 10 days of culture in the presence of ascorbic acid and β glycerophosphate, they expressed specific markers of mature osteoblast phenotype. The differentiation step correlates with the expression of different proteins such as ALP and collagen accumulation in the ECM. The mineralization of ECM begins approximately at 15–20 days of culture. After that, the cells programme their death by apoptosis [42].

UMR106 osteoblast-like cells are derived from a rat osteosarcoma induced by 32P. This immortalized cell line exhibits the characteristic osteoblast phenotype. The cells express high levels of specific ALP activity and produce type I collagen but they are unable to synthesize bone mineral phase in culture [39].

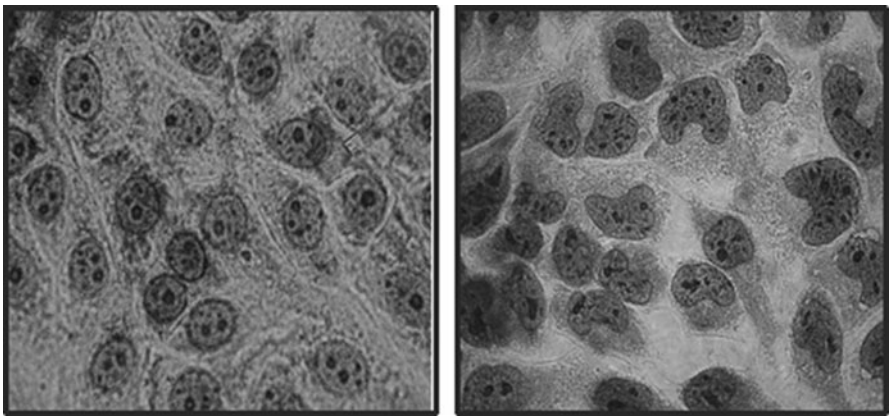

Fig. 7.3 MC3T3E1 osteoblast-like cells. The osteoblasts were cultured in DMEM at 37°C for 24 h, fixed and stained with Giemsa for microscopy observation (Magnification: 100×) (*Left* panel). UMR106 osteoblast-like cells. Osteoblasts were cultured in DMEM 37°C, 24 h, fixed and stained with Giemsa for microscopy observation (Magnification: 100×) (*Right* panel)

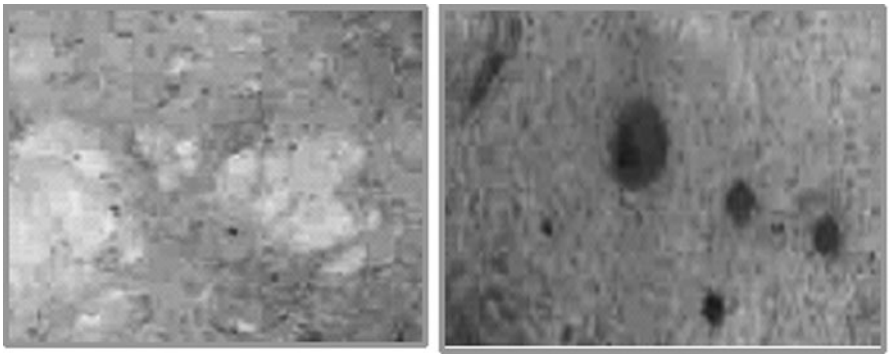

Fig. 7.4 Effect of TreVO long-term treatment on the mineralization of MC3T3E1 cells. Control cells (*Left* panel). Long-term treatment with 5 μM TreVO (*Right* panel)

This simple model of osteoblast-like cells in culture allows the investigation of pharmacological effects of many vanadium compounds. Specially, complexes of vanadyl(IV) cation with simple sugars (mono- and disaccharides, and related compounds such as polyhols and acids) were investigated [43, 44].

Practically all the vanadyl(IV)-sugar complexes synthesized in our laboratory were evaluated for their bioactivity on osteoblast cell lines in culture. This approach has allowed us to find an outstanding compound among this series: the complex of vanadyl(IV) cation with the disaccharide trehalose (TreVO) which displayed insulin mimetic activity [45]. Besides, in long term cultures carried out with the MC3T3E1 cell line [40], this complex revealed as a good osteogenic compound since it promoted type I collagen production and the mineralization of the ECM in the cultures (See Fig. 7.4) [40]. Moreover, it could also be established the mechanism of

action of this compound which exerted its mitogenic effect, at low doses, through the activation of the extracellular regulated kinase (ERK) pathway. On the other hand, it was demonstrated the participation of oxidative stress in the cytotoxic actions of this complex at high concentrations [39, 40].

Moreover, the bioactivity of vanadyl(IV) derivatives with flavonoids and related compounds have been also investigated with the aid of this cellular *in vitro* model to assess their osteogenic ability. In this context, a complex of vanadyl(IV) cation with the flavonoid Quercetin, also showed promissory osteogenic activity in osteoblasts in culture. Flavonoids are polyphenolic compounds obtained from plants. Recently they have aroused a great scientist interest due to their broad pharmacological activity. They present antioxidant, antitumoral and antibacterial properties [46–49].

The complex of Quercetin and vanadyl(IV) cation, QuerVO, was studied in cultures of MC3T3E1 and UMR106 cells. Cell proliferation was evaluated by the crystal violet bioassay. For studying cellular differentiation, two markers of osteoblast phenotype (ALP and collagen production) were analyzed. Finally, to get an insight into the putative mechanisms of action, studies on the effect of this complex on the activation of ERK pathway were performed and reported [50]. QuerVO displayed interesting osteogenic actions such as induction of the synthesis of collagen type I. The complex caused stimulation of ERK phosphorylation and this activation seems to be one of the possible mechanisms used by the complex to exert its biological effects.

Another interesting osteogenic oxovanadium (IV) derivative thoroughly studied for our group was the vanadyl(IV) complex with ascorbic acid (VOAsc) [51]. This complex significantly stimulated collagen production in osteoblasts and inhibited ALP activity in UMR106 cells. Besides, after 3 weeks of culture, VOAsc (5–25 μM) increases the formation of mineralization nodules in the ECM of MC3T3E1 cultures. At higher concentrations this complex stimulated cellular apoptosis in osteoblast cell lines.

On the other hand, the effects of vanadium(V) compounds such as metavanadate and decavanadate in bone fish cells have been investigated by Aureliano Alves and his group [52]. Short- and long-term studies were performed in VSa13, a fish bone-derived cell line. Metavanadate in short periods was less toxic than decavanadate. In long term studies the effects of both vanadium derivatives were similar. They stimulated cell proliferation but strongly impaired the mineralization process.

The reported results suggest that vanadium(IV) complexes display more effective osteogenic properties in osteoblasts in culture than vanadium(V) derivatives, although more research is required in this sense to get a deeper insight into the osteogenic properties of vanadium.

As bone homeostasis is the result of the balance between bone resorption and bone formation, we have studied the activation of macrophages because these cells are related with bone resorption. We investigated the effect of a complex of vanadyl(IV) cation with the non steroideal anti-inflammatory drug Aspirin, VOAspi, on a culture of murine macrophage RAW 264.7. VOAspi caused the activation of macrophages by a mechanism dependent on L-type calcium channel and the generation of nitric oxide. On the contrary, free vanadyl(IV) cation exerted cytoxic

effects by a mechanism independent of calcium channel and nitric oxide generation [53]. The studies on vanadium actions in osteoclasts and related cells are very scarce and merits more attention in the future.

7.4 Mechanism of Action

The putative mechanisms for the osteogenic actions of vanadium compounds are currently under exhaustive investigation. In fact, we have carried out different experiments in osteoblasts in culture to achieve this aim [37, 40, 54]. As an overview, at low concentrations, most vanadium derivatives behave as weak mitogens and promote osteoblast differentiation in a way similar to the insulin. Vanadium derivatives regulate osteoblastic proliferation, differentiation and stimulated the glucose consumption [55, 56]. Extracellular regulated kinases-1,2 (ERKs) and phosphatidyl inosytol-3 kinase (PI3-K) are the main intracellular transduction pathways used by vanadium to exert its biological effects. These pathways are stimulated as a result of the inhibition that vanadium derivatives cause on the protein tyrosine phosphatases (PTPases) [57, 58].

The model of osteoblastic cells in culture has allowed us to demonstrate the ability of low doses of TreVO to promote cell proliferation and to stimulate ERK phosphorylation in the MC3T3E1 osteoblastic cell line. This effect was totally abrogated by an inhibitor of MEK (PD98059) and wortmannin (an inhibitor of the PI3-K), but not by a mixture of free radical scavengers (vitamins E and C) [45]. These results suggest that low doses of the complex, which are mitogenic for MC3T3E1 cells, could act though the PI3K-MEK-ERK pathway and by a mechanism independent of free radicals. On the contrary, at higher doses, the vanadium complex inhibited cell proliferation of MC3T3E1 osteoblasts and the osteosarcoma UMR106 cell line. This effect was not blocked by neither wortmannin, nor PD98059 or by the mixture of vitamins C and E. However, high concentrations of the complex strongly increased ERK phosphorylation, an effect that was partially blocked by wortmannin, PD98059 or a mixture of vitamins E and C. In addition, the combination of these inhibitors showed an additive effect over the inhibition of ERK activation but not over the inhibition of cell proliferation [45]. Altogether these results indicate that, although high doses of vanadium stimulate ERK phosphorylation through the PI3K-MEK-dependent pathway and also through an oxidative mechanism, the inhibition of cell proliferation does not seem to be associated with the activation of these pathways.

On the other hand, there are some other mechanisms that may be involved in the osteogenic effects of vanadium such as the direct activation of a cytosolic protein tyrosine kinase [55, 59]. Results reported by our laboratory are in agreement with the latter observations. Insulin and TreVO stimulated the glucose consumption in osteoblast-like cells, but the PI3-K inhibitor wortmannin did not abrogate this effect. In addition, staurosporine at concentrations that do not affect PKC, was a potent inhibitor of the glucose consumption simulated by this vanadium(IV) complex.

[45]. In addition, the inhibition of glycogen synthase kinase-3 (GSK-3) is important for the activation of glycogen synthase [60]. Vanadium(IV) complexes inhibit GSK-3 through phosphorylation and in turn activate glycogen synthase promoting glucose consumption on osteoblats. In the presence of staurosporine, the vanadium derivatives failed to stimulate GSK-3 phosphorylation [44]. Altogether these results suggest that the cytosolic tyrosine protein kinase and GSK-3 may be involved in the insulin mimetic activity of the vanadyl(IV) compounds on osteoblast cell in culture.

7.5 *In Vivo* Osteogenic Effects of Vanadium

Several studies suggest that vanadium compounds ameliorate diabetic-related bone disorders, primarily by improving the diabetic state [61, 62].

Treatment in control and streptozotocin-induced diabetic female Wistar rats with bis(ethylmaltolato)oxovanadium(IV) (BEOV), was effective in incorporating vanadium into bone. In all treated groups, BEOV increased osteoid volume. In non-diabetic rats, BEOV increased cortical bone toughness, mineralization and bone formation [61] (Fig. 7.5).

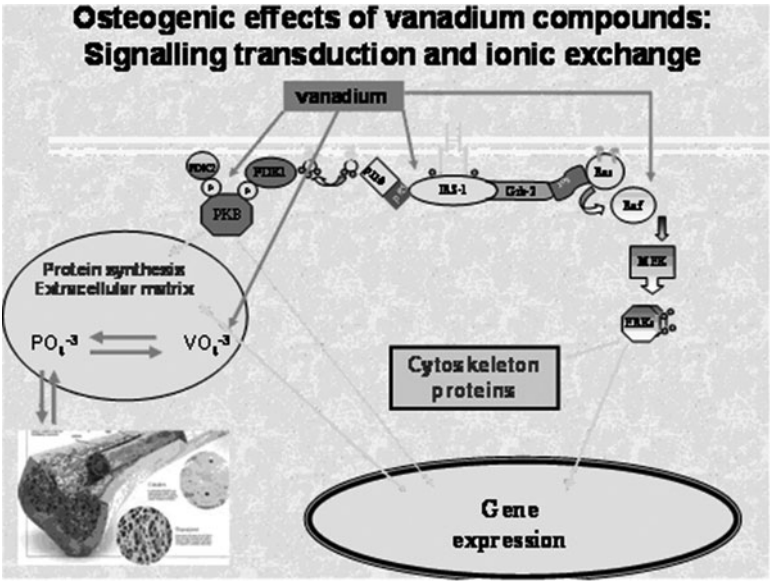

Fig. 7.5 In this figure it can be observed two of the most important signaling transduction pathways of insulin as well as the sites used by vanadium as an insulin enhancer. Both pathways regulate the expression of genes related to bone cell proliferation and differentiation as well as their action on proteins of the cytoskeleton which are related to cellular morphological changes. Moreover, vanadium compounds participate in ionic exchange with phosphate favoring its accumulation in bone tissue and potentiate effects on this tissue

Following the long-term administration of vanadyl acetylacetonate, trabecular thickness, mineral apposition rate and plasma osteoclacin in diabetic rats were either improved or normalized, however reduced bone mineral density was not increased [62].

In higher animals, vanadium has been demonstrated to be essential. After their mothers had been fed carefully formulated vanadium-deficient diets, second-generation goat kids suffered skeletal damage and died within 3 days of parturition [5]. In human beings vanadium essentiality has not been proven yet. Pharmacologic amounts of vanadium (i.e., 10–100 times normal intake) affect cholesterol and triglyceride metabolism, influence the shape of erythrocytes, and stimulate glucose oxidation and glycogen synthesis in the liver [5]. Moreover, clinical studies carried out in normal or diabetic patients indicated that orally administered vanadium(IV) showed low or no toxicity [63–65].

7.6 Risk Assessment for the Use of Vanadium Compounds as Potential Therapeutics Drugs: Cytotoxicity and Genotoxicity Studies

Despite the potential use of vanadium compounds either as insulinomimetic, osteogenic or anticancer drugs, its possible harmful effects argue against its clinical use. Understanding of the mechanisms underlying vanadium compounds toxicity is important in evaluating its use as a therapeutic drug.

The toxic effects of vanadium are related to the dose, cell line and vanadium nature (oxidation state, free or complexed). Studies concerning the mechanisms of action of vanadate showed that this compound induces gene expression, oxidative burst, changes in cytosolic calcium, tyrosine phosphorylation, enzyme activation or inhibition and also, morphological changes and cytoskeletal alterations [6, 66–71].

Several studies suggest that hydrogen peroxide is involved in vanadate-induced cell growth arrest and cell death [72–75].

However, a more recently study suggested that vanadate toxicity occurs by two distinct pathways, one dependent on and one independent of H_2O_2 production [76]. Vanadate concentrations that reduced cellular viability to approximately 60–70% of the control (10 μmol/L) did not induce H_2O_2 formation. A second hypothesis raised by these authors proposed that peroxovanadium compounds, produced once vanadate enters into the cells, are responsible for the cytotoxicity.

On the other hand, decreased cell viability induced by vanadyl sulphate in tumorogenic and non-carcinogenic cells has been also previously reported [77]. Moreover, we have also previously reported the cytotoxicity of a vanadium(V) derivative with salicylaldehyde semicarbaxone in osteoblasts in culture [78]. This complex caused cytotoxicity in the osteoblastic cells mainly through oxidative stress and through the activation of ERK pathways which, although it is classically recognized as a key transducer in the signal cascade mediating the cell proliferation, and differentiation

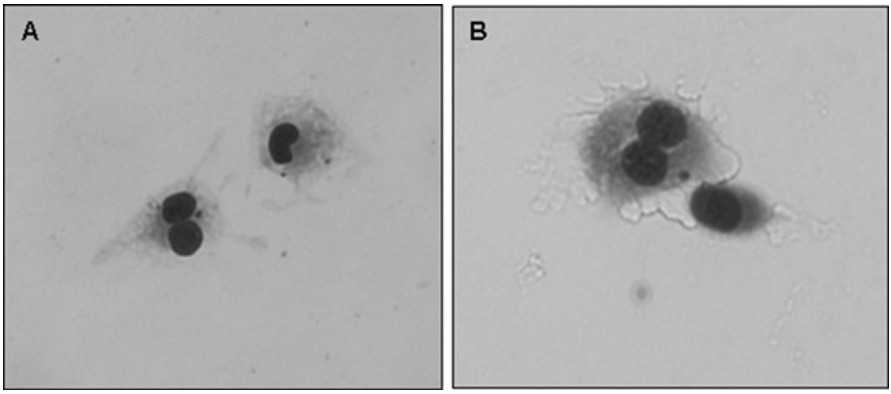

Fig. 7.6 Genotoxicity of VO(oda) in UMR106 cells (**a**) and MC3T3E1 osteoblasts (**b**). This picture shows the induction of micronucleus in binucleated cells stained with Giemsa (Magnification: 40×)

[79], some investigations have shown that the activation of ERK pathway can mediate cell cycle arrest and apoptotic and non apoptotic cell death [80].

On the other hand, even though vanadyl(IV) is less toxic than vanadium(V), it is always crucial to investigate the toxicity of vanadium(IV) derivatives intended to be used in therapeutics. Recently, we have reported an exhaustive study on a vanadyl(IV) complex with a multidentate oxygen donor oda=oxodiacetate, VO(oda) in osteoblast cell lines in culture [81]. The complex increased the level of ROS which correlated with a decreased in GSH/GSSG ratio, dissipation of the mitochondria membrane potential and promoted an increase in ERK cascade phosphorylation, which is involved in the regulation of cellular death and survival.

Considerable attention has attracted the assessment of the genotoxicity of vanadium compounds in recent years. Adverse effects of pentavalent and tetravalent vanadium compounds on chromosome integrity and segregation have been observed *in vitro*. In particular, we have studied the genotoxic effect of VO(oda) in two osteoblast cell lines (UMR106 and MC3T3E1) that revealed a twofold increase in the micronucleus frequency at 25 μM compared with control in UMR106 and at 10 μM in MC3T3E1. An example of a binucleated osteoblastic cell containing a micronucleus is depicted in Fig. 7.6 for both cell lines. Besides we have recently reported preliminary results on the increase in DNA strand breaks in a human colon adenocarcinoma cell line (Caco-2 cells) induced by VO(oda) [82]. In agreement with our results, vanadium(IV) compounds proved to be genotoxic in several *in vitro* systems, inducing micronuclei and chromosomal aberrations in human peripheral blood cells [83–85], and DNA strand breaks through the generation of free radicals [86, 87].

Pentavalent vanadium compounds have been also reported to induce genotoxic actions stimulating the increase in micronucleus frequency, DNA strand breaks, sister chromatid exchanges (SCE) and chromosomal aberrations in different *in vitro* systems [83, 84, 88–91].

These positive findings were confirmed in some *in vivo* studies in mice using acute intraperitoneal or intragastric administrations [92–94].

Moreover, the genotoxic potential *in vivo* by a subacute oral exposure of vanadyl sulphate has been evaluated. Effects on chromosome integrity and segregation, visualized as micronuclei, and primary DNA lesions detectable by comet assay, have been assessed in somatic and germ cells [95]. In summary, taken in consideration the multiple biological activities exerted by vanadium on critical cell mechanisms, even in the very low dose range [96, 97], it is suggested to maintain a cautious approach in the safety evaluation of vanadium compounds.

7.7 Concluding Remarks

The potential therapeutics actions of vanadium compounds at hard tissues have attracted the attention of scientists in the field of diabetes mellitus, bone disease, aging and cancer since vanadium compounds are store mainly in bones. The use of osteogenic primary or cloned lines in culture is a useful strategy to investigate the osteogenic properties of vanadium compounds. Although *in vitro* experiments showed that the toxicity actions of vanadium compounds seem to be related to the oxidation state of the element as well as the nature of the ligands in the coordination sphere and also, on the cell type in culture, *in vivo* reports show little, if any, toxicity in long-term administration. Vanadium compounds have demonstrated several interesting effects on biological processes such as cell proliferation, differentiation and mineralization of the ECM in bone cells. These effects convey to vanadium consideration as a potential therapeutic agent for several diseases. Finally, it is worthy to mention that further investigations are needed to completely elucidate the osteogenic mechanism of action of vanadium compounds, even though, currently most evidence point to the role of ERK pathway activation through the inhibitory effect on Protein tyrosine phosphatase (PTPase) activity, calcium channel and the expression of genes related to osteoblast differentiation. Moreover, although there are very few experimental works on this topic *in vivo*, some studies recently develop suggest the potential relevance of vanadium derivatives in the treatment of bone diseases.

Acknowledgements SBE, DAB and ALDV are members of the Carrera del Investigador CONICET (Argentina). This work was partially supported by grants from Universidad Nacional de La Plata (Argentina) (X345 and X 554), CONICET (PIP 1125) and the Agencia Nacional de Promoción Científica y Tecnológica (ANPCyT) (PICT 2218).

References

1. Myron DR, Zimmerman Shuler TR, Klevay LM, Lee DE, Nielsen FH (1978) Intake of nickel and vanadium by humans: a survey of selected diets. Am J Clin Nutr 31:527–531
2. Nielsen FH (1995) Vanadium in mammalian physiology and nutrition. In: Sigel H, Sigel A (eds) Metal ions in biological systems, Vanadium and its role in life. Marcel Dekker, New York

3. Nielsen FH (1984) Ultratrace elements in nutrition. Annu Rev Nutr 4:21–41
4. Nriagu JO (1998) Vanadium in the environment, Part 2: health effects. Wiley, New York/Chitester/Weinheim/Brisbane/Singapore/Toronto
5. Harland BF, Harden-Williams BA (1994) Is vanadium of human nutritional importance yet? J Am Diet Assoc 94:891–894
6. Cantley LC Jr, Josephson L, Warner R, Yanagisawa M, Lechene C, Guidotti G (1977) Vanadate is a potent (Na, K)-ATPase inhibitor found in ATP derived from muscle. J Biol Chem 252:7421–7423
7. Tsiani E, Fantus IG (1997) Vanadium compounds biological actions and potential as pharmacological agents. Trends Endocrinol Metab 8:51–58
8. Schwartz AV (2993) Diabetes mellitus: does it affect bone? Calcif Tissue Int 73:515–519
9. de Paula FJ, Horowitz MC, Rosen CJ (2010) Novel insights into the relationship between diabetes and osteoporosis. Diabetes Metab Res Rev 26:622–630
10. Schwartz AV (2003) Diabetes mellitus: does it affect bone? Calcif Tissue Int 73:515–519
11. Stankiewicz PJ, Tracey AS, Crans DC (1995) Inhibition of phosphate-metabolizing enzymes by oxovanadium(V) complexes. Met Ions Biol Syst 31:287–324
12. Plass W (2002) Transition metal centers in biological matrices: structure and function of vanadate in vanadium haloperoxidases and as phosphate analog. In: Rollnik H, Wolf D (eds) NIC symposium 2001, Proceedings, John von Neumann Institute for Computing, Jülich, NIC Series
13. Crans DC (2005) Fifteen years of dancing with vanadium. Pure Appl Chem 77:1497–1527
14. Steens N, Ramadan AM, Parac-Vogt TN (2009) When structural and electronic analogy leads to reactivity: the unprecedented phosphodiesterase activity of vanadates. Chem Commun (Camb) 28:965–967
15. Agata H, Asahina I, Yamazaki Y, Uchida M, Shinohara Y, Honda MJ, Kagami H, Ueda M (2007) Effective bone engineering with periosteum-derived cells. J Dent Res 86:79–83
16. Anderson HC (2003) Matrix vesicles and calcification. Curr Rheumatol Rep 5:222–226
17. Nijweidi Ehb PJ, Feyen JHM (1986) Cells of bone: proliferation, differentiation, and hormonal regulation. Physiol Rev 66:855–886
18. Kartsogiannis V, Ng KW (2004) Cell lines and primary cell cultures in the study of bone cell biology. Mol Cell Endocrinol 228:79–102
19. Eanes ED (2001) Amorphous calcium phosphate. Monogr Oral Sci 18:130–147
20. Eanes ED, Gillessen IH, Posner A (1970) A note on the crystal growth of hydroxyapatite precipitated from aqueous solutions. Mater Res Bull 5:377–383
21. Etcheverry SB, Ferrer EG, Gonzalez-Baró AC, Parajón-Costa BS, Williams PAM (2009) Vanadis´charms: from the mithology to the bioinorganic chemistry. J Arg Chem Soc 97:127–150
22. Anderson HC (1995) Molecular biology of matrix vesicles. Clin Orthop Rel Res 314:266–280
23. Nielsen FH (1995) Vanadium and its role in life. In: Sigel H, Sigel A (eds) Metal ions in biological systems. Marcel Dekker, New York
24. Barrio DA, Etcheverry SB (2010) Potential use of vanadium compounds in therapeutics. Curr Med Chem 17:3632–3642
25. Gresser MJ, Tracey AS (1990) Vanadates as phosphate analogs in biochemistry. In: Chasteen ND (ed) Vanadium in biological systems. Kluwer Academic, Dordrecht
26. Crans DC (1994) Enzyme interactions with labile oxovanadates and other oxometalates. Comm Inorg Chem 16:35–76
27. Etcheverry SB, Apella MC, Baran EJ (1984) A model study of the incorporation of vanadium in bone. J Inorg Biochem 20:269–274
28. Apella MC, Etcheverry SB, Baran EJ (1981) Untersuchung der symmetrischen Phosphat-Valenzschwingung in gemischten Calcium-Strontium-Apatiten. Z Naturforsch 36b:1190–1192
29. Narda GE, Pedregosa C, Etcheverry SB, Baran EJ (1990) Schwingungsspektroskopische Untersuchung einiger gemischter Calcium/Cadmium-Hydroxylapatite. Z Naturforsch 45b: 1133–1135

30. Narda GE, Apella MC, Etcheverry SB, Baran EJ (1984) Hydrolytisches und thermisches Verhalten von $Sn_3PO_4F_3$. Z Anorg Allg Chem 515:207–212
31. Etcheverry SB, Williams PAM, Baran EJ (1994) The interaction of the vanadyl(IV) cation with chondroitin sulfate A. Biol Trace Elem Res 42:43–52
32. Etcheverry SB, Williams PAM, Baran EJ (1996) Synthesis and characterization of a solid vanadyl (IV) complex of D-glucuronic acid. J Inorg Biochem 63:285–289
33. Etcheverrry S, Williams PAM, Baran EJ (1996) A spectroscopic study of the interaction of the VO^{2+} cation with the two components of chondroitin sulfate. Biol Trace Elem Res 51:169–176
34. Etcheverrry S, Williams PAM, Baran EJ (1996) A spectrophotometric study of the interaction of VO2+ with cytosine nucleotides. Biol Trace Elem Res 51:169–176
35. Anke M, Groppel B, Krause U (1991) The essentiality of the toxic elements aluminium and vanadium. In: Momcilovic B (ed) Trace elements in man and animals. IMI, Zagreb
36. Setyawati IA, Thompson KH, Yuen VG, Sun Y, Battell M, Lyster DM, Vo C, Ruth TJ, Zeisler S, McNeill JH, Orvig C (1998) Kinetic analysis and comparison of uptake, distribution, and excretion of ^{48}V-labeled compounds in rats. J Appl Physiol 84:569–575
37. Etcheverry SB, Cortizo AM (1998) Bioactivity of vanadium compounds on cells in culture. In: Nriagu JO (ed) Vanadium in the environment. Advances in environmental science and technology; Part A. Wiley, New York
38. Cortizo AM, Etcheverry SB (1995) Vanadium derivatives act as growth factor-minetic compounds upon differentiation and proliferation of osteoblast-like UMR106 cells. Mol Cell Biochem 145:97–102
39. Barrio DA, Etcheverry SB (2006) Vanadium and bone development: putative signalling pathways. Can J Physiol Pharmacol 84:677–686
40. Etcheverry SB, Barrio DA (2007) Vanadium and bone. Relevance of vanadium compounds in bone cells. In: Kustin K, Costa Pesoa J, Crans DC (eds) Vanadium: the versatile element, vol 15, American chemical society series. American Chemical Society, Washington, DC, p 974
41. Sálice VC, Cortizo AM, Gómez Dumm CL, Etcheverry SB (1999) Tyrosine phosphorylation and morphological transformation induced by four vanadium compounds on MC3T3E1 cells. Mol Cell Biochem 198:119–128
42. Quarles LD, Yohay DA, Lever LW, Caton R, Wenstrup RJ (1992) Distinct proliferative and differentiated stages of murine MC3T3-E1 cells in culture: an in vitro model of osteoblast development. J Bone Miner Res 7:683–692
43. Williams PAM, Barrio DA, Etcheverry SB, Baran EJ (2004) Characterization of oxovanadium(IV) complexes of D-gluconic and D-saccharic acids and their bioactivity on osteoblast-like cells in culture. J Inorg Biochem 98:333–342
44. Barrio DA, Cattáneo ER, Apezteguía MC, Etcheverry SB (2006) Vanadyl(IV) complexes with saccharides. Bioactivity in osteoblast-like cells in culture. Can J Physiol Pharmacol 84: 765–775
45. Barrio DA, Williams PA, Cortizo AM, Etcheverry SB (2003) Synthesis of a new vanadyl(IV) complex with trehalose (TreVO): insulin-mimetic activities in osteoblast-like cells in culture. J Biol Inorg Chem 8:459–468
46. Rice-Evans CA, Packer L (1998) Flavonoids in health and disease. Marcel Dekker, New York
47. Bravo A, Anacona JR (2001) Metal complexes of the flavonoid quercetin: antibacterial properties. Transit Met Chem 26:20–23
48. Cornard JP, Merlin JC (2001) Structural and spectroscopic investigation of 5-hydroxyflavone and its complex with aluminium. J Mol Struct 569:129–138
49. Kandaswami C, Lee LT, Lee PP, Hwang JJ, Ke FC, Huang YT, Lee MT (2005) The antitumor activities of flavonoids. In Vivo 19:895–909
50. Ferrer EG, Salinas MV, Correa MJ, Naso L, Barrio DA, Etcheverry SB, Lezama L, Rojo T, Williams PAM (2006) Synthesis, characterization, antitumoral and osteogenic activities of quercetin vanadyl(IV) complexes. J Biol Inorg Chem 11:791–801

51. Cortizo AM, Molinuevo MS, Barrio DA, Bruzzone L (2006) Osteogenic activity of vanadyl(IV)-ascorbate complex: evaluation of its mechanism of action. Int J Biochem Cell Biol 38:1171–1180
52. Tiago DM, Laizé V, Cancela ML, Aureliano M (2008) Impairment of mineralization by metavanadate and decavanadate solutions in a fish bone-derived cell line. Cell Biol Toxicol 24:253–263
53. Molinuevo MS, Etcheverry SB, Cortizo AM (2005) Macrophage activation by a vanadyl-aspirin complex is dependent on L-type calcium channel and the generation of nitric oxide. Toxicology 210:205–212
54. Etcheverry SB, Williams PA, Barrio DA, Salice VC, Ferrer EG, Cortizo AM (2000) Synthesis, characterization and bioactivity of a new VO^{2+}/aspirin complex. J Inorg Biochem 80:169–171
55. Cortizo AM, Salice VC, Vescina CM, Etcheverry SB (1997) Proliferative and morphological changes induced by vanadium compounds on Swiss 3T3 fibroblasts. Biometals 10:127–133
56. Etcheverry SB, Crans DC, Keramidas AD, Cortizo AM (1997) Insulin-mimetic action of vanadium compounds on osteoblast-like cells in culture. Arch Biochem Biophys 338:7–14
57. Swarup G, Cohen S, Garbers DL (1982) Inhibition of membrane phosphotyrosyl-protein phosphatase activity by vanadate. Biochem Biophys Res Commun 107:1104–1109
58. Tracey AS, Gresser MJ (1986) Interaction of vanadate with phenol and tyrosine: implications for the effects of vanadate on systems regulated by tyrosine phosphorylation. Proc Natl Acad Sci USA 83:609–613
59. Shisheva A, Shechter Y (1993) Role of cytosolic tyrosine kinase in mediating insulin-like actions of vanadate in rat adipocytes. J Biol Chem 268:6463–6469
60. Eldar-Finkelman H (2002) Glycogen synthase kinase 3: an emerging therapeutic target. Trends Mol Med 8:126–132
61. Facchini DM, Yuen VG, Battell ML, McNeill JH, Grynpas MD (2006) The effects of vanadium treatment on bone in diabetic and non-diabetic rats. Bone 38:368–377
62. Zhang SQ, Chen GH, Lu WL, Zhang Q (2007) Effects on the bones of vanadyl acetylacetonate by oral administration: a comparison study in diabetic rats. J Bone Miner Metab 25:293–301
63. Mukherjee B, Patra B, Mahapatra S, Banerjee P, Tiwari A, Chatterjee M (2004) Vanadium—an element of atypical biological significance. Toxicol Lett 150:135–143
64. Hirano S, Suzuki KT (1996) Exposure, metabolism, and toxicity of rare earths and related compounds. Environ Health Perspect 104:85–95
65. Fawcett JP, Farquhar SJ, Thou T, Shand BI (1997) Oral vanadyl sulphate does not affect blood cells, viscosity or biochemistry in humans. Pharmacol Toxicol 80:202–206
66. Yin X, Davidson AJ, Tsang SS (1992) Vanadate-induced gene expression in mouse C127 cells: roles of oxygen derived active species. Mol Cell Biochem 115:85–96
67. Fantus IG, Kadota S, Deragon G, Foster B, Posner B (1989) Pervanadate [peroxide(s) of vanadate] mimics insulin action in rat adipocytes via activation of the insulin receptor tyrosine kinase. Biochemistry 28:8864–8871
68. Trudel S, Pâquet MR, Grinstein S (1991) Mechanism of vanadate induced activation of tyrosine phosphorylation and of the respiratory burst in HL60 cells. Role of reduced oxygen metabolites. Biochem J 276:611–619
69. Secrist JP, Burns LA, Karnitz L, Koretzky GA, Abraham RT (1993) Stimulatory effects of the protein tyrosine phosphatase inhibitor, pervanadate, on T-cell activation events. J Biol Chem 268:5886–5893
70. Huyer G, Liu S, Kelly J et al (1997) Mechanism of inhibition of protein-tyrosine phosphatases by vanadate and pervanadate. J Biol Chem 272:843–851
71. Capella LS, Alcantara JSM, Moura-Neto V, Lopes AG, Capella MAM (2000) Vanadate is toxic to adherent- growing multidrug-resistant cells. Tumour Biol 21:54–62
72. Bay BH, Sit KH, Paramanantham R, Chan YG (1997) Hydroxyl free radicals generated by vanadyl[IV] induce cell blebbing in mitotic human Chang liver cells. Biometals 10:119–122
73. Huang C, Zhang Z, Ding M et al (2000) Vanadate induces p53 transactivation through hydrogen peroxide and causes apoptosis. J Biol Chem 275:32516–32522

74. Torres M, Forman HJ (2002) Vanadate inhibition of protein tyrosine phosphatases mimics hydrogen peroxide in the activation of the ERK pathway in alveolar macrophages. Ann N Y Acad Sci 973:345–348
75. Capella LS, Gefe MR, Silva EF et al (2002) Mechanisms of vanadate induced cellular toxicity: role of cellular glutathione and NADPH. Arch Biochem Biophys 406:65–72
76. Capella MAM, Capella LS, Valente RC, Gefé M, Lopes AG (2007) Vanadate-induced cell death is dissociated from H_2O_2 generation. Cell Biol Toxicol 23:413–420
77. Holko P, Ligeza J, Kisielewska J, Kordowiak AM, Klein A (2008) The effect of vanadyl sulphate ($VOSO_4$) on autocrine growth of human epithelial cancer cell lines. Pol J Pathol 59:3–8
78. Rivadeneira J, Barrio DA, Arrambide G, Gambino D, Bruzzone L, Etcheverry SB (2009) Biological effects of a complex of vanadium(V) with salicylaldehyde semicarbazone in osteoblasts in culture: Mechanism of action. J Inorg Biochem 103:633–642
79. Wang ZI, Bonner JC (2000) Mechanism of extracellular signal-regulated kinase ERK-1 and ERK-2 activation by vanadium pentoxide in rat pulmonary myofibroblasts. Am J Respir Cell Mol Biol 22:590–596
80. Blázquez C, Galve-Roperh I, Guzmán M (2000) The novo synthesized ceramide signals apoptosis in astrocytes via extracellular signal- regulated kinase. FASEB J 14:2315–2322
81. Rivadeneira J, Di Virgilio AL, Barrio DA, Muglia CI, Bruzzone L, Etcheverry SB (2010) Cytotoxicity of a vanadyl(IV) complex with a multidentate oxygen donor in osteoblast cell lines in culture. Med Chem 6:9–23
82. Di Virgilio AM, Rivadeneira J, Reigosa MA, Etcheverry SB (2010) XIV Congreso Latinoamericano de Genética, VIII Congreso de la Asociación Latinoamericana de mutagénesis, carcinogénesis y teratogénesis ambiental, XLIII de la Sociedad de Genética de Chile, XXXIX Confreso de la Sociedad Argentina de Genética. Book of Abstracts, pp 691, 2010
83. Migliore L, Bocciardi R, Macri C, Lo Jacono F (1993) Cytogenetic damage induced in human lymphocytes by four vanadium compounds and micronucleus analysis by fluorescence in situ hybridization with a centromeric probe. Mutat Res 319:205–213
84. Migliore L, Scarpato R, Falco P (1995) The use of fluorescence in situ hybridization with a β-satellite DNA probe for the detection of acrocentric chromosomes in vanadium-induced micronuclei. Cytogenet Cell Genet 69:215–219
85. Rodriguez-Mercado JJ, Roldan-Reyes E, Altamirano-Lozano M (2003) Genotoxic effects of vanadium(IV) in human peripheral blood cells. Toxicol Lett 144:359–369
86. Shi X, Jiang H, Mao Y, Ye J, Saffiotti U (1996) Vanadium (IV)- mediated free radical generation and related 2′-deoxyguanosine hydroxylation and DNA damage. Toxicology 106:27–39
87. Bay B, Sith K, Paramanamtham R, Chan Y (1997) Hydroxyl free radicals generated by vanadyl (IV) induce cell bleb bing in mitotic human Chang liver cells. Biometals 10:119–122
88. Owusu-Yaw J, Choen MD, Fernando SY, Wei CI (1990) An assessment of the genotoxicity of vanadium. Toxicol Lett 50:327–336
89. Rojas E, Valverde M, Herrera LA, Altamirano-Lozano M, Ostrosky-Wegman P (1996) Genotoxicity of vanadium pentoxide evaluated by the single cell gel electrophoresis assay in human lymphocytes. Mutat Res 359:77–84
90. Ramirez P, Eastmond DA, Laclette JP, Ostrosky-Wegman P (1997) Disruption of microtubule assembly and spindle formation as a mechanism for the induction of aneuploid cells by sodium arsenite and vanadium pentoxide. Mutat Res 386:291–298
91. Ivancsits S, Pilger A, Diem E, Schaffer A, Rudiger HW (2002) Vanadate induces DNA strand breaks in cultured human fibroblasts at doses relevant to occupational exposure. Mutat Res 519:25–35
92. Ciranni R, Antonetti M, Migliore L (1995) Vanadium salts induce cytogenetic effects in in vivo treated mice. Mutat Res 343:53–60
93. Altamirano-Lozano M, Valverde M, Alvarez-Barrera L, Rojas E (1996) Reprotoxic and genotoxic studies of vanadium pentoxide in male mice. Teratog Carcinog Mutagen 16:7–17

94. Mailhes JB, Hilliard C, Fuseler JW, London SN (2003) Vanadate, an inhibitor of tyrosine phosphatases, induced premature anaphase in oocytes and aneuploidy and polyploidy in mouse bone marrow cells. Mutat Res 538:101–107
95. Villani P, Cordelli E, Leopardi P, Siniscalchi E, Veschetti E, Fresegna AM, Crebelli R (2007) Evaluation of genotoxicity of oral exposure to tetravalent vanadium in vivo. Toxicol Lett 170:11–18
96. Sakurai H (1994) Vanadium distribution in rats and DNA cleavage by vanadyl complex: implication for vanadium toxicity and biological effects. Environ Health Perspect 102:1–4
97. Barceloux DG (1999) Vanadium. J Toxicol Clin Toxicol 37:265–278

Chapter 8
Vanadium in Cancer Prevention

Subhadeep Das, Mary Chatterjee, Muthumani Janarthan, Hari Ramachandran, and Malay Chatterjee

Abstract The pharmacological role of vanadium in health and disease remains one of the fascinating stories in biology. Recent studies have established vanadium as a novel regulator in assessing physiological and biochemical states of the animals. Vanadium exhibits biphasic effect, essentiality at low concentrations (0.05 μM) and toxicity at high doses (>10 μM). Vanadium inhibits growth of transformed cancer cells in culture. Various laboratories have confirmed the antitumorigenic potential of vanadium in liver, breast and colon cancer in vivo and various human cancer epithelial cell lines in vitro. Antiproliferative and induction of apoptosis may be the major mechanism of vanadium mediated inhibitions of cancer. Vanadium can play a central role in modulating phosphorylation states of various proteins in the cell and can affect many cellular processes regulated by cyclic AMP. In human vanadium is of interest pharmacologically but confirmation to its essentiality will require more significant information from experimental, clinical and epidemiological studies.

Keywords Vanadium • Cancer • DNA damage • Antiproliferative • Key regulator

S. Das • M. Chatterjee • M. Janarthan • M. Chatterjee (✉)
Chemical Carcinogenesis and Chemoprevention Laboratory, Department of Pharmaceutical Technology, Jadavpur University, Kolkata 700 032, West Bengal, India
e-mail: subhadeepdasfaea@gmail.com; mary.chatterjee@gmail.com; janarthan_mpharm@yahoo.co.in; mcbiochem@yahoo.com

H. Ramachandran
Department of Surgery, Columbia University, 17-401, 630W, 168th street, New York 10032, USA
e-mail: 2harikar@gmail.com

H. Michibata (ed.), *Vanadium: Biochemical and Molecular Biological Approaches*,
DOI 10.1007/978-94-007-0913-3_8, © Springer Science+Business Media B.V. 2012

8.1 Introduction

In present times, cancer is considered as one of the most fatal threats against civilization. At the late period of nineteenth century, a venture was pioneered by Dr. Stephen Paget in order to understand the underlying mechanism of metastasis [1] so as to develop a therapeutic to be used against cancer. From that very date, researchers and scientists have been engaged in enriching our machineries against cancer. Studies undertaken in the last three decades suggest that the dietary micronutrient vanadium could be a promising arsenal against cancer. At the beginning of nineteenth century the soft, ductile, silver-grey, nonplatinum group transition metal was introduced to us by Andres Del Rio and Nils Sefstorm separately [2]. Almost after 200 years of its discovery, it was found that various marine species have this metal as essential micronutrient [3]. This fact influenced nutritionists to consider vanadium as a dietary micronutrient. Vanadium has been documented in the list of 40 essential micronutrients and is required in trace amount for normal metabolism, proper growth and development of mammals [4]. Vanadium deficiency in nutrition results in growth inhibition, metabolism of thyroid and bones, disorders of generative function, disturbances of lipids and carbohydrate metabolic pathways [3–5]. Increased abortion and peritoneal death rates, growth impairment of tooth, bone and cartilage, decreased milk production during lactation [6], hepatic lipid and phospholipid changes [7], nutritional oedema [8] are usual physiological consequences of vanadium deficiency. Various dietary sources have been considered as the major source of exposure to vanadium for human population though it is present in very low concentration in diets (<1 ng/g) [9]. Vegetables like mushroom, dill seed, parsley, black pepper and foods like cereals, fresh fruits, shellfish are the common dietary sources enriched in vanadium [9–11]. Its intracellular concentration is approximately 20–200 nM. Vanadium is mostly accumulated in bone, kidney, spleen, liver, lung and blood [12]. Though this widely distributed but low abundant element is available in six oxidation states (-1, 0, $+2$, $+3$, $+4$ and $+5$); only $+4$ (vanadyl; VO^{2+}) and $+5$ (vanadate; $H_2VO_4^-$) are physiologically relevant [13, 14]. The pharmacological potentiality of this dietary micronutrient was initially exploited in the treatment of diabetes. Most of the vanadium salts like sodium metavanadate, sodium orthovanadate, vanadyl sulphate are orally administered to the individuals in insulin therapy which give them advantages over their predecessors [15]. Among the other pharmacological activities diuretic action, antiobesity, antihypertension, antihyperlipidemia, enhancement of oxygen affinity are needed to be mentioned [2]. Almost 50 years earlier the first attempt to exploit the pharmacological potentiality of vanadium in anticancer research was made [16]. This was just the opening of an avenue in cancer research. Later on, Thompson and his co-workers studied the chemopreventive effect of vanadium on 1-methyl-1-nitrosourea induced mammary cancer model in rats [17]. Antineoplastic effects of vanadium salts were established against rat liver tumors [18], fluid and solid Ehrlich ascites tumors [19], TA3Ha murine mammary carcinoma [20]. Some peroxovanadates have shown their inhibitory effects against

certain forms of leukemia. But we have to remember that the role of vanadium is not throughout beneficiary in cancer research, it has some detrimental role in the modulation of carcinogenesis. Being accumulated in considerably high amount vanadium may be responsible for haematological and biochemical alteration, renal toxicity, immunotoxicology and reproductive effect. The story of vanadium in the last three decades has shown its positive and negative sides, and thus gives rise to apparent controversies whether the dietary micronutrient could be a promising therapeutic against cancer. The story has its ups and downs and could be named as "The rise and fall of vanadium".

8.2 Physicochemical Properties of Vanadium

Vanadium, chemically classified as transition element, was placed in the fourth period of the VB group in the periodic table. The element is available in six oxidation states, namely −1, 0, +2, +3, +4, +5. Among these oxidation states, vanadic form (+3), vanadyl form (+4) and vanadate form (+5) are the most common [21]. Vanadium mainly occurs in uranium mines and is a constituent of titaniferous magnetites [22, 23]. In fossil fuels such as crude oil, coal, carbonaceous fossils vanadium present as a major trace element [21, 24]. Among the physiologically relevant form of vanadium, +4 (vanadyl) is the most stable form. But in presence of oxidizing agents, i.e. in oxygenated blood vanadium preferably exhibits its +5 oxidation state [25]. Vanadium can inhibit a number of enzymes. There are also a variety of enzymes which are stimulated by vanadium [26, 27]. The enzymes inhibited by vanadium include Na-K-ATPase, H-K-ATPase, phosphoenzyme ion-transport ATPase, myosine ATPase, dynein, adenylate kinase, phosphofructokinase, choline esterase. On the other side, glyceraldehyde-3-phosphate dehydrogenase, lipoprotein lipase, tyrosine phosphorylase, glucose-6-phosphate dehydrogenase, glycogen synthase, adenylate cyclase, cytochrome oxidase [28, 29] are stimulated by its action.

8.3 Pharmacology of Vanadium

At the turn of nineteenth century, some French physicians employed vanadium as a cure-all for ailments such as anaemia, diabetes, tuberculosis and chronic rheumatism [4]. Pharmacological exploitations have since been experiencing a current resurgence in these areas of research. Vanadium as vanadate in the cell has been proven to have specific role in the regulation of many enzymatic activities [30, 31], in generation of free radicals [32, 33], phosphorylation and dephosphorylation of proteins [34, 35]. Vanadium, the well-known prooxidant oxidises NADH and other intracellular reducing agents and generates active reducing form [36]. Tyrosine phosphorylation of a variety of cellular proteins is likely modulated by vanadium

through inhibition of protein tyrosine phosphatases. It also inhibits dephosphorylation of inositol phosphatases [37]. On the basis of its nutritional significance, physicochemical properties, distribution in tissues, it has been considered as a potent physiological regulator of the Na^+-K^+ pump [38, 39]. Vanadium as vanadate can mimic and potentiate the effect of growth factors like insulin [40], epidermal growth factor (EGF) on intact cells [41, 42]. Its insulinomimetic properties and its possible role in the alleviation of diabetic symptoms is one of the most prominent research interests. Vanadium, in vivo has been shown to exert insulin-like effects on transport, glucose oxidation, potassium uptake as well as on the activity of glycogen synthase in an isolated rat adipocytes and skeletal muscle [43]. By regulating the activity of secondary messengers, it can affect signal transduction in the cell. By activating PLC-coupled G-protein, vanadate stimulates consequently IP_3 synthesis in different cells [44, 45]. Increase in IP_3 levels leads to mobilization of Ca^{2+} from intracellular stores and the subsequent increase in intracellular Ca^{2+} level. This phenomenon is important in the stimulation of many cellular processes but excess Ca^{2+} can also be toxic [46]. Activation of adenylate cyclase by vanadium leads to increased cAMP level [47] but inhibition of cAMP production by vanadate and absence of effect on cAMP level were also described [48]. Thus vanadium can modulate many cAMP regulated cellular processes. On carbohydrate metabolism the effect of vanadium can be related to the reduction of the plasmatic glucose concentration. The vanadate ion stimulates 2,6-biphosphate fructose formation which influences the hormonal regulation of glycolysis and gluconeogenesis in liver [49]. The most important pharmacological significance of vanadium lies in glucose metabolism [50], lipoprotein lipase (LPL) activity [51], vanadate-dependent NADH oxidations-reductions [52], growth of red blood cells, adenylate cyclase activity and amino acid transport [53]. Vanadium at a low concentration takes a significant role in the modification of DNA synthesis and repair, but it appears cytotoxic at higher doses [21, 54]. The finding of unique properties of this inorganic micronutrient and its complexes may contribute in the maintenance of human health and development of therapy for the prevention of cancer.

8.4 *In Vivo* and *In Vitro* Studies

8.4.1 Breast

Fluid Ehrlich ascites tumor (EAT) appears as a spontaneous breast carcinoma in mice. Kopf-Maier and his group have established, among a group of metallocene dichloride, vanadocene dichloride (VDC) is capable of significant reduction of cell proliferation at very low concentration ($5–10 \times 10^{-6}$ mol/l) [55]. The antitumor activity of VDC against fluid EAT is reflected by accumulation in the nuclear heterochromatin [56], induction of mitotic aberration [57], transient suppression of mitosis, reversible cell accumulation in the late S and G_2 phase [58]. Vanadium

(IV) complex of 2-methylaminopyridine have been found to have similar activities on EAC cells like superoxide dismutase (SOD). M. M. El-Nagger et al. studied the antineoplastic effects of these complexes by intraperitonally administering them to Swiss albino mice infected with EAC cells. The value of EAC cells and EAC cell viability were found to be effectively decreased. Not only that, but activities of glutathione peroxide (GSH-Px) and glutathione reductase (GSH-R) also lowered along with significant elevation in the activities of SOD and glucose-6-phosphate dehydrogenase (G6PD) in Vanadium (IV) complex-treated mice [59]. A series of bisperoxovanadium compounds has been tested against DA3 murine mammary tumor model, in vivo. These compounds have also shown their efficacy against a panel of cell lines like MCF-7, NIH ADR, MB-231, MB-468 in vitro [60]. Metavan [bis(4,7-dimethyl-1,10-phenanthroline)sulfatooxovanadium] has been employed in the treatment of severe combined immunodeficient mouse xenograft models of human malignant glioblastoma and breast cancer and has been found to delay tumor progression, exhibit significant antitumor activity and prolong survival time [61]. In another study, it has been observed that vanadocene dichloride (VDC) and vanadocene acetylacetonate (VDacac) are effective chemical therapeutics against proliferation of glioblastoma cell lines and human mammary cancer cell lines. In a dose-dependent study VDC has been found to inhibit cell proliferation of BT-20 (breast cancer cell line), U373 (glioblastoma cell lines). The mechanistic study revealed that human cancer cell division is blocked by this organometallics through disruption of bipolar spindle formation [62].

In our laboratory, we have established the fact that the dietary supplementation of ammonium monovanadate in drinking water (0.5 ppm) causes significant reduction in tumor incidence, total number, multiplicity, size of the tumor cells in DMBA induced rat mammary carcinogenesis model [63]. Liver is the major organ for DMBA activation and detoxification [64]. This earlier information helps us to understand the underlying mechanism of anticarcinogenicity of vanadium. It acts through elevation of glutathione (GSH), glutathione-S-transferase (GST), cytochrome P450 (CYP) as well as inhibition of superoxide dismutase (SOD) and hepatic lipid peroxidation, indicating alteration of hepatic antioxidants along with phase I and phase II drug metabolizing enzymes. Later, in another study we have showed that only the mammary preneoplastic cells are sensitive to vanadium treatment, rather than the normal proliferating cells [65]. The additional information provided by this study was in connection with DNA repair through reduction of DNA protein cross-links, cell proliferation and induction of apoptosis. In a similar study, reduced metallothionein expression was observed immunohistochemically. Vanadium treatment slows down the hyperplasia occurrence and thus due to increased latency period delays the tumor appearance [66]. In another similar type of experiments, the effect of vanadium on DNA chain break was studied. In compare to DMBA control group, the DMBA+vanadium treated one gives almost 61% protection against single strand breaks. Vanadium (6.25 μM) imparts 62.9% protection against chromosomal aberration to DMBA induced cells [67]. The apoptogenicity of vanadium (100, 175, 250 μM) against human cancer cell line MCF-7 was studied by Chatterjee et al. through TUNEL assay and they confirmed

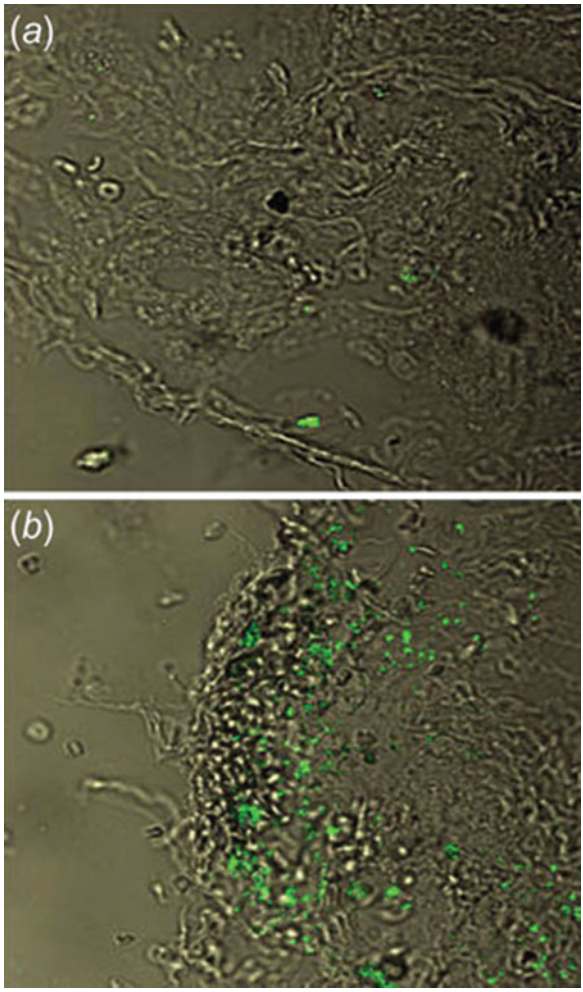

Fig. 8.1 Immunofluorescent localization of p53 in the mammary tissue of rats. p53 antibody was used at 1:100 dilution. (**a**) DMBA control (i.e., *group B*) stains very weakly for p53 and (**b**) DMBA with vanadium (i.e., *group C*) stains strongly for p53. Original magnification, ×100

that MCF-7 cells on vanadium treatment was likely to be apoptotic, rather than necrotic due to the presence of prominent apoptotic bodies [68]. Downregulation of Bcl2 and upregulation of p53 (Fig. 8.1), Bax are responsible for inhibition of cell proliferation and induction of apoptosis in vanadium treated DMBA induced rat mammary carcinogenesis (Fig. 8.2) [69].

8.4.2 Liver

The idea of considering vanadium as an effective chemopreventive agent against chemically induced hepatocellular carcinogenesis came from several studies. In our

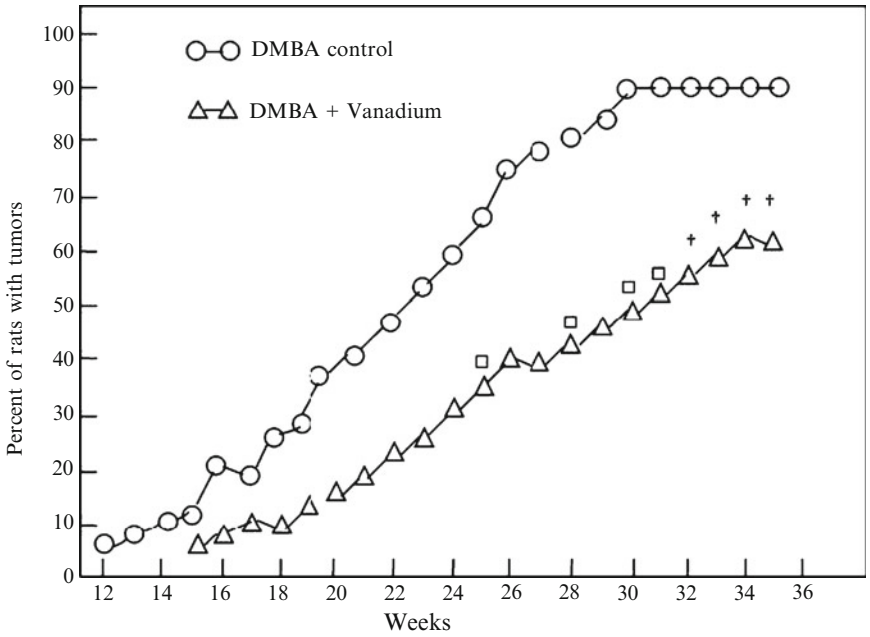

Fig. 8.2 Cumulative incidence of palpable mammary tumors (adenocarcinomas) in DMBA control (*group B*) as well as vanadium supplemented DMBA group (*group C*). DMBA was given to rats at 50 days of age at a dose of 0.5 mg per 100 g body weight via the tail vein. Ten animals were sacrificed for each time point following DMBA injection. Supplementation of vanadium in drinking water was started immediately after the carcinogen treatment and it continued for 35 weeks. □$p < 0.001$ and †$p < 0.05$ compared with the DMBA control (*group B*) by Fischer's exact probability test

laboratory we have studied the enhancement of activity of glutathione-s-transferase on oral administration of vanadium in a dose depended manner (100, 200, 400 nM for 30 days) in rat liver, kidney, small and large intestine mucosa. Moreover, this enhancement of enzyme activity is not associated with hepatic or renal toxicity as evidenced by glutamic pyruvic transaminase, serum glutamic oxaloacetate transaminase [70]. Some peroxovanadium compounds [bpv(Me_2Phen), bpv(OHpic)] have shown to be effective PTP inhibitors by Barry et al. [71]. In diethylnitrosamine induced hepatocarcinogenesis model of male Sprague-Dawley rats, supplementary vanadium (ammonium monovanadate) was given (0.5 ppm) to study its anticarcinogenicity. The vanadium treated group was found to have reduced incidence, number, multiplicity of hepatocytic nodules with respect to carcinogen induced group. Vanadium treated group also found to contain decreased number of altered liver cell foci (Table 8.1) [72]. In a phenobarbital promoted DENA induced hepatocarcinogenesis model of rats, supplementary vanadium has been proved to be potential therapeutic. The treatment group was appeared to have a decreased number of surface area of GGT-positive hepatocellular foci along with altered size distribution of visible persistent nodules [18]. In a similar study, it has been observed that DENA has

Table 8.1 Effect of vanadium supplementation (0.5 ppm) on the development persistent nodules in livers of rat initiated with DENA and promoted by PB

Group	No. of rats with nodules per total no. of rats	Nodule incidence (%)	Total no. of nodules	Average no. of nodules per nodule – bearing liver (nodule multiplicity)
A (carcinogen control)	10/10	100	383	38.3 ± 5.8[a]
C (carcinogen + vanadium for 20 weeks)	5/12	41.6[b]	52	10.4 ± 2.7[c]
E (vanadium treatment for 4 weeks before initiation)	7/12	58.3	136	19.4 ± 3.8[d]
G (vanadium supplementation 1 week after initiation and continued upto 20 weeks)	8/11	72.7	241	30.1 ± 4.7

[a]Each value represents the mean ± s.e.
[b]$P < 0.01$ as compared with group A by Fischer's exact probability test
[c]$P < 0.001$ as compared with group A
[d]$P < 0.02$

affected hematocrit value, RBC count, total WBC count, haemoglobin content with respect to normal. This adverse effect was found to be reversed in vanadium supplemented group. It also lowered plasma globulin content, prevented depletion of the plasma albumin concentration and thereby increased albumin to globulin ratio [73]. In order to find out a plausible mechanism of anticarcinogenic property of vanadium, it has been found that though it is not capable of altering the activities of hepatic phase I enzymes but of phase II ones like hydrocarbon hydroxylase, cytochrome P45062E1 (CYP2E1), UDP-glucoronyl transferase (UDPGT) [74, 75]. Chatterjee et al. further investigated the chemopreventive effects of vanadium in combination with vitamin D_3 against DENA – induced rat hepatocarcinogenesis model. Vitamin D_3 and vanadium in combination have been found to impart maximum protection against DENA-induced chromosomal aberrations and DNA strand breaks [76]. In another study their combinatorial effects reduced the number and area of placental glutathione-s-transferase positive altered hepatocyte foci (AHF) and nodules [77]. In the elevation of hepatic microsomal cytochrome P-450(Cyt. P-450), the combinatorial effect of vitamin D_3 and vanadium was found to be more efficient in contrast to their single effect. Furthermore, the combination also found to have significant role in reduction of GGT positive foci, cytosolic glutathione and glutathione-s-transferase (GST) [78]. A group of scientist from Poland synthesized V^{3+} complexes of cysteine, alanine and aspartic acid and exploited against hepatoma Morris 5123 cell lines. The probable route to cancer

cell death was assumed to be apoptotic [79, 80]. In a study conducted by our laboratory indicated sister chromatid co-efficient has significantly been reduced on vanadium supplementation through drinking water in a 2-acetylaminofluorene (2-AAF) induced rat hepatocarcinogenesis model [81]. The combined effect of vanadium and β-carotene has also been studied on DENA-PB induced rat liver carcinogenesis. In combination they imparted an additive effect in reduction of the expression of GST-positive AHF, the no. and size of hyperplastic nodules [82]. Vanadium has shown its anticlastogenic potentiality through inhibition of early hepatic cells. In addition, the GGT and PCNA expression were significantly reduced [83]. Later studies confirmed that the rise in the level of DNA base 8-OHdG, metallothionein, and trace elements in DENA-PB induced carcinogenesis and their significant reduction in vanadium supplemented group [84]. In another study from our laboratory, the elevation in the level of biomarkers like GGT positive foci, glycogen foci, PCNA, genotoxic DNA damage were investigated in chemically induced rat hepatocarcinogenesis and were found to be significantly lowered on vanadium treatment [85]. The anticlastogenic potential of this dietary micronutrient was established in a study where the formation of CA, SSB, DPC and tissue specific 8-OHdG are found to be inhibited by this dietary supplement [86]. The chemopreventive role of vanadium at the initiation stage of chemically induced hepatocarcinogenesis was investigated by the same author from our laboratory. The study confirmed that vanadium is capable of in limiting early molecular events and preneoplastic lesions through inhibition of DNA adduct and prevention of oxidative DNA damage in early stage of neoplasia [87]. In the expression of premalignant phenotype of the cell, metallothionein overexpression, DNA-protein crosses links, cell proliferation are found to have implicative role in rat liver preneoplasia. Vanadium as a chemopreventive agent has been found to have noteworthy impact on reduction of DPCs, CAs and MT immunoreactivity [88]. Dietary supplementation of vanadium is studied to have significant role on inhibition of formation 8-OHdG, DNA chain break along with in limiting cell proliferation in the initiation stage of neoplastic development in a two-stage (DENA-PB induced) hepatocarcinogenesis models [89]. In an in vitro study Na_2VO_3 has been established most effective against progressive growth of rat hepatoma H35-19 cells [90].

8.4.3 Colon

Colon cancer is one of most common type of epithelial malignancies [91]. Chemically induced rat colon carcinogenesis model has been studied several times in order to understand the chemopreventive effect of vanadium in this regard. In an earlier study vanadate, the potent mitogen was fed to 1,2-dimethylhydrazine induced mice colon carcinogenesis model. Vanadate at a concentration manner (10 or 20 ppm) was observed to elevate thymidine incorporation. But, it remains surprising non-influential in the development of large bowel tumors in DMH-treated

mice [92]. In our laboratory, we have carried out an investigation to establish the chemopreventive role of vanadium on DMH-treated colon carcinogenesis model in rats. We have observed that vanadium supplemented group (ammonium monovanadate, 0.5 ppm) contained reduced number of aberrant crypt foci (ACF), few colonic carcinomas and adenomas in contrast to only DMH-treated individuals. In addition, vanadium on one hand, elevated cyt p-450, liver GST activities, on other hand lowered PCNA index in ACF [93]. The study was further extended where we have seen the inhibitory effect of vanadium on the overexpression of GST-P positive foci. Additionally SOD activities in both liver and colon were found to be elevated upon vanadium treatment [94]. In another study it has been shown that the vanadium supplementation in drinking water significantly reduced the extent of DNA damage and chromosomal aberrations in colon cells, along with the activities of glutathione reductase and catalase [95]. The inhibitory effect of vanadium on DNA-protein cross-link and surface levels changes of ACF was well established in an in vivo study from our laboratory [96].

The individual PTP inhibitors orthovanadate and bpV(Phen) completely abrogated both the adenosine suppression of ERK1/2 activation and downregulation of cells surface DPPIV on HT-29 colon cancer cells [97]. In an in vitro study, synthesized VOHesp complex has exhibited its anticarcinogenicity against human colon carcinoma cell line Caco-2. The antioxidant activity of hesperidin complex has been enhanced in VOHesp as it became a better SOD mimic [98]. The fact that vanadium is an effective chemopreventive agent against DMH-induced rat colon carcinogenesis model is well established. Further studies have been performed to investigate the mechanism of its action of chemoprevention. O^6 – methylguanine (O^6-Meg) is a potent mutagen in DMH-induced colon cancer. Upon treatment with vanadium, the DNA adducts, O^6-Meg formation has significantly been lowered in contrast to the DMH-treated rats. Nuclear immunoexpression of p53 in vanadium treated group in compare to the extranuclear, random, irregular overexpression of p53 in DMH-control group supports for inhibitory effects of vanadium. Moreover an effective positive correlation between AI & p53 expression was observed in vanadium treated group rather than DMH-control one and iNOS mRNA expression has also significantly been reduced (Fig. 8.3) in vanadium supplemented group [99]. Vitamin D_3 is a well studied carcinogen inhibitor. Investigation was carried out in our laboratory to study the combinatorial effect of vitamin D_3 and vanadium in carcinogen induced rat colon cancer model. Fewer BrdU positive cells in vitamin D_3 and vanadium treated group (Group B, C and D) shows (Fig. 8.4) reduced BrdU immunopositivity when their carcinogen assaulted counterpart come in comparison. Vanadium and vitamin D_3 in combination has been established as effective inhibitor of colonic O^6 -Meg formation (HPLC fluorescence assay). Their combinatorial effect against DNA strand break also needs to be mentioned. The duo on one hand inhibits cell proliferation by downregulating antiapoptotic protein Bcl2 (Fig. 8.5) on the other hand it triggers apoptosis via elevation of p53 immunoexpression [100].

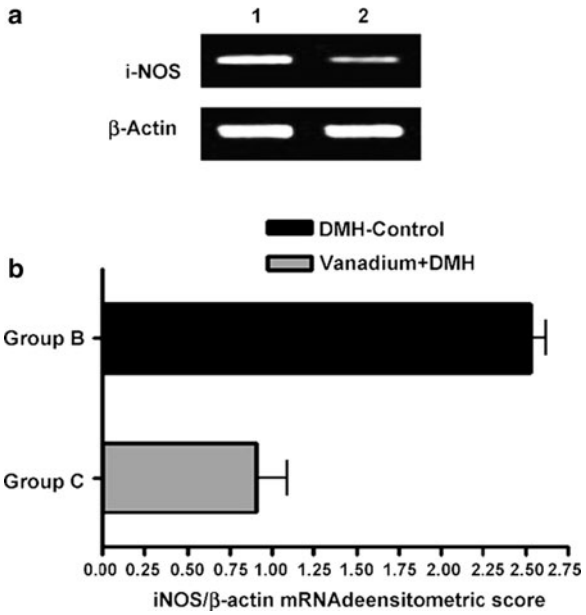

Fig. 8.3 RT-PCR analysis of iNOS mRNA expression in colon tumors. (**a**) RTPCR analysis of 30 cycles showing the representative blots of iNOS mRNA transcripts (*upper bands*) and _-actin mRNA transcripts (*lower bands*) in colonic tumor tissues from DMH control (*lane 1*) and vanadium treated (*lane 2*) animals. (**b**) Densitometric quantitaions of the agarose gel band is presented as a bar diagram, and the band intensities represented in the form of ratio of densitomentric scores (iNOS/_-actin). Mean ratio and S.E. were calculated from the signal obtained from ten different samples in each group. iNOS mRNA levels (iNOS mRNA/_-actin mRNA) were significantly lowered in vanadium treated group (*group C*) than that of DMH controls (*group B*) ($P < 0.001$)

8.4.4 Prostate

Metavan, a most potent anticancer, multitargated vanadium complex, has been passed successfully against tumor cells derived from prostate cancer patients [61] Sodium orthovanadate (Na_3VO_3) and vanadylsulphate ($VOSO_4$) have been exploited successfully against human prostate (DU145) cancer cell line in a dose dependent manner. It has been suggested that vanadium as a pro-apoptotic factor affects the protein kinase activities through inhibition of phosphatases [101, 102].

8.4.5 Lung

Inhibitory effect of sodium orthovanadate against human epithelial A549 cancer cell line has been established by Klein et al. in an in vitro study [102]. Vanadium (III) –L-cysteine compound like [VIII$(Hcys)_3$]. 2HCL.2.5H_2O has been studied by a group of scientist in order to evaluate its antimetastatic effect against 3,4-benzopyrene treated Wistar rats [103].

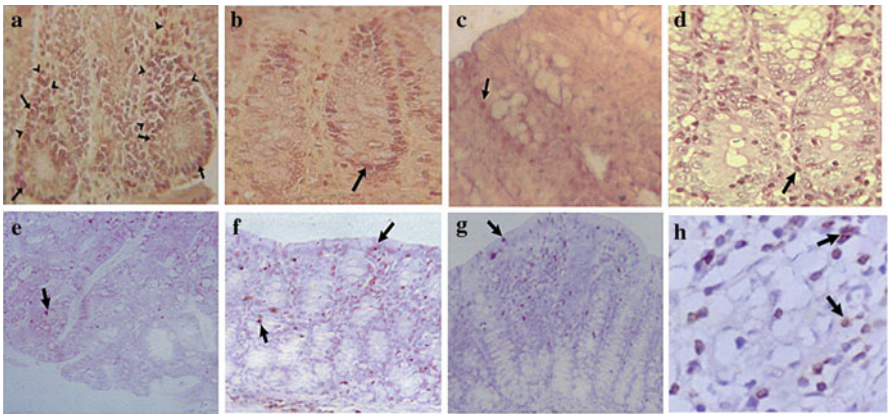

Fig. 8.4 Representative immunohistochemistry pictures of BrdU labeled cell proliferation and TUNEL positive apoptotic cells in colon tissues of rats in presence or absence of Vanadium (V) and/or 1, 25-dihydroxy-vitamin D_3 (Vitamin D_3). Brown-stained (*arrow*) cells are undergoing cell proliferation (**a**, **b**, **c**, **d**) or apoptosis (**e**, **f**, **g**, **h**). Approximately 50 crypt columns per site per animal were randomly chosen and 10 rats were examined per group. (**a**) (100×) represents DMH control group. Highly proliferative zones are marked by arrowhead; (**b**, **c**, **d**) (100×) respectively represents V-treated (*Group B*), vitamin D_3 treated (*Group C*) and V+Vitamin D_3 treated (*Group D*) DMH group. (**e**) (40×) represents DMH control group with few TUNEL positive cells in colonic crypts. (**f**, **g**) (40×) and (**h**) (150×) respectively show colonic crypts with TUNEL positive cells from V, Vitamin D_3 and V+Vitamin D_3 treated group

8.4.6 Pancreas

Vanadate with somatostatin causes dephosphorylation of membrane proteins through inhibition of epidermal growth factor(EGF). This may be the probable mechanism of inhibitory effect of human pancreatic cancer cell as evidenced in MIA PaCa-2 cell line [104].

8.4.7 Bone

Most of the vanadium we intake is accumulated in our bone which generate a concept of using vanadium in the treatment of bone tumor metastasis. Vanadium(IV) being complexed with aspirin using poly(β-propiolactone) as delivery system has been successfully used against UMR106 osteosarcoma cells to investigate its antineoplasticity [105]. Cytotoxity of other vanadyl and pervanadate has been evaluated against osteoblast (MC3T3E1) and osteosarcoma (UMR106) cell line in vitro [106]. Vanadium in a dose dependent manner induces ROS formation, cytotoxicity and thiobarbituric acid reactive substances (TBARS) formation in the

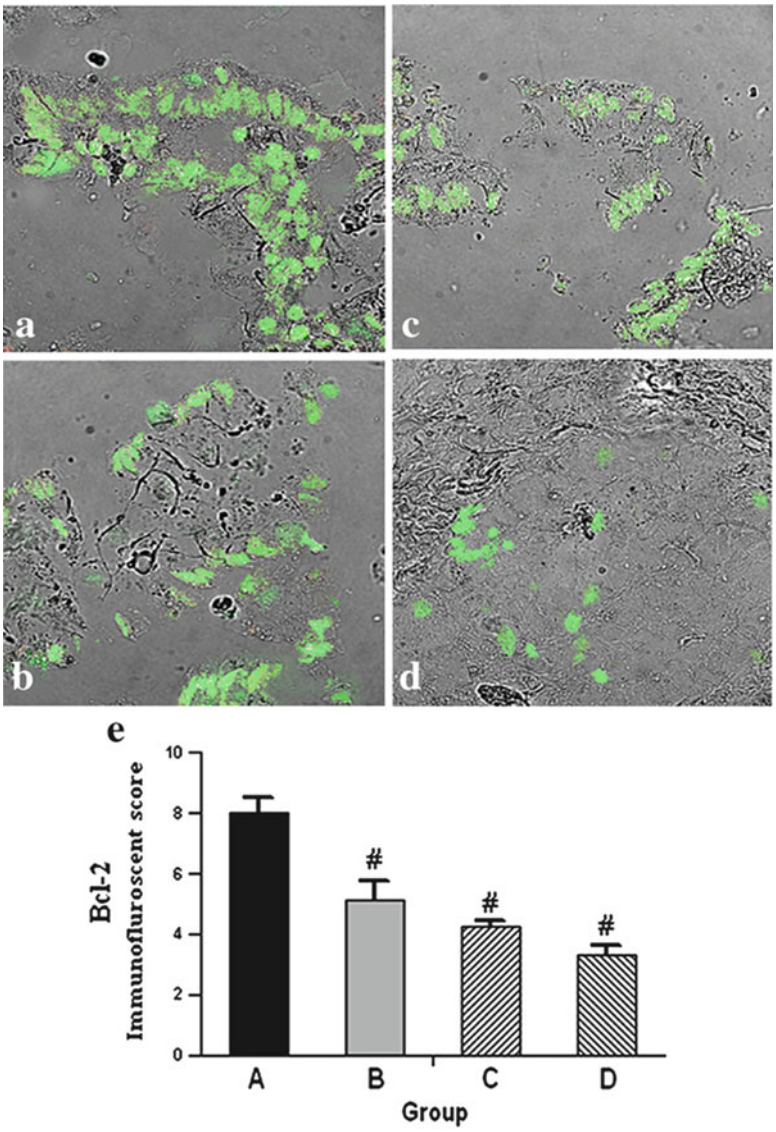

Fig. 8.5 Bcl-2 immunofluorescence in colon tissues of rats. (**a**, **b**, **c**, **d**) Immunofluorescent localization of Bcl-2. Bcl-2 antibody was used at 1:400 dilutions. (**a**) DMH control (*Group A*) stains very strongly for Bcl-2 and (**b**, **c**, **d**) DMH with vanadium (V) and/or 1, 25- dihydroxy-vitamin D3 (Vitamin D3) (*Group B*, *C*, *D*) stains weakly for Bcl-2 with a gradual decrease of expression in V+DMH (**b**), Vitamin D3 + DMH (**c**) and V+Vitamin D3 + DMH (**d**) treated group respectively. Original magnification, ×200. (**e**) Graph represents Bcl-2 immunofluorescent score in DMH challenged colon tissues in presence or absence of vanadium and/or vitamin D3. Each bar represents the mean value ± S.E calculated from 8 slides/rat and 10 rats/group. #Pb0.001 when compared to DMH control group

concerned cells. In a recent study, the fact has been established that the key events of tumorigenesis, cell adhesion, migration and clonogenicity have been inhibited by TreVo, GluVo in UMR106 osteosarcoma cells [107].

8.5 Epidemiological Study

Fallico et al. carried out a longitudinal retrospective case-control study on the populations of the Etna massif as a consequence of vanadium assimilation through diet and its effects on diabetes mellitus, heart arrhythmia, renal lithiasis and arterial hypertension. They hypothesized that vanadium has a protective role on the mentioned pathologies. It was observed in this study that the healthy controls have turned out to have higher concentrations of V in the blood and urine compared to the cases. Further and more longitudinal studies are needed on representative groups to verify and confirm their hypothesis [108]. A team led by Jaroslav Lener have performed a 3-year follow-up of some indicators like hematological and cytogenetic status, cellular and specific immunity, sperm lipids level in some school children (10–12 years) exposed to vanadium pentoxide emission from metallurgical plant in their vicinity. The finding is long-term exposure to vanadium emissions had no negative impact on their health. Furthermore, significant higher values of T-lymphocyte mitotic activity in children from immediate proximity of the plant producing vanadium indicated that vanadium have an elevated activity of cellular immunity [109].

8.6 Mechanisms of Action

Micronutrients like vitamin D, lycopene, folate, calcium are currently undergoing clinical trials to investigate their pharmacological potentiality [110]. Selenium is the most evidenced inorganic nutrient which has happened to be a promising chemopreventive agent. Although, less known than selenium, vanadium is gaining importance for its potential chemopreventive effects [111]. Cancer morbidity and mortality were reduced when vanadium in its various forms placed in the diets of the experimental model [17, 72, 73]. Daily supplementation of $VOSO_4$ (25 ppm) in diet inhibited induction of mammary carcinogenesis in experimental model and reduced both the number of cancer incidences and average number of tumors [72]. Further studies have shown its inhibitory effect on DMBA, DENA and DMH induced carcinogenesis. But, very scanty mechanistic data of its chemopreventive properties against cancer over a large population area is available. The well-known biochemical effect of vanadium elevation is decreased lipid peroxidation leading to an increase in oxidative protection processes [63]. The other mentionable biochemical activities are elevated cytochrome P450 expression, increased glutathione level and glutathione-S-transferase activity, lowered superoxide dismutase activity and last but not the least, elevation of Phase II conjugated enzymes; UDP-glucose

dehydrogenase, UDP-glucoronyl transferase [63, 74, 112]. Possibly, it also elevated the detoxifying enzyme activities. Due to presence of structural similarity to PO_4^{3-}, VO_4^{3-} interacted with phosphate processing enzymes and participated in metabolic pathways of carbohydrates and lipids. All these together highlighted the beneficial activity of vanadium.

Vanadium supplementation in diets of chemically induced carcinogenesis model is a result of minimized DNA instability – evidenced from a number of studies. But, no suggested mechanisms account for the decreased DNA alkylation. Vanadium predominates as oxoanions (VO_4^{3-}) in aqueous solution [113–115] and thus exhibit nucleophilic character which in turn attack the electrophilic alkylating agent. The ability of vanadium salts in the inhibition of DNA damage, when subjected to an alkylating assault was demonstrated by Wilker et al. The fact that oxospecies such as $V_3O_9^{3-}$ detoxified alkylating agent through hydrolysis to yield corresponding alcohols was revealed from NMR-spectroscopic analysis. For example, vanadates transformed ethyl iodide (CH_3CH_2I) and $(CH_3CH_2O)SO_2$ to ethanol (CH_3CH_2OH) [115].

It is evidenced that Na_3VO_4 gives greater protection to DNA alkylation than Na_3SeO_4. This is because VO_4^{3-} is a better nucleophile than SeO_4^{3-} due to presence of greater charge density. Vanadate brings equilibrium between various species, depending upon concentration, solution pH and oxygenation levels. We cannot say conclusively that this "carcinogen interception" mechanism exactly occur within cells. Only a significant interaction between inorganic species and alkylating carcinogens is discussed here.

Some other possible mechanisms proposed by the scientists are increased activity of phosphodiesterase [116], inhibition of protein phosphatases [117], or generation of reactive oxygen species and oxidative stress [118].

8.7 Toxicity vs. Beneficiary Action

Toxicity of vanadium compounds to the exposed groups depends on its dose, route of administration, time span of exposure and nature of the compound itself [2, 111]. A series of toxicity and pharmacokinetic studies have been performed on experimental animal models, but very scanty data are available on clinical studies and long-term effect on humans. In a clinical trial, the effect of $VOSO_4$ was studied in 31 weight training athletes. There was no significant effect of treatment on blood viscosity, hematological indices and biochemistry [119]. Oral administration of $NaVO_3$ has shown minimal side-effects like mild gastrointestinal intolerance [120]. Twelve healthy adults were orally administered vanadium (125 mg/day) in the form of diammonium vanadotartarate to investigate its effect on serum cholesterol effect. But, no changes in levels of serum cholesterol, lipoprotein pattern, haemoglobin, blood urea were observed [121]. Another study was performed to investigate the toxicity of ammonium vanadyltartarate administered orally to human subjects. Only cramps and diarrhea were observed where high-doses (4,325, 4,225 mg) were

given to them. No statistical changes occurred in triglycerides, cholesterol, blood lipids, phospholipids which is indicative of the absence of toxicity. Unpredictable vanadium absorption is suggested by varying amounts of vanadium excretion [122]. Oxytartarovanadate was administered at a level of 4.5 mg V/day for 16 months to patient, who showed no sign of toxicity throughout the study [123]. Vanadium is appeared to be more toxic when inhaled rather ingested. Vanadium pentoxide fume from several industries was proved to be causative agents of acute chemical pneumonitis, pulmonary oedema to acute tracheobronchitis [124]. In an epidemiological study, it has been established that inhalative exposure to vanadium pentoxide was responsible for DNA instability in workers from a vanadium pentoxide factory [125]. As an additional note, toxicity of vanadate and vanadyl salts was observed only at remarkably higher doses in compare to the usual amount ingested through diets. So it is evident, that under normal environmental and nutritional condition of exposure vanadium would not be hazardous to human health [5]. The effect of this transition metal on animal physiology and their individual response to the treatment might be influenced by plasma and cellular binding proteins (including catecholamines and glutathione), severity of diseases (including gastrointestinal and renal function), exercise, stress and genetic predisposition [126]. These factors would be accounted in determining proper dose, route and time of exposure of vanadium compounds in cancer treatment. Therapeutic advantage of oral administration, and available options for lessening toxicities warrant development of safe and effective pharmacological formulations.

8.8 Conclusions

An objective of this review has been to provide comprehensive picture of current biological, chemical and clinical research on vanadium. There is heightened need to draw together the numerous threads and present a coherent picture of the various research endeavors.

The present study demonstrates vanadium mediated inhibition of different forms of cancer and illustrates an emerging concept of chemoprevention through inhibition. Vanadium functions as an inhibitor of cancer through modulation of cell proliferation and apoptosis. Authors suggest that by induction of oxidative stress or inhibition of phosphatases. Ortho or metavanadates affects the activities of protein kinase which are adjusted during cell growth. An additional question is whether the antiproliferative effect of vanadium will allow employing such compounds as auxiliary drugs in certain types of cancer. The extensive use of this element together with its complex chemistry and the narrow threshold between essential and toxic doses makes it crucial to understand as much as possible about vanadium. Ultimate determination of essentiality for human will depend on the greater understanding of the fundamental biochemical roles of vanadium.

There is however no studies or reports on the pharmacokinetics of vanadium metabolism in human subject and thus additional studies are warranted to determine

the optimum effective dose of vanadium in inhibiting cancer in human. The need of the moment is to improve the experimental design, interpret the observed effect and encourage their use as templates for further development of more effective and safe chemopreventive compound.

The data summed up here add another layer to the already highly complex word of vanadium that could prove to have a stronger antitumor activity.

However we need to collect significant information from experimental, clinical, and epidemiological result before we support any public health recommendation. To do this we need more research and more exchanges within the scientific communities of basic and applied research disciplines.

Acknowledgement We thank Subrata Pramanik (M. Pharm.), Rohullah Roien (M. Pharm.) and Dr. Kaushik Roy for their continuous help and support for the preparation of the manuscript.

References

1. Paget S (1889) The distribution of secondary growths in cancer of the breast. Lancet 1: 571–573
2. Mukherjee B, Patra B, Mahapatra S et al (2004) Vanadium-an element of atypical biological significance. Toxicol Lett 150:135–143
3. Almedeida M, Filipe S, Hunianes M et al (2001) Vanadium haloperoxidases from brown algae of the Laminariaceae family. Photochemistry 57:633–642
4. French RJ, Jones PJ (1993) Role of vanadium in nutrition: metabolism, essentiality and dietary consideration. Life Sci 52:339–346
5. Domingo JL (1996) Vanadium: a review of the reproductive and developmental toxicology. Reprod Toxicol 10:175–182
6. Anke M, Groppel B, Kosla T et al (1986) New research on vanadium deficiency in ruminants. In: Anke M et al (eds) Supplement-symposium: new trace elements. Friedrich-Schiller-Universitat, Jena, pp 1266–1275
7. Menon AS, Rau M, Ramasarma T et al (1980) Vanadate inhibit mevalonate synthesis and activates NADH oxidation in microsomes. FEBS Lett 114:139–141
8. Golden MH, Golden BE (1981) Trace elements. Potential importance in human nutrition with particular reference to zinc and vanadium. Br Med Bull 37:31–36
9. Barceloux DG (1999) Vanadium. J Toxicol Clin Toxicol 37:265–278
10. Byrne AR, Kosta L (1978) Vanadium in foods and in human body fluids and tissues. Sci Total Environ 10:17–30
11. Badmaev V, Prakash S, Majeed M (1999) A review of its potential role in the fight against diabetes. J Altern Complement Med 5:273–291
12. Mongold JJ, Cros GH, Vian L et al (1990) Toxicological aspects of vanadyl sulphate on diabetic rats*:* effects on vanadium levels and pancreatic B-cell morphology. Pharmacol Toxicol 67:192–198
13. Philips TD, Nechay BR, Heidelbaugh ND (1983) Vanadium: chemistry and the kidney. Fed Proc 42:2969–2973
14. Nechay BR (1984) Mechanisms of actions of vanadium. Annu Rev Pharmacol Toxicol 24:501–524
15. Orvig C, Thompson KH, Battell M et al (1995) Vanadium compounds as insulin mimics. Met Ions Biol Syst 31:575–594

16. Kieler J, Gromek A, Nissen N (1965) Studies on the antineoplastic effect of vanadium salts. Acta Chir Scand Suppl 343:154–164
17. Thompson HJ, Chasten ND, Meeker LD (1984) Dietary vanadyl (IV) sulphate inhibits chemically-induced mammary carcinogenesis. Carcinogenesis 5:849–851
18. Bishayee A, Chatterjee M (1995) Inhibition of altered liver cell foci and persistent nodule growth by vanadium during diethylnitrosamine-induced hepatocarcinogenesis in rats. Anticancer Res 15:455–462
19. Harding MM, Mokdsi G (2000) Antitumor metallocenes: structure-activity studies and interactions with biomolecules. Curr Med Chem 7:1289–1303
20. Murthy MS, Rao LN, Kuo LY et al (2000) Antitumor and toxicologic properties of the organometallic anti-cancer agent vanadocene dichloride. Inorg Chem Acta 152:117–124
21. WHO (1988) Vanadium. Environmental Health Criteria No. 80. Geneva
22. Baroch EF (1983) Vanadium and vanadium alloys. In: Seidel A (ed) Encyclopedia of chemical technology, vol 23. Wiley, New York, pp 673–687
23. Rosenbaum JB (1983) Vanadium compounds. In: Seidel A (ed) Encyclopedia of chemical technology, vol 23. Wiley, New York, pp 688–704
24. Al-Swaidan HM (1993) Determination of vanadium and nickelin oil products from Saudi Arabia by inductively coupled plasma mass spectrometry (ICP/MS). Anal Lett 26:141–146
25. Crans DC (1998) Chemistry of relevance to vanadium in the environment. In: Nriagu JO (ed) Vanadium in the environment. Part 1: chemistry and biochemistry. Wiley, New York, pp 73–96
26. Dafnis E, Sabatini S (1994) Biochemistry and pathophysiology of vanadium. Nephron 67:133–143
27. Crans DC, Bunch RL, Theisen LA (1989) Interaction of race levels of vanadium (IV) and vanadium (V) in biological systems. J Am Chem Soc 111:7597–7607
28. Erdmann E, Werdan K, Krawietz W et al (1984) Vanadate and its significance in biochemistry and pharmacology. Biochem Pharmacol 33:945–950
29. Nechay BR, Nanninga LB, Nechay PSE et al (1986) Role of vanadium in biology. Fed Proc 45:123–132
30. Ueki H, Okuhama R, Gresser MJ et al (1988) Interaction of vanadate with uridine and adenosine monophosphate: formation of ADP and ATP analogues. J Am Chem Soc 110:5869–5874
31. Wenzel UO, Fouqueray B, Biswas P et al (1995) Activation of mesangial cells by the phosphatase inhibitor vanadate. J Clin Invest 95:1244–1252
32. Ding M, Gannett PM, Rojanasakul Y et al (1994) One-electron reduction of vanadate by ascorbate and related free radical generation at physiological pH. J Inorg Biochem 55: 101–112
33. Shi X, Wang P, Jiang H et al (1996) Vanadium (IV) causes 2′-deoxyguanosine hydroxylation and deoxyribonucleic acid damage via free radical reaction. Ann Clin Lab Sci 26:39–49
34. Imbert V, Peyron JF, Far F et al (1994) Induction of tyrosine phosphorylation and T-cell activation by vanadate peroxide, an inhibitor of protein tyrosine phosphatases. Biochem J 297:163–173
35. Yamaguchi M, Oishi H, Araki S et al (1995) Respiratory burst and tyrosine phosphorylation by vanadate. Arch Biochem Biophys 323:382–386
36. Kalyani P, Vijaya S, Ramasarma T (1992) Characterisation of oxygen free radicals generated during vanadate-stimulated NADH oxidation. Mol Cell Biochem 111:33–40
37. Bencherif M, Lukas RJ (1992) Vanadate amplifies receptor-mediated accumulation of inositol tris-and tetrakis phosphatase activities. Neurosci Lett 134:157–160
38. Cantley LC Jr, Cantley LG, Josephson L (1978) A characterisation of vanadate interactions with the (Na, K)-ATPase. Mechanistic and regulatory implications. J Biol Chem 253: 7361–7368
39. Cantley LC, Aisen P Jr (1979) The fate of cytoplasmatic vanadium implication on (Na, K)-ATPase inhibition. J Biol Chem 254:1781–1784
40. Brichard SM, Henquin JC (1995) The role of vanadium in the management of diabetes. Trends Pharmacol Sci 16:265–270

41. Macara IG (1986) Activation of $^{45}Ca^{2+}$ influx and $^{22}Na^{+}/H^{+}$ exchange by epidermal growth factor and vanadate in A431 cells is independent of phosphatidylinositol turnover and is inhibited by phorbol ester and diacylglycerol. J Biol Chem 261:9321–9327
42. Stern A, Yin X, Tsang S-S et al (1993) Vanadium as a modulator of cellular regulatory cascades and oncogene expression. Biochem Cell Biol 71:103–112
43. Roden M, Liener K, Fűrnsinn C et al (1993) Non-insulin like action of sodium orthovanadate in the isolated perfused liver of fed non-diabetic rats. Diabetologia 36:602–607
44. Tertrin-Clary C, DeLaLlosa-Hermier MP, Roy M et al (1992) Activation of phospholipase C by different effectors in rat placement cells. Cell Signal 4:727–732
45. Zick Y, Sagi-Eisenberg R (1990) A combination of hydrogen peroxide and vanadate concomitantly stimulates protein tyrosine phosphorylation and polyphosphoinositide breakdown in different cell lines. Biochemistry 29:10240–10245
46. Richelmi P, Mirabelli F, Salis A et al (1989) On the role of mitochondria in cell injury caused by vanadate-induced Ca^{2+} overload. Toxicology 57:29–44
47. Schmitz W, Scholz H, Erdmann E et al (1982) Effect of vanadium in the +5, +4 and +3 oxidation states on cardiac force of contraction, adenylatecyclase and $(Na^{+} + K^{+})$-ATPase activity. Biochem Pharmacol 31:3853–3860
48. Madsen KL, Porter VM, Fedorak RN (1994) Vanadium reduces sodium-dependent glucose transport and increases glycolytic activity in LLC-PK1 epithelia. J Cell Physiol 158:459–466
49. Pilkis SJ, El-Maghrabi MR (1988) Hormonal regulation of hepatic gluconeogenesis and glycolysis. Annu Rev Biochem 57:755–783
50. Cupo MA, Donaldson WE (1987) Chromium and vanadium effects on glucose metabolism and lipid synthesis in the chick. Poult Sci 66(1):120–126
51. Sera M, Tanaka K, Morita T et al (1990) Increasing effect of vanadate on lipoprotein lipase activity in isolated rat fat pads. Arch Biochem Biophys 279(2):291–297
52. Coulombe RA Jr, Briskin DP, Keller RJ et al (1987) Vanadium dependent oxidation of pyridine nucleotide in rat liver microsomal membranes. Arch Biochem Biophys 255(2): 267–273
53. Hajjar JJ, Fucci JC, Rowe WA et al (1987) Effect of vanadate on amino acid transport in rat jejunam. Proc Soc Exp Biol Med 184:403–409
54. Leonard A, Gerber GB (1994) Mutagenecity, carcinogenecity and teratogenicity of vanadium compounds. Mutat Res 317:81–88
55. Kopf-Maier P, Wagner W, Hesse B et al (1981) Tumor inhibition by metallocenes: activity against leukemias and detection of the systemic effect. Eur J Cancer 17:665–669
56. Kopf-Maier P, Krahl D (1983) Tumor inhibition by metallocenes: ultrastructural localisation of titanium and vanadium, in treated tumor cells by electron energy loss spectroscopy. Chem Biol Interact 44:317–328
57. Kopf-Maier P (1982) Development of necroses virus, activation and giant cell formation after treatment of Ehrlich ascites tumor with metallocene dichloride. J Cancer Res Clin Oncol 103:145–164
58. Kopf-Maier P, Wagner W, Liss E (1981) Cytokinetic behaviour of Ehrlich ascites tumor after in vivo treatment with cis-diamminedichloroplatinum (II) and metallocene dichloride. J Cancer Res Clin Oncol 201:21–30
59. El-Naggar MM, El-Waseef AM, El-Halafawy KM et al (1998) Antitumor activities of vanadium (IV), manganese(IV), iron(III), cobalt(II) and copper(II) complexes of 2-methylaminopyridine. Cancer Lett 133:71–76
60. Scrivens PJ, Alaoui MA, Giannini G et al (2003) Cdc-25A inhibitory properties and antineoplastic activity of bisperoxovanadium analogues. Mol Cancer Ther 2:1053–1059
61. D'Cruz OJ, Uckun FM (2002) Metavan: a novel oxovanadium (IV) complex with broad spectrum anticancer activity. Expert Opin Investig Drugs 11:1829–1836
62. Navara CS, Benyumov A, Vassilev A et al (2001) Vanadocenes as potent anti-proliferative agents disrupting mitotic spindle formation in cancer cells. Anticancer Drugs 12(4):369–376
63. Bishayee A, Oinam S, Basu M et al (2000) Vanadium chemoprevention of 7, 12-dimethylbenz(a) anthracene-induced rat mammary carcinogenesis: probable involvement of

representative hepatic phase I and II xenobiotic metabolizing enzymes. Breast Cancer Res Treat 63(2):133–145
64. Moore CJ, Tricomi WA, Gould MN (1986) Interspecies comparison of polycyclic aromatic hydrocarbon metabolism in human and rat mammary epithelial cells. Cancer Res 46:4946–4952
65. Ray RS, Roy S, Ghosh S et al (2001) Suppression of cell proliferation, DNA protein cross-links, and induction of apoptosis by vanadium in chemical rat mammary carcinogenesis. Anticancer Drugs 12(4):369–376
66. Ray RS, Roy S, Samanta S et al (2005) Protective role of vanadium on the early process of rat mammary carcinogenesis by influencing expression of metallothionein. GGT-positive foci and DNA fragmentation. Cell Biochem Funct 23(6):447–456
67. Ray RS, Basu M, Ghosh B et al (2005) Vanadium, a versatile biochemical effector in chemical rat mammary carcinogenesis. Nutr Cancer 51(2):184–196
68. Ray RS, Rana B, Swami B et al (2006) Vanadium mediated apoptosis and cell cycle arrest in MCF7 cell line. Chem Biol Interact 63(3):239–247
69. Ray RS, Ghosh B, Rana A et al (2006) Suppression of cell proliferation, induction of apoptosis and cell cycle arrest: chemopreventive activity of vanadium in vivo and in vitro. Int J Cancer 120(1):13–23
70. Bishayee A, Chatterjee M (1993) Selective enhancement of glutathione S-transferase activity in liver and extrahepatic tissues of rat following oral administration of vanadate. Acta Physiol Pharmacol Bulg 19(3):83–89
71. Posner BI, Faure R, Burgess JW et al (1994) Peroxovanadium compounds. A new class of potent phosphotyrosine phosphatase inhibitors which are insulin mimetics. J Biol Chem 269(6):4596–4604
72. Bishayee A, Chatterjee M (1995) Inhibitory effect of vanadium on rat liver carcinogenesis initiated with diethylnitrosamine and promoted by phenobarbital. Br J Cancer 71(6): 1214–1220
73. Bishayee A, Karmakar R, Mandal A et al (1997) Vanadium-mediated chemoprotection against chemical hepatocarcinogenesis in rats: haematological and histological characteristics. Eur J Cancer Prev 6(1):58–70
74. Bishayee A, Roy S, Chatterjee M (1999) Characterization of selective induction and alteration of xenobiotic biotransforming enzymes by vanadium during diethylnitrosamine-induced chemical rat liver carcinogenesis. Oncol Res 11(1):41–53
75. Chakraborty A, Selvaraj S (2000) Differential modulation of xenobiotic metabolizing enzymes by vanadium during diethylnitrosamine-induced hepatocarcinogenesis in Sprague-Dawley rats. Neoplasma 47(2):81–89
76. Basak R, Saha BK, Chatterjee M (2000) Inhibition of diethylnitrosamine-induced rat liver chromosomal aberrations and DNA-strand breaks by synergistic supplementation of vanadium and 1alpha,25-dihydroxyvitamin D(3). Biochim Biophys Acta 1502(2):273–282
77. Basak R, Chatterjee M (2000) Combined supplementation of vanadium and 1alpha,25-dihydroxyvitamin D3 inhibit placental glutathione S-transferase positive foci in rat liver carcinogenesis. Life Sci 68(2):217–231
78. Basak R, Basu M, Chatterjee M (2000) Combined supplementation of vanadium and 1alpha,25-dihydroxyvitamin D(3) inhibit diethylnitrosamine-induced rat liver carcinogenesis. Chem Biol Interact 128(1):1–18
79. Bukietyńska K, Podsiadly H, Karwecka Z (2003) Complexes of vanadium(III) with L-alanine and L-aspartic acid. J Inorg Biochem 94(4):317–325
80. Osińska-Królicka I, Podsiadły H, Bukietyńska K et al (2004) Vanadium(III) complexes with L-cysteine-stability, speciation and the effect on actin in hepatoma Morris 5123 cells. J Inorg Biochem 98(12):2087–2098
81. Chakraborty T, Ghosh S, Datta S et al (2003) Vanadium suppresses sister-chromatid exchange and DNA-protein crosslink formation and restores antioxidant status and hepatocellular architecture during 2-acetylaminofluorene-induced experimental rat hepatocarcinogenesis. J Exp Ther Oncol 3(6):346–362

82. Chattopadhyay MB, Mahendrakumar CB, Kanna PS et al (2004) Combined supplementation of vanadium and beta-carotene suppresses placental glutathione S-transferase-positive foci and enhances antioxidant functions during the inhibition of diethylnitrosamine-induced rat liver carcinogenesis. J Gastroenterol Hepatol 19(6):683–693
83. Chakraborty T, Chatterjee A, Saralaya MG et al (2006) Vanadium inhibits the development of 2-acetylaminofluorene-induced premalignant phenotype in a two-stage chemical rat hepatocarcinogenesis model. Life Sci 78(24):2839–2851
84. Chakraborty T, Chatterjee A, Saralaya MG et al (2006) Chemopreventive effect of vanadium in a rodent model of chemical hepatocarcinogenesis: reflections in oxidative DNA damage, energy-dispersive X-ray fluorescence profile and metallothionein expression. J Biol Inorg Chem 11(7):855–866
85. Chakraborty T, Chatterjee A, Dhachinamoorthi D et al (2006) Vanadium limits the expression of proliferating cell nuclear antigen and inhibits early DNA damage during diethylnitrosamine-induced hepatocellular preneoplasia in rats. Environ Mol Mutagen 47(8):603–615
86. Chakraborty T, Pandey N, Chatterjee A et al (2006) Molecular basis of anticlastogenic potential of vanadium in vivo during the early stages of diethylnitrosamine-induced hepatocarcinogenesis in rats. Mutat Res 609(2):117–128
87. Chakraborty T, Chatterjee A, Rana A et al (2007) Carcinogen-induced early molecular events and its implication in the initiation of chemical hepatocarcinogenesis in rats: chemopreventive role of vanadium on this process. Biochim Biophys Acta 1772(1):48–59
88. Chakraborty T, Swamy AH, Chatterjee A et al (2007) Molecular basis of vanadium-mediated inhibition of hepatocellular preneoplasia during experimental hepatocarcinogenesis in rats. J Cell Biochem 101(1):244–258
89. Chakraborty T, Chatterjee A, Rana A et al (2007) Suppression of early stages of neoplastic transformation in a two-stage chemical hepatocarcinogenesis model: supplementation of vanadium, a dietary micronutrient, limits cell proliferation and inhibits the formations of 8-hydroxy-2′-deoxyguanosines and DNA strand-breaks in the liver of sprague-dawley rats. Nutr Cancer 59(2):228–247
90. Kordowiak AM, Klein A, Goc A et al (2007) Comparison of the effect of VOSO4, Na3VO4 and NaVO3 on proliferation, viability and morphology of H35-19 rat hepatoma cell line. Pol J Pathol 58(1):51–57
91. Greenle RT, Murry T, Wingo PA (2000) Cancer statistics, 2000. CA Cancer J Clin 50:7–33
92. Kingsnorth AN, LaMuraglia GM, Ross JS et al (1986) Vanadate supplements and 1, 2-dimethylhydrazine induced colon cancer in mice: increased thymidine incorporation without enhanced carcinogenesis. Br J Cancer 53(5):683–686
93. Kanna PS, Mahendrakumar CB, Chakraborty T et al (2003) Effect of vanadium on colonic aberrant crypt foci induced in rats by 1, 2 dimethyl hydrazine. World J Gastroenterol 9(5):1020–1027
94. Kanna PS, Mahendrakumar CB, Chatterjee M et al (2003) Vanadium inhibits placental glutathione S-transferase (GST-P) positive foci in 1,2-dimethyl hydrazine induced rat colon carcinogenesis. J Biochem Mol Toxicol 17(6):357–365
95. Kanna PS, Mahendrakumar CB, Indira BN et al (2004) Chemopreventive effects of vanadium toward 1,2-dimethylhydrazine-induced genotoxicity and preneoplastic lesions in rat colon. Environ Mol Mutagen 44(2):113–118
96. Kanna PS, Saralaya MG, Samanta K et al (2005) Vanadium inhibits DNA-protein cross-links and ameliorates surface level changes of aberrant crypt foci during 1,2-dimethylhydrazine induced rat colon carcinogenesis. Cell Biol Toxicol 21(1):41–52
97. Tan EY, Richard CL, Zhang H et al (2006) Adenosine downregulates DPPIV on HT-29 colon cancer cells by stimulating protein tyrosine phosphatase(s) and reducing ERK1/2 activity via a novel pathway. Am J Physiol Cell Physiol 291(3):C433–C444
98. Etcheverry SB, Ferrer EG, Naso L et al (2008) Antioxidant effects of the VO(IV) hesperidin complex and its role in cancer chemoprevention. J Biol Inorg Chem 13(3):435–447

99. Samanta S, Swamy V, Suresh D et al (2008) Protective effects of vanadium against DMH-induced genotoxicity and carcinogenesis in rat colon: removal of O(6)-methylguanine DNA adducts, p53 expression, inducible nitric oxide synthase downregulation and apoptotic induction. Mutat Res 650(2):123–131
100. Samanta S, Chatterjee M, Ghosh B et al (2008) Vanadium and 1, 25 (OH)2 vitamin D3 combination in inhibitions of 1,2, dimethylhydrazine-induced rat colon carcinogenesis. Biochim Biophys Acta 1780(10):1106–1114
101. Holko P, Ligeza J, Kisielewska J et al (2008) The effect of vanadyl sulphate (VOSO4) on autocrine growth of human epithelial cancer cell lines. Pol J Pathol 59(1):3–8
102. Klein A, Holko P, Ligeza J et al (2008) Sodium orthovanadate affects growth of some human epithelial cancer cells (A549, HTB44, DU145). Folia Biol (Krakow) 56(3–4):115–121
103. Papaioannou A, Manos M, Karkabounas S et al (2004) Solid state and solution studies of a vanadium(III)-L-cysteine compound and demonstration of its antimetastatic, antioxidant and inhibition of neutral endopeptidase activities. J Inorg Biochem 98(6):959–968
104. Hierowski MT, Liebow C, Schally AV et al (1985) Stimulation by somatostatin of dephosphorylation of membrane proteins in pancreatic cancer MIA PaCa-2 cell line. FEBS Lett 179(2):252–256
105. Cortizo MS, Alessandrini JL, Etcheverry SB et al (2001) A vanadium/aspirin complex controlled release using a poly(beta-propiolactone) film. Effects on osteosarcoma cells. J Biomater Sci Polym Ed 12(9):945–959
106. Cortizo AM, Bruzzone L, Molinuevo S et al (2000) A possible role of oxidative stress in the vanadium-induced cytotoxicity in the MC3T3E1 osteoblast and UMR106 osteosarcoma cell lines. Toxicology 147(2):89–99
107. Molinuevo MS, Cortizo AM, Etcheverry SB (2008) Vanadium(IV) complexes inhibit adhesion, migration and colony formation of UMR106 osteosarcoma cells. Cancer Chemother Pharmacol 61(5):767–773
108. Fallico R, Ferrante M, Fiore M et al (1998) Epidemiological research into the consequences of vanadium assimilated through diet and of its effects on human health following research carried out on people from the Etna massif. J Prev Med Hyg 39:74–79
109. Lener J, Kučera J, Kodl M et al (1998) Health effects of environmental exposure to vanadium. In: Nriagu JO (ed) Vanadium in the environment. Part 2: health effects. Wiley, New York
110. Greenwald P, Milner JA, Anderson DE et al (2002) Micronutrients in cancer chemoprevention. Cancer Metastasis Rev 21:217–230
111. Evangelou AM (2002) Vanadium in cancer treatment. Crit Rev Oncol Hematol 42:249–265
112. Bishayee A, Banik S, Marimuthu P et al (1997) Vanadium-mediated suppression of diethylnitrosamine-induced chromosomal aberrations in rat hepatocytes and its correlation with induction of hepatic glutathione and glutathione-S-transferase. Int J Oncol 102:413–423
113. Crans DC, Rithner CD, Theisen LA (1990) Application of time-resolved vanadium-51 2D NMR for quantitation of kinetic exchange pathways between vanadate monomer, dimer, tetramer, and pentamer. J Am Chem Soc 112:2901–2908
114. Heath E, Howarth OW (1981) Vanadium-51 and oxygen-17 nuclear magnetic resonance study of vanadate(V) equilibria and kinetics. J Chem Soc Dalton 1981:1105–1110
115. Hamilton EE, Wilker JJ (2004) Inorganic oxo compounds reacts with alkaline agents: implication for DNA damage. Angew Chem Int Ed Engl 43(25):3290–3292
116. Kawabe K, YoshikawaY AY et al (2006) Possible mode of action for insulin mimetic activity of vanadyl (IV) compounds in adipocytes. Life Sci 78:2860–2866
117. Zhang Z, Leonard SS, Huang C et al (2003) Role of oxygen species and MAPKs in vanadate-induced G2/M phase arrest. Free Radic Biol Med 34:1333–1342
118. Molinuevo MS, Barrio DA, Cortizo AM et al (2004) Antitumoral properties of two new-vanadyl(IV) complexes in culture: role of apoptosis and oxidative stress. Cancer Chemother Pharmacol 53:163–172
119. Fawcett JP, Farquhar SJ, Thou T et al (1997) Oral vanadyl sulphate does not affect blood cells, viscosity or biochemistry in humans. Pharmacol Toxicol 80:202–206

120. Goldfine AB, Simonson DC, Folli F et al (1995) Metabolic effects of sodium metavanadate in humans with insulin-dependent and noninsulin-dependent diabetes mellitus in vivo and in vitro studies. J Clin Endocrinol Metab 80:3311–3320
121. Somerville J, Davies B (1962) Effect of vanadium on serum cholesterol. Am Heart J 64:54–56
122. Dimond EG, Caravace J, Benchimol A (1963) Vanadium, excretion, toxicity, lipid effect in man. Am J Clin Nutr 12:49–53
123. Schroeder HA, Balassa JJ, Tipton IH (1963) Abnormal trace metals in man- Vanadium. J Chronic Dis 16:1047–1071
124. Nemery B (1990) Metal toxicity and the respiratory tract. Eur Respir J 3(2):202–219
125. Ehrlich VA, Nersesyan AK, Atefie K et al (2008) Inhalative exposure to vanadium pentoxide causes DNA damage in workers: results of a multiple end point study. Environ Health Perspect 116(12):1689–1693
126. Maines MD (1994) Modulating factors that determine interindividual differences in response to metals. In: Mertz W et al (eds) Risk assessment of essential elements. ILSI Press, Washington, DC, pp 21–39

Chapter 9
Cardiovascular Protection with Vanadium Compounds

Kohji Fukunaga and Md Shenuarin Bhuiyan

Abstract Protein kinase B/Akt plays a critical role in the regulation of cardiac hypertrophy, angiogenesis and apoptosis. The evidences that elevation of Akt in cardiomyocytes *in vivo* and *in vitro* protects against apoptosis after ischemia/reperfusion injury provide possibility that agents targeting Akt activation become a novel therapeutic strategy for limiting myocardial injury following ischemia. Vanadium compounds inhibiting protein tyrosine phosphatases are potent activator of the Akt signaling pathways and elicit cardioprotection in heart ischemia/reperfusion injury along with cardiac functional recovery in rats. In addition, vanadium compounds has strong anti-hypertrophic in the pressure overload-induced hypertrophy in ovariectomized and aortic-banded rats. The elevation of Akt activity and Akt-dependent eNOS phosphorylation are central roles on vanadium compound-induced anti-hypertrophy and heart failure in the ovariectomized and aortic-banded rats. Taken together, vanadium compounds are potential therapeutics for ischemia/reperfusion-induced myocardial injury and heart failure associated with hypertension in the postmenopausal women.

Keywords Cardiovascular disease • Hypertrophy • Endothelial nitric oxide synthase • Postmenopausal women • Protein kinase B • Protein tyrosine phosphatase • Vanadium compounds

K. Fukunaga (✉) • M.S. Bhuiyan
Department of Pharmacology, Graduate School of Pharmaceutical Sciences, Tohoku University, 6-3 Aramaki-Aoba, Aoba-ku, Sendai 980-8578, Japan
e-mail: fukunaga@mail.pharm.tohoku.ac.jp; shenuarin@hotmail.com

H. Michibata (ed.), *Vanadium: Biochemical and Molecular Biological Approaches*,
DOI 10.1007/978-94-007-0913-3_9,

9.1 Introduction

In the cardiovascular system, protein kinase B (PKB)/Akt plays an important role in the regulation of cardiac hypertrophy, angiogenesis, and apoptosis [1–5]. The Akt subfamily comprises three mammalian isoforms, PKBα/Akt1, PKBβ/Akt2 and PKBγ/Akt3, which are products of distinct genes and share a conserved structure that includes three functional domains: an N-terminal pleckstrin homology domain, a central kinase domain, and a C-terminal regulatory domain containing the hydrophobic motif phosphorylation site [FxxF(S/T)Y] [6]. Among the three Akt genes, only Akt1 and Akt2 are highly expressed in the heart. Consistent with the general trophic function of Akt, the Akt1 whole-genome-knockout mice weigh approximately 20% less than wild-type littermates and have a proportional reduction in size of all somatic tissues, including the heart [7, 8]. In contrast, Akt2-knockout mice have only a modest reduction in organ size [9]. Thus, data from Akt-knockout mice support a critical role specifically for Akt1 in normal growth of the heart [10]. The observation that acute activation of Akt in cardiomyocytes *in vivo* and *in vitro* protects against apoptosis after ischemia/reperfusion injury provide possibility that agents targeting Akt activation become a novel therapeutic strategy for limiting myocardial injury following ischemia [11].

9.2 Cardioprotection with Vanadium Compound in Myocardial Infarction

9.2.1 Vanadium Compounds as Akt Activator

Vanadium compounds are potent activator of the Akt signaling pathways [12–15] and elicit cardioprotection in heart ischemia/reperfusion injury along with cardiac functional recovery in rats [1, 2, 15, 16]. Vanadium compounds inhibit protein tyrosine phosphatases [12, 13] and promote an increase in protein tyrosine phosphorylation, leading to the upregulation of Akt [12, 14]. An increase in tyrosine phosphorylation in the heart via increased tyrosine kinase activity has been implicated in the signal transduction pathway of cardioprotection by ischemic preconditioning [17–19] which is the most potent endogenous mechanism to limit myocardial infarct size. Among several oxidation states of vanadium II to V, vanadium ion in living cells exists exclusively as vanadyl (IV) cation and a small amount as vanadate (V) anion [20]. Furthermore, vanadyl (VO^{2+}) compounds, of oxidation state IV, under physiological conditions are subject to oxidation by a variety of oxidants, including molecular oxidant and vanadate compounds, of oxidation state V are thought to undergo reduction to state IV in the cell [21–24]. To develop a novel therapeutic drug to protect cardiomyocytes from heart diseases, we selected a novel vanadyl (IV) compound having the VO^{2+} chelate, bis(1-oxy-2-pyridinethiolato) oxovanadium(IV), [VO(OPT)], which is a potent activator of the Akt signaling pathway both *in vivo* and *in vitro* [12–14, 25].

9.2.2 Pharmacotoxicity of Vanadium Compounds

The toxicity of vanadium compounds is low. The most common toxic effects reported for inorganic vanadium compounds are diarrhea, decreased food uptake, dehydration and reduced body weight gain [14] which can, however, be corrected by adding sodium chloride to drinking water, adjusting the pH of the solution to neutrality and by gradually increasing the dose of vanadium [26, 27]. Organic vanadium compounds were much safer than inorganic vanadium salts and do not cause any gastrointestinal discomfort, hepatic or renal toxicity [25, 28]. Along with the previous studies, we also did not found any gastrointestinal, hepatic or renal toxicity in the VO(OPT) treated rats [29, 30].

Recent work has demonstrated that vanadium compounds inhibited serum- and growth factor-stimulated mitogenesis [31, 32] and possess anti-tumor activity [33, 34]. Many other studies have, however, failed to detect any change in the levels of urea, creatinine, glutamic oxaloacetic transaminase and glutamic pyruvic transaminase, indices of kidney and liver functions [35–37]. Moreover, no significant changes in the histopathology of several tissues, including the liver, spleen, stomach, heart and lung, have been observed among control and vanadyl sulfate-treated animals [38]. Electron microscopic examination of *ob/ob* mice treated with vanadate for 47 days revealed no sign of hepatotoxicity [27].

In patients treated with vanadium salts, gastrointestinal discomfort was the most common toxic effect, which could be corrected by decreasing the dose level [39]. Moreover, clinical studies have been of short duration (up to 6 weeks) and utilized lower doses than those administered in animal experiments; thus, the long-term toxicity of vanadium in humans remains to be explored. Clearly, at present, there is no consensus on the toxic effects of vanadium compounds, and detailed and systematic investigations are needed to evaluate the toxicity of various vanadium compounds before undertaking long-term clinical trials in humans. It should be noted that use of chelating agents and organo-vanadium compounds, such as VO(OPT), have shown significantly reduced vanadium toxicity and may serve as more potent cardioprotective agents than inorganic vanadium salts.

9.2.3 Cardioprotection of VO(OPT) in Ischemia/Reperfusion Injury

We tested whether VO(OPT) treatment has cardioprotective effect against myocardial ischemia/reperfusion injuries in rats. Rats were subjected to 30 min ischemia followed by 24 h reperfusion to define the cytoprotective effect of VO(OPT) (0.5 and 1.25 mg V/kg) on myocardial infarct size. The infarct sizes in the VO(OPT) treated group ($53 \pm 7\%$ and $37 \pm 2\%$ in 0.5 and 1.25 mg V/kg, respectively) were significantly smaller than that in the vehicle group ($67 \pm 4\%$) [1]. This observation indicated that VO(OPT) has cardioprotective effect on ischemia/reperfusion induced myocardial infarction.

Sodium orthovanadate restores ischemia-induced decrease in Akt phosphorylation on Ser-473 in the gerbil hippocampus, thereby rescuing hippocampal neurons from ischemia-induced cell death [40]. Akt activation has been shown to reduce cardiomyocyte apoptosis, thereby preventing myocardial injury after transient ischemia [11]. We confirmed that post-treatment with VO(OPT) significantly rescues decreased Akt activity after myocardial ischemia/reperfusion and the preserved Akt activity possibly accounts for the VO(OPT)-induced cytoprotective action in cardiomyocytes. Activated Akt is believed to suppress apoptosis through phosphorylation of several substrates, including the Bcl-2 family member, Bad [41] and Forkhead transcription factors (FOXO) [42, 43]. We confirmed downstream targets of Akt to mediate anti-apoptotic signaling in cardiomyocytes. Significant decrease in phosphorylation of Bad and Forkhead transcription factors (FKHR and FKHRL1) are closely correlated with decreased Akt activity following myocardial ischemia/reperfusion injury. Phosphorylation of Bad and Forkhead transcription factors were markedly potentiated in cardiomyocytes by treatment with VO(OPT), similar to its response to Akt activity. These results suggest that both Bad and FOXOs are Akt targets and mediate cardioprotective action by inhibiting them following treatment with VO(OPT). Like FKHR, FKHRL1 has been shown to induce apoptosis in the brain [44] and fibroblasts through up-regulation of the Fas ligand expression and activation of the death receptor pathway [45]. We also found significantly increased expression of both Fas ligand and Bim after myocardial ischemia/reperfusion and significant inhibition by treatment with VO(OPT) [1].

Recent findings showed that FKHRL1 is regulated by Akt activity in endothelial cells and that FKHRL1 dephosphorylation promotes apoptosis by negatively regulating FLIP expression [46]. Moreover, Akt was found to rescue endothelial cells from Fas/Fas ligand-mediated cell death through up-regulation of FLIP level [47]. Similar with the previous studies, we found significant FLIP degradation after ischemia/reperfusion [48, 49] and treatment with VO(OPT) significantly increased FLIP expression in cardiomyocytes. The increased FLIP expression was correlated with decreased Fas ligand expression in VO(OPT)-treated group compared with vehicle-treated group. Taken together, inactivation of FKHR and FKHRL1 by treatment with VO(OPT) after ischemia/reperfusion likely promotes expression of FLIP, thereby inhibiting cardiomyocyte [1] apoptosis

Cardiomyocyte apoptosis is one of the major contributors in the development of myocardial infarct [50], which is related to the pathogenesis of heart failure after ischemia. Accumulating evidences indicate that apoptosis, different type of cell death form necrosis, plays essential role in cardiomyocyte death after ischemia/reperfusion [50]. Therefore, we examined whether VO(OPT) has anti-apoptotic effects in cardiomyocytes by measuring Caspase 3, Caspase 7 and Caspase 9 processing as a marker of apoptosis. Interestingly, short-term infusion of VO(OPT) significantly reduced cardiomyocyte apoptosis after ischemia/reperfusion as indicated by dose-dependent inhibition of Caspase-3, -7 and -9 processing [3]. The results confirm anti-apoptotic effects of VO(OPT) against myocardial ischemia/reperfusion injury.

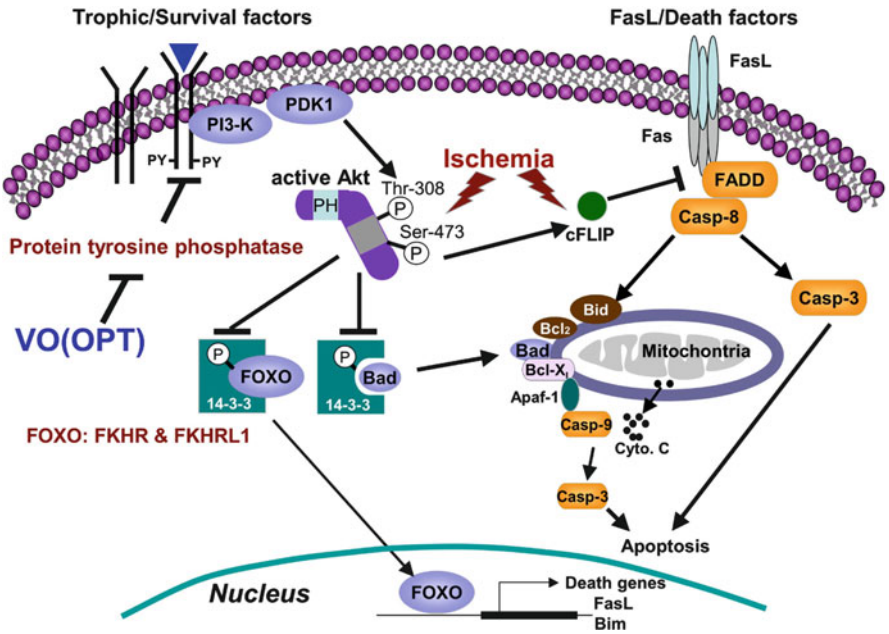

Fig. 9.1 Putative mechanism of myocardial protection by VO(OPT). Binding of trophic/survival factors to tyrosine kinase receptors activate Akt through PI3K and phosphatidylinositol-dependent kinase-1(PDK1) activation. Ischemia/reperfusion caused inactivation of Akt, thereby promoting apoptotic pathways including the Bad, Forkhead transcription factors (FOXO; FKHR and FKHRL-1) and FLIP via the Fas pathways. Treatment with VO(OPT) activates and/or preserves Akt activity after ischemia-reperfusion leading to the phosphorylation and thereby inactivation of Bad and Forkhead transcription factors thus preventing apoptosis by Fas ligand and Bim. VO(OPT) treatment also preserves ischemia-reperfusion induced breakdown of FLIP and thereby preventing cell death via Fas pathways. Therefore, the cytoprotective action of VO(OPT) is mediated by the Akt-Forkhead transcription factor-FLIP mediated pathway

VO(OPT) treatment protects the heart form ischemia/reperfusion-induced cardiac injury, thereby improving cardiac contractile dysfunction in rats. VO(OPT) induced cardioprotection is mainly elicited by Akt activation after myocardial ischemia/reperfusion. Akt activation induces phosphorylation of proapoptotic protein Bad, thereby reducing mitochondria-dependent apoptosis. Moreover, VO(OPT) treatment abolished dephosphorylation of forkhead transcription factors after ischemia/reperfusion injury, thereby inhibiting expression of Fas ligand and Bim. Furthermore, VO(OPT) treatment after ischemia/reperfusion promoted expression of FLIP through Akt activation, thereby further inhibiting activation of Fas/Fas-ligand intracellular signal. Taken together, VO(OPT) treatment at reperfusion is likely beneficial as a cardioprotective drug in subjects undergoing reperfusion therapy following a myocardial infarction (Fig. 9.1).

9.3 Cardioprotection of Vanadium Compounds in the Postmenopause

9.3.1 Cardiovascular Diseases in the Postmenopausal Women

Menopause is the permanent cessation of menstruation and ovarian follicular production of estrogens and progesterone. The mean age at menopause is 51 years, and 95% of women reach menopause between the ages of 45 and 55 [51]. Over the past 20 years, numerous observational, retrospective, interventional, and meta-analytic studies [52] as well as studies using animal models have supported the hypothesis that ovarian steroids exert important protective actions in women and the absence of sex hormones after menopause makes postmenopausal women more vulnerable than younger premenopausal women to cardiovascular diseases (CVD). Indeed, CVD is the leading cause of morbidity and mortality among postmenopausal women in westernized societies [53] and accounts for nearly half of all deaths in women [54]. The Framingham study showed that the incidence of CVD is higher among postmenopausal than in premenopausal women, even among women of the same age [55]. Women who also experience early menopause, both naturally and surgically (bilateral oophorectomy), also have increased risk of coronary events [56].

Approximately 1 in 8 women above age 55 years has undergone bilateral oophorectomy before reaching natural menopause [56, 57]. Bilateral oophorectomy may be performed for a benign disease or for prophylaxis against ovarian cancer, and is usually performed along with hysterectomy (in nearly 90% of cases) [58]. Of the more than 600,000 hysterectomies performed annually in the United States, approximately half include bilateral oophorectomy [59]. In addition, the practice of prophylactic oophorectomy has increased over time and became more than doubled between 1965 and 1990 [60]. Meanwhile, reports now link premenopausal oophorectomy with serious health consequences including premature death, cardiovascular and neurologic disease, and osteoporosis in addition to menopausal symptoms, psychiatric symptoms, and impaired sexual function [61]. The preponderance of evidence suggests that bilateral oophorectomy is associated with increased cardiovascular risk and premature death, and that oophorectomy at a young age further increases this risk [62]. Estrogen therapy started early after surgical or natural menopause at a young age appears to reduce this risk [62–65].

Clinical and experimental studies have established that sex influences the patterns of LV hypertrophy [66]. In response to pressure overload, such as hypertension or aortic stenosis, human male hearts exhibit LV dilatation or eccentric hypertrophy, whereas female hearts tend to maintain normal chamber size but develop increased wall thickness, consistent more with concentric hypertrophy [67]. Evidences of sex hormones influence on the patterns of hypertrophy is revealed from studies demonstrating that physiological replacement of 17β-estradiol, the main circulating

form of estrogen in premenopausal women, to ovariectomized female mice limits pressure overload–induced LV hypertrophy [68, 69].

Despite well established models of myocardial hypertrophy and heart failure using rodents, there has been lack of suitable animal models to study postmenopausal hypertension and hypertrophic cardiac remodeling. Although nonhuman primates, sheep, rabbits, mice and rats have all been used as models of various menopausal changes [70], progress in elucidating the mechanisms responsible for postmenopausal hypertension and hypertrophic remodeling has been hampered by the lack of a suitable animal model. Therefore, despite impressive progress in the diagnosis and treatment of hypertrophy, more research on postmenopausal cardiac decompensation under stress is absolutely needed, and adequate animal models are critical to fill the gap between basic science discovery and clinics. An ideal model of postmenopausal cardiac hypertrophy and heart failure should meet various requirements to mimic a complex syndrome characterized by cardiac, hemodynamic and neurohumoral alterations as close as possible. We focused on the molecular mechanisms that contribute to cardioprotective effects of estrogen on LV hypertrophy in response to pressure overload in a rat model of postmenopausal phenotypes to develop novel therapeutic strategy instead of hormone replacement therapy in the postmenopausal women.

9.3.2 Development of Postmenopausal Cardiac Hypertrophy Models

There have been attempts to elucidate the cardioprotective effect of estrogen in pressure overload induced hypertrophy by using ovariectomized animals [71, 72], however, these have rarely taken into account the effect of menopause on cardiac adverse remodeling and the transition to heart failure. In any case, there is no normotensive animal model that exhibits hypertrophy and decompensation with postmenopausal phenotypes. Female spontaneously hypertensive rats (SHR) represent some postmenopausal phenotypes as they stop cycling at age 10–12 months and have low estradiol levels comparable to postmenopausal women [73]. However, the sex difference in blood pressure no longer exists because of the increase in blood pressure in old females, whereas blood pressure in male SHR remains fairly stable after age 8 months [73]. Dahl salt-sensitive (DS) hypertensive rats also represent some characteristics of postmenopause as they exhibit increases in blood pressure with aging [74]. When the young female DS rats are ovariectomized and fed a high-salt diet, the blood pressure increases to higher levels than in intact females [74]. Still it is not known at what age these animals cease cycling and what happens to their blood pressure after cessation of cycling. In addition to the rat models, the follicular-stimulating hormone receptor knockout mouse also exhibits some of the characteristics of postmenopausal women [75]. These mice have low plasma estradiol levels, have functionally active estrogen receptors, increased testosterone

levels, hypertension, hypercholesterolemia, and weight gain when compared with their wild-type counterparts [75]. However, these animals did not exhibit increased oxidative stress or endothelial dysfunction at age of 14–16 weeks, factors common to postmenopausal women [75].

To produce left ventricular pressure overload in the ovariectomized rats, we introduced a model of transverse aortic constriction in the abdominal aorta between the right and left renal arteries [2, 4, 76]. Serum estrogen level was significantly decreased following ovariectomy (OVX) compared with the sham rats (sham: 56.6 ± 8.3 pg/ml; OVX: 3.6 ± 2.3 pg/ml). Pressure overload (PO)-induced hypertrophy had no effect on the serum estrogen level as seen both in the PO (60.8 ± 13.6 pg/ml) and OVX-PO (3.4 ± 1.2 pg/ml) group rats. Following ovariectomy, body weight (BW) was significantly increased compared to sham animals. Significant increases in LV weight were also seen in the OVX-PO group compared to sham, OVX and PO groups without significant changes in right ventricle weight.

9.3.3 Anti-hypertrophic Effect of VO(OPT)

Consistent with my previous observation, LV weight and LW significantly increased in the ovariectomized pressure overloaded (OVX-PO) group compared with the OVX group, without significant changes in right ventricle weight [2]. VO(OPT) (2.5 mgV/kg, p.o.) treatment on the sham and OVX rats have no effect on the morphometric parameters [4]. VO(OPT) treatment significantly and dose-dependently decreased the elevated LV weights and lung weight (LW). Notably, the ratio of HW to BW markedly increased in OVX-PO group compared with OVX group. VO(OPT) (2.5 mg/kg) treatment significantly inhibited the elevated the HW/BW ratio ($P < 0.01$ vs. OVX-PO) (Fig. 9.2). The LW/BW ratio was also significantly increased in OVX-PO group compared with OVX group. VO(OPT) treatment dose-dependently decreased the elevated LW/BW ratio. Moreover, oral treatment with VO(OPT) (2.5 mg V/kg) for 14 days have no effect on HW/BW ratio and HW/LW ratio in sham-operated animals [4].

Since treatment with VO(OPT) (1.25 and 2.5 mg V/kg) restored HR and MABP, we evaluated LV functions in OVX-PO heart with or without treatment of VO(OPT). Consistent with my previous observation [2], left ventricular end diastolic pressure (LVEDP) was significantly increased in the OVX-PO group compared with OVX group. VO(OPT) treatment dose-dependently restored elevated LVEDP. Similarly, left ventricular developed pressure (LVDP) significantly increased in OVX-PO group and VO(OPT) treatment dose-dependently restored elevated LVDP. The rate of LV contraction (+dp/dt) and relaxation (−dp/dt) also significantly increased in OVX-PO [2] and VO(OPT) treatment dose-dependently restored the elevated LV contraction (+dp/dt) and relaxation (−dp/dt). In agreement with earlier studies [29, 30], the treatment with VO(OPT) containing 2.5 mg V/kg resulted in slight decrease in body weight and food intake compared to vehicle treated rats but these changes are not significant [4].

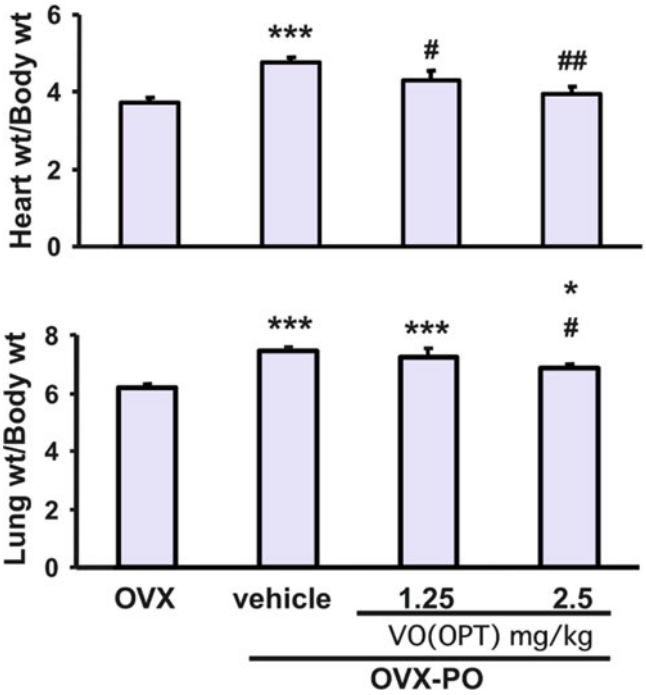

Fig. 9.2 Effect of VO(OPT) on heart weight (HW)/body weight (BW) (**a**) and lung weight (LW)/body weight BW (**b**) ratio. Each bar represents the mean ± S.E.M.*, $P < 0.05$ and ***, $P < 0.001$ versus OVX group; #, $P < 0.05$ and ##, $P < 0.01$ versus OVX-PO-vehicle treated group (Modified from [4])

9.3.4 Impaired Cardiac Akt/eNOS Signaling in Postmenopause

Akt phosphorylation at Ser-473 was significantly reduced in the hearts of OVX-PO rats compared with the OVX group, indicating that Akt signaling is markedly impaired in pressure overload-induced heart failure concomitant with severe cardiac hypertrophy. Akt Thr-308 phosphorylation also decreases only in the OVX-PO group. To define the role of Akt activity in cardiac hypertrophy and heart failure, we evaluated the time course of cardiac hypertrophy, heart failure, and the left ventricular Akt activity. Heart weigh/body weight ratio is increased time dependently from 1 to 4 weeks following PO in OVX rats [4]. LV Akt phosphorylation at Ser 473 was increased 1 week after PO, thereafter decreased time dependently with significant decreased level observer 4 weeks after PO in OVX rats. On the contrary, no significant change was observed in the total Akt level [4]. Importantly, VO(OPT) treatment markedly and dose-dependently increased Akt activity as assessed by increased phosphorylation at Ser 473 and at Thr 308 (Fig. 9.3).

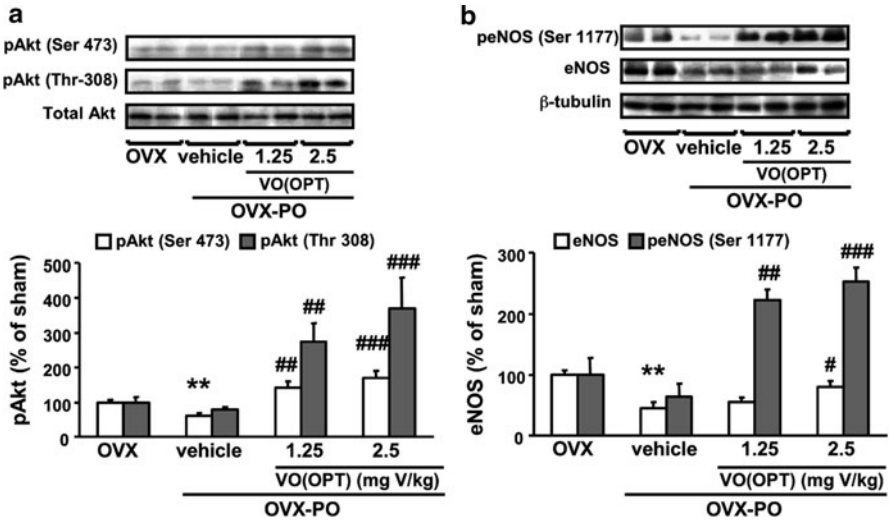

Fig. 9.3 Effects of VO(OPT) on Akt and eNOS phosphorylation in the left ventricle. Representative Western blot analysis using cell extracts from OVX (n = 8), OVX-PO-vehicle (n = 8), OVX-PO-VO(OPT) containing 1.25 mg/kg vanadium (V 1.25) (n = 8) and OVX-PO-VO(OPT) containing 2.5 mg/kg vanadium (V 2.5) (n = 8) treated hearts probed with phospho-Akt (Ser-473) and phospho-Akt (Thr-308) (**a**) and eNOS and phospho-eNOS (Ser 1179) (**b**). Data are expressed as percentages of the value of OVX rats. Each column represents the mean ± S.E.M. **, $P < 0.01$ versus the OVX group; ## $P < 0.01$ and ### $P < 0.001$ versus the OVX-PO-vehicle treated group (Modified from [4])

Since eNOS is physiological substrate for Akt in human vascular endothelial cells [77], we determine whether VO(OPT)-induced Akt activation results in increased eNOS phosphorylation and its activity. The time course studies revealed that both eNOS and Akt mediated eNOS phosphorylation at Ser 1179 decreased time dependently following PO-treatment with significant decreased level observed 4 weeks after PO in OVX rats [4]. Consistent with our previous observation [2], we also observed severe impairment of eNOS expression following OVX-PO treatment. I here found a slight but not significant reduction of eNOS phosphorylation at Ser 1179. Notably, VO(OPT) treatment dose-dependently increased eNOS phosphorylation (Fig. 9.3). VO(OPT) also significantly increased eNOS expression.

9.3.5 Prevention of β-Adrenergic Induced Heart Attack with VO(OPT)

β-adrenoceptor (β-AR) agonists differently affect heart rate during the estrous cycle in female rats and in ovariectomized rats with or without estrogen replacement [78]. Ovariectomy also increases susceptibility to the effects of β-AR agonists

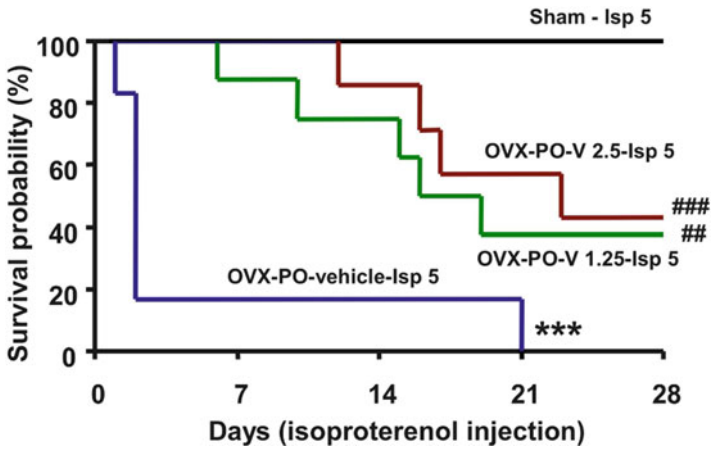

Fig. 9.4 Kaplan-Meier survival analysis following chronic isoproterenol treatment. Five mg/kg isoproterenol (Isp 5) was administered daily to sham, sham-PO, OVX, OVX-PO-vehicle, OVX-PO-VO(OPT) containing 1.25 mg/kg vanadium (V 1.25) and OVX-PO-VO(OPT) containing 2.5 mg/kg vanadium (V 2.5) treated groups. Survival over 28 days was monitored. ***, $P < 0.001$ versus the sham group; ##, $P < 0.01$ and ###, $P < 0.001$ versus the OVX-PO-vehicle treated group (Modified from [4])

[79]. Importantly, Kam et al. [80] demonstrated that β-AR stimulation with isoproterenol led to a significantly greater increase in electrical stimulation-induced Ca^{2+} elevation, Ca^{2+}-uptake through cardiac L-type Ca^{2+} channels, heart rate and contractility in hearts of ovariectomized rats compared to sham rats. These responses were rescued by estrogen replacement. Several studies hypothesized that excessive adrenergic activation could initiate the progression from compensated LV hypertrophy in hypertension to cardiac dysfunction and that this effect is primarily through adverse LV remodeling.

Similar with aortic banding [2], chronic administration of β-AR agonist to rats led to adverse cardiac injury through impaired Akt-eNOS signaling pathways and ovariectomy further aggravated the cardiac injury suggesting the cardioprotective role of ovarian hormones [4]. Kaplan-Meier survival data in indicate that chronic β-adrenergic stimulation with isoproterenol has no effect of the survival of sham and pressure overloaded female rats (Fig. 9.4). Remarkably, treatment with isoproterenol on the ovariectomized rats tended to increase mortality with a survival rate of 84% at 28 days. Interestingly, the most significant mortality occurred in the OVX-PO rats with a survival rate of 0% at 21 days following chronic β-adrenergic stimulation (Fig. 9.4) [4]. These observations indicate that decompensation against cardiac stress such as isoproterenol treatment occurs only in OVX and OVX-PO rats. Treatment with the Akt activator VO(OPT) dose dependently increased survival following acute cardiac stress caused by chronic β-adrenergic stimulation [1, 3], suggesting that cardiac remodeling and recovered cardiac functions by

VO(OPT) treatment contributes the reduced mortality (Fig. 9.4). Thus, simultaneous impairment of Akt-eNOS signaling by ovariectomy contributed to cardiac decompensation during PO-induced hypertrophy, deteriorated heart functions and thereby increased mortality during chronic β-adrenergic stimulation. Potentiation of the Akt and eNOS signaling pathways by treatment with VO(OPT) after OVX-PO likely contributes to increased survival following acute cardiac stress caused by chronic β-adrenergic stimulation. These results contribute to our understanding of the mechanisms underlying increased cardiac injuries in postmenopausal women by chronic β-adrenergic activation and bear relevance to further clinical management strategies to prevent adverse cardiac remodeling.

9.4 Crosstalk of Estrogen Receptor and Akt/eNOS Signaling

9.4.1 Cardioprotection Through Estrogen Receptor

Both *in vivo* and *in vitro* studies indicates that estrogen have cardioprotective effects. However, despite these positive results, hormone replacement therapy has not been shown to consistently lower blood pressure in postmenopausal women. Moreover, in women who have experienced surgical menopause, estrogen replacement therapy also did not result in significant sustained reductions in blood pressure. The mechanisms responsible for increased prevalence of cardiovascular diseases in postmenopausal women are complex and multifaceted. They are not nearly so simple as a reduction in estradiol. We focused on evaluating the molecular mechanisms responsible cardiac injuries in postmenopausal women and characterized the postmenopausal OVX-PO model to provide a suitable animal model to quantitatively evaluate some of the mechanisms and hoped that the information could be extrapolated to women.

Ovarian hormones are believed to possess cardiovascular protective effects, and they seem to play a role in the gender-related differences in the development of hypertension in experimental models [81, 82]. Naturally, ovariectomy causes a significant reduction in estradiol and progesterone levels [74, 83]. Comparison of estradiol levels with MABP in DS rats suggests that the OVX-induced increase in MABP is associated with decreased levels of plasma estrogen because estradiol replacement was able to prevent the OVX-induced hypertension [74]. Moreover, estradiol supplementation did not markedly alter circulating progesterone levels in both young and aged DS rats [74]. Furthermore, progesterone levels did not correlate with the difference in MABP between the OVX and OVX-estrogen groups in DS rats [74]. This lack of effect of progesterone supports previous reports in deoxycorticosterone salt hypertension showing that progesterone had no effect on the development of hypertension in OVX rats [82].

9.4.2 Stimulation of Akt/eNOS Signaling Through Estrogen Receptor

Signaling through phosphatidylinositol 3-kinase (PI3K)/Akt pathway is important for the physiological growth and inhibition of pathological hypertrophy [11, 84, 85]. Moreover, physiological hypertrophy induced by exercise training also requires the activation of myocardial Akt. By contrast, pathological hypertrophies induced by pressure overload cause an inactivation of Akt signaling pathway [86]. It is evident that the E2-activated PI3K/Akt pathway functions as one of the acute nongenomic actions of E2 in various types of cells [87]. Studies indicate that young women possess higher levels of nuclear-localized phospho-Akt (Serine 473) relative to comparably aged men or postmenopausal women [88] and Phospho-Akt (Serine 473) is also localized to the nucleus of cultured cardiomyocytes after exposure to E2 [88]. Previous studies have demonstrated that OVX-reduced Akt activation occurs with decreased myocyte contractile function and impaired intracellular calcium handling, whereas E2-upregulated Akt is associated with restored cardiac contractility and intracellular calcium homeostasis [89]. Moreover, activation of the PI3K/Akt pathway is required for E2-suppressed apoptosis and E2-protected myocardial function in the heart following ischemia [68]. Estrogen receptor a mediates increased activation of PI3K/Akt signaling and improved myocardial function in female hearts following acute ischemia [90]. Recent study also suggests that E2-mediated improvement in cardiac function following trauma-hemorrhage is mediated by an increase in cardiac Akt activation [91]. In endothelial cells, estrogen receptors localize to caveolae and their stimulation activate eNOS activity via PI3K/Akt signaling [92, 93]. Strikingly, Grasselli et al. [94] demonstrated that estrogen receptor alpha and eNOS form a complex and translocate to nucleus to bind to the estrogen response element in the promoter region of telomerase catalytic subunit gene, thereby leading to the increase telomerase activity. Since the telomerase activity is critical to determine the lifespan of a cell. This is the first report to define enhancement of telomerase activity by eNOS activation and NO production.

9.4.3 Stimulation of Nitric Oxide Production Through Estrogen Receptor

Men and postmenopausal women may have less endogenous nitric oxide (NO) production, shown by less vasoconstriction following inhibition of NO synthase by L-N-monomethyl-arginine (L-NMMA), than premenopausal women. After estrogen therapy, L-NMMA resulted in greater constriction consistent with estrogen restoring vascular NO activity to levels seen in premenopausal women [95]. Other studies have shown improvement in endothelial function with estrogen therapy

with a greater improvement in hypertensive postmenopausal women [96]. Acute estrogen deprivation after oophorectomy in healthy women results in impaired endothelium-dependent vasodilatation as a result of reduced NO availability [97]. Estrogen therapy improves endothelium-dependent vasodilatation after oophorectomy and also natural menopause [98]. However, among a broader sample of postmenopausal women, HRT results in improved flow-mediated dilation only among women with no cardiovascular risk factors [99, 100]. Studies indicate that estrogen activates eNOS activity through Akt pathway, thereby promoting NO production in heart [87]. Moreover, estrogen mediated Akt activation results in eNOS activation in cultured human endothelial cells [77] and in intact elastic and muscular arteries in vivo [101]. Upregulation of PI3K/Akt by administration of E2 results in endothelial nitric oxide synthase activation via a transcription-independent mechanism [77]. Localization and activity of eNOS are regulated by making a complex with a chaperone protein, heat shock protein 90 and caveolin-3 in cardiomyocytes, especially in caveolae [102]. I also found significantly increased expression of the eNOS regulatory proteins like HSP-90 and caveolin-3 in the hearts of the OVX rats and pressure overload downregulated their expression on the OVX-PO rats [2]. More extensive studies are required to determine temporal changes and immunohistochemical localization of HSP-90 and eNOS after OVX-PO.

Under physiological conditions, myosin light chain (MLC) phosphorylation correlates with increased maximum tension or dp/dt values [103]. In the postmenopausal hypertrophy rat model, I found that phosphorylation was markedly increased only in OVX-PO rats. By contrast, total MLC content was significantly decreased in OVX-PO rats. The increased MLC phosphorylation/total MLC ratio was likely associated in part with an increase in $\pm dP/dt_{max}$ in heart contractile function [2]. Nitric oxide in vascular smooth muscle activates soluble guanylyl cyclase (sGC) to increase cGMP formation, thereby leading to a decrease in $[Ca^{2+}]_i$ with subsequent inhibition of myosin light chain phosphorylation and contraction [104, 105]. My data suggest that ovariectomy followed by pressure overload subsequently increases MLC phosphorylation accompanied by increased cardiac contractility, as observed particularly in OVX-PO rats (Fig. 9.5).

Detailed *in vivo* and *in vitro* studies suggest that underlying mechanisms of estrogen mediated cardioprotection against myocardial hypertrophy are multifold. Estradiol-mediated activation of PI3K signaling blocks angiotensin II- or endothelin-1-initiated cardiomyocyte hypertrophy in vitro via upregulation of the gene encoding modulatory calcineurin-interacting protein (MCIP), a calcineurin antagonist. 17b-estradiol stimulates both the transcriptional transactivation and mRNA stability of the MCIP gene. Interestingly, Estradiol-induced PI3K signaling to MCIP up-regulation does not occur through AKT, as indicated by silencing Akt [106]. As the MCIP1 gene utilizes four different promoters, in a cell context-specific fashion, and so a detailed in vivo analysis is required to further clarify this effect.

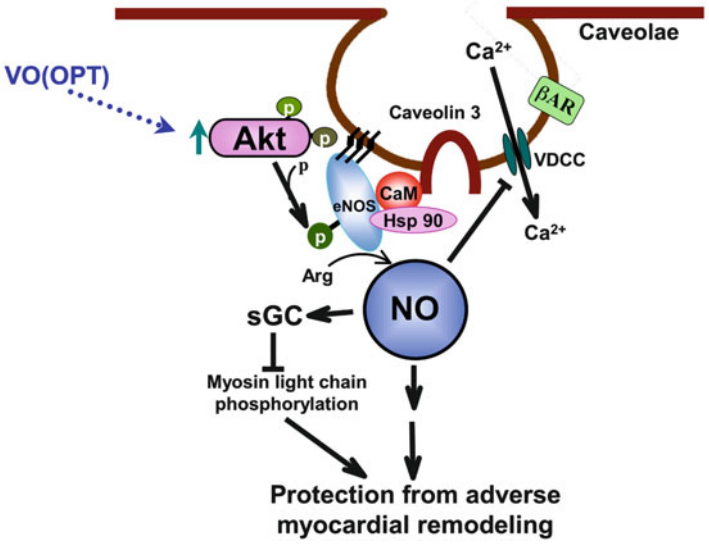

Fig. 9.5 Putative mechanism of VO(OPT) mediated cardioprotection. In normal female heart, eNOS is localized to the caveolae through its interaction with caveolin 3 and compartmentalized with L-type Ca^{2+} channel and b-aderenergic receptor. Activation of Akt signaling ultimately leads to eNOS phosphorylation, eNOS activation and thereby activates nitric oxide signaling pathways. The resulting combination of these effects subsequently confers ventricular dilation and cardioprotection. Pressure overload-induced hypertrophy severely impairs eNOS and Akt signaling pathways, thereby imbalances the NO mediated cardioprotective action. Treatment with VO(OPT) activate the Akt activity and enhances Akt mediated eNOS activity and subsequently confers cardioprotection against myocardial hypertrophy

9.5 Conclusion

Despite numerous studies on postmenopausal cardiac remodeling in hypertension and hypertrophy, we are just beginning to understand the pathophysiology of postmenopausal cardiovascular diseases. Particularly in light of the disappointing cardioprotective results obtained in several clinical trials with hormone replacement therapy, the mechanisms underlying estrogen-mediated cardioprotective action merit further study. In normal female heart, estrogen-mediated increased Akt-eNOS signaling restores the impaired nitric oxide signaling pathways and subsequently confers cardioprotection. In our postmenopausal model of cardiac hypertrophy by ovariectomy and pressure overload, impaired Akt-eNOS signaling imbalances the physiological protective mechanism by nitric oxide. Therefore, menopause likely accounts for cardiac decompensation against chronic stress through impairment of functions of eNOS and Akt signaling, and showed increased mortality following acute cardiac stress caused by chronic β-adrenergic stimulation. The novel model of postmenopausal cardiac decompensation using OVX-PO rats and elucidation of the mechanisms of detrimental cardiac remodeling are attractive for testing

cardioprotective drugs in hypertension-induced cardiac injury in postmenopausal women. Furthermore, Akt/eNOS signaling is central dogma of cardiac remodeling following ischemia and hypertension and vanadium compound therapy instead of HRT is clinically relevant for cardioprotection not only in ischemic injury but also postmenopausal heart disease.

References

1. Bhuiyan MS, Shibuya M, Shioda N, Moriguchi S, Kasahara J, Iwabuchi Y, Fukunaga K (2007) Cytoprotective effect of bis(1-oxy-2-pyridinethiolato)oxovanadium (IV) on myocardial ischemia/reperfusion injury elicits inhibition of Fas ligand and Bim expression and elevation of FLIP expression. Eur J Pharmacol 571:180–188
2. Bhuiyan MS, Shioda N, Fukunaga K (2007) Ovariectomy augments pressure overload-induced hypertrophy associated with changes in Akt and nitric oxide synthase signaling pathways in female rats. Am J Physiol Endocrinol Metab 293:E1606–E1614
3. Bhuiyan MS, Takada Y, Shioda N, Moriguchi S, Kasahara J, Fukunaga K (2008) Cardioprotective effect of vanadyl sulfate on ischemia/reperfusion-induced injury in rat heart in vivo is mediated by activation of protein kinase B and induction of FLICE-inhibitory protein. Cariovasc Ther 26:10–23
4. Bhuiyan MS, Shioda N, Shibuya M, Iwabuchi Y, Fukunaga K (2009) Activation of endothelial nitric oxide synthase by a vanadium compound ameliorates pressure overload-induced cardiac injury in ovariectomized rats. Hypertension 53(1):57–63
5. Oudit GY, Sun H, Kerfant BG, Crackower MA, Penninger JM, Backx PH (2004) The role of phosphoinositide-3 kinase and PTEN in cardiovascular physiology and disease. J Mol Cell Cardiol 37:449–471
6. Hanada M, Feng J, Hemmings BA (2004) Structure, regulation and function of PKB/AKT: a major therapeutic target. Biochim Biophys Acta 1697:3–16
7. Cho H, Thorvaldsen JL, Chu Q, Feng F, Birnbaum MJ (2001) Akt1/PKBalpha is required for normal growth but dispensable for maintenance of glucose homeostasis in mice. J Biol Chem 276:38349–38352
8. Yang ZZ, Tschopp O, Hemmings-Mieszczak M, Feng J, Brodbeck D, Perentes E, Hemmings BA (2003) Protein kinase B alpha/Akt1 regulates placental development and fetal growth. J Biol Chem 278:32124–32131
9. Woulfe D, Jiang H, Morgans A, Monks R, Birnbaum M, Brass LF (2004) Defects in secretion, aggregation, and thrombus formation in platelets from mice lacking Akt2. J Clin Invest 113:441–450
10. Dorn LLGW, Force T (2005) Protein kinase cascades in the regulation of cardiac hypertrophy. J Clin Invest 115:527–537
11. Matsui T, Tao J, del Monte F, Lee KH, Li L, Picard M, Force TL, Franke TF, Hajjar RJ, Rosenzweig A (2001) Akt activation preserves cardiac function and prevents injury after transient cardiac ischemia in vivo. Circulation 104:330–335
12. Ou H, Yan L, Mustafi D, Makinen MW, Brady MJ (2005) The vanadyl (VO^{2+}) chelate bis(acetylacetonato)oxovanadium(IV) potentiates tyrosine phosphorylation of the insulin receptor. J Biol Inorg Chem 10:874–886
13. Theberge JF, Mehdi MZ, Pandey SK, Srivastava AK (2003) Prolongation of insulin-induced activation of mitogen-activated protein kinases ERK 1/2 and phosphatidylinositol 3-kinase by vanadyl sulfate, a protein tyrosine phosphatase inhibitor. Arch Biochem Biophys 420:9–17
14. Mehdi MZ, Srivastava AK (2005) Organo-vanadium compounds are potent activators of the protein kinase B signaling pathway and protein tyrosine phosphorylation: mechanism of insulinomimetics. Arch Biochem Biophys 440:158–164

15. Takada Y, Hashimoto M, Kasahara J, Aihara K, Fukunaga K (2004) Cytoprotective effect of sodium orthovanadate on ischemia/reperfusion-induced injury in the rat heart involves Akt activation and inhibition of fodrin breakdown and apoptosis. J Pharmacol Exp Ther 311: 1249–1255
16. Liem DA, Gho CC, Gho BC, Kazim S, Manintveld OC, Verdouw DD, Duncker DJ (2004) The tyrosine phosphatase inhibitor Bis(Maltolato)oxovanadium attenuates myocardial reperfusion injury by opening ATP-sensitive potassium channels. J Pharmacol Exp Ther 309:1256–1262
17. Fryer RM, Schultz JE, Hsu AK, Gross GJ (1999) Importance of PKC and tyrosine kinase in single or multiple cycles of preconditioning in rat hearts. Am J Physiol 276:1229–1235
18. Przyklenk K, Kloner RA (1998) Ischemic preconditioning: exploring the paradox. Prog Cardiovasc Dis 40:517–547
19. Vahlhaus C, Schulz R, Post H, Rose J, Heusch G (1998) Prevention of ischemic preconditioning only by combined inhibition of protein kinase C and protein tyrosine kinase in pigs. J Mol Cell Cardiol 30:197–209
20. Sakurai H, Shimomura S, Fukuzawa K, Ishizu K (1980) Detection of oxovanadium (IV) and characterization of its ligand environment in subcellular fractions of the liver of rats treated with pentavalent vanadium (V). Biochem Biophys Res Commun 96:293–298
21. Shi X, Dalal SN (1992) Superoxide-independent reduction of vanadate by rat liver microsomes/NAD(P)H: vanadate reductase activity. Arch Biochem Biophys 295:70–75
22. Elberg G, Li J, Shechter Y (1994) Vanadium activates or inhibits receptor and non-receptor protein tyrosine kinases in cell-free experiments, depending on its oxidation state. J Biol Chem 269:9521–9527
23. Willsky GR, White DA, McCabe BC (1984) Metabolism of added orthovanadate to vanadyl and high-molecular-weight vanadates by *Saccharomyces cerevisiae*. J Biol Chem 259: 13273–13281
24. Huyer G, Liu S, Kelly J, Moffat J, Payette P, Kennedy B, Tsaprailis G, Gresser MJ, Ramachandran C (1997) Mechanism of inhibition of protein-tyrosine phosphatases by Vanadate and pervanadate. J Biol Chem 272:843–851
25. Reul BA, Amin SS, Buchet JP, Ongemba LN, Crans DC, Brichard SM (1999) Effect of vanadium complexes with organic ligands on glucose metabolism: a comparison study in diabetic rats. Br J Pharmacol 126:467–477
26. Strout HV, Vicario PP, Saperstein R et al (1989) The insulin-mimetic effect of vanadate is not correlated with insulin receptor tyrosine kinase activity or phosphorylation in mouse diaphragm *in vivo*. Endocrinology 124:1918–1924
27. Meyerovitch J, Farfel Z, Sack J et al (1987) Oral administration of vanadate normalizes blood glucose levels in streptozotocin-treated rats: characterization and mode of action. J Biol Chem 262:6658–6662
28. Srivastava AK (2000) Anti-diabetic and toxic effects of vanadium compounds. Mol Cell Biochem 206:177–182
29. Sakurai H, Sano H, Takino T, Yasui H (2000) An orally active antidiabetic vanadyl complex, bis(1-oxy-2-pyridinethiolato)oxovanadium(IV), with $VO(S_2O_2)$ coordination mode; in vitro and in vivo evaluations in rats. J Inorg Biochem 80:99–105
30. Takeshita S, Kawamura I, Yasuno T et al (2001) Amelioration of insulin resistance in diabetic ob/ob mice by a new type of orally active insulin-mimetic vanadyl complex: bis(1-oxy-2-pyridinethiolato) oxovanadium (IV) with VO(S2O2) coordination mode. J Inorg Biochem 85:179–186
31. Fantus IG, Tsiani E (1998) Multifunctional actions of vanadium compounds on insulin signaling pathways: evidence for preferential enhancement of metabolic versus mitogenic effects. Mol Cell Biochem 182:109–119
32. Faure R, Vincent M, Dufour M et al (1995) Arrest at the G2/M transition of the cell cycle by protein-tyrosine phosphatase inhibition: studies on a neuronal and a glial cell line. J Cell Biochem 59:389–401
33. Djordjevic C (1995) Antitumor activity of vanadium compounds. Met Ions Biol Syst 31: 595–616

34. Liasko R, Kabanos TA, Karkabounas S et al (1998) Beneficial effects of a vanadium complex with cysteine, administered at low doses on benzo (alpha) pyrene-induced leiomyosarcomas in Wistar rats. Anticancer Res 18:3609–3613
35. Blondel O, Bailbe D, Portha B (1989) *In vivo* insulin resistance in streptozotocin diabetic rats – evidence for reversal following oral vanadate treatment. Diabetologia 32:185–190
36. Al-Bayati MA, Giri SN, Raah OG (1990) Time and dose response study of the effects of vanadate in rats: changes in blood cells, serum enzymes, protein, cholesterol, glucose, calcium and inorganic phosphate. J Environ Pathol Toxicol Oncol 10:206–213
37. Bishayee A, Cecchin F (1995) Time course effects of vanadium supplements on cytosolic reduced glutathione level and glutathione S-transferase activity. Biol Trace Elem Res 48: 275–285
38. Mongold JJ, Cros GH, Vian L et al (1990) Toxicological aspects of vanadyl sulphate on diabetic rats: effects on vanadium levels and pancreatic B-cell morphology. Pharmacol Toxicol 67:192–198
39. Goldfine AB, Simonson DC, Folli F et al (1995) *In vivo* and *in vitro* studies of vanadate in human and rodent diabetes mellitus. Mol Cell Biochem 153:217–231
40. Kawano T, Fukunaga K, Takeuchi Y, Morioka M, Yano S, Hamada J, Ushio Y, Miyamoto E (2001) Neuroprotective effect of sodium orthovanadate on delayed neuronal death after transient forebrain ischemia in gerbil hippocampus. J Cereb Blood Flow Metab 21: 1268–1280
41. Datta SR, Dudek H, Tao X, Masters S, Fu H, Gotoh Y, Greenberg ME (1997) Akt phosphorylation of BAD couples survival signals to the cell-intrinsic death machinery. Cell 91:231–241
42. Burgering BMT, Kops GJPL (2002) Cell cycle and death control: long live Forkheads. Trends Biochem Sci 27:352–360
43. Fukunaga K, Ishigami T, Kawano T (2005) Transcriptional regulation of neuronal genes and its effect on neural functions: expression and function of forkhead transcription factors in neurons. J Pharmacol Sci 98:205–211
44. Shioda N, Han F, Moriguchi S, Fukunaga K (2007) Constitutively active calcineurin mediates delayed neuronal death through Fas-ligand expression via activation of NFAT and FKHR transcriptional activities in mouse brain ischemia. J Neurochem 102:1506–1517
45. Brunet A, Bonni A, Zigmond MJ, Lin MZ, Juo P, Hu LS, Anderson MJ, Arden KC, Blenis J, Greenberg ME (1999) Akt promotes cell survival by phosphorylating and inhibiting a Forkhead transcription factor. Cell 96:857–868
46. Skurk C, Maatz H, Kim HS, Yang J, Abid MR, Aird WC, Walsh K (2004) The Akt-regulated forkhead transcription factor FOXO3a controls endothelial cell viability through modulation of the caspase-8 inhibitor FLIP. J Biol Chem 279:1513–1525
47. Suhara T, Mano T, Oliveira BE, Walsh K (2001) Phosphatidylinositol 3-Kinase/Akt signaling controls endothelial cell sensitivity to fas-mediated apoptosis via regulation of FLICE-inhibitory protein (FLIP). Circ Res 89:13–19
48. Rasper DM, Vaillancourt JP, Hadano S, Houtzager VM, Seiden I, Keen SL, Tawa P, Xanthoudakis S, Nasir J, Martindale D, Koop BF, Peterson EP, Thornberry NA, Huang J, MacPherson DP, Black SC, Hornung F, Lenardo MJ, Hayden MR, Roy S, Nicholson DW (1998) Cell death attenuation by 'Usurpin', a mammalian DED-caspase homologue that precludes caspase-8 recruitment and activation by the CD-95 (Fas, APO-1) receptor complex. Cell Death Differ 5:271–288
49. Imanishi T, Murry CE, Reinecke H, Hano T, Nishio I, Liles WC, Hofsta L, Kim K, O'Brien KD, Schwartz SM, Han DK (2000) Cellular FLIP is expressed in cardiomyocytes and down-regulated in TUNEL-positive grafted cardiac tissues. Cardiovasc Res 48:101–110
50. Gottilieb RA, Engler RL (1999) Apoptosis in myocardial ischemia–reperfusion. Ann NY Acad Sci 874:412–426
51. Belchetz PE (1994) Hormonal treatment of postmenopausal women. N Engl J Med 330: 1062–1071

52. Turgeon JL, McDonnell DP, Martin KA, Wise PM (2004) Hormone therapy: physiological complexity belies therapeutic simplicity. Science 304:1269–1273
53. Gorodeski GI (2002) Update on cardiovascular disease in post-menopausal women. Best Pract Res Clin Obstet Gynaecol 16:329–355
54. Mosca L, Manson JE, Sutherland SE, Langer RD, Manolio T, Barrett-Connor E (1997) Cardiovascular disease in women: a statement for healthcare professionals from the American Heart Association. Writing Group. Circulation 96:2468–2482
55. Kannel WB (1983) Prevalence and natural history of electrocardiographic left ventricular hypertrophy. Am J Med 3:4–11
56. Howe HL (1984) Age-specific hysterectomy and oophorectomy prevalence rates and the risks for cancer of the reproductive system. Am J Public Health 74:560–563
57. Howard BV, Kuller L, Langer R, Manson JE, Allen C, Assaf A, Cochrane BB, Larson JC, Lasser N, Rainford M, Van Horn L, Stefanick ML, Trevisan M (2005) Risk of cardiovascular disease by hysterectomy status, with and without oophorectomy: the Women's Health Initiative Observational Study. Circulation 111: 1462–1470
58. Melton LJ 3rd, Bergstralha QEJ, Malkasian GD, O'Fallon WM (1991) Bilateral oophorectomy trends in Olmsted County, Minnesota, 1950–1987. Epidemiology 2:149–152
59. Whiteman MK, Hillis SD, Jamieson DJ, Morrow B, Podgornik MN, Brett KM, Marchbanks PA (2008) Inpatient hysterectomy surveillance in the United States, 2000–2004. Am J Obstet Gynecol 198(34):e1–e7
60. Keshavarz H, Hillis SD, Kieke BA, Marchbanks PA (2002) Hysterectomy surveillance-United States, 1994–1999. MMWR Surveill Summ 51:1–8
61. Shuster LT, Gostout BS, Grossardt BR, Rocca WA (2008) Prophylactic oophorectomy in premenopausal women and long term health- a review. Menopause Int 14:111–116
62. Lobo RA (2007) Surgical menopause and cardiovascular risks. Menopause 14:562–566
63. Lokkegaard E, Jovanovic Z, Heitmann BL, Keiding N, Ottesen B, Pedersen AT (2006) The association between early menopause and risk of ischaemic heart disease: influence of hormone therapy. Maturitas 53:226–233
64. Rossouw JE, Prentice RL, Manson JE, Wu L, Barad D, Barnabei VM, Ko M, LaCroix AZ, Margolis KL, Stefanick ML (2007) Postmenopausal hormone therapy and risk of cardiovascular disease by age and years since menopause. JAMA 297:1465–1477
65. Dubey RK, Imthurn B, Barton M, Jackson EK (2005) Vascular consequences of menopause and hormone therapy: importance of timing of treatment and type of estrogen. Cardiovasc Res 66:295–306
66. Leinwand LA (2003) Sex is a potent modifier of the cardiovascular system. J Clin Invest 112:302–307
67. Hayward CS, Kelly RP, Collins P (2000) The roles of gender, the menopause and hormone replacement on cardiovascular function. Cardiovasc Res 46:28–49
68. Patten RD, Pourati I, Aronovitz MJ, Baur J, Celestin F, Chen X, Michael A, Haq S, Nuedling S, Grohe C, Force T, Mendelsohn ME, Karas RH (2004) 17beta-estradiol reduces cardiomyocyte apoptosis in vivo and in vitro via activation of phospho-inositide-3 kinase/Akt signaling. Circ Res 95:692–699
69. Van Eickels M, Grohe C, Cleutjens JP, Janssen BJ, Wellens HJ, Doevendans PA (2001) 17beta-estradiol attenuates the development of pressure-overload hypertrophy. Circulation 104:1419–1423
70. Thorndike EA, Turner AS (1998) In search of an animal model for postmenopausal diseases. Front Biosci 3:c17–c26
71. Fang Z, Carlson S, Chen Y, Oparil S, Wyss J (2001) Estrogen depletion induces NaCl-sensitive hypertension in female spontaneously hypertensive rats. Am J Physiol Regul Integr Comp Physiol 281:R1934–R1939
72. Peng N, Clark J, Wei C, Wyss J (2003) Estrogen depletion increases blood pressure and hypothalamic norepinephrine in middle-aged spontaneously hypertensive rats. Hypertension 41:1164–1167

73. Fortepiani LA, Zhang H, Racusen LC, Roberts LJ II, Reckelhoff JF (2003) Characterization of an animal model of postmenopausal hypertension in SHR. Hypertension 41:640–645
74. Hinojosa-Laborde C, Craig T, Zheng W, Ji H, Haywood JR, Sandberg K (2004) Ovariectomy augments hypertension in aging female Dahl salt sensitive rats. Hypertension 44:405–409
75. Javeshghani D, Touyz R, Sairam M, Virdis A, Neves M, Schiffrin E (2003) Attenuated responses to angiotensin II in follitropin receptor knockout mice, a model of menopause-associated hypertension. Hypertension 42:761–767
76. Bhuiyan MS, Fukunaga K (2010) Characterization of an animal model of post menopausal cardiac hypertrophy and novel mechanisms responsible for cardiac decompensation using ovariectomized pressure-overloaded rats. Menopause 17:213–221
77. Haynes MP, Sinha D, Russell KS, Collinge M, Fulton D, Morales-Ruiz M, Sessa WC, Bender JR (2000) Membrane estrogen receptor engagement activates endothelial nitric oxide synthase via the PI3-kinase-Akt pathway in human endothelial cells. Circ Res 87:677–682
78. Ciric O, Susic D (1980) Effect of isoprenaline on blood pressure and heart rate in different phases of the oestrous cycle. Endokrinologie 76:274–278
79. Thawornkaiwong A, Preawnim S, Wattanapermpool J (2003) Upregulation of beta 1-adrenergic receptors in ovariectomized rat hearts. Life Sci 72:1813–1824
80. Kam KW, Kravtsov GM, Liu J, Wong TM (2005) Increased PKA activity and its influence on isoprenaline-stimulated L-type Ca^{2+} channels in the heart from ovariectomized rats. Br J Pharmacol 144:972–981
81. Cambotti LJ, Cole FE, Gerall AA, Frolich ED, Macphee AA (1984) Neonatal gonadal hormones and blood pressure in the spontaneously hypertensive rat. Am J Physiol 247: E258–E264
82. Crofton JT, Share L (1997) Gonadal hormones modulate deoxycorticosterone-salt hypertension in male and female rats. Hypertension 29:494–499
83. David FL, Carvalho MHC, Cobra ALN, Nigro D, Fortes ZB, Rebouças NA, Tostes RCA (2001) Ovarian hormones modulate endothelin-1 vascular reactivity and mRNA expression in DOCA-salt hypertensive rats. Hypertension 38:692–696
84. Kureishi Y, Luo Z, Shiojima I, Bialik A, Fulton D, Lefer DJ, Sessa WC, Walsh K (2000) The HMG-CoA reductase inhibitor simvastatin activates the protein-kinase Akt and promotes angiogenesis in normocholesterolemic animals. Nat Med 6:1004–1010
85. Fujio Y, Nguyen T, Wencker D, Kitsis RN, Walsh K (2000) Akt promotes survival of cardiomyocytes in vitro and protects against ischemia-reperfusion injury in mouse heart. Circulation 101:660–667
86. Kemi OJ, Celi M, Wisloff U, Grimaldi S, Gallo P, Smith GL, Condorelli G, Ellingsen O (2008) Activation or inactivation of cardiac Akt/mTOR signaling diverges physiological from pathological hypertrophy. J Cell Physiol 214:316–321
87. Simoncini T, Hafezi-Moghadam A, Brazil DP, Ley K, Chin WW, Liao JK (2000) Interaction of oestrogen receptor with the regulatory subunit of phosphatidylinositol-3′-OH kinase. Nature 407:538–541
88. Camper-Kirby D, Welch S, Walker A, Shiraishi I, Setchell KD, Schaefer E, Kajstura J, Anversa P, Sussman MA (2001) Myocardial Akt activation and gender: increased nuclear activity in females versus males. Circ Res 88:1020–1027
89. Ren J, Hintz KK, Roughead ZK, Duan J, Colligan PB, Ren BH, Lee KJ, Zeng H (2003) Impact of estrogen replacement on ventricular myocyte contractile function and protein kinase B/Akt activation. Am J Physiol Heart Circ Physiol 284:H1800–H1807
90. Wang M, Wang Y, Weil B, Abarbanell A, Herrmann J, Tan J, Kelly M, Meldrum DR (2009) Estrogen receptor beta mediates increased activation of PI3K/Akt signaling and improved myocardial function in female hearts following acute ischemia. Am J Physiol Regul Integr Comp Physiol 296:R972–R978
91. Hsu JT, Kan WH, Hsieh CH, Chowdhry MA, Bland KI, Chaudry IH (2009) Mechanism of salutary effects of estrogen on cardiac function following trauma-hemorrhage: Akt-dependent HO-1 up-regulation. Crit Care Med 37:1–7

92. Chen Z, Yuhanna IS, Galcheva-Gargova Z, Karas RH, Mendelsohn ME, Shaul PW (1999) Estrogen receptor alpha mediates the nongenomic activation of endothelial nitric oxide synthase by estrogen. J Clin Invest 103:401–406
93. Chambliss KL, Yuhanna IS, Mineo C, Liu P, German Z, Sherman TS, Mendelsohn ME, Anderson RG, Shaul PW (2000) Estrogen receptor alpha and endothelial nitric oxide synthase are organized into a functional signaling module in caveolae. Circ Res 87:e44–e52
94. Grasselli ANS, Colussi C, Aiello A, Benvenuti V, Moretti F, Sacchi A, Bacchtt S, Gaetano C, Capogrossi MC, Pontecrvi A, Farsetti A (2008) Estrogen receptor alpha and endothelial nitric oxide synthase nuclear complex regulates transcription of human teromerase. Circ Res 103:34–42
95. Majmudar NG, Robson SC, Ford GA (2000) Effects of the menopause, gender, and estrogen replacement therapy on vascular nitric oxide activity. J Clin Endocrinol Metab 85:1577–1583
96. Higashi Y, Sanada M, Sasaki S, Nakagawa K, Goto C, Matsuura H, Ohama K, Chayama K, Oshima T (2001) Effect of estrogen replacement therapy on endothelial function in peripheral resistance arteries in normotensive and hypertensive postmenopausal women. Hypertension 37:651–657
97. Virdis A, Ghiadoni L, Pinto S, Lombardo M, Petraglia F, Gennazzani A, Buralli S, Taddei S, Salvetti A (2000) Mechanisms responsible for endothelial dysfunction associated with acute estrogen deprivation in normotensive women. Circulation 101:2258–2263
98. Sanada M, Higashi Y, Nakagawa K, Tsuda M, Kodama I, Kimura M, Chayama K, Ohama K (2002) Hormone replacement effects on endothelial function measured in the forearm resistance artery in normocholesterolemic and hypercholesterolemic postmenopausal women. J Clin Endocrinol Metab 87:4634–4641
99. Herrington DM (1995) Dehydroepiandrosterone and coronary atherosclerosis. Ann NY Acad Sci 774:271–280
100. Kelemen M, Vaidya D, Waters DD, Howard BV, Cobb F, Younes N, Tripputti M, Ouyang P (2005) Hormone therapy and antioxidant vitamins do not improve endothelial vasodilator function in postmenopausal women with established coronary artery disease: a substudy of the Women's Angiographic Vitamin and Estrogen (WAVE) trial. Atherosclerosis 179: 193–200
101. Guo X, Razandi M, Pedram A, Kassab G, Levin ER (2005) Estrogen induces vascular wall dilation: mediation through kinase signaling to nitric oxide and estrogen receptors a and b. J Biol Chem 280:19704–19710
102. Fulton D, Gratton J-P, Sessa WC (2001) Post-translational control of endothelial nitric oxide synthase: why isn't calcium/calmodulin enough? J Pharmacol Exp Ther 299:818–824
103. Solaro RJ (1986) Protein phosphorylation and cardiac myofilaments. In: Solaro RJ (ed) Protein phosphorylation in heart muscle. CRC, Boca Raton, pp 129–156
104. Pabla R, Curtis MJ (1996) Effect of endogenous nitric oxide on cardiac systolic and diastolic function during ischemia and reperfusion in the rat isolated perfused heart. J Mol Cell Cardiol 28:2111–2121
105. Schmidt HHHW, Lohmann SM, Walter U (1993) The nitric oxide and cGMP signal transduction system: regulation and mechanism of action. Biochim Biophys Acta 1178: 153–175
106. Pedram A, Razandi M, Aitkenhead M, Levin ER (2005) Estrogen inhibits cardiomyocyte hypertrophy *in vitro*. Antagonism of calcineurin-related hypertrophy through induction of MCIP1. J Biol Chem 280:26339–26348

Chapter 10
Inhalation Toxicity of Vanadium

Farida Louise Assem and Leonard Stephen Levy

Abstract This section presents an overview of the toxicology of vanadium and inorganic vanadium compounds following inhalation. The well known respiratory effects associated with inhalation of vanadium compounds are the main focus, since they have been found to be the most sensitive endpoint following exposure to vanadium compounds in a number of occupational settings. We will also take a brief look at the possible mechanisms underlying these respiratory effects and how health standard-setting bodies have interpreted the current dataset in relation to human health risk assessment and setting of occupational and general population standards.

Keywords Occupational • Environmental • Toxicology • Respiratory • Mechanisms • Mode of action • Genotoxicity • Inflammation • Carcinogenicity

10.1 Occupational and Environmental Sources and Routes of Exposure to Vanadium Compounds

Vanadium is a naturally occurring element, present in many different mineral forms in the earth's crust. Natural release of vanadium to the environment occurs from weathering of soil and rock, continental dusts, marine aerosols and volcanic activity. However anthropogenic activity contributes to environmental vanadium levels to a greater extent than natural sources. Anthropogenic input of vanadium to the

F.L. Assem
ICF International, 9300 Lee highway, Fairfax, VA 22031, USA
e-mail: lAssem@icfi.com

L.S. Levy (✉)
Institute of Environment and Health, Cranfield University, Cranfield, Bedfordshire MK43 0AL, UK
e-mail: len.levy@cranfield.ac.uk

H. Michibata (ed.), *Vanadium: Biochemical and Molecular Biological Approaches*,
DOI 10.1007/978-94-007-0913-3_10,

atmosphere arises primarily from industrial sources involved in fuel combustion e.g. power plants and oil refineries.

In humans, inhalation and oral exposure routes are the most important; dermal is not considered to be a significant route of vanadium exposure and unlike certain other metals such as nickel and cobalt, vanadium has not been associated with dermal sensitisation.

For the general population, ingestion is the major exposure route with food being the major source of vanadium (mainly in the form of VO^{2+} (vanadyl, V(IV)) or HVO_4^{2-} (vanadate, V(V)). Dietary intakes range from 0.01 to 0.02 mg/day; average intake from drinking water is approximately 5–10-fold less [1]. Daily intakes of vanadium (i.e. vanadyl sulphate and sodium metavanadate) from dietary supplements may exceed intake levels from food and water, although vanadium as an essential element in humans has not been confirmed. General population intake of vanadium from the air is relatively low compared to intake from food, although smokers may be exposed to higher levels of vanadium contained in cigarette smoke.

Occupational exposure to vanadium oxide-containing particles may arise during the production of certain steels, handling of vanadium pentoxide (V_2O_5)-containing catalysts and pigments or colouring agents where vanadium is used. Exposure to vanadium may also occur during the cleaning of oil-fired boilers and furnaces, since organically-complexed vanadium contained in crude oil and coal can in part be converted into V_2O_5 during combustion.

10.2 Some Current Classifications and Health Standards for Vanadium

A summary of some current and draft occupational and general population health standards and classifications for carcinogenicity is given in Table 10.1. Irritation of the eyes and respiratory tract and other effects on the lungs as a result of over-exposure to vanadium metal and its compounds in occupational settings has been well documented [6] and health standards have generally been recommended based on respiratory tract irritation effects in humans [3, 4] or in experimental animals [5].

10.3 Respiratory Tract Irritation Effects of Inorganic Vanadium

Respiratory tract irritation effects in workers exposed to vanadium compounds for short or longer durations are well known. Similar irritation effects are found in studies with experimental animal, although evidence of lung tumours seen in mice exposed to V_2O_5 in a long-term cancer bioassay has not been reported in workers exposed long-term to vanadium or its inorganic compounds in the workplace.

Table 10.1 Summary of health standards and recommendations (occupational and general population) for long-term repeated exposure to vanadium and its compounds

Agency	Year	Standard/classification	Description	Basis for standard
IARC [2]	2006	Group 2B (V_2O_5). There is *inadequate evidence* in humans for the carcinogenicity of vanadium pentoxide. There is *sufficient evidence* in experimental animals for the carcinogenicity of vanadium pentoxide	Possibly carcinogenic to humans	Based on significantly increased incidences of alveolar/bronchiolar neoplasms in mice and increases in male rats. Absence of human epidemiological data on the carcinogenicity of V_2O_5
ACGIH [3]	2008	0.05 mg V/m^3 (V_2O_5)	Workplace: TLV (8 h TWA) V_2O_5 (respirable fraction of dust or fume, as V_2O_5)	Chronic upper airway irritation based on human data from Kiviluoto et al. [4]
ACGIH [3]	2008	A3 (V_2O_5)	Confirmed animal carcinogen with unknown relevance to humans	Clear evidence of carcinogenic effects in mice and equivocal evidence in rats from the NTP study [5]. No available human epidemiological data on the carcinogenicity of vanadium
ATSDR [1]	2009	0.0001 mg vanadium/m^3 (V_2O_5 dust), (draft)	General population: Chronic-Duration ≥1 yr Inhalation Minimal Risk Level (MRL)	Non-cancer respiratory endpoints in rats exposed to V_2O_5 in the NTP study [5], specifically degeneration of epiglottis respiratory epithelium was used as the point of departure
US EPA[a]	1996/1988	–	General population: Reference concentration (RfC) and carcinogenicity assessment	RfC not assessed during last review in 1996 Carcinogenicity assessed in 1988, prior to NTP study

[a]Under assessment, final revised assessment due in 2012

10.3.1 Respiratory Tract Irritation in Vanadium-Exposed Workers

Studies in humans have demonstrated that acute and long-term exposure to vanadium dust in the form of vanadyl or vanadate results in eye and/or respiratory tract irritation in workers sometimes coupled with a green discolouration of the tongue, a typical sign of vanadium exposure, but with an absence of adverse effects on pulmonary function [7–11].

In a volunteer study, nine volunteers were exposed to respirable V_2O_5 (<5 μm) at a nominal concentration of 1 mg/m^3 (n = 2), 0.25 mg/m^3 (n = 5) or 0.1 mg/m^3 (n = 2), for 8 h [10]. Toward the end of exposure to 1 mg/m^3, coughing was evident in the volunteers, while delayed onset of this symptom manifest in volunteers exposed to lower concentrations of V_2O_5. No other symptoms or changes in pulmonary function were found.

Levy et al. [9] reported respiratory irritation in male boiler workers exposed to high levels of V_2O_5 (0.05–5.3 mg/m^3) during the conversion of an oil power plant to coal. Shifts lasted for approximately 10 h/6 days per week, and the conversion job took approximately 4–6 weeks. Exposure to other metals, (chromium, iron, nickel and copper) metal fume and respiratory tract irritants (carbon monoxide, nitrogen dioxide, hydrogen sulphide, sulphur dioxide and ozone) were either undetected or present at low or transient levels (within the OSHA permissible exposure limits at the time). The major symptoms reported by questionnaire (n = 55) were: cough with sputum, sore throat, dyspnoea on exertion, chest pain or discomfort, headache, runny nose or sneezing eye irritation and wheezing. Wheezing was also recorded in 27/70 (39%) workers upon examination by a physician. Bronchitis was the most common clinical diagnosis in the 70/100 workers seen by a physician. The median latency period was 1 week.

Longer-term exposure i.e. several months to several years to vanadium compounds can result in similar respiratory effects such as cough or wheezing [7, 11]. Bronchial hyper-responsiveness to inhaled histamine or exercise challenge has also been reported in 12/40 vanadium plant workers exposed to typical TWA concentrations (assessed over a 1 week period) of <0.05–1.53 soluble vanadium mg/m^3, with persistent respiratory symptoms [11]; workers were exposed to vanadium in ore and in the vanadate and vanadyl form, in addition to SO_2, and NH_3 other respiratory tract irritants. Wheezing was also more common among male workers exposed to vanadium compared to matched controls (typical TWA concentration during time of study: <0.03 mg total V/m^3; 20% particles <5 μm; typical concentrations over several years: <0.5 mg total V/m^3; higher exposures evident during dustier tasks), while no clinically relevant differences in lung function [7] or haematological or clinical parameters were found [12].

Lung function tests following both short-term and long-term exposure, appeared to be unchanged [7, 10, 11]. In summary, acute and/or sub-acute occupational exposure to vanadium compounds results in symptoms of respiratory tract irritation

(e.g. cough, wheezing, dyspnoea, sore throat, epiphora (excessive tear production)); longer-term exposure may also result in similar respiratory tract irritation effects. Recovery is generally evident, following removal from exposure [8, 11, 13].

10.3.2 Respiratory Tract Irritation in Vanadium-Exposed Experimental Animals

Respiratory effects in animals exposed to vanadium compounds support the findings in workers and also show that compound solubility (and thus bioavailability) influences the timing of the onset of effects. Knecht et al. [14] illustrated this in an acute exposure study in cynomolgus monkeys exposed to either V_2O_5 or a soluble solution of vanadate aerosol. Delayed impaired lung air-flow (assessed 1 day after exposure) was associated with an increase in neutrophils in bronchoalveolar lavage fluid (BAL) in monkeys exposed to a single nominal V_2O_5 aerosol concentration of 5 mg/m^3 for 6 h. This compares to an immediate impairment of lung function in monkeys exposed by intrabronchial aerosolisation to a single dose of soluble vanadium (vanadate solution, 0.38 or 0.76 M vanadium) [14]. This finding is supported by the results of Pierce et al. [15], who reported pulmonary inflammation, characterised by an influx of neutrophils into the lungs of female CD rats, following single exposures to $NaVO_3$, $VOSO_4$ or V_2O_5 by intratracheal instillation. The authors noted that the onset and magnitude of the response was dependent on compound solubility; influx was highest in $VOSO_4$-treated rats and double the concentration of vanadium in the form of V_2O_5 compared to the more soluble $NaVO_3$ or $VOSO_4$ was required to elicit a response. Similarly, male BALB/cJ mice (n = 4/group), given a single dose of $NaVO_3$ (50 μg/mouse) by intratracheal instillation exhibited a time-dependent increase in neutrophils, macrophages and apoptotic lung cells in BAL fluid [16].

Sub-acute inhalation (full body) exposure of rats and mice to V_2O_5 (2–32 mg/m^3) for 6 h/day, 5 days/week for 16 days demonstrated increases in relative lung weights associated with pulmonary inflammation i.e. increased total cell number, protein, neutrophils, and lysozyme in BAL, without evidence of immunological effects [5]. Fibrosis was also found in rats exposed for 13 days to 4 mg/m^3, but only in mice exposed for 2 years. In mice pulmonary lesions were both duration and concentration-related. Knecht et al. [17] demonstrated a similar response in sub-chronically exposed cynomolgus monkeys (n = 8 per group), given up to 0.5 mg V_2O_5/m^3 (6 h/day 5 days/week for 26 weeks) and noted that repeated exposure did not lead to a cellular immune response, enhanced bronchial reactivity, or an exacerbation of the acute responsivity reported by Knecht et al. [14], suggesting that the animals developed some measure of tolerance as a result of repeated exposure [17]. However, the series of studies conducted by the NTP, found a progressive worsening of effects over time and in relation to exposure concentration. Increased relative lung weights associated with inflammation or fibrosis (rats only)

were also seen in rats and mice exposed to V_2O_5 for 3 months, ≥2 mg/m^3 (males) and ≥4 mg/m^3 (females), in addition to epithelial hyperplasia in the distal airways and alveolar ducts and alveoli at ≥2 mg/m^3. Epithelial cells appeared morphologically similar to bronchioles and were larger and rounded in appearance. Inflammation (accumulation of macrophages with abundant foamy cytoplasm) was apparent in rat alveoli adjacent to the epithelial hyperplasia. These changes were similar to those seen in the 16 day NTP study [5]. Squamous metaplasia located in an area of hyperplasia was observed in a female rat exposed at the highest concentration (16 mg V_2O_5/m^3). At higher exposure levels than those resulting in pulmonary effects in rats (≥4 mg/m^3 in females, ≥8 mg/m^3 in males) hyperplasia and metaplasia of the nasal respiratory epithelium was seen, and inflammation (influx of lymphocytes and neutrophils) at the highest concentration. Exposure-related changes in lung function were evident at ≥4 mg/m^3, which were indicative of restrictive disease.

In terms of chronic exposure, the only available study is the 2 year NTP [5] cancer bioassay in groups of F334/N rats and B6C3F$_1$ mice (50/sex). Exposure to particulate aerosols of V_2O_5 (mean mass median aerodynamic diameter: 1.2 and 1.3 μm in the chambers of rats and mice, respectively) at concentrations of 0, 0.5, 1 or 2 mg/m^3 (rats) 0, 1, 2 or 4 mg/m^3 (mice) for 6 h per day, 5 days per week, for 104 weeks caused a range of lung and respiratory tract non-neoplastic effects, somewhat similar to those observed following shorter exposure durations. The findings of the study have been well documented and discussed in the literature [18–21]. Respiratory effects included concentration-related chronic inflammation and interstitial fibrosis in the lungs of both species at all except the lowest exposure. Upper and lower respiratory tract pathology, including alveolar and bronchiolar epithelial hyperplasia, was observed at all treatment exposures and of particular interest was the finding of squamous metaplasia associated with keratin production in the alveoli of male and to a lesser extent female rats at 2 mg V_2O_5/m^3, extending occasionally to the distal airways in males. Nasal epithelial changes of varying intensity were also observed in both species at some exposures. This study is of particular relevance as the pathological changes in the lungs and respiratory tract are generally consistent with the reported changes in exposed humans and, therefore, provide a convincing base for standard setting in the absence of reliable human data.

10.4 Lung Cancer

There are currently no epidemiological studies available that have assessed the potential for inorganic vanadium compounds to cause occupational lung cancer. One of the reasons for this is probably the difficulty in finding well-defined cohorts exposed to specific vanadium compounds. Another issue is the need to address co-exposures to other known lung carcinogens, such as tobacco smoke, asbestos, crystalline silica, and metals (chromium (VI) and nickel), which would confound results. In addition, although a number of positive *in vitro* studies have

demonstrated the genotoxic potential of vanadium compounds, there are limited studies available in humans. Indeed only two are currently available, one of which reported negative results [22], the other reported positive results for increases in markers of DNA damage in vanadium-exposed workers [23]. Overall the weight of evidence for the genotoxic potential for vanadium *in vivo* in animals and humans is equivocal; nonetheless the positive findings *in vitro* remain indicating a potential for carcinogenic effects in occupationally-exposed workers that needs exploration. These data are discussed in more detail later on in the section. The limited dataset on carcinogenicity has led to a understandable reliance by standard and classification-setting agencies on the 2 year NTP [5] study in rats and mice.

In the NTP study [5], alveolar/bronchiolar neoplasms were seen in all male rat groups (including controls) at levels that exceeded historic controls (4/50 (8%), 10/49 (20%), 6/48 (13%), and 9/50 (18%) in the 0, 0.5, 1, and 2 mg/m^3 groups respectively). The numbers of tumours in V_2O_5-treated male rats were not statistically greater than control levels, although surprisingly, they were still considered by the study authors to be treatment-related. The tumours, alveolar/bronchiolar adenomas, were described as distinct masses, typical of spontaneously occurring tumours, while alveolar/bronchiolar carcinomas were larger with, in some cases, local invasion or metastasis. In contrast to the concentration-related non-neoplastic inflammatory lesions that were seen in the lung, larynx and nasal passages of all V_2O_5-exposed groups, there was no exposure-response relationship in the occurrence of these tumours. Similar, though less frequent, lung tumours were also seen in female rats; 3/49 (6%; adenomas) in the 0.5 mg/m^3 group, 1/50 (2%; adenoma) in the 1 mg/m^3 group and 1/50 (2%; carcinoma) in the 2 mg/m^3 group, compared to none in controls. In mice the incidences of alveolar/bronchiolar neoplasms (adenomas and carcinomas) were significantly increased in all treated groups (males: 22/50 (44%), 42/50 (84%), 43/50 (86%), 43/50 (86%); females 1/50 (2%) 32/50 (64%) 35/50 (70%) 32/50 (64%)), but surprisingly, there was no concentration-response relationship.

These tumours arose from a background of widespread and marked inflammatory changes which affected the whole of the lung and respiratory tract. Furthermore, the numbers of lung tumours in rats were relatively few, not concentration-related as one would expect for a causal relationship, and not remarkable compared to historical controls (0–6% for the NTP-2000 diet) for this strain [20]. These findings, coupled with the lack of observed mutagenicity of V_2O_5 *in vivo* in mice [5] do not suggest that V_2O_5 is a classical genotoxic carcinogen. Rather, it might be interpreted as a weak and local (to the lung) carcinogen acting through a secondary (non-genotoxic) mechanism. A typical "lung particle overload" response from an inert insoluble particle would normally evoke a dose-related increase in lung tumours (alveolar/bronchiolar and carcinomas) in rats, and a negative response in mice, although there would have been dose-related inflammatory responses in both species. This was not the case for the NTP [5] studies and it is difficult to assess what contribution the particle overload effect might have made to the overall pathological outcome, as the particle size would have guaranteed penetration to the deep lung (including alveoli) and V_2O_5 is described as sparingly soluble in water (0.1–0.8 g/100 cm^3; [2]).

10.5 Genotoxicity of Inorganic Vanadium

To date, there are no studies available in humans or experimental animals which have assessed genotoxic effects in the lung following inhalation exposure to inorganic vanadium compounds. Investigations on genotoxicity have been limited to non point-of-contact organs/systems such as the blood and male reproductive cells. Nonetheless, these studies provide *in vivo* and *in vitro* evidence of the potential for genotoxic effects of certain inorganic vanadium compounds in some cells, raising the possibility of potential genotoxic effects of V_2O_5 in the lung. However, experimental evidence of such effects still in the lung remains to be demonstrated.

10.5.1 Evidence of Genotoxic Effects in Vanadium Pentoxide-Exposed Workers

To date, there are only two studies available on the genotoxic effects of vanadium in workers [22, 23]. Both studies investigated systemic genotoxicity in cells isolated from blood; genotoxic effects in lung cells have not been investigated. A study by Ehrlich et al. [23] on DNA damage in vanadium production workers found no increase in the frequency of DNA strand breaks in leucocytes isolated from 52 exposed workers compared to non-exposed controls ($n = 52$), but reported changes in a number of genotoxic markers of chromosomal instability; increased frequency of DNA base oxidation, micronuclei (MN), nucleoplasmic bridge and nuclear bud formation, necrosis and a reduction in DNA repair in lymphocytes from exposed workers ($n = 23$) compared with matched controls ($n = 24$). Findings were associated with a seven-fold higher median plasma vanadium levels in exposed workers (2.2 μg/L) compared with matched controls (0.3 μg/L). The lack of evidence of DNA strand breaks in leucocytes of exposed workers supports similar negative findings in a study by Ivancsits et al. [22] in V_2O_5-exposed factory workers ($n = 49$); no differences in DNA strand-breaks, oxidative damage (8-OHdG assay) or SCE were observed in leukocytes of occupationally-exposed compared to unexposed controls ($n = 12$). Median serum vanadium concentrations in exposed individuals (5.38 μg/L) and controls (2.54 μg/L) in this study [22] were higher than in the study by [23]. These two studies suggest that some cell types may be more susceptible than others to the genotoxic effects of V_2O_5.

10.5.2 Evidence of Genotoxic Effects of Vanadium in Experimental Animals and In Vitro

Conflicting evidence of genotoxic effects is also reported in studies on experimental animals exposed to inorganic vanadium compounds. The NTP 2002 study on V_2O_5

found no increase in the frequency of MN in normochromatic erythrocytes (NCEs) in the peripheral blood of male and female B6C3F1 mice exposed to V_2O_5 (at 1, 2, 3, 8 or 16 mg/m^3, equivalent to 0.6, 1.1, 1.7, 4.5 or 9 mg V/m^3, for 6 h/day for 3 months) in the absence of signs of bone marrow toxicity measured using the difference in the ratio of PCEs to NCEs [5]. Vanadium blood concentrations in female mice ($n = 4$ or 5) exposed to 4 mg/m^3 V_2O_5 measured as part of the NTP (2002) study, were approximately 1 μg/g blood (equivalent to ~1 mg/L) on day 26 and 54, which were several-fold lower than vanadium concentrations in the lungs [21]. In several studies on more soluble forms of inorganic vanadium administered via oral or intraperitoneal (i.p.) routes, single exposure (or for Na_3VO_4 also repeated exposure) of experimental animals to $VOSO_4$, Na_3VO_4 or NH_4VO_3 induced an increase in MN in bone marrow PCEs and the number of hypo- and/or hyperploid BMCs [24–26] with some evidence of a dose-dependent increase in aneuploidy [26]. Chromosomal aberrations in BMCs were only reported following a single exposure to $VOSO_4$ [24]. Attia et al. [27] reported negative results for MN in bone marrow PCEs of male mice given Na_3VO_4 (1.4, 4.2 and 6.9 mg V/kg bw) by i.p. injection, although a dose-dependent increase in the frequency of hyperhaploid sperm was observed. Treatment of rats with 0.5 ppm vanadium (NH_4VO_3) in drinking water for 28 or 103 days did not result in an increase in hepatic DNA damage (oxidative, strand breaks, DNA-protein cross-links) or in the frequency of hepatocytes with structural chromosomal aberrations or aneuploidy [28, 29]. These *in vivo* studies may indicate a potential for V(IV) and V(V) compounds to induce MN and aneuploidy in some cells, although the data are inconsistent. However, the results emphasize the importance of exposure route in determining the target dose at which genotoxic effects may be apparent, show differences in the response of various cell types and are suggestive of differences in the types of potential genotoxic effects of V(IV) and V(V) compounds.

Overall the findings from *in vitro* studies support positive findings *in vivo*. While vanadium compounds have generally been found to be negative in bacterial gene mutation assays, which is not uncommon for metal compounds (e.g. Mn, Co, Ni), in some cell systems vanadium compounds have been shown to cause DNA-damage, clastogenicity and aneugenicity. *In vitro* experiments by Ivancsits et al. [22], in support of investigations of genotoxic effects in V_2O_5-exposed workers, showed a significant increase in DNA strand breaks in cultured fibroblasts at occupationally-relevant concentrations, while similar effects in whole blood leukocytes and lymphocytes we found only at concentrations of vanadium >50 μg/l which equates to the upper end of the range of serum vanadium concentrations determined for V_2O_5-exposed workers. Several studies have also shown induction of DNA single strand breaks to varying degrees in some human cells (lymphocytes, fibroblasts, leukocytes; HeLa cancer cells) exposed to either V_2O_5, $VOSO_4$, or Na_3VO_4 but not others (mucosal cells) [30–32]. Evidence of DNA double strand breaks, possibly via vanadyl-mediated radical formation, was reported in cells exposed to vanadyl ($VOSO_4$) [31].

Data on clastogenic effects *in vitro* are similarly mixed with regards to the cell system used. V_2O_5 was positive in an *in vitro* V79 micronucleus assay but

failed to induce MN in Syrian hamster embryos [33]. While a concentration-related increase in the frequency of hyperdiploid cultured human lymphocyte cells (from three donors), treated with V_2O_5 (0.01–1 μg V/ml for 24 h) has been reported, although variability in the individual response was observed [34]. V_2O_5 (0.05 and 0.5 μg V/ml) induced persistent and transmissible genomic instability (dicentric chromosomes, nucleoplasmic bridges, MN and aneuploidy) in telomerase reverse transcriptase-negative (hTERT–, wild type), but not hTERT+, human BJ fibroblasts, and tetraploidy in hTERT+, but not hTERT- cells, which suggests that the type of genomic instability in human cells may depend on expression of telomerase [35].

In summary, vanadium (IV) and (V) compounds are potentially genotoxic to some cells; however, there is currently a lack of data on the genotoxic effects of V_2O_5 and other vanadium compounds on lung cells and given the variability in response of various cell systems, it is unclear whether genotoxic effects in the lung would occur. The genotoxic response is also dependent on the internal dose and is therefore related to exposure route. It is difficult to make direct comparisons on the potency of vanadium compounds and the valency between these studies, since the routes of administration differ and the internal dose is not known for most of these studies. However, the *in vitro* data suggest differences in effects following treatment with V(IV) and V(V) compounds i.e. V(IV) appears to induce double strand DNA breaks, whereas V(V) compounds do not. The overall weight of evidence from all genotoxic studies suggests a possible genotoxic potential for V(IV) and V(V) compounds.

10.6 Potential Mechanisms of Genotoxicity, Respiratory Effects and Cancer

The mechanisms underlying vanadium-induced *in vivo* genotoxicity and carcinogenicity observed in mice have not been established, however *in vitro* studies are available that have investigated the role of vanadium-induced reactive oxygen species (ROS) and various vanadium species formed *in vivo*.

10.6.1 Mechanisms of Genotoxicity

In cell-free systems, vanadium appears to induce DNA-damage by generating ROS, which then react with DNA. In particular $VOSO_4$, V(IV) has been shown to mediate DNA damage by generation of hydroxyl radicals ($^{\cdot}OH$) via a Fenton-like reaction involving reaction of V(IV) with generated H_2O_2 [36–38].

In cellular systems, however, the mechanisms appear to be somewhat more complicated. Investigations into the mechanism of action of vanadate (Na_3VO_4)-mediated increase in DNA single strand breaks in human fibroblasts showed no coincidental increase in oxidative damage (8-OHdG adducts) or double strand

breaks suggesting a mechanism other than one mediated by ROS [22]. Indeed, it has been suggested that generation of peroxovanadium species from vanadyl and peroxide may be responsible for the some of the observed biological effects of V(IV and V) [39, 40]. Although the exact mechanisms of vanadium-mediated genotoxicity are not clear, H_2O_2 may play a major role in certain toxic endpoints, since several studies that have shown an increase in effects of V(IV and V) with the addition of super oxide dismutase (SOD), perhaps due to the generation of H_2O_2 during the dismutation of O^{2-} [36, 37, 39].

Ramírez et al. [34] investigated the effects of V_2O_5-treatment on spindle formation. Immunofluorescence analysis using anti-β-tubulin antibody showed that V_2O_5 treatment disrupted microtubule assembly, indicating that V(V), V_2O_5 interacts directly with tubulin. Further experiments by the same authors with purified tubulin revealed that V_2O_5 inhibited tubulin polymerisation and stimulated depolymerisation, suggesting that the aneuploidy observed in V_2O_5-treated cultured human lymphocyte may be caused by inhibition of microtubule assembly leading to disruption of spindle formation [34]. The exact mechanism of this interaction has not been elucidated, although the authors speculated that V(V) interacts directly with sulfhydryl-containing amino acid residues within tubulin [34]. Based on these data International Agency for Research on Cancer (IARC) [2] considered that the aneugenic effects may be explained by inhibition of microtubule polymerization, but noted that it is not clear whether these effects are related to oxidative damage or to direct interaction with vanadium ions. IARC also noted that indirect inhibitory effects of V_2O_5 on enzymes involved in DNA synthesis and repair also contribute to genotoxicity [2].

10.6.2 Pathways for Respiratory Irritation and Inflammation

The underlying mechanisms of the respiratory effects following inhalation exposure of humans and experimental animals have been investigated in cell culture in a number of different studies. These studies have focused on effects of vanadium exposure on expression of various inflammatory cytokines and transcription factors. In one such study, sodium vanadate ($NaVO_3$) induced a concentration-dependent increase in tumour necrosis factor α (TNF-α) mRNA and protein levels in murine macrophage Raw264.7 cells, via ROS generation and the activation and subsequent binding of nuclear factor-κB (NF-κB) to the TNF-α promoter [41]. Activation of NF-κB has been shown to promote cell proliferation and has been linked to carcinogenesis [42]. In an *in vivo* study, Pierce et al. [15] reported that TNF-α was not detected in BAL fluid taken 10 days after a single exposure of female rats to $NaVO_3$, $VOSO_4$ or V_2O_5, however mRNA expression of chemokines macrophage inflammatory protein 2 (MIP-2) and KC, primary mediators of pulmonary inflammatory response in rats, were found [15].

In bronchial epithelial cells or perfused lung, $VOSO_4$ treatment has been found to induce protein or mRNA expression of several inflammatory cytokines such as

interleukin (IL)-1β, IL-8 and IL-1α [43, 44] and a zinc finger protein (which is induced by TNF-α) that inhibits NF-κB activity and TNF-mediated apoptosis, [43]. The mRNA expression of some other genes involved in inflammatory responses were also found to be up-regulated; these include prostaglandin-endoperoxide synthase 2 (cyclooxygenase-2, COX-2), chemokine ligand 1 and 3 [43].

In a study by Wang et al. [16] on $NaVO_3$-exposed mice, addition of the H_2O_2 scavenger, catalase reduced the inflammatory response (influx of neutrophils and increase in apoptotic lung cells) to control levels; addition of SOD ($O_2^{\cdot -}$ scavenger) or deferoxamine (inhibitor of $^{\cdot}OH$ generated by Fenton-like reactions) only slightly diminished the response. The authors suggested that NADPH oxidase and the mitochondrial electron transport (MET) chain are involved in vanadium-induced ROS generation, a hypothesis which is supported by a reduction in ·OH generation in the presence of the MET-inhibitor rotenone and NADPH-inhibitor [16].

10.6.3 Proposed Modes of Action for Lung Cancers in Mice

IARC in the Monograph on V_2O_5 [2], acknowledged the lack of a clear mode of action (MOA) for the development of tumours observed in mice following inhalation exposure to V_2O_5, and concluded that the induction of dominant lethal mutations in mice may result from one, or a combination, of genotoxic MOAs [2]. The draft ATSDR toxicological assessment for vanadium [1] concluded that redox cycling occurs between V(IV) and V(V) species and that vanadium acts as a phosphate analogue, interacting with a number of enzymes, a possible mechanism to explain various toxicological effects associated with vanadium exposure. The authors acknowledged that there is a lack of information to fully explain effects *in vivo*.

These and other potential MOAs are described by the general schematic in Fig. 10.1.

In one permutation, inhaled V_2O_5 (V(V)) may interact directly with tubulin, inhibiting microtubule assembly leading to disruption of spindle formation [34]. In another permutation, ROS generated by V(V) may induce genetic damage rather than direct interaction of vanadium species with nuclear targets. Based on the available data IARC [2] considered that the aneugenic effects may be explained by inhibition of microtubule polymerization, but noted that it is not clear whether these effects are related to oxidative damage or to direct interaction with vanadium ions. IARC also noted that indirect inhibitory effects of V_2O_5 on enzymes involved in DNA synthesis and repair also contribute to genotoxicity [2]. Following induction of genotoxic effects, ROS generated by inflammation or vanadium species (derived from V_2O_5) may then activate cell signalling cascades [45] involved in cell proliferation and growth, fixing genetic damage and leading ultimately to tumour formation. Data from a recent *in vivo* study in three different strains of mice also suggested a tumour promotion role for V_2O_5 which was associated with susceptibility to V_2O_5-induced pulmonary inflammation [45]. There is limited *in vivo* evidence to fully support a proposed MOA, however *in vitro*

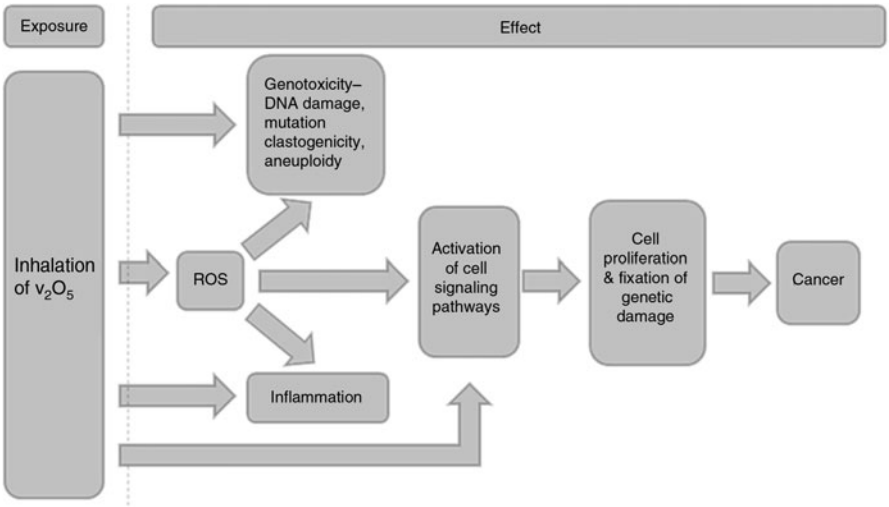

Fig. 10.1 Simple schematic of proposed possible mode of actions for lung tumours in mice following inhalation of V_2O_5 (ROS; reactive oxygen species)

data are available indicating potential for the various steps in these pathways. Findings from a number of *in vitro* studies suggest that V(IV) and V(V) compounds activate cell signalling cascades involved in cell differentiation and proliferation [46–49]. For example, in mouse epidermal C141 cells, vanadate was found to act on or upstream of phosphatidylinositol-3 kinase (PI3-K), activating a number of downstream proteins involved in control of cell cycle regulation [47, 48] including mitogen-activated protein kinases (MAPKs) ERK1&2 (mammalian extracellular signal-regulated kinases 1 and 2), which are involved in cell proliferation in response to growth factors, and p38, which is involved in cell differentiation, cell cycle regulation, cell death and inflammation [49]. More recently, ERK1&2 activation have been demonstrated *in vivo* in lung tissue from mice exposed to inhaled V_2O_5 [45]. V(IV) (as $VOSO_4$) was demonstrated to active MAPK signalling pathways via PI3-K [46]. Other studies have demonstrated a role for p53 tumour-suppressor gene in vanadate-induced apoptosis [50] and cell cycle (S phase) arrest [51]. Capella et al. [39] hypothesised that Na_3VO_4-induced cell death is related to induction of p21 Ras proteins, which are involved in signal transduction to the MAPK cascade. Indeed, evidence suggests that p21 K-*ras* gene may play a tumour suppressive role in mouse lung tumours as a high frequency of Ras mutations have been identified in human and mouse tumours, and elevated MAPK signalling in alveolar bronchiolar carcinomas (6/7) taken from B6C3F1 mice exposed to V_2O_5, correlated with K-*ras* mutation and loss of heterozygosity (loss of wild type K-*ras* allele) [52].

Vanadium species also appear to be involved in activation of a different PI3-K pathway involving vascular endothelial growth factor (VEGF), a potent mitogen involved in tumour progression and activation of angiogenesis in several cancer types [53].

Many of these studies have demonstrated that activation of the MAPK pathway is attenuated by the presence of antioxidants indicating ROS-initiated phosphorylation of protein targets as a potential mechanism [54, 55]. However, several other studies have shown that V(V) species (vanadate and the pervanadate species diperoxovanadate and monoperoxovanadate) are able to interact directly with certain phosphatases such as recombinant protein tyrosine phosphatase (PTP) 1B, [40, 56]. Huyer et al. [40] suggested that vanadium (IV) is likely to be a less potent inhibitor of PTP since it does not form a structure analogous to phosphate and does not mimic the transition state of PTP; they have cited publications that have reported V (IV) as being a less effective inhibitor of Na, K-ATPases than V (V). The relevance in *in vivo* systems is unclear since previous studies in cellular systems have confirmed that V (V) is quickly reduced to V (IV) in the presence of NADPH [42] although whether continual inter-conversion between the two states takes place has not been fully demonstrated.

Clearly, the situation is complex and there are a number of critical data gaps that, if filled, would help to clarify the MOA for the lung tumours in V_2O_5-exposed mice and whether these induced tumours have any relevance for human risk assessment.

References

1. ATSDR (2009) Draft toxicological profile for vanadium, draft for public comment. U.S. Department of Health and Human Services, Public Health Service Atlanta, Georgia
2. IARC (2006) Cobalt in hard metals and cobalt sulfate, gallium arsenide, indium phosphide and vanadium pentoxide. IARC monographs on the evaluation of carcinogenic risks to humans, vol 86. IARC, Lyon, pp 227–292
3. Cincinnati OH (2009) American conference of governmental industrial hygienists. Vanadium pentoxide, Signature Publications, pp 1–9. In: Documentation of the threshold limit values and biological exposure indices, 7th ed.: ACGIH
4. Kiviluoto M, Rasanen O et al (1979) Effects of vanadium on the upper respiratory tract of workers in a vanadium factory. A macroscopic and microscopic study. Scand J Work Environ Health 5:50–58
5. NTP (2002) NTP toxicology and carcinogensis studies of vanadium pentoxide (CAS No. 1314-62-1) in F344/N rats and B6C3F1 mice (inhalation). Natl Toxicol Program Tech Rep Ser 507:1–343
6. Parkes WR (1994) Occupational lung disorders, 3rd edn. Butterworth-Heinemann Ltd., Oxford
7. Kiviluoto M (1980) Observations on the lungs of vanadium workers. Br J Ind Med 37:363–366
8. Musk AW, Tees JG (1982) Asthma caused by occupational exposure to vanadium compounds. Med J Aust 1:183–184
9. Levy BS, Hoffman L et al (1984) Boilermakers' bronchitis. Respiratory tract irritation associated with vanadium pentoxide exposure during oil-to-coal conversion of a power plant. J Occup Environ Med 26:567–570
10. Zenz C, Berg BA (1967) Human responses to controlled vanadium pentoxide exposure. Arch Environ Health 14:709–712
11. Irsigler GB, Visser PJ et al (1999) Asthma and chemical bronchitis in vanadium plant workers. Am J Ind Med 35:366–374
12. Kiviluoto M, Pyy L et al (1981) Clinical laboratory results of vanadium-exposed workers. Arch Environ Health 36:109–113

13. Zenz C, Bartlett JP et al (1962) Acute vanadium pentoxide intoxication. Arch Environ Health 5:542–546
14. Knecht EA, Moorman WJ et al (1985) Pulmonary effects of acute vanadium pentoxide inhalation in monkeys. Am Rev Respir Dis 132:1181–1185
15. Pierce LM, Alessandrini F et al (1996) Vanadium-induced chemokine mRNA expression and pulmonary inflammation. Toxicol Appl Pharmacol 138:1–11
16. Wang L, Medan D et al (2003) Vanadium-induced apoptosis and pulmonary inflammation in mice: role of reactive oxygen species. J Cell Physiol 195:99–107
17. Knecht EA, Moorman WJ et al (1992) Pulmonary reactivity to vanadium pentoxide following subchronic inhalation exposure in a non-human primate animal model. J Appl Toxicol 12: 427–434
18. Assem FL, Levy LS (2009) A review of current toxicological concerns on vanadium pentoxide and other vanadium compounds: gaps in knowledge and directions for future research. J Toxicol Environ Health B Crit Rev 12:289–306
19. Duffus JH (2007) Carcinogenicity classification of vanadium pentoxide and inorganic vanadium compounds, the NTP study of carcinogenicity of inhaled vanadium pentoxide, and vanadium chemistry. Regul Toxicol Pharmacol 47:110–114
20. Ress NB, Chou BJ et al (2003) Carcinogenicity of inhaled vanadium pentoxide in F344/N rats and B6C3F1 mice. Toxicol Sci 74:287–296
21. Dill JA, Lee KM et al (2004) Lung deposition and clearance of inhaled vanadium pentoxide in chronically exposed F344 rats and B6C3F1 mice. Toxicol Sci 77:6–18
22. Ivancsits S, Pilger A et al (2002) Vanadate induces DNA strand breaks in cultured human fibroblasts at doses relevant to occupational exposure. Mutat Res 519:25–35
23. Ehrlich VA, Nersesyan AK et al (2008) Inhalative exposure to vanadium pentoxide causes DNA damage in workers: results of a multiple end point study. Environ Health Perspect 116:1689–1693
24. Ciranni R, Antonetti M et al (1995) Vanadium salts induce cytogenetic effects in in vivo treated mice. Mutat Res 343:53–60
25. Leopardi P, Villani P et al (2005) Assessment of the in vivo genotoxicity of vanadate: analysis of micronuclei and DNA damage induced in mice by oral exposure. Toxicol Lett 158:39–49
26. Mailhes JB, Hilliard C et al (2003) Vanadate, an inhibitor of tyrosine phosphatases, induced premature anaphase in oocytes and aneuploidy and polyploidy in mouse bone marrow cells. Mutat Res 538:101–107
27. Attia SM, Badary OA et al (2005) Orthovanadate increased the frequency of aneuploid mouse sperm without micronucleus induction in mouse bone marrow erythrocytes at the same dose level. Mutat Res 583:158–167
28. Chakraborty T, Chatterjee A et al (2006) Vanadium limits the expression of proliferating cell nuclear antigen and inhibits early DNA damage during diethylnitrosamine-induced hepatocellular preneoplasia in rats. Environ Mol Mutagen 47:603–615
29. Chakraborty T, Chatterjee A et al (2006) Vanadium inhibits the development of 2-acetylaminofluorene-induced premalignant phenotype in a two-stage chemical rat hepatocarcinogenesis model. Life Sci 78:2839–2851
30. Kleinsasser N, Dirschedl P et al (2003) Genotoxic effects of vanadium pentoxide on human peripheral lymphocytes and mucosal cells of the upper aerodigestive tract. Int J Environ Health Res 13:373–379
31. Wozniak K, Blasiak J (2004) Vanadyl sulfate can differentially damage DNA in human lymphocytes and HeLa cells. Arch Toxicol 78:7–15
32. Rojas E, Valverde M et al (1996) Genotoxicity of vanadium pentoxide evaluate by the single cell gel electrophoresis assay in human lymphocytes. Mutat Res 359:77–84
33. Gibson DP, Brauninger R et al (1997) Induction of micronuclei in Syrian hamster embryo cells: comparison to results in the SHE cell transformation assay for National Toxicology Program test chemicals. Mutat Res 392:61–70

34. Ramirez P, Eastmond DA et al (1997) Disruption of microtubule assembly and spindle formation as a mechanism for the induction of aneuploid cells by sodium arsenite and vanadium pentoxide. Mutat Res 386:291–298
35. Glaviano A, Nayak V et al (2006) Effects of hTERT on metal ion-induced genomic instability. Oncogene 25:3424–3435
36. Shi X, Jiang H et al (1996) Vanadium(IV)-mediated free radical generation and related 2′-deoxyguanosine hydroxylation and DNA damage. Toxicology 106:27–38
37. Shi X, Wang P et al (1996) Vanadium(IV) causes 2′-deoxyguanosine hydroxylation and deoxyribonucleic acid damage via free radical reactions. Ann Clin Lab Sci 26:39–49
38. Sakurai H (1994) Vanadium distribution in rats and DNA cleavage by vanadyl complex: implication for vanadium toxicity and biological effects. Environ Health Perspect 102(Suppl 3): 35–36
39. Capella LS, Gefe MR et al (2002) Mechanisms of vanadate-induced cellular toxicity: role of cellular glutathione and NADPH. Arch Biochem Biophys 406:65–72
40. Huyer G, Liu S et al (1997) Mechanism of inhibition of protein-tyrosine phosphatases by vanadate and pervanadate. J Biol Chem 272:843–851
41. Ye J, Ding M et al (1999) Induction of TNFalpha in macrophages by vanadate is dependent on activation of transcription factor NF-kappaB and free radical reactions. Mol Cell Biochem 198:193–200
42. Valko M, Rhodes CJ et al (2006) Free radicals, metals and antioxidants in oxidative stress-induced cancer. Chem Biol Interact 160:1–40
43. Li Z, Stonehuerner J et al (2005) Discrimination of vanadium from zinc using gene profiling in human bronchial epithelial cells. Environ Health Perspect 113:1747–1754
44. Huang YC, Wu W et al (2002) Activation of EGF receptors mediates pulmonary vasoconstriction induced by residual oil fly ash. Exp Lung Res 28:19–38
45. Rondini EA, Walters DM et al (2010) Vanadium pentoxide induces pulmonary inflammation and tumor promotion in a strain-dependent manner. Part Fibre Toxicol 7:9
46. Pandey SK, Theberge JF et al (1999) Phosphatidylinositol 3-kinase requirement in activation of the ras/C-raf-1/MEK/ERK and p70(s6k) signaling cascade by the insulinomimetic agent vanadyl sulfate. Biochemistry 38:14667–14675
47. Zhang Z, Gao N et al (2004) The role of phosphatidylinositol-3 kinase in vanadate-promoted S phase entry. Mol Cell Biochem 255:239–245
48. Zhang Z, Gao N et al (2004) Vanadate activated Akt and promoted S phase entry. Mol Cell Biochem 255:227–237
49. Zhang Z, He H et al (2002) MAPKs mediate S phase arrest induced by vanadate through a p53-dependent pathway in mouse epidermal C141 cells. Chem Res Toxicol 15:950–956
50. Huang C, Zhang Z et al (2000) Vanadate induces p53 transactivation through hydrogen peroxide and causes apoptosis. J Biol Chem 275:32516–32522
51. Zhang Z, Chen F et al (2002) Vanadate induces G2/M phase arrest in p53-deficient mouse embryo fibroblasts. J Environ Pathol Toxicol Oncol 21:223–231
52. Devereux TR, Holliday W et al (2002) Map kinase activation correlates with K-ras mutation and loss of heterozygosity on chromosome 6 in alveolar bronchiolar carcinomas from B6C3F1 mice exposed to vanadium pentoxide for 2 years. Carcinogenesis 23:1737–1743
53. Lee M, Hwang JT et al (2006) Critical roles of AMP-activated protein kinase in the carcinogenic metal-induced expression of VEGF and HIF-1 proteins in DU145 prostate carcinoma. Biochem Pharmacol 72:91–103
54. Wang YZ, Bonner JC (2000) Mechanism of extracellular signal-regulated kinase (ERK)-1 and ERK-2 activation by vanadium pentoxide in rat pulmonary myofibroblasts. Am J Respir Cell Mol Biol 22:590–596
55. Zhang Z, Leonard SS et al (2003) Role of reactive oxygen species and MAPKs in vanadate-induced G(2)/M phase arrest. Free Radic Biol Med 34:1333–1342
56. Freire AC, Aoyama H et al (2003) Relationship between phosphatase activity and cytotoxic effect of two protein phosphatase inhibitors, okadaic acid and pervanadate, on human myeloid leukemia cell line. J Enzyme Inhib Med Chem 18:425–429

Index

H. Michibata (ed.), *Vanadium: Biochemical and Molecular Biological Approaches*,
DOI 10.1007/978-94-007-0913-3, © Springer Science+Business Media B.V. 2012